ACTA MINERALOGICA PAKISTANICA

1SSN 0257-3660

VOLUME NO. 9 1998

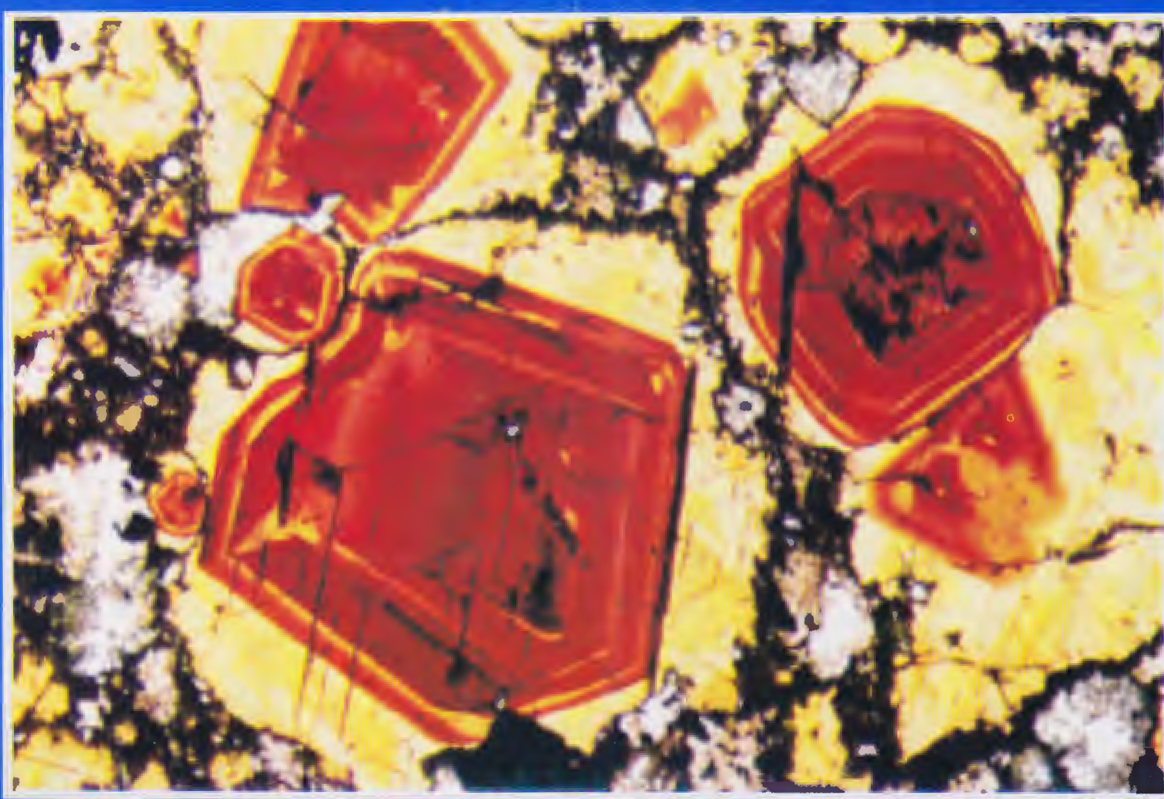

NATIONAL CENTRE OF EXCELLENCE IN MINERALOGY
UNIVERSITY OF BALOCHISTAN,
QUETTA, PAKISTAN

VOLUME 9 **1998**

ACTA MINERALOGICA PAKISTANICA

An annual publication of the Centre of Excellence in Mineralogy, Quetta Pakistan

On the Cover	Zoning in Sphalerite grains from sediment-hosted Lead-Zinc-Barite mineralized area, District Khuzdar, Pakistan. (Transmitted light, X5). Photo courtesy of Shamim Ahmad Siddiqui.

Address for correspondence	Editor, Acta Mineralogica Pakistanica, Centre of Excellence in Mineralogy, University of Balochistan, Quetta. Pakistan. Phone No. (081) 9211323, Fax No. (081) 9211285 cem@minerals.qta.sdnpk.undp.org
ISSN	0257-3660
Copyright	Centre of Excellence in Mineralogy, University of Balochistan, Quetta.
Price for Volume 9	Rs. 200.00, US$12.00, UK£8.00 (includes postage and handling)
Type setting and composing	Mohammad Ahmad Farooqui
Printed at	Print Point, Art School Road, Quetta.

Published in December each year.

ACTA MINERALOGICA PAKISTANICA
VOLUME 9, 1998

CONTENTS

ARTICLES

SHORT COMMUNICATIONS

REPORTS

ACTA MINERALOGICA PAKISTANICA
Volume 9 (1998)

Article Reference
AMP9.1998/001-006/ISSN.0257-3660

CONTROL OF PHYSICO-CHEMICAL CONDITIONS ON THE MINERALOGICAL CHARACTERISTICS OF WEATHERING PROFILE OF ANORTHOSITIC ROCKS OF SURYUN AREA, KOREA

***ABID MURTEZA KHAN*[1] AND *SOO JIN KIM*[2]**
[1] Engineering Consultants International (Pvt.) Limited, Karachi, Pakistan.
[2] Department of Geological Sciences, Soel National University, Soel 151-742, Korea.

ABSTRACT

The physico-chemical condition along the weathering profile of anorthositic rocks of Suryun area. Korea, have produced three distinct zones or horizons which show a characteristic trend in mineral distribution. Generally kaolinite, chlorite, gibbsite, vermiculite, geothite and hematite are abundant in the upper zones while hallosite. illite, interstratified minerals become abundant in the middle zone. Hydrated halloysite (10A°) is predominant in the lower zone. Smectite, manganese minerals are epidote are distributed as minor minerals in both middle and lower zones. Quartz is present in all three zones while chromium and titanum are concentrated in the upper zone. The pH value, oxidation potential, water activity and intensity of weathering are the main controlling factors in the formation of these zones.

INTRODUCTION

The physico-chemical condition controls the formation of secondary mineral phases and their abundance and distribution in specific horizon of weathering profile. According to Anand et.al (1985) the chemical micro-environment within the same horizon accounts for the formation of different products.

The weathering profile of Suryun Anorthositic rocks in South Korea shows three distinct zones or horizons (Fig.1) that differ in nature and relative abundance of minerals (Khan 1990). The presence of good outcrop of weathering profile has provided an excellent opportunity to study the mineralogical variations along different zones. The paper describes the control of physico-chemical condition on the mineralogy of each zone of weathering profile in Suryun area.

MATERIAL AND METHODS

Samples from all the three zones of weathering profile were collected, packed in air tight polythene bags and placed in plastic bottles in order to preserve its natural state. The particle size of the samples were determined by wet sieving and by the sedimentation and centrifuge methods. pH of the samples were also determined. Fe-oxide impurities were removed by the method of Mehra and Jackson (1960). For X-ray diffraction analysis, Rigaku RAD-C diffractometer operated at 30Kv, 10mA with nickel filtered Cuk radiation was used. A JEOL Model JEM200CX transmission electron microscope, operated at 160 Kv and JEOL JSM-35, scanning electron microscope was used for electron microscopy. Polished thin sections were analysed by JEOL-JCXA-733 superprobe for chemical analysis. The instrument operated under condition of 12 mA beam current and 2 m of beam diameter. ZAF caliberation was made by applying Bense and Albee's method (1968). pH determination was carried out using DP-135 pH/ion meter.

RESULTS

X-RAY DIFFRACTION

The X-ray diffraction analyses of bulk rock samples and centrifuged samples of weathering profile indicate that there is a distinct variation of mineral assemblage in three zones and each zone is characterized by index minerals. The X-ray diffraction patterns of major minerals are shown in Figure 2. Each zone also differs in texture.

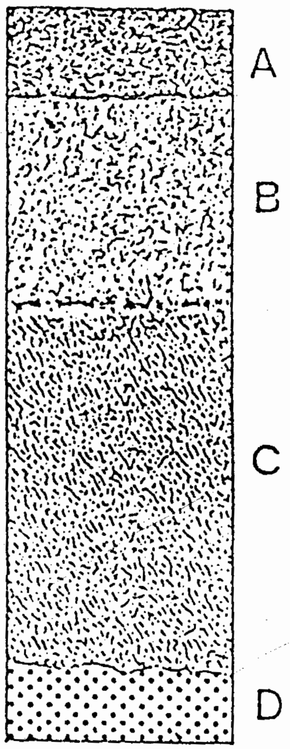

Figure 1. Generalized columnar section of kaolin deposit of Suryun area. A; upper red zone, B; middle pink zone, C; lower white zone and D; host rock anorthosite.

The upper red zone is devoid of relict texture and contains kaolinite, halloysite (7A°), gibbsite, chlorite, illite, goethite, hematite, vermiculite and quartz, kaolinite, gibbsite, goethite and hematite form characteristic minerals of this zone. The middle pink zone shows relict texture preserved and consists of halloysite (10A° and 7A°), kaolinite, smectite, interstratified minerals, vermiculite, goethite, illite, quartz and managanese oxide. Halloysite is more abundant than Kaolinite, Gibbsite occurs in traces. The characteristic minerals include hydrated (10A°) and dehydrated (7A°) halloysite, illite, smectite and interstratified minerals. The mineral assemblage of the lower white zone include halloysite, smectite. illite, kaolinite, interstratified minerals, quartz and altered grains of feldspar. Halloysite (10A°) forms the characterisitc mineral of this zone. The lower white zone is marked by firm to weakly preserved texture.

Table 1. Electron microprobe analyses of weathering profile and fresh anorthosite rock: 1;Upper reddish brown zone, 2; Middle pink zone, 3;Lower white zone, 4;Fresh anorthositic rock

Percent Oxides	Sample No. AH-D1 1	AH-D2 2	AH-D3 3	AH-10 4
SiO_2	44.13	47.31	48.58	52.55
Al_2O_3	35.40	45.66	37.53	26.13
TiO_2	1.28	0.04	0.01	0.37
Cr_2O_3	0.03	0.01	0.08	0.05
FeO	17.35	3.15	0.30	3.78
MgO	0.32	0.32	2.04	2.60
MnO	0.09	0.03	0.05	0.06
CaO	0.03	0.56	5.62	10.14
Na_2O	0.42	0.94	2.94	3.77
K_2O	0.76	1.98	2.91	0.65
Total	100.00	100.00	100.00	100.00
Si/Al	1.24	1.03	1.29	2.00

MORPHOLOGY

The scanning electron micrograph (SEM) and transmission electron micrographs (TEM) of minerals are shown in Figure 3. The smectite display honey comb structure (Fig.3A) while vermiculite shows lamellar morphology (Fig. 3B). The halloysite and kaolinite display different shapes. The former show tubular form (Fig. 3C) while the later a vermiform shape (Fig. 3D) respectively. The illite and chlorite also show platy or lamellar structure but the former is more fine grained than the later.

CHEMICAL ANALYSES

The bulk chemical composition of the three zones were obtained by using electron microprobe. The chemical data is given in Table 1. The relative changes of the contents of major oxides on different stages of weathering along the profile are shown in Figure 4.

The alkali and alkaline earth (Na, K, Mg, Ca) show rapid leaching from upper horizon to lower one. SiO_2 content shows only slight variation. Al_2O_3 shows concentration in the upper horizon. The Si/Al ratio varies in different horizons (Av.2.00-1.03) and shows ratio of 1.03 in the middle horizon indicating enrichment of halloysite. The FeO content which shows total Fe content is

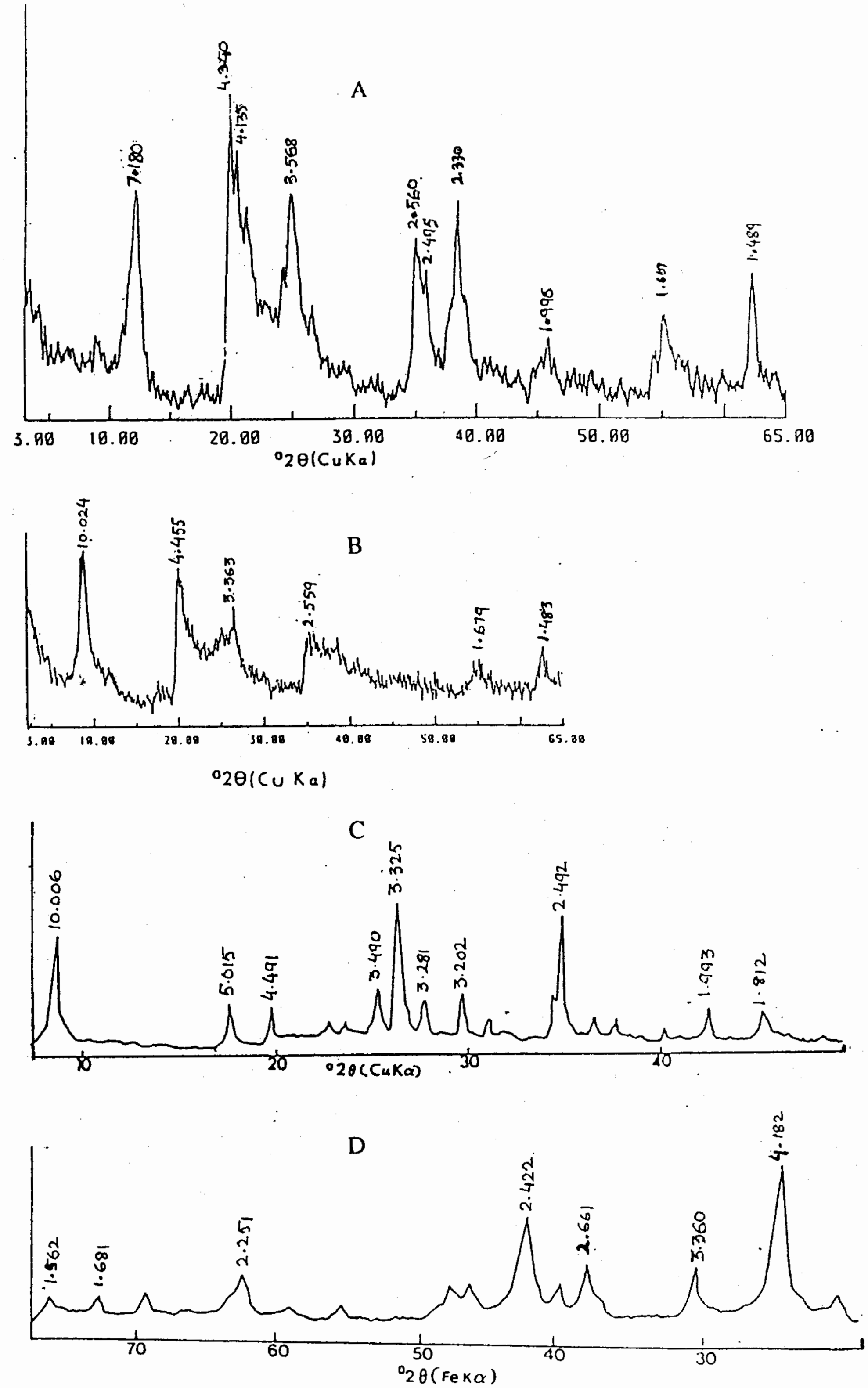

Figure 2. X-ray powder diffraction pattern of A) kaolinite, B) halloysite, C) illite, D) geothite.

Table 2. Physico-chemical environment along zones of weathering profile; Arrow indicates direction of increase.

Physical Characteristics	Physico-chemical Environment			
	Water Activity	Degree of Leaching	Oxidation Potential	pH Value
Upper Red Zone Red to brown, fine subangular grains, friable in consistency, relict texture absent, 0.5 to 1.5m thick	↓	↑	↑	↓
Middle Pink Zone Light brown to pink, medium- to fine-grained, relict texture preserved, microfracture and veinlets common,~ 2.5m thick				
Lower White Zone Firm weakly preserved relict texture, numerous veins and veinlets, thickness from 3m to 5m.				

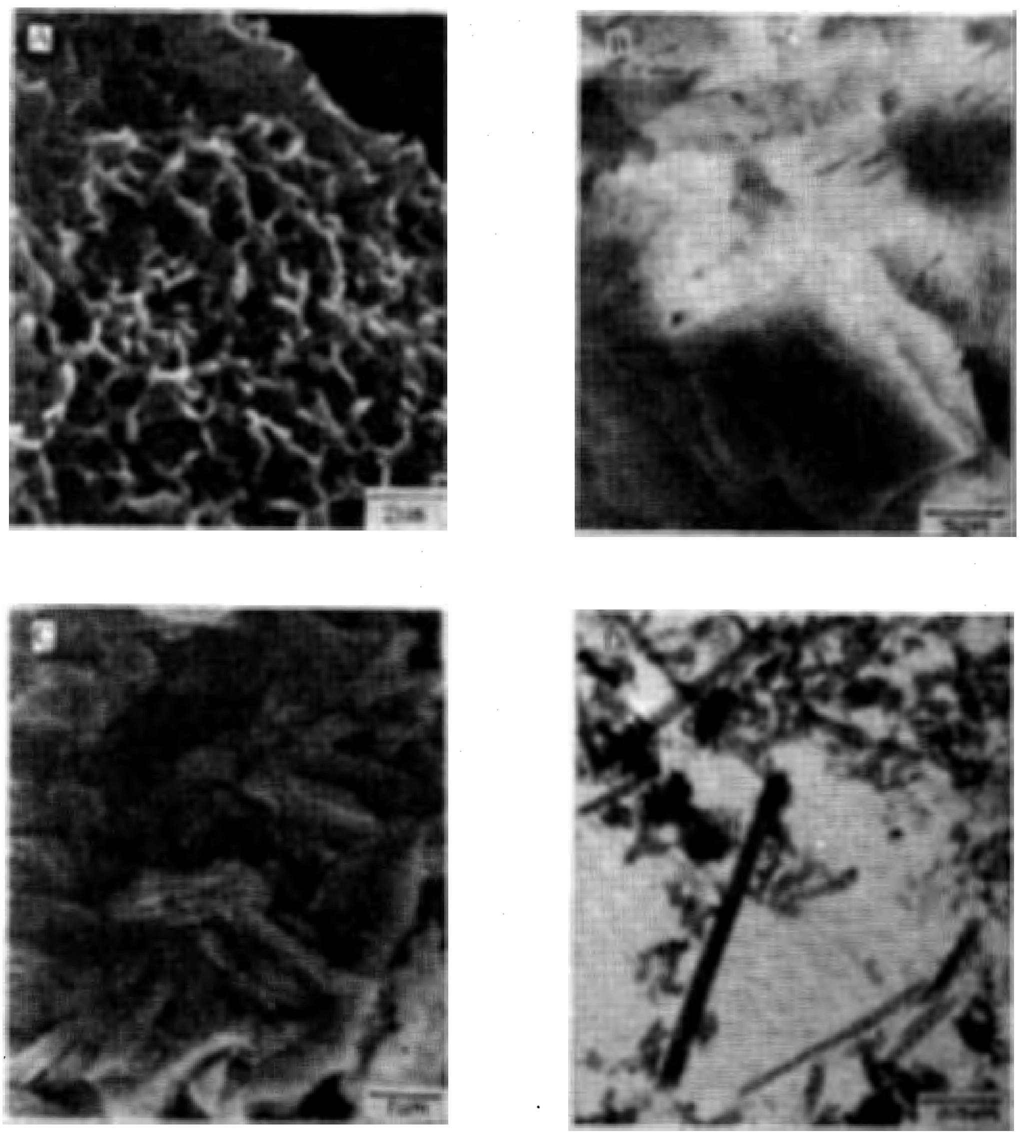

Figure 3. Scanning electron micrographs of A) smectite B) Kaolinite, C) illite, and transmission electron micrograph of halloysite (D).

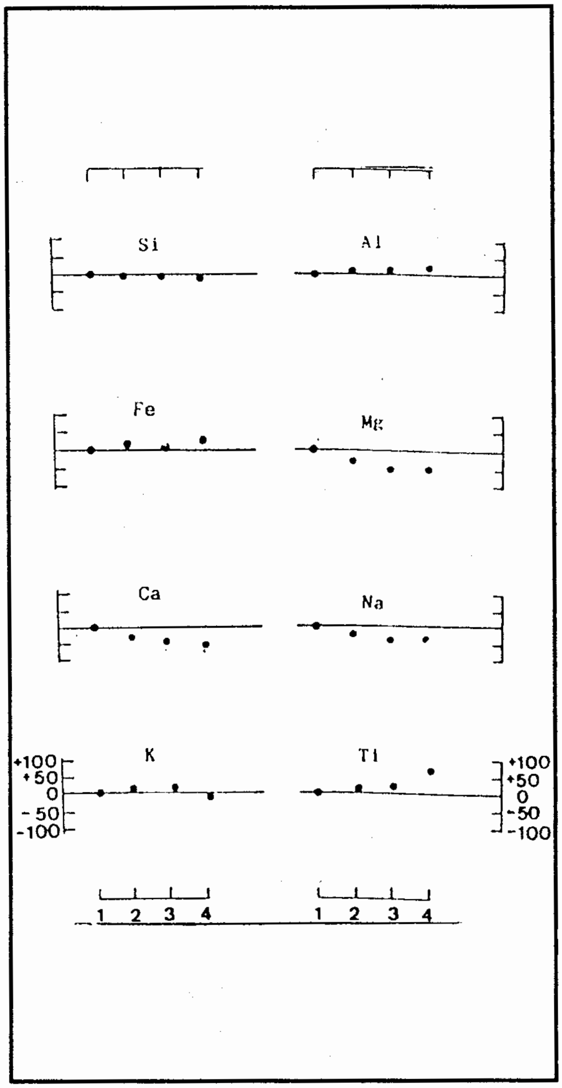

Figure 4. Relative changes of concentration of major element during the weathering of anorhyositic rocks (recalculated from the content of oxides). The ordinate in each diagram is the % chage in content. Numbers in adcissa indicate the samples: 1) fresh rock: 2) lower zone: 3) middle zone: 4) upper zone of oxides.

also concentrated in the upper horizon.

The CaO is depleted very rapidly in upper and middle zone. In lower zone the content of CaO show intermediate values. Mg. show rapid leaching in upper horizon but is retained in middle and lower horizons. Titanium and chromium occur as minor elements and show a gradual increase in content during initial weathering conditions. In upper zone they show high concentration.

pH

The pH value for all the three zones were determined. The upper red zone gives value between 5.00 to 5.22, the middle pink zone shows a value between 5.30 to 5.60 and the lower white zone in a range of 5.80 to 7.70.

CONCLUSIONS

The physico-chemical condition along the weathering profile of Suryun anorthositic rocks (Table 2) have resulted in the formation of three distinct zones each of which is characterized by specific mineral assemblage that indicate the environment of formation. The upper red zdfones show intense leaching condition, low pH value (5-5.22) and high oxidation potential thus favouring the formation of kaolinite, gibbsite, goethite, hematite and ferrihydrite. Vermiculite, dehydrated halloysite ($7A_o$), chlorite and illite occur as minor mineral. The medium leaching condition, intermediate pH value (5-3-5.6) and low to medium oxidation state that prevails in the middle pink zone has produced wide range of clay minerals including halloysite, kaolinite, vermiculite, smecitite, interstratified minerals and illite. The slow solution speed resulted in the concentration of mobile elements thus favouring the formation of 2:1 layered minerals. Poor microdrainage caused low Si level in soil solution and has produced partially enclosed or protected environment conducive to the formation of smectite. Fe released on weathering is precipitate3d as goethite as a result of low to medium oxidation state.

The lower white zone shows high pH value (5.80 to 7.70), reducing environment and high water activity as it usually lie in water table. Dominant mineral formation include hydrated halloysite (10A°) while kaolinite, illite, interstratified minerals occur as minor associated minerals. High water saturation and relatively high pH value in this zone have resulted in the abundance of 10A° halloysite.

The bulk composition of zones of weathering profile shows good correlation with mineral composition. Leaching of Na, K, Ca increases towards the upper zone. High content of Al_2O_3 and FeO in upper zone explains abundance of gibbsite & iron oxide minerals. CaO & MgO show retention on middle zone as interlayer cations. Titanium and Chromium are concentrated in the upper zone.

ACKNOWLEDGEMENTS

The author is greatful to Mr. Zaheer Mirza, Chief Executive Officer/Chairman and Mr. Khalid Mirza, Director Highways Engineering Consultants International (Pvt) Ltd. for their support in preparation and presentation of this paper. Mr. Bashar is acknowledged for typing the manuscript.

REFERENCES

Anand, R.R., Gikes, R.J., Armitage, T.M., and Hilluyer T.W., 1985. Feldspar weathering in lateritic saprolite. Clay & Clay Minerals. 33, 31-45.

Appleman, D.E. and Evince, H.T. Jr., 1973. Job 9214 Indexing and least squares refinement of powder diffraction data. U.S.G.S, Computer contribution 22, US National Tech. Info. Serv. PB2-16188.

Bence, A.E., and Albee, A.L.,1968. Empirical correction factors for the electron microanalysis of silicates and oxides. Joun. Geo. 76, 362-403.

Khan, A.M., 1990. Mineralogy and Genesis of Suryun Kaolin deposits, Ph.D dissertation (unpublished), Seoul National University, Soel, South Korea.

Mehra, O.P. and Jackson, M.J., 1960. Iron oxide from soils and clays by a dithionite system buffered with sodium bi-carbonate. Clays & Clay Min. 7, 317-327.

Manuscript Received 10th August 1997
Revised Manuscript Received 1st October 1997
Accepted 1st October 1997

ACTA MINERALOGICA PAKISTANICA
Volume 9 (1993)

Article Reference
AMP9.1998/007-019/ISSN.0257-3660

LANDSLIDES AND GAPING FISSURES IN SOR RANGE-ZHARAI AREA, QUETTA DISTRICT, PAKISTAN

AKHTAR MOHAMMAD KASSI AND DIN MOHAMMAD KAKAR
Department of Geology, University of Balochistan, Quetta, Pakistan

ABSTRACT

The Sor Range-Degari coal field of Quetta District is composed mostly of mudstone, sandstone, limestone and rarely conglomerate beds of the Eocene Ghazij Formation and the Kirther Formation. The area contains various ancient landslides and huge gaping fissures which involve strata of the coal-bearing Ghazij Formation and the overlying Kirther Formation. The Ghazij Formation, comprising mainly the incompetent strata, is highly susceptible to erosion, making high angle, generally concave-upward, slopes of 5- 30%. Limestone of the Kirther Formation makes high peaks and nearly vertical scarpments.

At least 4 ancient landslides of fairly large size, mappable on 1:50,000 scale and many others, which are comparatively smaller, but of highly variable sizes, are found on high angle-slopes of the Ghazij Formation in the area. Various huge gaping fissures (incipient landslides) are also present in the Zharai area. Dips across these gaping fissures, situated on the dip-slope of the Kirther Limestone, change drastically from 36 degrees in the lower part to nearly horizontal in the upper reaches suggesting down-slope movement and subsidence of the limestone mass. Fissures are several hundred meters long and gaps across them 40cm to nearly 3m wide which gradually decrease at depth. Area covered is estimated as over 120,000 sq.m and may involve up to 21 million cubic m of limestone and claystone material. These gaping fissures, along with the on-going downslope movements in the Zharai area, are posing threat to the life and property. Therefore, study of the contributing factors and monitoring of the landslides in Sor Range area will be of immense value for putting forward proposals with a view avoiding and/or minimizing high risk to the life and property.

INTRODUCTION

Landslides, the downward and outward movement of slope-forming rock material, have caused considerable damage to public and private property and a high number of casualties throughout the world. Losses can be greatly reduced by carefull evaluation of the potentially unstable slopes and applying the acquired information in planning, designing and organizing the use of hillside areas.

The most important factors that are directly related to the landslides are the bed rock geology, slope conditions, precipitation, ground water conditions, seismicity and the occurrence of ancient landslides. Therefore, analysis of slope stability is essentially required wherever developmental plans are to be carried out. Development on or near ancient landslides must be carried out with great care and only after careful engineering geologic studies of the concerned area.

This paper is the first attempt to present the geological conditions of the ancient and active landslides in the Sor Range-Zharai area. The presence of wide gaping fissures near the peak of the Habib Rahi Limestone member of the Kirther Formation in Zharai area and other ancient landslides of fairly large size and several small ones involve millions of cubic meters of rock material and pose high risk to life and property. The purpose is to draw attention of the concerned authorities and mine owners/companies and miners of the area to

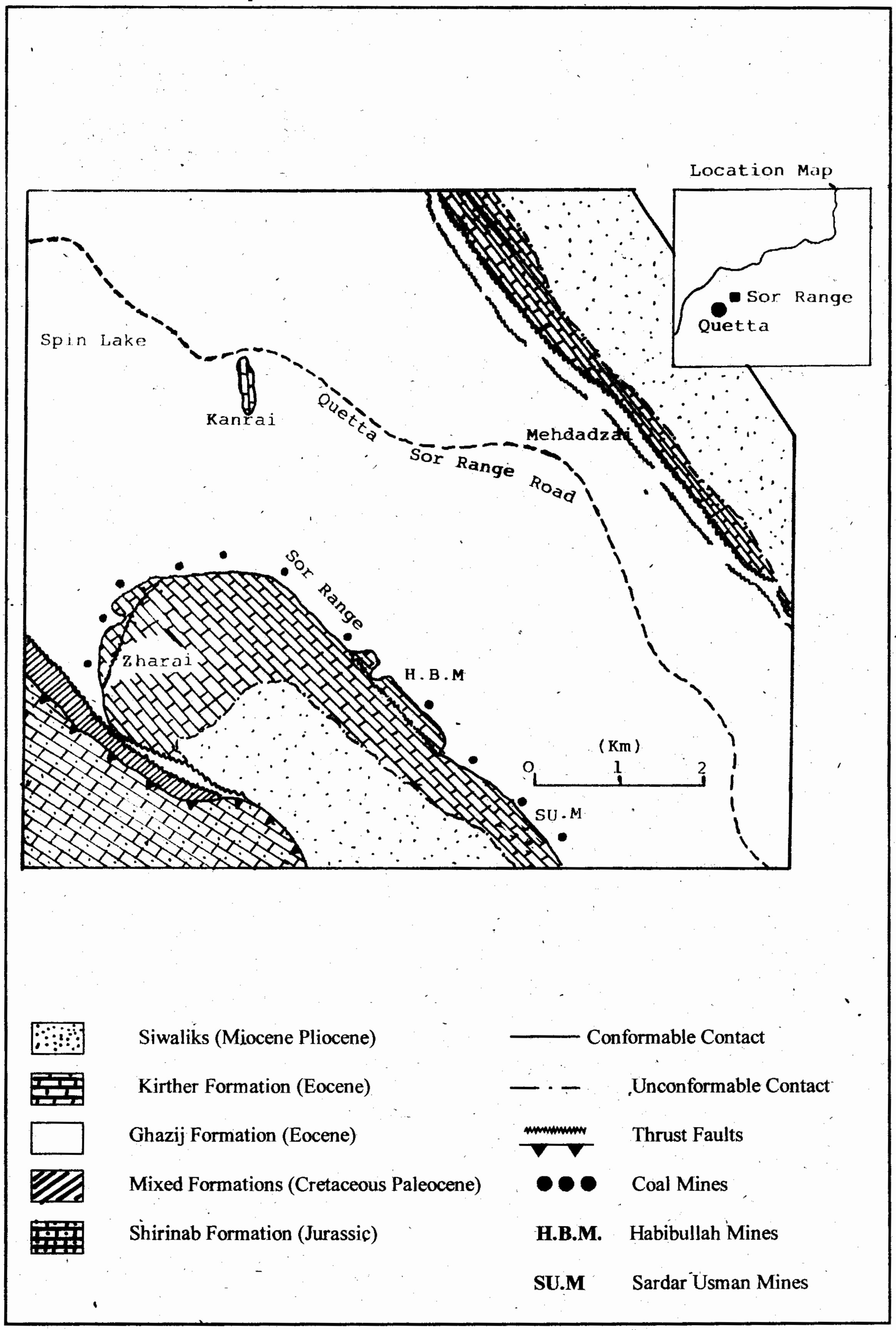

Figure 1. Geological map of the Sor Range-Zharai area.

the magnitude of high risk involved.

GEOLOGY OF THE AREA

The Sor Range-Zharai area is situated on the junction between Kirther and Sulaiman belts at the edge of Quetta Syntaxis (Fig. 1) which comprises sedimentary rocks of Jurassic to Pleistocene age (Kakar and Kassi 1997). Landslides are mainly associated with the slope of Eocene Ghazij Formation, also involving the overlying Kirther Formation. The Ghazij Formation is composed of over 1000m thick succession of dominantly claystone/siltstone interbedded with minor sandstone, conglomerate and coal seams. The lower part (over 750m thick) is dominantly claystone/siltstone of olive grey colour with occasional sandstone beds. The middle part (30-75m thick) contains higher proportions of sandstone, a thick conglomerate bed and various coal seams. However, the proportion of claystone/siltstone is still higher. The upper part (up to 230m thick) is composed mainly of claystone/siltstone of yellowish grey, maroon, red and pale green and yellowish grey colours with only a few beds of sandstone. The claystone is calcareous, gypsiferous, carbonaceous, splintery and fissile. It has been proposed (Hunting Survey Corporation 1960, Shah 1977, Iqbal 1969a, Kassi et al. 1987, Kakar and Kassi 1997) that the Ghazij Formation is a deposit of deltaic environment in which the lower claystone/siltstone dominant part comprises the prodeltaic clays of marine origin.

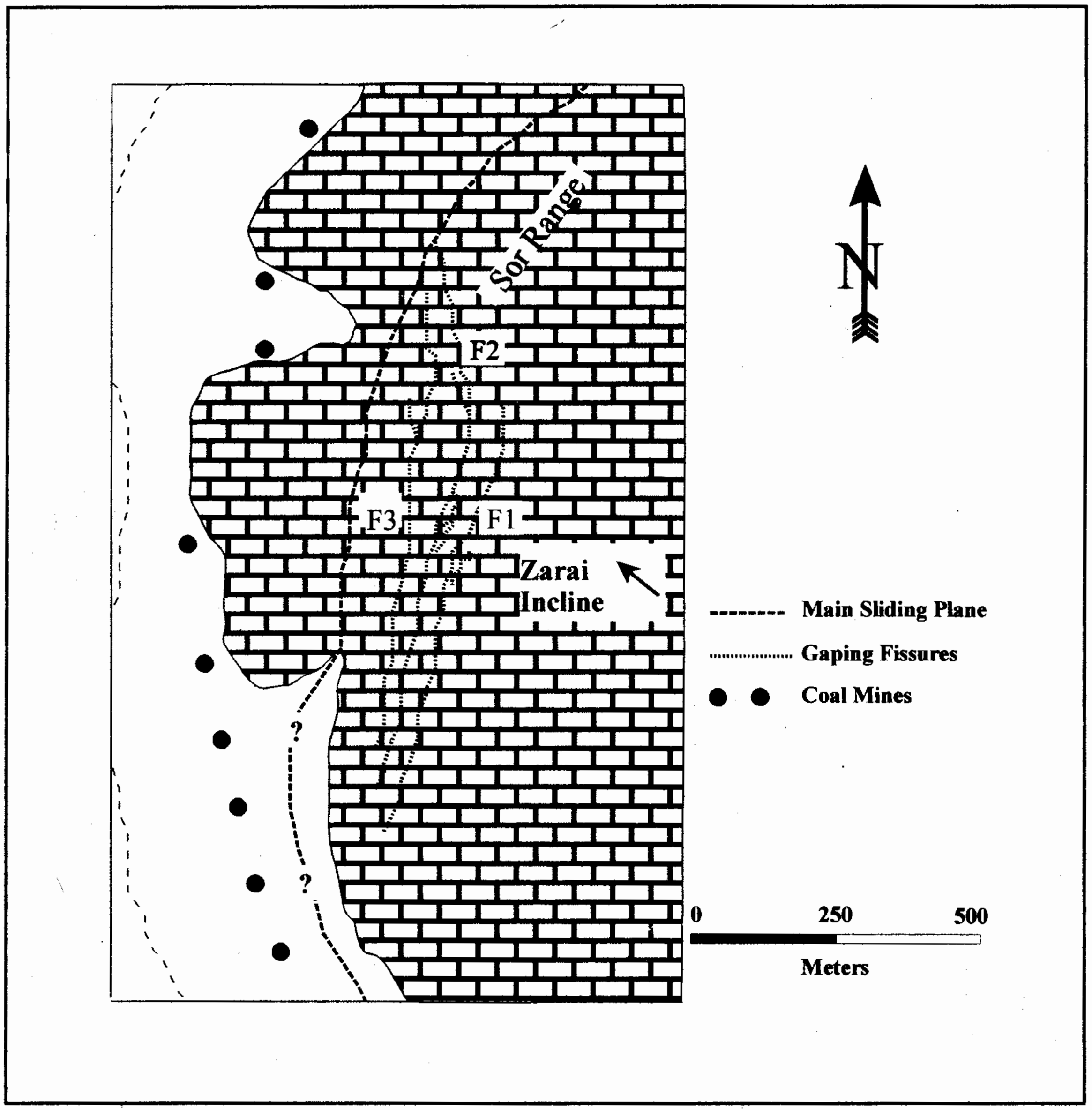

Figure 2. Geological map of the gaping fissures near Zharai area. Symbols are same as in Fig. 1

The overlying Kirther Formation comprises 158-201m thick limestone(Habaib Rahi Limestone member) in its lower part and up to 250 m thick chocolate-coloured claystone/siltstone with minor arenaceous limestone and sandstone (Sirki member) in the upper part. The limestone member is thick bedded, compact, cream coloured and highly fossiliferous.

The area (Fig.1) comprises NW-SE trending Obeshtakai Anticline between the Zarghun Ghar and Sor Range and a doubly plunging Sor Range Syncline further south-west. The southern limb of this syncline is cut off and overturned by a major thrust, the Ushbull thrust, bringing the older rocks of the Jurassic Chiltan Limestone and Cretaceous Parh Group in contact with the early Eocene Ghazij Formation. Another major structural feature is the NW-SE trending Dokan Thrust-Wrench Zone within the northern limb of the Obeshtakai Anticline (Fig. 1). The Obeshtakai Anticline is broad and complex containing many other minor thrust/ wrench faults. The anticline has the incompetent, claystone/siltstone succession of the Ghazij Formation in its core and thick bedded and competent limestone of the Kirther Formation in its limbs. The Ghazij Formation, being incompetent is highly susceptible to erosion, and formes high-angle concave-up slopes which is generally starting from nearly 5% in the core of Obushtakai Anticline and reach up to 30% in the limbs near the overlying Kirther Formation. The Kirther Formation makes high peaks and nearly vertical escarpments which f... northeast turning to the north and northwest.

GAPING FISSURES / INCIPIENT LANDSLIDES

Three major fissures F1, F2 and F3 (Fig. 2,4,5) are present on the northwestern nose of the Sor Range Syncline near the top of the curved peak of Kirther Formation north of Zharai. In this locality the strike of the beds is N36E and dip angle (to SE) gradually decreases upward (northwestward) across the fissures. The dip angle decreases from 36 SE to 32 SE, 26 SE and 15 SE north westward towards the peak, across fissures F1, F2 and F3 respectively, showing progressive subsidence of the limestone mass. Dip of the fissures vary from 75 degree west to almost vertical. Lateral movement gaps across these fissures vary between 40cm and 3m (measured on January 4, 1992) and appear to decrease gradually at depth. Actual depth of the fissures is not observable as these have been blocked by rock material fallen from the edges. However, the maximum observable depth in one locality is up to 40m. This implies that downslope movement, whenever initiated, will be westward, towards the coal mines and residential areas.

Area covered by the fissures (Fig. 2) between the highest reaches of the peak of Kirther Formation, just above the westward facing escrapments, and the fissure F1, is nearly 1km long and has the maximum width of nearly 240 m. If average width is taken as 120m then the estimated covered area is over 120,00 meter^2. If the average thickness of the Habib Rahi limestone member of the Kirther Formation is taken as 175m (Mohsin et al. 1991) a rough estimate of the volume of limestone alone in the covered area will be at least 21 million cubic m . This estimate does not include volume of material of upper part of the Ghazij Formation involved. Fissures have been observed further westward, downslope, above the coal mines which indicate movements during the past. Near the western peak the sides along fissures have moved downslope for up to 3-4 m forming "terrasets" and the dips here are almost horizontal.

The westward decrease in dip angle of the limestone ridge, across the fissures, indicates subsidence of the limestone mass which, along with other contributing factors, may be a response of the human activities downslope especially excavations of coal and other material. These open fissures obviously receive all the surface run-off and the sediment load which lubricate the slip zones along the fissures and therefore decrease friction between the shearing blocks. Fissures have caused disruption of the roots of vegetation (Fig. 5) which indicates that movements along fissures have occurred quite recently.

In view of the huge volume of rock material involved, it will be almost impossible to stabilize the potential slide, near Zharai area. However, careful monitoring and supervision is required which involving precise measurement of the position of fixed points on the surface and regular checking of displacements in horizontal and vertical directions. These measurements must be recorded verses time and systematically analyzed (Kobold 1968). The volume of the moving rock material is calculated on the basis of these measurements. Any acceleration of the displacement must be interpreted as a possible warning of rupture inside the mass. Differences in the velocity profiles indicate discontinuous creep of mass and possible formation of a rock slide (Jaeger 1968, Muller 1946).

ANCIENT LANDSLIDES

Landsliding in Sor Range-Zharai area has been commonly occurring during the past and the process is still going on. At least 4 ancient landslides of fairly large sizes, mapable on a scale of 1:50,000, have been shown (Fig.1, 10). Two of them near Nal Khaizai, east of the Habibullah Mines (Fig 1, 6) are apparently dormant but under the prevailing conditions they may be reactivated at any favorable moment. Considerable amount of movements along the landslides north of Zharai area have occurred. The presence of gaping fissures, described in the previous section, indicates that these landslides are still active. Furthermore, many other small scale landslides (Fig. 7,8) may be found on slopes of the Ghazij Formation. A landslide (Fig. 7) occurred quite recently (January, 1991) and blocked mouth of the mine. Fortunately, at that time there was no labour inside, otherwise it would have caused a number of casualties. Another landslide occurred in December 1991 near Mehdadzai village in Obeshtakai Nala (Fig. 9) and blocked a road used for mining purpose. Fortunately, a home located within 100m distance of the slide was not affected.

Studies world over have shown that most landslides in any particular year have occurred in areas of previous landsliding (Nilsen et al. 1976, 1979, Frane 1974). It has been shown that 55% of recorded landslides in 1968-69 and 69% of those in 1972-73 took place within 600 m distance of the ancient landslides. Commonly the new landslides consist simply of renewed movements along the old landslides as a result of natural causes such as earthquakes, unusually intense rainfalls and/or modification of slopes by the activities of man (Morton 1971). Therefore, distribution of ancient landslides is a key to predicting future landslide activity of both natural and man-modified slopes.

Apart from the ancient landslides that exist in the Sor Range-Zharai area, there are many large erratically oriented limestone fragments/blocks of the Kirther Formation on slopes of the Ghazij Formation (Fig. 10) which have been transported downslope. A 600m long and 100m wide limestone block (Kanrai) of the Kirther Formation lies near Spin Karez (Fig. 1) which has been transported at least 1-2 km from its original position. The presence of this block can not be explained by tectonic relationship with the surrounding lower Ghazij Formation and thus, in view of the presence of ancient landslides, its presence near Spin Karez may only be justified by sliding.

CAUSES OF LANDSLIDES

Several factors contribute to the generation of landslides, most of which are interrelated. These have been exhaustively described by Nilsen et al. (1976, 1979; Table 4) among which the most important are the inherent geological characters, location of pre-existing faults and fractures, precipitation, slope, geometry of slope and its relationship to the bedding planes, presence of ancient landslides, seismicity (Early and Skempton 1972, Prior and Stephens 1972, Briggs 1974).

In Sor Range-Zharai area the highly incompetent nature of the Ghazij Formation, tectonic structure of the area, high angle slopes and scant vegetation provides the base for instability of slopes. It has been observed (Nilson et al. 1976) that 74% of the landslides in 1968-69 and 80% in 1972-73 in San Francisco Bay region of USA took place on slopes steeper than 15% (8.5 degree), whereas slope in Sor Range area reaches up to 30%. Rain fall is a major factor causing continued movement as it saturates the ground, thereby, adding weight, decreasing friction and raising the internal pore pressure (Prior and Stephens 1972). In Sor Range and surrounding region the average annual rainfall and snowfall is over 26mm, most of which is received between December and March (Imperial Gazetteer of India, Provincial Series, Balochistan 1984). Studies on the relationship of rainfall to erosional and run-off conditions and to the reactivation and/or occurrence of the landslides have not been carried out in Sor Range-Zharai area. However, it seems that claystone/siltstone succession of the Ghazij Formation are highly susceptible to erosion as they quickly absorb and become saturated with water.

The presence of several ancient landslides of fairly large sizes and several small ones is another factor which indicates that landslides may be reactivated and/or downslope movements may continue intermittently over a long period of time. The presence of gaping fissures indicates that the slopes are unstable and the process of sliding may continue. Seismicity along numerous active faults in the nearby area is a common phenomenon (Quittmeyer et al. 1979) which contributs to the landsliding (Youd and Hoose 1978). Tremors of sufficient intensity, if coincide with conditions of high pore-water pressure and loss of intergranular contact, could result in initiation of downslope movements (Minard 1974). Soviet authors (Solonenko 1972) believe that extremely large landslides are generally triggered by earthquakes and designate these phenomena as seismo-gravitational.

Other contributing factors, specially with reference to the Sor Range-Zharai area, are:

1) Human activities like mining, cutting and removal of material from the slopes, construction, deforestation and pumping out of mine water which may have caused lowering of pore-water pressure

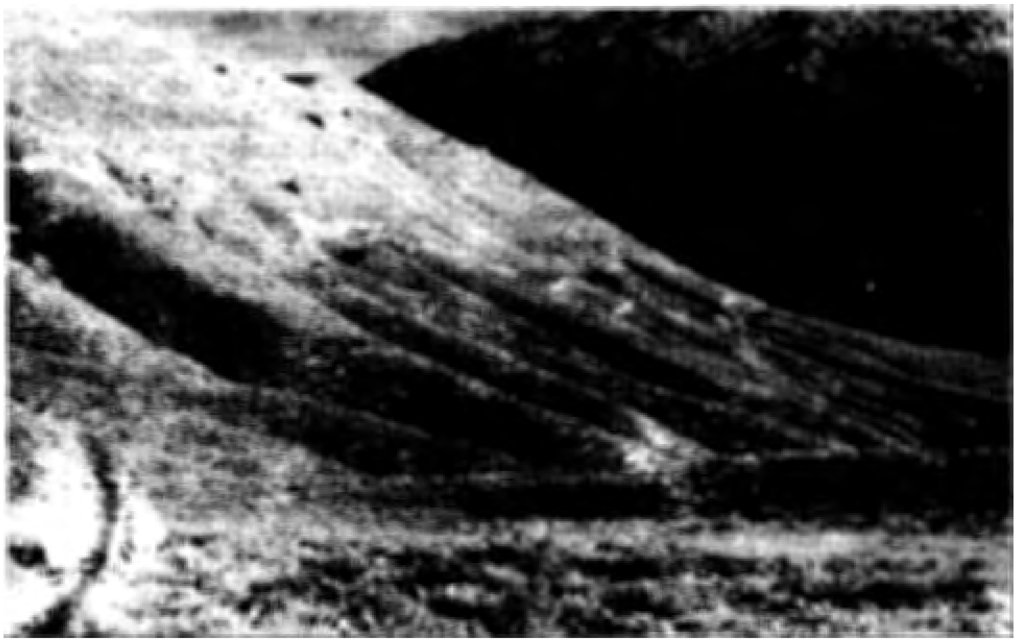

Figure 3. Photograph showing outline of fissures NW of Zharai area along which sliding has taken place during the past. Note the coal mining activity and residences nearby.

Figure 4. Photograph of the gapping fissure north of the Zharia China area.

Figure 5. Photograph showing disrupted, vegetation across the fissures north of Zharai area.

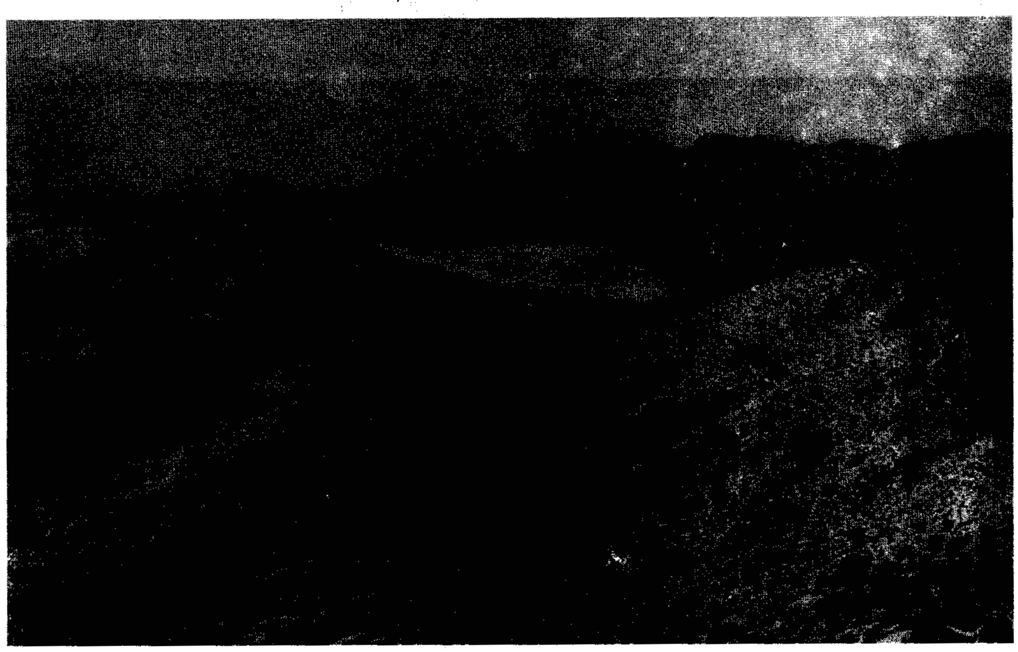

Figure 6. Photograph of ancient landslide near Nal Khezai east of Habibullah Mines. Steep scarps to the right side of the Photograph is the Habib Rahi Limestone member of the Kirther Formation (Eocene). Flat lying recent deposits cause by ponding of water behind slumped blocks.

Figure 7. Photograph showing the landslide which have blocked the mouth of a mine, the incident occurred on January 1991.

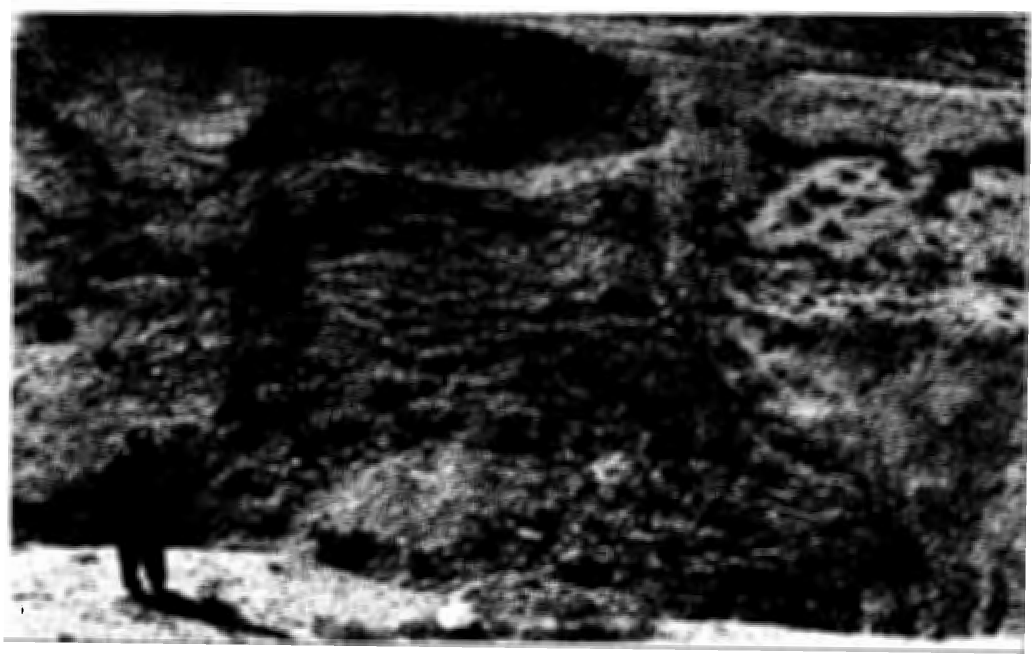

Figure 8. Small scaled rockslide within the Ghazij Formation near Spin Karez. Man in the bottom left of the photograph demonstrates the scale.

and thus may have contributed to the subsidence of overlying strata and/or initiation of cracks and fissures. Human activities include steepening of slope, adding and pumping out of water and placing of extra loads on slopes which altogether increase the possibility of landsliding.

2) Lack and/or scarcity of vegetation on slopes which protects the ground from erosion and bind the soil to the bed rock, thereby diminishing the likelihood of landsliding (Rice and Foggin 1971; Frane 1974). In Sor Range-Zharai area vegetation is scant, slope surface of the Ghazij Formation has virtually no protection at all against the erosion, therefore erosion rate must be very high. During rainy season the stream drawing surface run-off from the Ghazij Formation is highly turbid with high amount of mud content.

3) Creep of soil and rock causing slow, day to day, downslope movement of slope forming material under the influence of gravity.

4) Unusual chemical weathering and degradation of shale.

TYPES OF LANDSLIDES

Landslides are of many types, varying greatly in size, shape, geometry, rate of movement and the type of material involved. The general shape and appearance of landslides (Fig 11. after Eckel 1958), nomenclature used and types are given by Varnes (1968). Different types of landslidings move dwonslope with wide range of speeds (Eckel 1958) among which the rapidly moving landslides (rock fall and earth flows) may pose a great threat to life and property, whilst, the slower moving landslides (slumps and debris slides) gradually cause increasing amount of damage, but the expected movements can be anticipated.

Landslides occurring in the Sor Range-Zharai area are mostly slides and slumps of Varnes (1968). Slides result from shear failure along one or several surfaces. The slided material may be broken up and deformed or fairly cohesive or intact. A cohesive landslide is called a slump. Both slides and slumps are found in the Sor Range-Zharai area. It has been observed that slides in Sor Range-Zharai area are often small scale features (Fig. 8) and found on the slope of the Ghazij Formation. Whereas large scale features found near the Nal Khaizai (Fig. 6) and north of Zharai (Fig. 1), involving both the Kirther and Ghazij formations, are slumps. The speed of movement in slumps and slides may range from very slow to extremely rapid (1ft/5 years to 10ft/second, Eckel 1958), therefore, these could cause great damage. Slumps are more common which have caused movements along concave upwards and spoon shaped slip faces. Steep scarps and flanking walls are commonly formed and water is ponded behind slumped blocks (Fig. 6) which further promote the sliding, thus the surrounding area become prone to slope failure once the first slump has occurred.

DISCUSSION AND PROPOSALS

The gaping fissures north of the Zharai area, occurrence of the ancient landslides, high angle of slop (up to 30%) within the Ghazij Formation and the presence of thick (158-210 m) limestone of the Kirther Formation, forming nearly vertical cliffs, over a thick incompetent argillaceous succession of the Ghazij Formation, which are highly susceptible to erosion and weathering are the main characteristics of the Sor Range-Zharai area. Based on comparison of these characters with those of the slope-stability categories of Nilsen et al. (1979), we suggest that the Sor Range-Zharai area falls within category 5 of Nilsen et al. (1979) i.e. highly susceptible to landsliding having "high risk" to life and property. Slope stability categories for land-use planning suggest that in areas of "high risk" urban development is usually inappropriate. During a landslide in Mantaro River valley in Peru (Kojan et al. 1972) the slide movement reached a velocity of 120-140 km/hour because of the height difference of about 1500m and accomplished within 3-4 minutes. The disastrous slide destroyed several villages and 450 people lost their lives. In view of these, it would be most reasonable to prepare a detailed slope stability map of the area and to carry out research on causes of landslides and to monitor movements along fissures near Zhari China. Research on contributing factors, specially the effects and correlation to rainfalls, seismicity and storms etc. should be carried out. Studies have shown that a simplified system of landslide prediction is possible (Nilsen and Turner 1975). By plotting a cumulative graph of precipitation, one could estimate when the ground would be saturated (after 250-380mm) after the precipitation. Also of particular interest would be the behavior of argillaceous sequences and clay minerals of the Ghazij Formation with the moisture and surface run-off.

The existence of ancient landslides in the area indicates that landsliding will continue in future, therefore, development on or near the landslides must be subject to careful site investigation.

Accurate mapping of ancient landslides, slope conditions and bedrock geology should prove to be a valuable aid in determining slope stability on regional basis. Photo interpretative mapping of landslides has widely been used (Watson 1971,

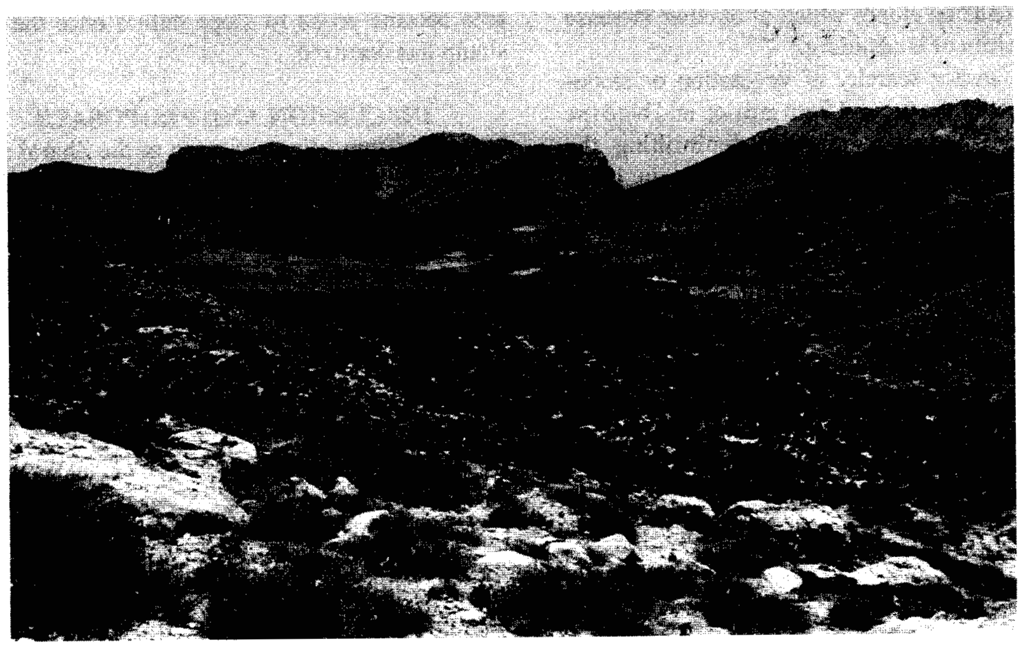

Figure 9. Another view of the ancient landslide near Nal Khezai east of Habibullah Mines.

Figure 10. Photograph of the huge erratic block of the Kirther Formation near Spin Karez (center) which has been transported by sliding.

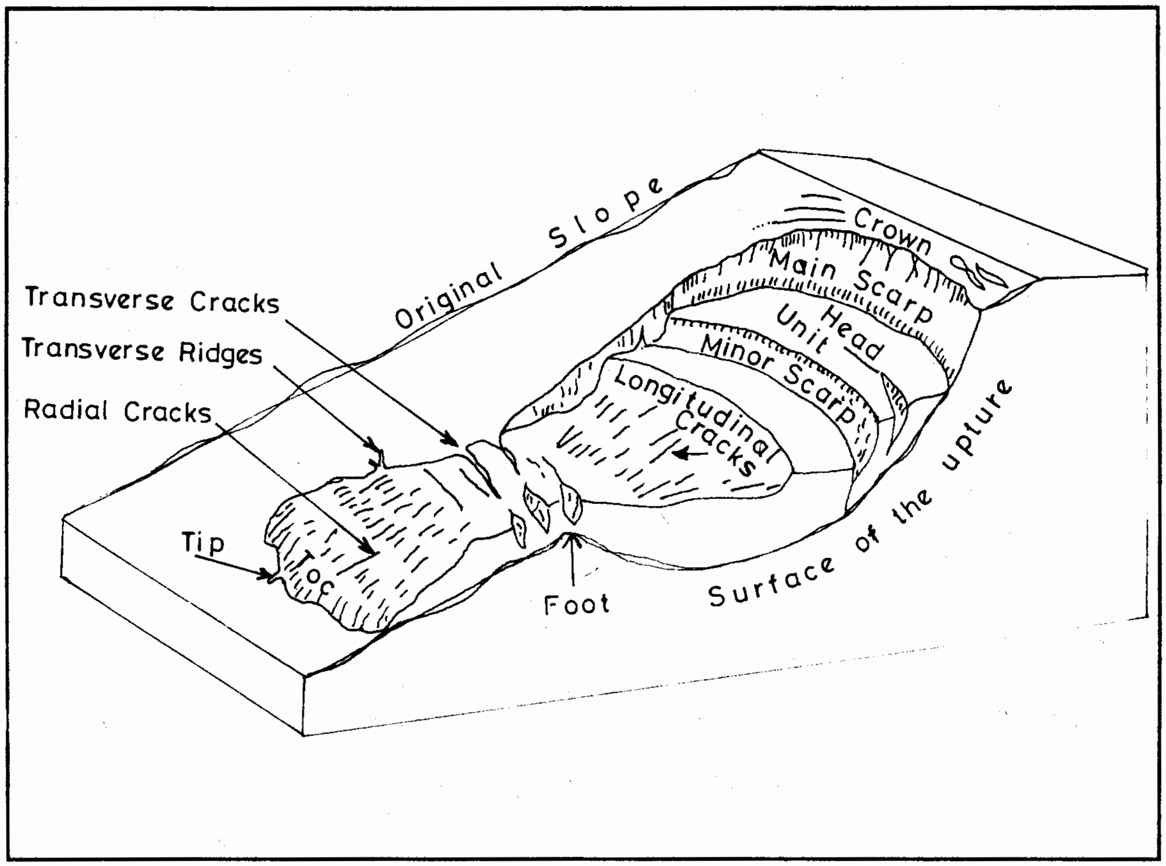

Figure 11. Shape and appearance of landslides (after Eckel 1958).

Kojan et al. 1972) and is particularly useful for regional reconnaissance studies and permits rapid determination of the relative distribution of current landsliding and ancient landslide deposits. Black and white aerial photographs at scales of 1:20,000 to 1:30,000 are generally suitable for most regional mapping purposes (Nilsen et al. 1979).

Landslide deposits are characterized by small isolated ponds, lakes and closed depressions, natural springs, abrupt and irregular changes in slope and drainage patterns, steep curved escarpments at the upper edge of the deposit, disturbed vegetation and flat areas within slopes that might appear suitable for construction.

The effects of deforestation and/or behavior of vegetation with the process of erosion and weathering are also of special interest. Earthquakes play a major role in the initiation and triggering of landslides and occur commonly in the affected area. It will be highly interesting to study the effects of earthquakes on landslides, especially on the fissures in Zhari area. Maldenado et al. (1992) have shown relationship of the landslide of north of Zhari area to the disastrous Quetta Earthquake of 1935- although they have misinterpreted these particular landslides as a series of normal faults and graben structures. Little is known about the effects of seismic waves passing through the landslide deposits and marginally stable slopes, thus, scientists are unable to predict about the landslides and their specific effects.

Many landslides have resulted from the modification of natural slopes by man, commonly in areas that might at first appear to be stable (Nilsen et al. 1976). In Sor Range-Zharai area the excavation of coal seams, thicknesses of which vary from 0.5 to 2m, is in progress. Over 5 million tons of coal have already been mined out (Mohsin et al. 1991). This must have caused subsidence of the overlying mass of the upper Ghazij Formation and the Kirther Formation. Furthermore, cutting of slopes for the construction of roads, buildings and loading of slopes may also have minor contribution.

Some of the mine owners use explosives for mining purpose, for cutting coal and associated rocks. The Habibullah Mines Limited has launched two 500 m long inclines north of Zharai, just near the fissures, across the bedding of the Kirther Formation, in order to reach the underlying coal seams in the middle part of the Ghazij Formation. They have cut across nearly 200 m thick limestone of the Kirther Formation and another 300m of the

Ghazij Formation using explosives. Repeated explosions must have caused vibrations and shaking of the surrounding rocks. Gaping fissures, along with the other contributing factors, may have been caused by a large number of repeated underground explosions.

Geological hazards are not private matters, but concern the public in general. It is, therefore, the responsibility of the government to protect the public interest. Landslides are local phenomena, consequently local agencies on district-level and mine owners have the key responsibility for reducing risk from landslide hazards. Consideration of slop-stability and land-use planing requires proper precautions and the role of various professionals involved. Local agencies and mine owners along with geologists and engineers have the greatest responsibility for ensuring that slope-stability analysis is carried out prior to the land-use planning. Nilsen et al. (1979) have offered basic guidelines, some of them are relevant to the problem of slope-stability of the Sor Range-Zharai area, which are given as under:

1. Slope-stability hazards must be identified and communicated to all those who might be interested in or potentially affected by them.
2. Special attention must be paid to landslide hazards when preparing comprehensive landuse policy, plans and implementation strategies.
3. When potential slope stability hazards have been identified in developing areas, make and implement appropriate plans for mitigating the hazards. In this connection the first step would be proper and systematic monitoring of the fissures. This proposal may specifically be applied to the fissures that exist north of the Zharai. Necessary precautionary measures for example, relocation of the residents in the risk areas, avoidance of removal of material from the toes of the slopes, stability of slopes, removal of the structure from the highest risk area, prevention of excessive water infiltration in the fissures and disaster preparedness plan, particularly in the seismically active areas, should be taken. Root areas of slides should be studied in detail. A broad zone penetrated by cracks inclined to the slope is indicative of deep reaching slide.
4. Evaluate potential slope-stability hazards by using maps of appropriate scale and detail before any contemplated development or structure reaches the site selection or design stage.
5. See that all proposals for development on slopes of questionable stability are thoroughly reviewed by competent professionals.
6. Adequate regular inspection of human activities on slope areas are required to ensure safety.

CONCLUSIONS

1. The existing geological and other conditions in Sor Range -Zharai area are such that slopes are unstable and highly susceptible to landsliding and the risk to life and property of the residents on these slopes is high.
2. The area, specially the ominous fissures north of Zharai area, require proper and systematic monitoring and study to understand slope-stability and causes and factors relevant to the landsliding in the area.
3. Proper safety measures are required and cautions/guidelines, adopted elsewhere in the developed countries, need to be imposed in the area in order to mitigate risk to life and property of the residents.

REFERENCES

Briggs, R.P., 1974. Map of the overdip slopes that can effect landsliding in Allegheny Country, Pennsylvania: U.S. Geol. Surv. Misc. Field Studies Map, MF-543, Scale 1:125,000.

Early, K.E. and Skempton, A.W., 1972. Investigations of the landslide at Wlaton's Wood, Stafordshire: Quart. Jor. Eng. Geology, 5, p. 19-41.

Eckel, E.B., ed. 1958. Landslides and engineering practice: Washington D.C. Highway Reasearch Board Spec.Rept.29 NAS-NRC 554, 232p.

Frane, P.A., 1974. Landslides in the M.Sizer area, Santa Clara, County, Clifornia: Califorinia State Univ., San Jose, M. S. Thesis, 67p.

Hunting Survey Corporation, 1960. Reconnaissance Geology of part of West Pakistan: Toronto, Canada, 550p.

Imperial Gazetter of India, Provicial Series, Balochistan, 1984: New Quetta Book Stall, Jinnah Road, Quetta.

Iqbal, M.W.A., 1969, Maga-Fauna from the Ghazij Formation (Lower Eocene) in Quetta-Sharigh area, West Pakistan: Mem. Geol. Surv. Pakistan, Palaeontologica Pakistanica, Vol. 5.

Jaeger, C., 1968, Discontineous creep of masses: Water Power, 20, p. 197-8.

Kakar, D.M. and Kassi, A.M., 1997. Lithostratigaghy, sedimentology and petrology of the Ghzij Formation, Sor Range Quetta District, Pakistan: Acta Mineralogica Pakistanica, 8, p. 73-85.

Kassi, A.M., Qureshi, A.R. and Kaker, D.M., 1987. Sedimentology of the Ghazij Formation, Kach area, Balochistan: Geol. Bull. Univ. Peshawar, 20, p. 53-62.

Kobold, F., 1968. Methodes geodesiques pour la determination des movements de roches ou de terrains dans les zones de glissmment. L Entrepise, Zurich, 67, p. 1007-160.

Kojan, E., Foggin, G.T. III, and Rice, R.M., 1972. Prediction and analysis of debris slide incidence by photogrammetry, Santa Vnez-San Rafael Mountain, California: Internt. Geol. Cong., 24th, Proc. Sec. 13, p. 124-131.

Maldonado, F., Mengal, J.M. and Khan, S.H., 1992. Fault scarps related to the 1935 Quetta Earthquake, Quetta, Balochistan vince, West-Central Pakistan: Abstract: Geophysical Union.

Minard, J.P., 1974. Slump blocks in the Atlantic Highlands of new Jersey; U.S. Geol. Sur. Prof.. Paper 898,24p.

Mohsin, A.K., Asif, N.R., Memon, A.R., Saleem, M. and Khan, A.L., 1991. Coal resources of Sor Range Block, Sor Range-Degari Coal Field, Balochistan, Pakistan: Inf. Release No. 463, Coal Resources, Geol. Surv. Pakistan.

Morton, D.M., 1971. Seismically triggered landslides in the area above the San Fernando Valley: U.S. Geol. Surv. Prof. Paper 733, p. 99-104.

Muller, L., 1946. The rock slide in the Vajont Valley; Rock Mechenics and Eng. Geol., 2, p. 148-212.

Nilsen, T.H., Taylor, F.A. and Dean, R.M., 1976. Natural conditions that control landsliding in the San Fransisco Bay Region - An analysis based on data from the 1968-69 and 1972-73 rainy seasons: U.S. Geol. Surv. Bull. 1424, 35p.

Nilsen, T.H. and Turner, B.L., 1975. The influence of rainfall and ancient landslide deposition on recent landslides (1952-1971) in urban areas of Contra Costa Country, California: U.S. Geol. Surv. Bull. 1388.

Nilsen, T.H., Wright, R.H., Volasic, T.C., Spangle, W.E., Spangle, W. and Associates, 1979. Relative slope stability and land-use planning in the San-Francisco Bay Region, California: U.S. Geol. Surv. Professional Paper 944.

Prior, D.B., and Stephens, N., 1972. Some movement patterns of temprate mudflows- Examples from northeastern Ireland: Geol. Soc. America Bull., 83, p. 2533-544.

Quittmeyer R.C., Farah, A. and Jacob, K.H., 1979. The seismicity in Pakistan and its relation to surface faults **In** Farah, A. and Dejong, K.A., (eds.), Geodynamics of Pakistan: Geol. Surv. Pakistan, Quetta.

Rice R.M. and Foggin, G.T., 1971. Effects of high intensity storms in soil slippage on mountanous watershed in southern California: Water Res. Research, 7, p. 1485-1496.

Shah, S.M.1 (Ed.), 1977. Stratigraphy of Pakistan: Mem 12. Geol. Surv. Pakistan.

Solonenko, V.P., 1972. Siesmogenic distruction of mountain slopes: 24th Inter. Geol. Congress, Montereal, Section 13 Eng. Geol., p. 117-147.

Varnes, L.J., 1958. Landslide types and processes, in Eckel, E.B. (ed.) Landslides and engineering practice: Washington, D.C. Highway Research Board, Spec. Rept. 29, Nas-NRC 644, p. 20-47.

Watson, Fan 1971. A preliminary report on new photogeological studies to detect unstable natural slopes: Quart. Jour. Eng. Geology, 4, p. 133-137.

Youd, T.L. and Hoose, S.L., 1978. Historic ground failures in north California associated with earthquakes: U.S. Geol. Surv. Prof. Paper 993.

Manuscript Received 8th October 1998
Revised Manuscript Received 3rd March 1999
Accepted 1st September 1999

ACTA
MINERALOGICA
PAKISTANICA
Volume 9 (1998)

Article Reference
AMP9.1998/021 -026/ISSN0.257-3660

HYDROTHERMAL ALTERATION OF VARIOUS ROCK SUITES FROM SINJRANI VOLCANIC GROUP OF CHAGAI BALOCHISTAN

GHULAM NABI[1], MUHAMMAD AYUB[1] AND MEHRAB KHAN[2]
[1] Department of Geology, University of Balochistan, Quetta. Pakistan
[2] Centre of Excellence in Mineralogy, University of Balochistan, Quetta, Pakistan

ABSTRACT
The rock samples collected from the Sanjrani Volcanic Group at Mashkai Chah (Chagai district), were examined in thin sections. This short paper reports the results of petrographic observations and the alteration process of minerals present various siuts of rocks. Two types of minerals observed during the study. The primary mineral are original component of the rocks, whereas the secondary minerals are the altered products of primary minerals.

INTRODUCTION

Out crops of Sanjrani Volcanic rocks occur in the western part of Balochistan in the Chagai district (Fig. 1). The volcanism here occurred in double volcanic chains, the Raskoh Arc and Chagai Arc (Siddiqui 1996). The Raskoh Arc is called as frontal arc, whereas Chagai Arc is considered as the rear main arc (Siddiqui 1996). The Sanjrani volcanic rocks, belong to Chagai Volcanic Arc.

In regional tectonic context Chagai Volcanic Arc belongs to Zagros -Chitral convergence zone (Powel 1979, Sengor et al 1988). This convergence was initiated during Late Cretaceous due to intra oceanic convergence in the Neotethys (Siddiqui 1996). The Chaghi Volcanic Arc is about 500km long and 150km wide. It also extends towards west in Iran and towards north in Afghanistan. This arc is convex towards south (Farah et al 1984 , Siddiqui 1996) and is terminated by the Chaman Noshki Transform Fault in the east.

In the Chagai Volcanic Arc several episodes of volcanism occurred during Late Cretaceous to Pleistocene. The Late Cretaceous volcanic activity was most widespread during which large amount of volcanic rocks were formed in the area. These rocks are designated as Sanjarani Volcanic Group.

Many foreign geologists visited the Chaghai Arc including Nigel (1975), Sillitoe (1978) and Arthuran et al (1982). They interpreted the Chagai Arc as Andean type calc alkaline magmatic belt, constructed on the southern leading edge of the Afghan micro-plate. Sanjrani Volcanic Group is the oldest rock unit of the Chagai Arc (Sillitoe and Khan 1977) and is composed of sub-marine stratified intercalation of volcanic lava flows and pyroclastics including agglomerate, volcanic breccia, volcanic conglomerate and tuff. The initial petrological and petrochemical studies show that they belong to tholeiitic Island Arc Series (Siddiqui et al 1986, Siddiqui 1996).

RESULTS OF MICROSCOPIC STUDY

The samples selected for the microscopic study were collected from five different units of volcanic rocks belonging to Sanjrani Volcanic Group. The delected samples were fresh and show no sign of weathering They range from rhyolite to andesite through rhyodacite, latite and dacite mostly exposed

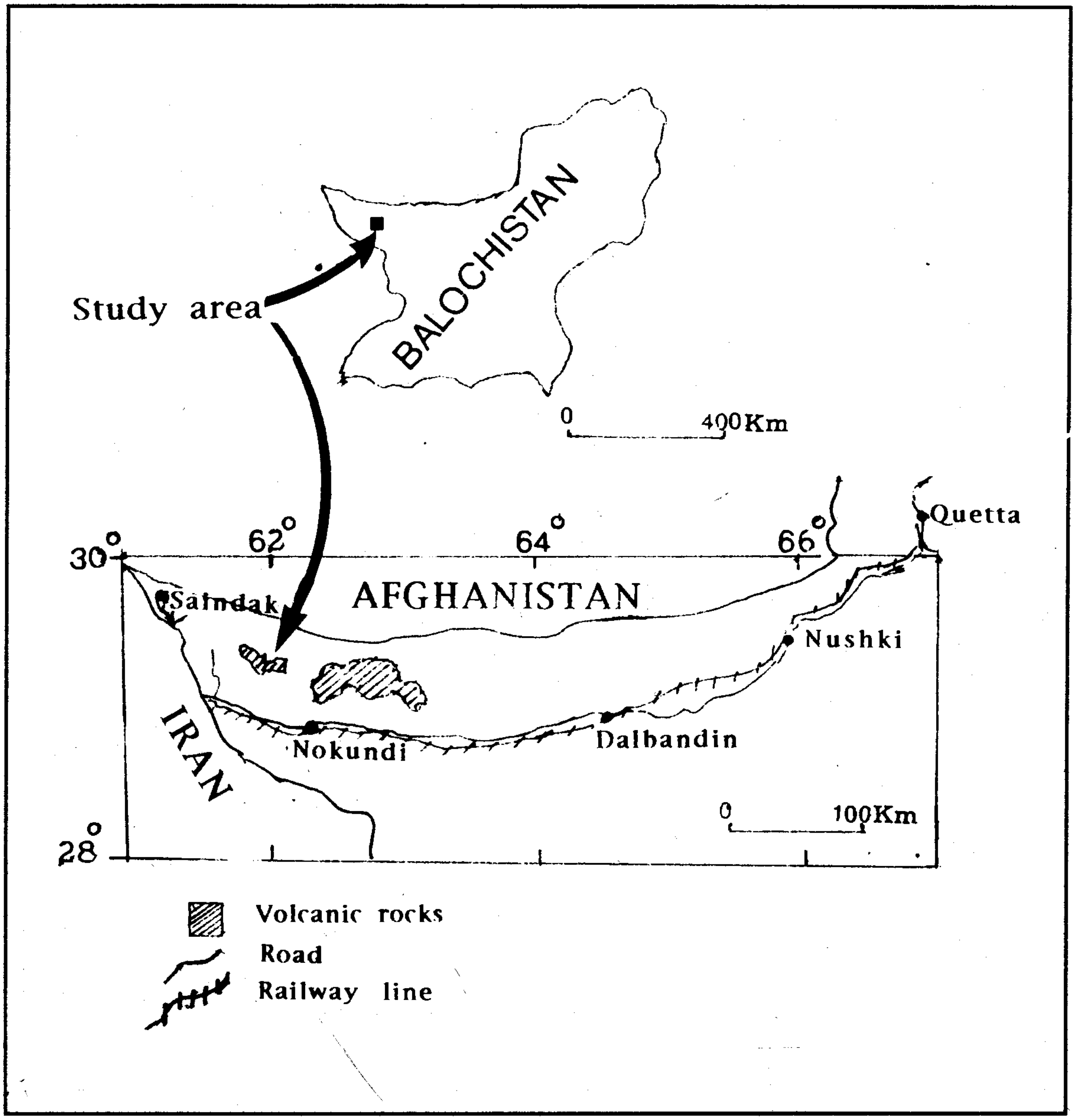

Figure 1. Location map of the study area

around Mashkai chah area (Nabi et al. 1997).

The observed mineral species of these rocks are classified into two categories, primary and secondary (Table 1). Primary minerals are the original rock-constituents, whereas the secondary minerals are altered primary minerals.

The phenocrysts of primary minerals are composed of k-feldspar, plagioclase, quartz, hornblende, pyroxene and some opaque minerals. Plagioclase and k-feldspar are mostly dominant, quartz is sub-ordinate to plagioclase and k-feldspar in amount. Hornblende pyroxene and opaque minerals are very small in quantity. Groundmass is highly altered. Most of primary minerals of groundmass, such as Plagioclase, k-feldspar and volcanic glass are replaced by secondary minerals. The alteration progressed mainly along the cracks and cavities developed in groundmass area.

The plagioclase and K-feldspar phenocrysts are replaced partly by fine grained quartz, sericite, kaolinite, and small amount of epidote. At places euhedral grains of epidote are crowded in the center of plagioclase (Plate.1). The mafic constituents (hornblende and pyroxene) have completely been altered to chlorite, uralite and epidote, and occur as pseudomorphs of the original hornblende (Plate.2). Pyroxene is altered to uralite.

The process of alteration of opaque minerals with oxidization is as fellows:-

The ilmenite reacted with free oxygen

producing magnetite, anatase and small amount of maghemite, then maghemite reacted with water to form goethite. The oxygen available for this chemical reaction and oxidization phenomenon is from the alteration of major constituent minerals. The four sequences of alteration process of opaque minerals are given in Box 1.

CHEMICAL ANALYSES

One sample of rhyolite, five samples of andesite and three samples of dacite were analysed for major element analysis (Table 2). In SiO_2 versus major elements plots (Fig. 2) a correlation of alkalies and Al_2O_3 with SiO_2, is noticeable which has been interpreted as the result of sub-marine alteration.

Box 1. Alteration processes of opaque minerals in the rocks of Sinjarani Volcanic Group

$6(Na_{0.70}K_{0.30})AlSi_3O_8$(Plagioclase)$+2H_2O=2KAl_3Si_3O_{10}(OH)_2$(Sericite)$+12SiO_2$(quartz)$+O_2+4Na^++4e^-$	(I)
$3FeTiO_3$(Ilmenite)$+O_2=Fe_3O_4$(Magnetite)$+3TiO_2$(Anatase)	(II)
$4Fe_3O_4$(Magnetite)$+O_2=6Fe_2O_3$(Maghematite)	(III)
Fe_2O_3(Magmatite)$+H_2O=2FeOOH$(Goethite)	(IV)

Table 1. Modal analysis of primary minerals and alteration minerals. A; abundant, M; moderate, R; rare, N; nil.

	Primary Minerals						Secondary Minerals				
Rock Type	Quartz	k-feldspar	Plagioclase	Hornblende	Pyroxene	Biotite	Kaolinite	Epidote	Sericite	Chlorite	Fe- Oxide
Rhyolite	A	A	A	M	N	R	M	N	R	N	M
Rhyodacite	A	M	A	M	N	R	M	N	M	R	M
Latite	M	R	A	M	N	R	M	N	M	R	M
Dacite	M	R	A	M	N	R	R	N	R	R	M
Hornblende Andesite	M	R	A	M	N	R	N	R	N	M	M
Pyroxene Andesite	M	N	A	R	M	R	N	R	R	R	M

Table 2. Average whole rock chemistry (major oxides) of Sinjrani volcanic rocks

Rock Types	*Rhyolite*	*Andesite*					*Dacite*		
Sample No.	*Rhy*	*An-1*	*An-2*	*An-3*	*An-4*	*An-5*	*Da-1*	*Da-2*	*Da-3*
Major Oxides									
SiO_2	72.08	51.86	59.50	61.80	59.00	61.47	67.81	67.05	64.33
TiO_2	0.37	1.50	0.84	1.00	1.15	0.76	0.98	0.49	0.40
Al_2O_3	13.86	16.40	16.55	17.00	14.70	16.00	12.30	15.90	17.11
Fe_2O_3	0.86	2.73	8.05	6.70	7.14	7.33	6.47	3.79	4.43
FeO	1.67	6.97	2.18	2.50	2.10	2.28	2.81	2.50	1.55
MnO	0.06	0.18	0.16	0.10	0.14	0.13	0.09	0.09	0.10
MgO	0.53	6.12	3.33	2.50	3.11	2.90	2.07	0.61	2.59
CaO	1.33	8.40	5.42	4.90	8.14	5.04	5.93	4.44	5.30
Na_2O	3.08	3.36	3.97	4.30	2.95	3.64	2.67	5.74	4.24
K_2O	5.05	1.33	2.01	2.90	1.06	2.54	0.86	1.79	1.09
P_2O_3	0.18	0.35	0.39	0.49	0.43	0.18	0.30	0.20	0.14
H_2O	0.53	0.80	0.50	-	-	-	-	-	-

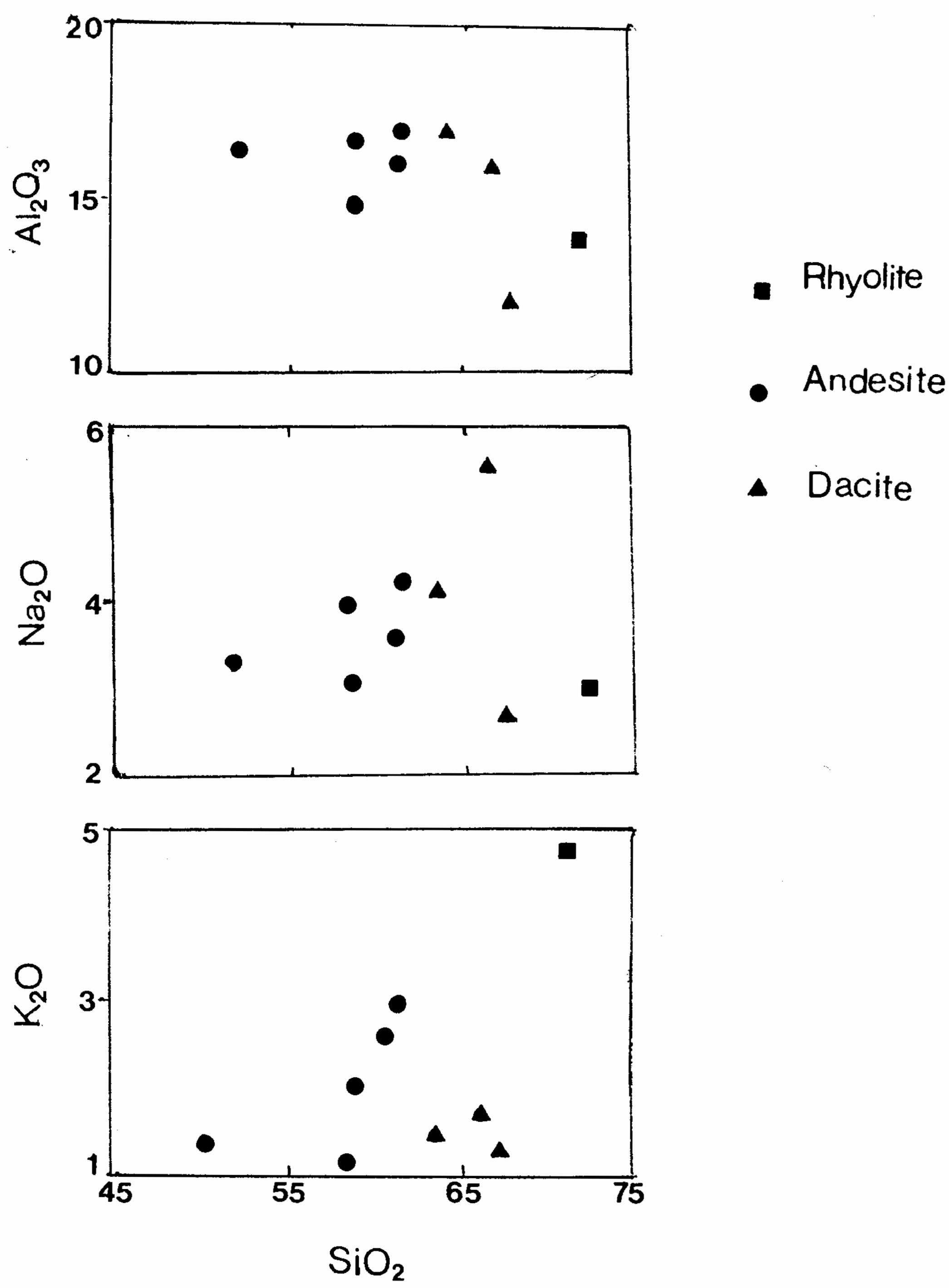

Figure 2. SiO_2 versus major element oxides plots for various Sinjrani volcanic rocks.

CONCLUSIONS

The rock of Sanjarani Volcanic Group show indiscriminate alteration by hydrothermal solution. Microscopically the prophylitic alteration is characterized by the presence of minerals such as kaolinite, sericite, epidote, chlorite and uralite. K-feldspar appear cloudy due to alteration to kaolinite. Sericite was formed along the fractures in plagioclase. The mafic constituents were altered to chlorite, epidote and uralite. The alteration of opaque minerals progressed in four steps: 1) ilmenite, 2) magnetite, 3) maghemite and finally 4) goethite. Finally it is concluded that these rocks have undergone such alteration processes as thermal activity, hydrate effects and oxidization, suggesting hydrothermal alteration.

REFERENCES

Arthurton, R. S., Farah, A. and Ahmed, W., 1982. The Late Cretaceous-Cenozoic History of Western Balochistan Pakistan, the northern margin of the Makran subduction complex, **In**: Leggett, J. K., ed., Trench Fore-arc Geology: Geol. Soc. London, Spec. Pub., V. 10, p. 343-385.M

Nabi, G., Siddiqui, S.A, and Baloch, M. A. 1997. Petrographic study of the rocks around Mashkay Chah Chagai District Balochistan. Acta Mineralogica Pakistanica. V. 8, p. 96-105.

Nigell, R. H., 1975, Reconnaissance of the Geology and ore mineralization in part of the Chagai District Balochistan, Pakistan: Project Report PK-27, U. S. Geol. Surv., 550p.

Powell, C. M., 1979. A speculative tectonic history of Pakistan and surrounding: Some constraints from the Indian Ocean. **In**: Frah, A. and Dejong K.A eds. Geodynamic of Pakistan: Geol. Surv. of Pakistan, p. 5-24.

Sengor, A. M. C., Altinar, D., Cin, A., Ustammer, T. and Hsu, K, J., 1988. Origin and assembly of Tethyside orogenic collage at the expense of Gondwanaland. **In**: Charles, M. G. A and Hallan, A., eds., Gondwana and Tethys: Geol. Soc. Spec, Pup 37, Oxford Univ. Press. p. 119-181.

Siddiqui, R. H. and Khan, W. 1986. A comparison of hydrothermal alteration in porphyry copper mineralization in Chagai calc- alkaline magmatic belt, Balochistan Pakistan: Acta Mineralogica Pakistanica, V. 2, p. 100-106.

Siddiqui, R. H., 1996. Magmatic Evolution of Chagai-Raskoh Arc Terrane and its implication for porphyry copper mineralization. Geolocica, Geosci. Lab., G.S.P. Islamabad. V. 2, No. 1, p. 87-120.

Sillitoe. R. H., 1978. Metallogenic evolution of a collision mountain belt in Pakistan: a preliminary analysis. Jour. Geol.Soc. London, V. 125, p. 377-387.

Sillitoe, R. H and Khan, S. N. 1977. Geology of Saindak porphyry copper deposit Pakistan Inst. Min. Metall Sec. B, v.86

Manuscript Received 8th October 1998
Revised Manuscript Received 25th December 1998
Accepted 1st September 1999

Plate 1. Euhederal grains of epidote crowded in the centre of plagioclase

Plate 2. Pseudomorph of epidote after the original hornblende

ACTA
MINERALOGICA
PAKISTANICA
Volume 9 (1998)

Article Reference
AMP9.1998/027-036/ISSN.0257-3660

GENETICALLY TWO DIFFERENT TYPES OF BASALTIC ROCKS FROM BELA OPHIOLITE BALOCHISTAN, PAKISTAN

MEHRAB KHAN[1], EDWIN GNOS[2], A. SALAM KHAN[1] AND KHALID MAHMOOD[1]
[1] Centre of Excellence in Mineralogy, University of Balochistan, Quetta Pakistan.
[2] Mineralogisch-Petrographisches Institute, Baltzerstrasse 1, 30312 Bern Switzerland.

ABSTRACT

Genetically two different types of basaltic rocks are distinguished in the Bela area. These are: i) the mid-oceanic-ridge related basalts ii) Microdioritic or gabbroic Fe-rich tholeiites and alkaline basalts related to hotspot.

The mid-oceanic ridge basalts (MORB) are aphanitic to fine grained, plagioclase and augite are the most common minerals with rare phenocrysts of olivine. These basalts show narrow SiO_2 range (46-49%), with FeO/MgO ratio (1.25-2.2) and the K_2O content is (0.05-0.13). These geochemical signatures are in a close resemblance with the mid-oceanic ridge basalts. Microdioritic or gabbroic, Fe-rich tholeiites and alkaline basaltic rocks with reunion hotspots (Deccan trap), chemistry, capping or intruding the MORB. The microgabbroic plutons and sills cover as much as 30% of the area and are related to some Fe-rich tholeiites or alkaline sub marine extrusive (amygdaloidal pillows, titan-aug·'e phyric tephrites and olivine-basalts). Some tholeiitic microgbbros contain enclaves from the red and dark sedimentary series along with mid- oceanic ridge basaltic rocks. The mineral and whole rock chemistry of the microgabbro and alkaline basalts give signatures of within plate alkali basalt. These alkaline volcanic rocks and microgabbroic Fe-rich tholeiites are believed to have been generated during the northward drift of Indo-Pakistani plate over the active Reunion hotspot. A hornblende concentrate from an alkaline rock yielded an $^{39}Ar/^{40}Ar$ plateau age of 70.9± 0.7 Ma. (Gnos et al. 1998).

INTRODUCTION

The "Bela ophiolite" is the largest piece of oceanic lithosphere in the western belt of Pakistan and forms a N-S oriented, 300 km long; 10-60 km wide, strip between Karachi and Khuzdar (Fig. 1). Magnetic data indicate that the northern part of the ophiolite is offset along sinistral fault and that the ophiolite continues south to the coast of the Arabian sea covered by alluvium, Zaigham (1991). The Bela oceanic lithosphere consists of two units of different age. True ophiolitic outcrops can be found north of Sunaro, and some relics farther south (Fig. 1). Nearly all the southern areas belong to a tectonically lower accretionary wedge unit (pillow lavas or sheet flows associated with pelagic sediments) of older material, Gnos et al; (1998). The volcanic sequence is well exposed between Uthal and Sunaro (Fig. 1). The volcanics are directly overlain by Red pelagic sediments (radiolarian cherts, red shales, and red to greyish calciturbidites). These are capped or intruded by doleritic to microdioritic or gabbroic Fe-rich tholeiites and alkaline rocks. On the basis of gravimetry, Zaigham and Malik (1992) estimated a total thickness of 1000m for the volcanic rocks of the Bela ophiolites. This paper presents petrographical and geochemical properties of different kinds of basaltic and intrusive rocks of the Bela ophiolite and discuss their genetic relationship.

MID-OCEANIC RIDGE BASALTS AND ASSOCIATED SEDIMENTS

The volcanic rocks occur as pillow lavas and

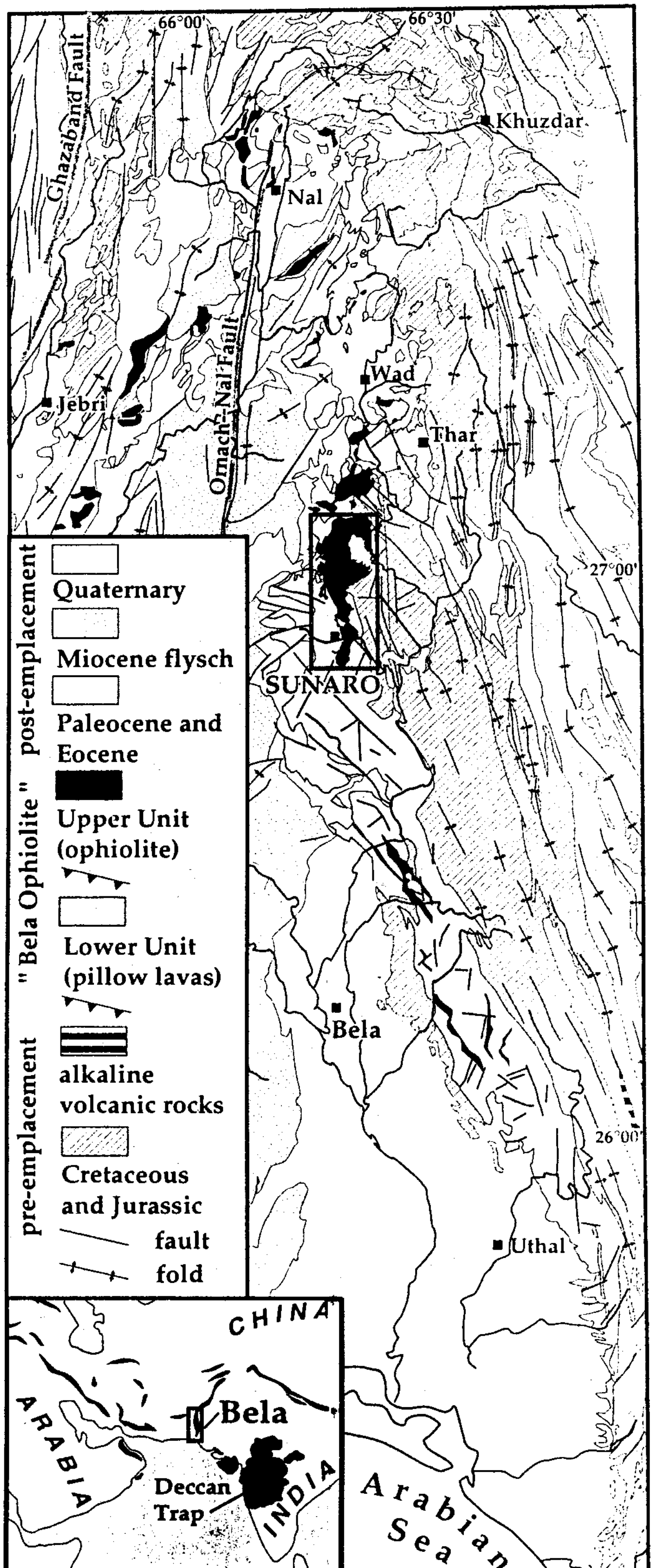

Figure 1. Overview map of the Bela oceanic lithosphere asemblage based on Hunting Survey Corporation (1960), Ahsan et al. (1988) and Gnos et al. (1998).

sheet flows that have enriched mid-oceanic ridge basalt (MORB) chemistry (Ahmed 1991; Sarwar 1992; Gnos et al. 1998; Khan 1999) covered by a Mn-enriched horizon, red pelagic sediments (radiolarian cherts, shales and calciturbidites). The pillow lavas at places interbedded with red pelagic sediments having a thickness of upto 5 m. The radiolarian cherts are well bedded and occasionally well laminated. The age of this unit is (MORB, directly overlying by red pelagic sediments) Aptian/Albian (110 M.y. old) to Lower Maastrichtian (70 M.y. old), based on radiolarian biostratigraphy (Sarwar 1992; Gnos. et al; 1998). The pillow lavas have been metamorphosed to green schist facies during a sea-floor hydrothermal process (Sarwar 1992). The diameter of the individual pillow varies from cm to m . Normally the pillows are tightly packed and contain very little interstitial material. Nearly all pillows show chilled margins, which are 1 to 3 cm thick. Within the chilled margin glassy material predominates and rarely contains variolites. Individual flows, are 2.0 to 22 m thick. The basalts are brown or greenish grey on weathered surfaces, and grey to dark greenish grey on fresh surfaces, fine grained, hypocrystalline, holocrystalline, and porphyritic. The rocks are predominantly composed of plagioclase and augite. Whereas ilmenite and magnetite are ubiquitous accessory minerals. Plagioclase sometimes is zoned. scattered phenocrysts of olivine, but rarely hypersthene, are also found.

LATE MAGMATIC (INTRUSIVE AND VOLCANIC) ROCKS RELATED TO HOTSPOT

The intrusive rocks are doleritic to microdioritic, Microgabbroic or gabbroic Fe-rich tholeiitic plutons and sills, while volcanic rocks are alkaline sub marine basalts.

The doleritic to microgabbroic plutons and sills, and alkaline rocks cover as much as 30% of the area and doleritic to microgabbroic related to some tholeiitic (Gnos et. al 1998). The sills and plutons are light brownish to greenish grey to grey on weathered surfaces and greenish grey to grey on fesh surfaces. Individual sills are less than 1 m to 140 m in thickness. Some of the microgabbroic plutones are several kilometres across. Ophitic and subophitic texture dominates the plutons and sills. Some of them show porphyritic, glomeroporphyritic and suboptitic texture. The microgabbroic sills are composed of small to large anhedral to subhedral grains of plagioclase (oligoclase-andesine), clinopyroxene (diopside), chlorite partly replaced plagioclase and pyroxene. It also contains hornblende, biotite, and opaque minerals. Whereas doleritic sills, are composed of plagioclase (andesine-clear-cloudy laths of 2mm), anhedral to subhedral grains of clinopyroxene (diopside), chlorite replaces plagioclase and pyroxene. It also contains hornblende and opaque minerale (magnetite-ilmenite).

The alkali basalts consist of anhedral to euhedral laths (upto 1-2mm) of plagioclase and partly chloritized, clinopyroxene, hornblende as occasional phenocryst (upto 4.5 mm) and partly replaced by chlorite. It also contains magnetite, sphene, apatite and glass in ground mass. The alkali basalts are characterized by amygdaloidal structure. The amygdules are filled up with calcite, epidote, quartz and chlorite are also observed. The titanaugite phyric tephrites, and olivine basalts and subaerial lavas (flows with scoriaceous texture) are composed of titanaugite, clinopyroxene (diopside), olivine, amphibole, chlorite and phlogopite, ilmenite are also present. Some microgabbroic intrusions contain fragments of chert, red shale, black shale along with basaltic rocks and these intrusions as well as amygdaloidal basalt, titanaugite phyric tephrites and olivine basalts cut the MORB related basalts, and pelagic sediments.

GEOCHEMICAL CHARACTERISTICS VOLCANIC AND ASSOCIATED BASALTIC INTRUSIONS

The section presents a brief description of geochemical characteristics of the volcanic and associated intrusive rocks of the Bela ophiolite. Selected samples for whole rock chemistry and mineral chemistry were analysed for this study.

MINERAL CHEMISTRY

Six least altered samples, four from alkali basalts and two from microgabbro , were selected for mineral chemistry to identify genesis of these rocks. Chemical data of clinopyroxene phenocryst and their cations ratios (on the basis of six oxygen) are given in Table 1.

The composition of clinopyroxenes of alkali basalts and microgabbros are plotted on Tio_2-MnO-Na_2O diagram (Fig. 2) of Nisbet and Pearce (1977). Most of the samples of the alkali basalts plot in the field of within-plate alkali basalts (WPA) or close to it. However, a few samples plot in the field of ocean floor basalts (OFB) along the boundary separating the field of within plate alkali basalt.

The samples of the microgabbro plot in the field of within- plate alkali basalt (WPAB), or in the field representing all environments and a numebr of samples in volcanic arc basalts (VAB). None of them plot in the field of ocean floor basalts (OFB).

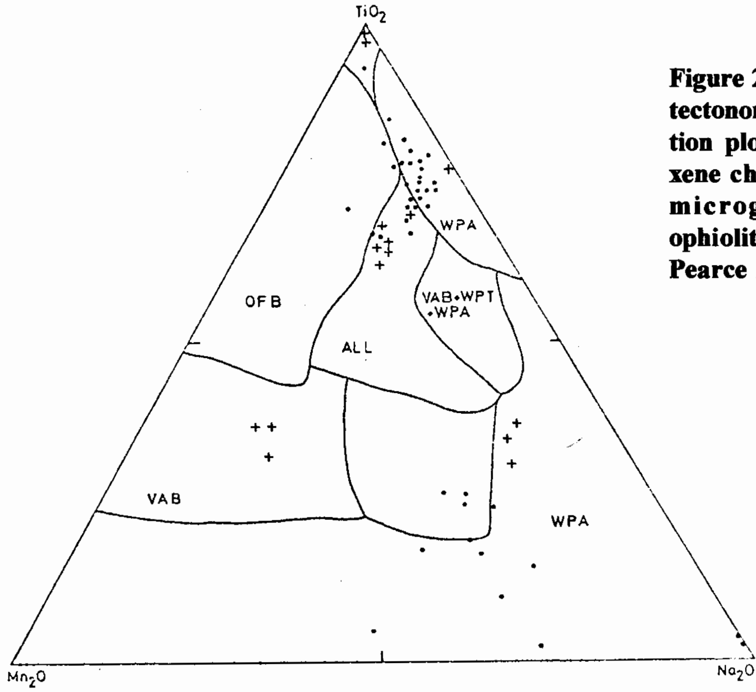

Figure 2. TiO_2-MnO-Na_2O tectonomagamatic discrimination plot based on clinopyroxene chemistry of basalt and microgabro from Bela ophiolite (after Nisbet and Pearce 1977).

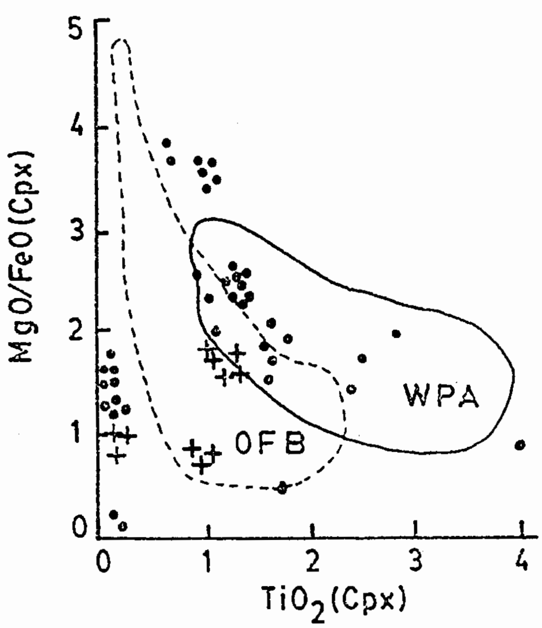

Figure 3. TiO_2 versus MgO/FeO plot for clinopyroxene chemistry of basalts and microgabbro from the Bela ophiolite (after Nisbet and Pearce 1977).

Table 1. Chemical Composition (in wt%) of clinopyroxenes in basalts and microgabbro from the Bela ophiolite.

	Major Oxides											Cation ratios on the basis of 6 oxygen.											
Sample No.	SiO_2	TiO_2	Al_2O_3	FeO	MnO	Cr_2O_3	MgO	CaO	Na_2O	K_2O	Total	Si	Ti	Al	Fe	Mn	Cr	Mg	Ca	Na	K	Total	MgO/FeO
95-18 Microgabbro	51.780	0.300	1.580	13.460	0.430	0.000	13.430	18.990	0.170	0.000	100.180	1.950	0.000	0.070	0.420	0.010	0.000	0.750	0.760	0.010	0.000	10.000	0.990
	51.320	0.390	1.730	13.030	0.490	0.000	13.780	18.440	0.160	0.010	99.360	1.940	0.010	0.070	0.410	0.010	0.000	0.770	0.750	0.010	0.000	10.000	1.000
	51.600	0.300	1.740	12.830	0.370	0.000	13.540	19.030	0.140	0.010	99.590	1.950	0.000	0.070	0.400	0.010	0.000	0.760	0.770	0.010	0.000	10.000	1.000
95-21 Alkali Basalt	51.090	1.560	2.540	9.430	0.190	0.000	15.070	18.720	0.440	0.030	99.130	1.910	0.040	0.110	0.290	0.000	0.000	0.840	0.750	0.030	0.000	10.000	1.590
	50.690	1.590	3.120	8.060	1.190	0.110	15.440	19.560	0.410	0.020	99.240	1.890	0.040	0.130	0.250	0.000	0.000	0.850	0.780	0.020	0.000	10.000	1.900
	50.240	1.520	3.210	8.950	0.250	0.060	15.350	18.540	0.470	0.040	98.680	1.890	0.040	0.140	0.280	0.000	0.000	0.860	0.740	0.030	0.000	10.010	1.700
	53.110	0.090	29.670	0.510	0.000	0.000	0.080	10.910	4.980	0.210	99.380	1.800	0.000	1.180	0.010	0.000	0.000	0.000	0.430	0.290	0.000	9.740	1.220
95-38 Alkali Basalt	52.560	0.240	4.170	10.210	0.230	0.000	16.820	12.320	0.440	0.020	97.040	1.990	0.000	0.180	0.310	0.000	0.000	0.930	0.490	0.030	0.000	9.950	1.650
	53.010	0.000	0.980	8.860	0.110	0.020	4.370	2.930	0.290	0.000	20.440	0.720	0.000	0.270	1.720	0.020	0.000	1.550	0.750	0.130	0.000	11.200	0.500
	50.050	0.220	6.010	11.500	0.350	0.480	15.420	12.020	0.640	0.040	98.780	1.890	0.000	0.260	0.360	0.010	0.010	0.870	0.480	0.040	0.000	9.990	1.300
	51.610	0.160	4.630	10.570	0.270	0.380	16.440	12.140	0.520	0.030	96.800	1.940	0.000	0.200	0.330	0.000	0.010	0.920	0.490	0.030	0.000	9.960	1.550
	52.920	0.220	3.810	10.070	0.230	0.030	16.920	12.290	0.380	0.010	96.920	1.970	0.000	0.160	0.350	0.000	0.000	0.940	0.490	0.020	0.000	9.940	1.680
	49.910	0.250	6.530	10.600	0.220	0.010	14.750	11.180	0.580	0.070	94.270	1.920	0.000	0.290	0.340	0.000	0.000	0.080	0.460	0.240	0.000	9.930	1.390
	49.680	0.310	6.300	11.560	0.340	0.070	14.940	11.850	0.650	0.060	95.810	1.900	0.000	0.280	0.370	0.010	0.000	0.850	0.480	0.040	0.000	9.970	1.290
97-69 Alkali Basalt	51.030	1.130	3.000	5.840	0.040	0.250	15.850	21.850	0.310	0.000	99.130	1.890	0.030	0.130	0.170	0.000	0.000	0.870	0.860	0.020	0.000	10.010	2.800
	49.920	1.530	3.760	6.170	0.040	0.300	15.420	21.800	0.530	0.000	99.330	1.850	0.040	0.160	0.190	0.000	0.000	0.850	0.870	0.020	0.000	10.020	2.490
	50.240	1.310	3.670	6.150	0.170	0.300	15.500	22.000	0.360	0.000	99.750	1.860	0.360	0.010	0.190	0.000	0.000	0.850	0.870	0.020	0.000	10.020	2.500
	49.730	1.180	3.660	6.270	0.090	0.260	15.470	21.970	0.320	0.010	98.990	1.860	0.030	0.160	0.190	0.000	0.000	0.860	0.880	0.020	0.000	10.030	2.460
	49.930	1.340	3.600	6.440	0.090	0.310	15.540	22.120	0.320	0.000	99.740	1.850	0.030	0.150	0.200	0.000	0.000	0.860	0.880	0.020	0.000	10.030	2.400

Table 1. (Contd...)

Sample	Major Oxides											Cation ratios on the basis of 6 oxygen.											
	SiO_2	TiO_2	Al_2O_3	FeO	MnO	Cr_2O_3	MgO	CaO	Na_2O	K_2O	Total	Si	Ti	Al	Fe	Mn	Cr	Mg	Ca	Na	K	Total	MgO/FeO
	43.200	4.390	5.260	11.170	0.260	0.010	11.110	19.030	0.520	0.080	95.090	1.730	0.130	0.040	0.370	0.000	0.000	0.660	0.810	0.040	0.000	10.030	1.000
97-100 Alkali Basalt	50.550	1.260	2.690	9.220	0.270	0.000	14.960	19.300	0.320	0.000	98.600	1.900	0.030	0.110	0.290	0.000	0.000	0.840	0.780	0.020	0.000	10.000	1.600
	49.990	1.180	2.980	9.350	0.300	0.000	14.840	19.210	0.310	0.000	98.200	1.890	0.030	0.130	0.290	0.000	0.000	0.830	0.780	0.020	0.000	10.010	1.580
	50.690	1.310	2.620	8.970	0.190	0.000	14.880	19.270	0.350	0.010	98.330	1.910	0.030	0.110	0.280	0.000	0.000	0.830	0.780	0.260	0.000	10.000	1.650
	42.620	0.050	21.070	5.180	0.000	0.010	0.000	26.210	0.010	0.000	95.190	3.400	0.000	1.980	0.310	0.000	0.000	0.000	2.240	0.000	0.000	20.440	0.000
	31.100	30.080	6.210	1.300	0.000	0.020	0.010	29.010	0.000	0.000	97.760	1.020	0.750	0.240	0.030	0.000	0.000	0.000	1.030	0.000	0.000	8.090	0.000
	31.270	31.130	5.700	1.080	0.000	0.010	0.000	28.890	0.000	0.000	98.120	1.030	0.770	0.220	0.020	0.000	0.000	0.000	1.020	0.000	0.000	8.080	0.000
	31.210	30.230	5.660	1.520	0.000	0.000	0.130	28.260	0.000	0.010	7.070	1.040	0.790	0.220	0.040	0.000	0.000	0.000	1.010	0.000	0.000	8.080	0.080
	50.270	1.090	2.050	8.000	0.230	0.000	15.050	19.800	0.330	0.000	96.860	1.920	0.030	0.090	0.020	0.000	0.000	0.850	0.810	0.020	0.000	10.000	1.870
	51.570	1.050	2.030	8.470	0.310	0.000	15.940	19.270	0.340	0.000	99.020	1.920	0.020	0.080	0.260	0.010	0.000	0.880	0.770	0.020	0.000	10.000	1.880
95-591 Micro- gabbro	51.290	0.990	2.530	4.610	0.070	0.340	15.490	22.790	0.240	0.000	98.000	1.910	0.020	0.110	0.440	0.000	0.010	0.860	0.910	0.010	0.000	10.000	3.350
	51.790	1.040	2.540	4.610	0.050	0.300	16.120	23.370	0.230	0.000	100.080	1.900	0.020	0.110	0.140	0.000	0.000	0.880	0.920	0.010	0.000	10.010	3.690
	52.720	0.830	2.000	4.370	0.090	0.370	16.330	63.570	0.240	0.000	100.570	1.920	0.020	0.080	0.130	0.000	0.010	0.880	0.920	0.010	0.000	10.010	3.700
	51.660	0.800	1.990	4.100	0.080	0.350	16.160	23.160	0.240	0.000	98.560	1.920	0.020	0.080	0.120	0.000	0.010	0.890	0.920	0.010	0.000	10.010	3.900
	50.760	1.290	3.240	6.250	0.180	0.030	15.130	22.630	0.330	0.000	99.840	1.880	0.030	0.140	0.190	0.000	0.000	0.830	0.890	0.020	0.000	10.020	2.400
	49.980	1.760	2.960	8.190	0.160	0.010	14.470	20.930	0.320	0.000	98.820	1.880	0.050	0.130	0.250	0.000	0.000	0.810	0.840	0.020	0.000	10.010	0.560
	48.330	2.290	4.480	8.840	0.210	0.000	13.820	20.840	0.320	0.000	99.160	1.820	0.060	0.190	0.270	0.000	0.000	0.770	0.840	0.020	0.000	10.020	1.560
	35.480	1.660	2.690	7.720	0.160	0.020	15.620	20.740	0.300	0.000	84.440	1.820	0.050	0.140	0.290	0.000	0.000	1.060	1.020	0.020	0.000	10.250	2.000
	50.550	1.540	3.200	7.450	0.080	0.060	14.940	21.530	0.270	0.000	99.860	1.880	0.040	0.140	0.230	0.000	0.000	0.820	0.850	0.020	0.000	10.010	1.960
	50.500	1.570	3.200	7.280	0.120	0.010	15.180	21.520	0.310	0.000	99.730	1.870	0.040	0.140	0.000	0.000	0.000	0.840	0.850	0.020	0.000	10.010	2.080

The TiO_2 versus MgO/FeO plot (Fig.3) of the clinopyroxene of Nisbet and Pearce (1977), most of the samples plot either in the field of within-plate alkali (WPA) or in the combined field of within plate alkali (WPA) and ocean floor basalts (OFB). However, some of them plot outside the both fields.

To conclude majority of the samples of the alkali basalts and the microgabbro have closer affinity with the within- plate alkali basalts.

WHOLE ROCK CHEMISTRY

Nine rock samples were selected for major and trace elements determination (Table 2). These include 5 volcanic and 4 intrusive (microgabbro/ microdiorite) rocks. Both volcanic and intrusive rocks are plotted on SiO_2 versus Na_2O+K_2O (alkali) diagram (Fig. 4) of Le Base et al. (1986) for rock classification. Majority of the volcanic and intrusive rocks samples fall in the field of basalt, two in the field of tepherite/basanite, one in the field of andesite and one in the field of trachydacite. When plotted in a diagram based on SiO_2 versus FeO/MgO (after Miyashiro, 1974) all the samples plot in the field of tholeiite and non of the samples plot in the Calc-alkaline field (Fig. 5).

Table 2. Major and trace elements of various volcanic and associated intrusive rocks from Bela Ophiolites.

	Rock Types / Major and Trace Elements	Microdiorite	Basanite	Trachydacite	Microgabbro	Alkali basalt	Microgabbro	Ocean floor basalt	Tepherite	Microgabbro
	Sample No.	**95-18**	**95-21**	**95-48**	**95-97**	**95-98**	**95-140**	**95-147**	**95-174**	**96-419**
Major elements wt. %	SiO_2	60.01	44.1	65.17	49.6	46.74	49.69	49.71	43.37	50.52
	TiO_2	0.76	1.68	0.74	2.66	0.97	2.73	2.23	2.79	2.76
	Al_2O_3	13.93	15.49	14.33	12.91	14.44	12.78	13.76	12.65	12.89
	Fe_2O_3	9.87	6.14	6.76	15.05	8.94	14.9	13.76	8.99	14.97
	MnO	0.17	0.11	0.25	0.21	0.23	0.23	0.2	0.05	0.21
	MgO	2.1	4.4	0.2	5.79	7.1	4.75	6.24	1.19	4.83
	CaO	6.06	14.24	0.73	9.04	12.79	7.53	10.77	13.41	8.65
	Na_2O	4.31	4.04	5.05	3.32	4.23	3.27	2.67	6.7	2.99
	K_2O	0.31	1.54	3.04	0.51	0.05	0.8	0.13	0.18	0.74
	P_2O_5	0.13	0.19	0.18	0.27	0.11	0.28	0.24	0.59	0.32
	GV	2.82	7.21	3.15	0.99	4.36	1.99	0.71	9.04	1.56
	SUM	100.46	100.14	99.62	100.36	99.92	98.96	100.43	98.96	100.45
	FeO/ MgO	4.7	1.39	33.8	2.59	1.25	3.1	2.2	7.55	3.07
Trace elements ppm	Ba	88	271	842	176	18	229	66	354	235
	Cr	3	126	15	35	609	8	68	16	10
	Cu	17	14	6	167	123	91	130	58	84
	Nb	4	21	123	11	21	16	9	63	16
	Ni	2	76	5	53	158	40	67	35	40
	Pb	3	2	5	3	1	4	4	4	4
	Rb	14	22	65	18	10	23	10	11	21
	Sr	188	431	139	267	149	349	242	590	323
	Th	0	0	10	-1	-1	2	0	6	0
	V	138	349	32	386	263	382	381	318	390
	Y	33	20	80	35	28	47	32	24	45
	Zn	57	29	174	88	86	108	101	55	117
	Zr	82	95	645	156	864	268	138	227	254

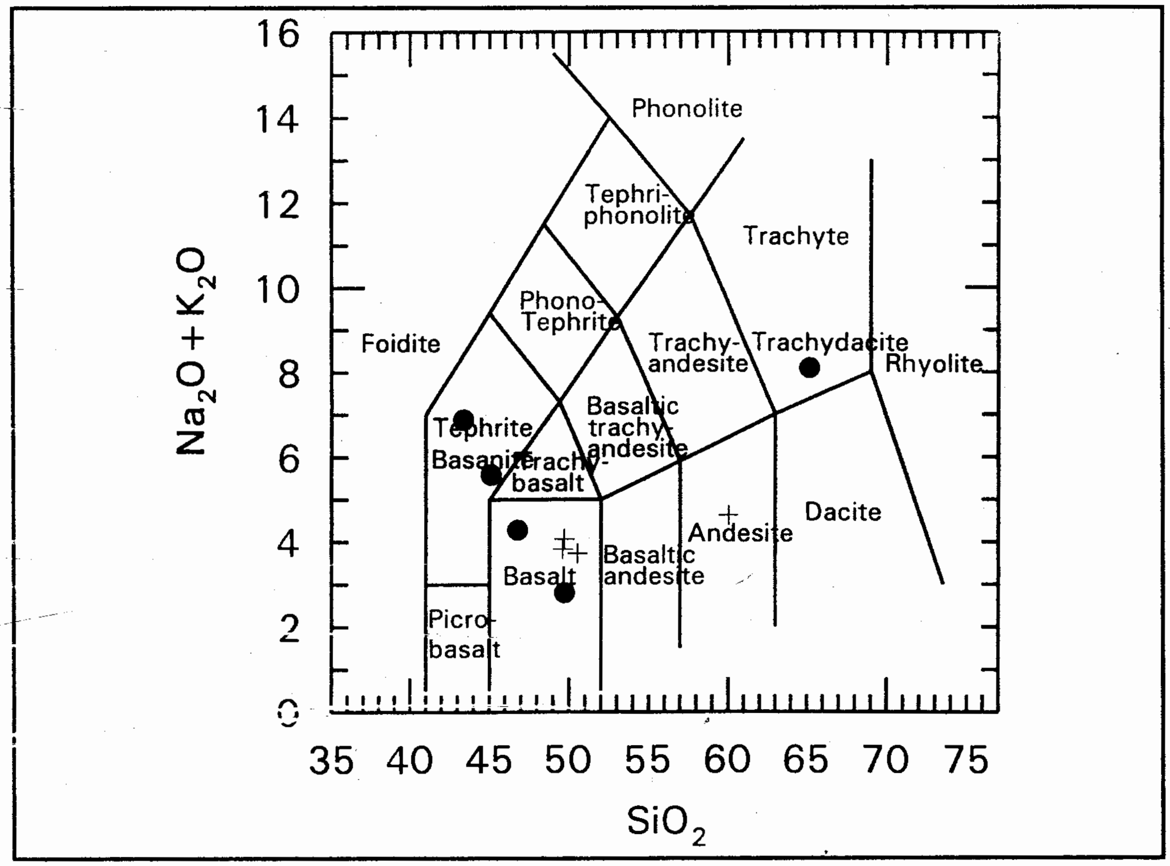

Figure 4. Alkali versus SiO_2 plot of volcanic (•) and intrusive (+) rocks of the Bela ophiolite (after Le Bas et al. 1986).

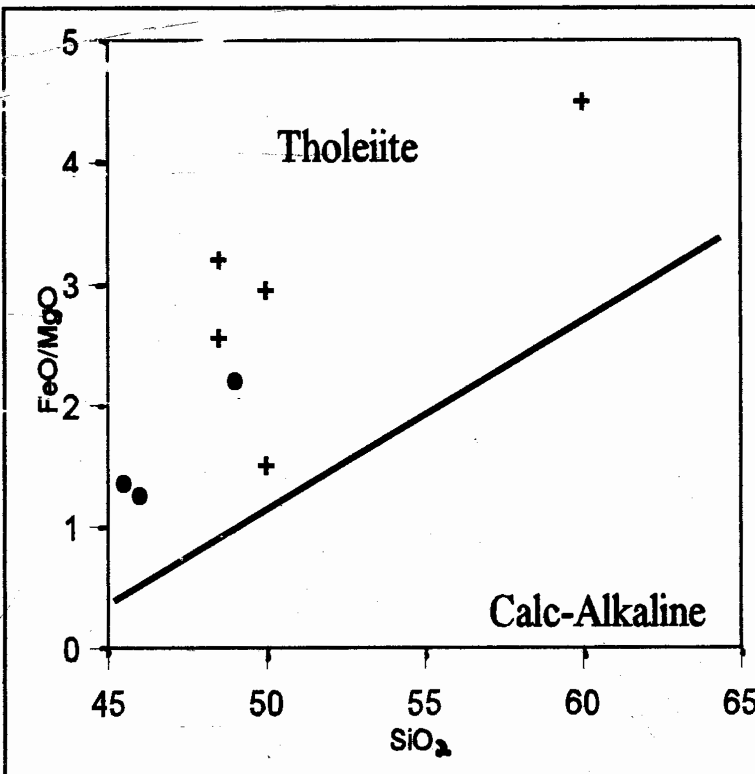

Figure 5. SiO_2 versus FeO/MgO plot for volcanic and intrusive rocks of the Bela ophiolite (after Miyashiro 1974).

When plotted on the triangular tectono-discrimination diagram (Fig. 5) involving Nb- Zr-Y (after Meschede 1986). The rocks show a wide spread pattern.Two basalt samples plot in the field of within plate alkali basalts(WPA) and one each in the field of E-MORB and WPA+WPT, WPT+VAB. The intrusive rocks plot mostly in the combined field of within plate tholeiite and volcanic arc basalt (WPT+VAB) and one in the field of N-MORB. When plotted on another triangula tectono-discrimination diagram (Fig. 6) involving Ti-Zr-Y (after Pearce and Cann 1973), most of the volcanic and intrusive rocks fall in the field of D (Within plate basalt) and only one volcanic rock fall in the field of B (Ocean floor basalt) and non of them fall in the field of A (Island-arc basalt) and in the field of C (Calc-alkaline basalt).

DISCUSSION AND CONCLUSION

Magmas originated in different tectonic environments have specific geochemical charateristics, so geochemical data of the igneous rocks can provide significant clues for the recognition of past tectonic environments (Wilson 1991). However, the geochemical recognition of some magma is more complex, when they share charateristics of two or more tectonic settings.

As far as classification for magma series is concerned, most of the samples of the volcanic and associated basaltic intrusive rocks plot either in the field of alkaline series or tholeiitic series (Fig. 4 and 5). The tholeiitic rocks may occur in all tectonic setting, however they can be distinguished on the basis of SiO_2 content range, FeO/MgO, TiO_2 and K_2O content (Miyashiro 1974). The basalts of the mid- oceanic ridge are characterised by narrow SiO_2 range (47- 52%). With FeO/ MgO less than 1.7 and low K_2O content (<0.40%) (Miyashiro 1974). Two of the basalts (95-98 and 95-147) cleary fall in the category of mid-oceanic ridge basalt (MORB). The SiO_2 content ranges from 46 to 49, FeO/MgO ratio is 1.25 to 2.2 and the K_20 content is 0.05 to 0.13 (Table 2). Most of the micro gabbro and remaining basalt (95-174) seems to be hotspot related. Various discrimination plots of mineral chemistry (Fig. 2 and 3) and whole rock chemistry (Fig. 6 and 7) of both volcanic and intrusive rocks from the study area give signatures of both within plate alkali basalt (WPAB) and mid-oceanic ridge basalts (MORB).

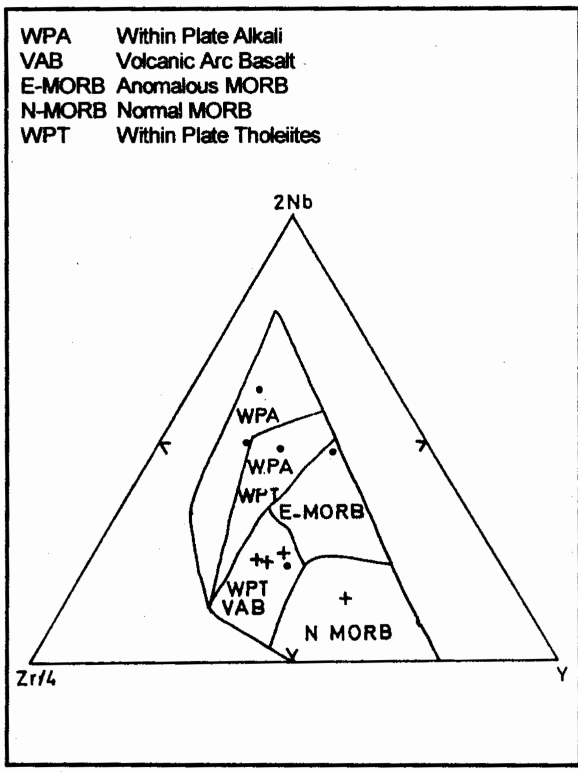

Figure 6. Nb-Zr-Y tectonomagmatic discrimination diagram for volcanics (•) and intrusives (+) of the Bela ophiolite (after Meschede 1986).

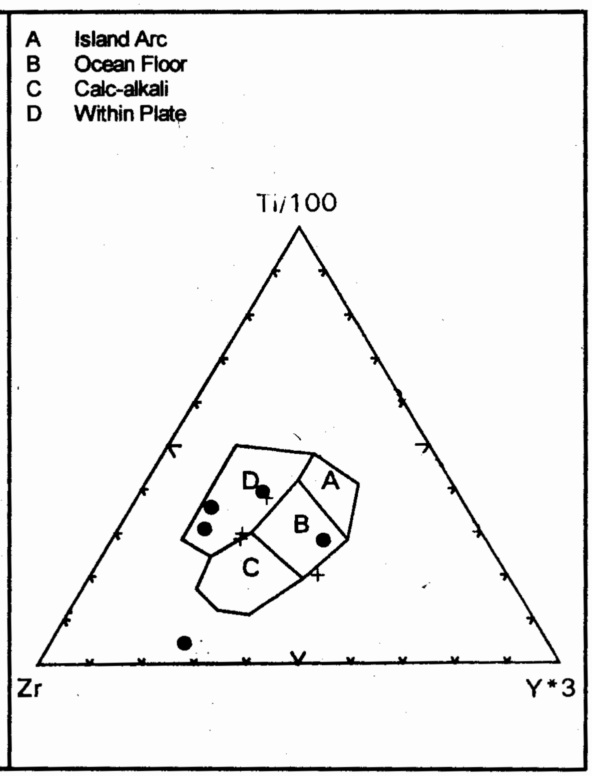

Figure 7. Ti-Zr-Y discrimination diagram for volcanic (•) and intrusive rocks (+) of the Bela ophiolite (after Pearce and Cann 1973).

The mid-oceanic ridge basalts of the Bela oceanic lithosphere formed in Aptian- Albian, prior to the separation of Indian from Madagascar. During the late Cretaceous to Eocene, oceanic crust was consumed between the African-Arabian and India-Seychelles plates in response to the counterclockwise breakup of India-Seychelles plate (Gnos et al. 1998; Khan 1999). During the northward drift of India–Seychelles passed over the active Reunion hot spot, caused the intrusions of doleritic to microdioritic or gabbroic Fe- rich tholeiites and alkaline rocks into the Indian oceanic lithosphere or the continental margin. The hot spot related rocks yield the age of 70Ma (Gnos et al. 1998). Intraoceanic subduction initiated between 70 and 65 Ma, obduction onto the Indian passive margin occurred during the formation of Deccan traps at ≈66, and final thrusting onto the continental margin ended in the early Eocene ≈50 Ma (Gnos et al 1998, Khan 1999). During the emplacement of ophiolites, the active Reunion hot spot was located below the Indian oceanic lithosphere andthis indicates that the subduction was initiated very close to the Reunion hotsopt. The presence of hotspot related rocks in the sedimentary successio of the Jamburo Group (Paleocence-Eocene) suggests that part of the oceanic lithosphere was close to the continental margin. After the emplacement of Fe–tholeiitic and alkaline magmatism related to the Reunion hot spot, the Bela oceanic lithosphere along with hot spot related rocks emplaced onto the Indian continental margin. The ophiolite, along with Reunion hot spot traveled in Tertiary onto the Indian continental margin to its present position.

We conclude that genetically two different types of basaltic rocks are present in the Bela area: i) the mid-oceanic ridge related basalts and ii) microdioritic or gabbroic Fe- rich tholeiites and alkaline basalts related to hot spot.

REFERENCES

Ahmed, Z.,1991, A supra-subduction origin of the Bela ophiolite indicated by acidic rocks, Khuzdar District, Pakistan. Acta. Miner. Pakistan; 5, p. 9-24.

Ahsan, S.N., Akhtar T. and Ali Khan, Z., 1988, Petrology of the Bela-Khuzdar ophiolites, Baluchistan, Pakistan; Geological Survey of Pakistan Inf. Rel., 307, 24p.

Edwin Gnos, Mehrab Khan, Khalid Mahmood, Abdul S. Khan, Nasser A. Shafique and Igor M. Villa., 1998, Bela oceanic lithosphere assemblage and its relation to the Reunion hotspot. Terra Nova, Vol 10, p. 90-95.

Hunting Survey Corporation (HSC), 1960, Reconnaissance geology of part of West Pakistan: repo[illegible] published for Government of Pakistan by the Government of Canada, Toronto, 550 p.

Khan, Mehrab, 1999, Petrological and structural studies of the ophiolites of the Baran Lak area, Bela- Khuzdar, District, Balochistan, Pakistan. Ph. D. Thesis (unpublished) University of Balochistan, Quetta, Pakistan, 147 p.

Le Bas, M. J., Le Maitre, R. W. , Streckeisen, A., and Zanettin, B., 1986, A chemical classification of volcanic rocks based on the total alkali - silica diagram. Jour. Petrol. 27, p. 745-750.

Meschede, M., 1986, A method of discriminating between different types of mid- oceanic ridge basalts and continental tholeiites with the Nb-Zr-Y diagram. Chem. Geol. 56, p. 207-223

Miyashiro, A., 1974, Volcanic rock series in island arcs and active continental margins. Am. Jour. Sci. 274 p 321-55.

Nisbet, E.G., and Pearce, J.A., 1977, Clinopyroxene composition in mafic lavas from different tectonic setting. Cont. Min. Pet. 63, p. 149-160.

Pearce, J.A. and Cann, J., 1973, Tectonic setting of basic volcanic rocks using trace element analysis; Earth and Planetary Science letters. 19, p. 290-300.

Sarwar, G.,1992, Tectonic setting of the Bela ohiolites, southern Pakistan. Tectonophysics 207, p. 359-381.

Wilson, M., 1991, Igneous petrogenesis. Unwin Hyman, London. 466p.

Zaigham, N. A. and Malik, K.A; 1992. Upward continuity filtering of the Uthal gravity data. Acta Miner.Pakistan; 6, p. 149-158.

Zaigham, N. A; 1991, Bela Ophiolite and associated mineralization in southern part of Axial- belt of Pakistan Unpublished doctoral dissertation, University of Karachi Pakistan, 370p.

Manuscript Received 27th October 1998
Revised Manuscript Received 2nd June 1999
Accepted 1st September 1999

ACTA
MINERALOGICA
PAKISTANICA
Volume 9 (1998)

Article Reference
AMP9.1998/037-054/ISSN.0257-3660

LITHO AND STREAM SEDIMENTS' GEOCHEMICAL STUDIES FOR GOLD AND BASE METALS IN AREAS AROUND TIMARGARA AND SAMARBAGH, DISTRICT DIR, NORTHERN PAKISTAN

MOHAMMAD TAHIR SHAH[1], ALI SARWAR[2], WALEED AHMAD[2] and SHAMIM AHMAD SIDDIQUI[3]

[1]National Centre of Excellence in Geology, University of Peshawar, Peshawar Pakistan
[2]Sarhad Development Authority, Peshawar Pakistan
[3]Center of Excellence in Mineralogy, University of Balochistan, Quetta Pakistan

ABSTRACT

The area of study (about 900 sq. km.) lies within the Kohistan arc terrane in the northern part of Pakistan. It is located immediately north of the Main Mantle Thrust (MMT) in Dir district. It has a complex geology and is mainly composed of amphibolites, metadiorites, metagabbro-norites, metagranodiorites, metagranites and metavolcanics with subordinate amount of hornblendites, ultramafites and tonalites. The area has already been investigated for preliminary geology, however, no detail geochemical investigation has been carried out for precious and base metals mineralization. This study has main emphasis on the rocks and stream sediments (both pan-concentrates and -80 mesh fine fraction) geochemical survey for gold and base metals in order to delineate areas likely to contain mineralization and be worthy of follow-up work.

The area has been divided in to 56 drainage cells ranging from 2-50 km^2 with an average density of about one site per 15 km^2. From each cell a pan-concentrate and -80 mesh fine fraction were collected for mineralogical and geochemical studies. The visible gold as piece (>0.5mm), speck (0.5-0.3mm) and color (<0.3mm) was identified in the pan concentrates of certain streams, mainly in the north eastern and north western portion of the study area. However, no nugget of gold has been noticed in the pan-concentrates. The specks and colors are generally angular to subangular, sometime irregular to rectangular in shape and bright yellow in color. The pan concentrates are dominantly composed of magnetite whereas zircon, quartz, pyroxene, garnet, hornblende, feldspar, tourmaline, chromite and rock fragments occur as minor constituents. The floats were also examined for alteration and other geological phenomenon at each site.

Samples of Rocks and stream sediments (both pan-concentrates and fine fraction) have been analyzed for Au, Ag, Cu, Zn, Pb, Co, Ni, and Cr. The geochemical data have been displayed and evaluated by considering various geostatistical methods. Geochemical maps have also been prepared on the basis of single and multi-eliments consideration in order to pin point areas of most interest. These studies show that pan-concentrates have higher concentration of base metals as compared to that of fine fraction and are, therefore, silicate-bounded rather than sulfide-bound in stream sediments. The higher concentration of Cu, Pb, Zn, Ni, Cr, Co and Ag could be related to the bed rock rather than to specific mineralization in the area. The anomalous gold, however, could not be directly related to the bed rock but it could possibly be related to the existence of gold-bearing mineralization, most probably in the form of quartz veins, in the north and north-eastern part of Samarbagh area. Further detail geochemical survey is, therefore, recommended for follow-up in the region.

INTRODUCTION

The area of study covers about 900 sq km and is situated between latitude 34°47" N to 35°N and longitude 71°34" E to 71°55"E in Dir district, northern Pakistan (Fig. 1). It covers most part of the Jandul valley (toposheet 38-N/9) and Timargara and Midan area (toposheet 38-N/13). The central, north-eastern and north- western portion of the area has high relief while the southeastern and southwestern part is occupied by smaller hillocks. Steep walled valleys with slope of more than 45° are the common topographic features of the area. Topographically the northern and central part of the area is characterized by sharp and steeply dipping mountain ridges bounded by sloping features in two directions.

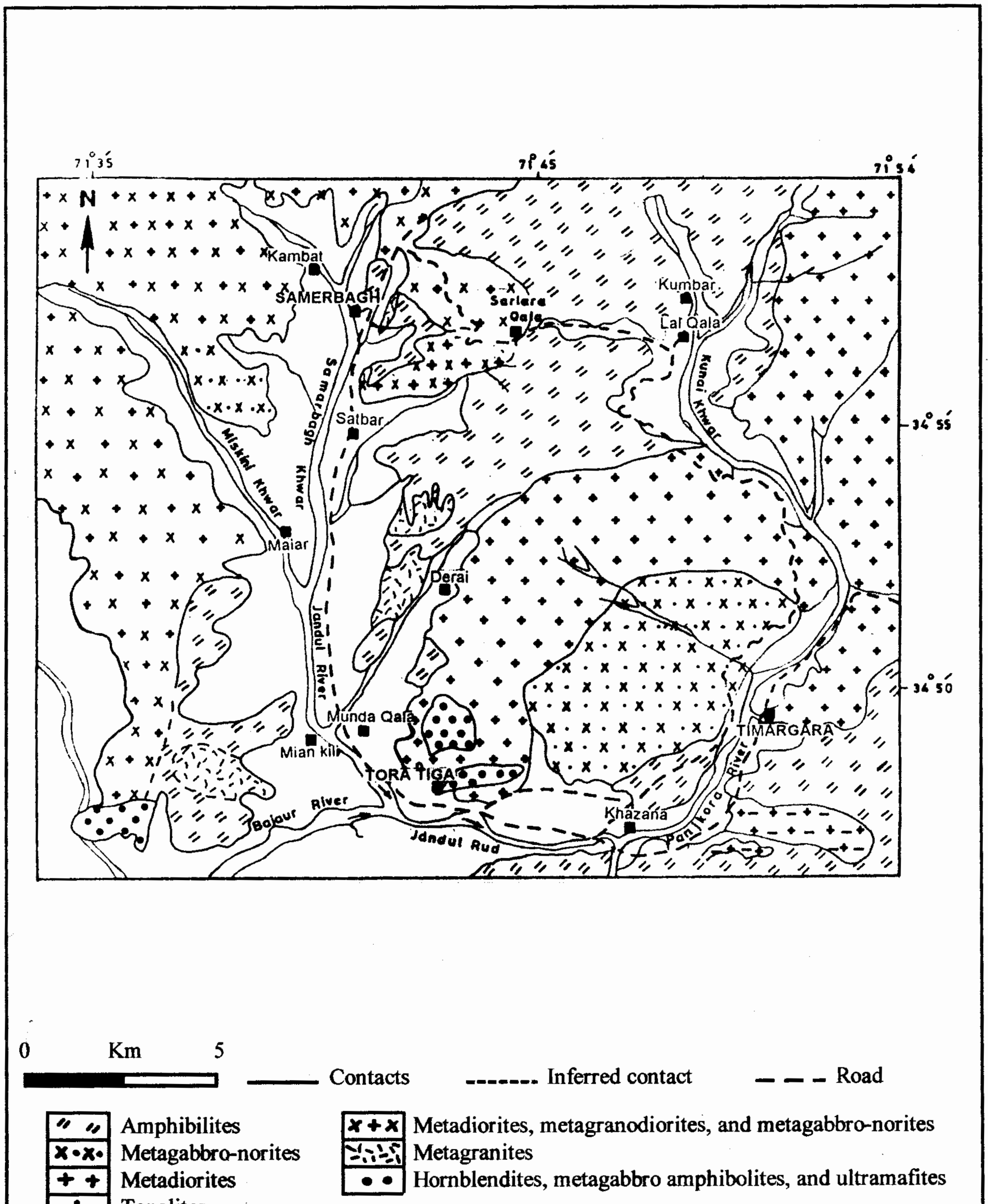

Figure 1. Geological Map of Timargara and Samarbagh areas, District Dir, N.W.F.P. Pakistan (modified after Kakar et al. 1971, Chaudhry et al. 1974 and Butt et al. 1980).

The area generally drains into the Panjkora river by various streams (i.e. Samarbagh, Miskini and Kunai streams). In western part of the study area, two big streams such as Samarbagh Khawar and Miskini Khawar join each other near Mayar and flow downward towards Munda Qala in the south. It then joins the main Bajaur Khawar near Munda Qala. The Bajaur Khawar flowing towards east and falls into the Panjkora river near Khazana village (Fig. 1). The north-eastern part of the area is drained into the Kunai Khawar. This stream flows downwards and falls in to the Panjkora river in the south. The area around Timargara is directly drained into Panjkora river by various small streams. Most of the steams of the area are seasonal, except few, and carry sufficient discharge during rainfall. The drainage system of the area is flat bottomed and most of the streams join each other at acute angles, producing dendritic drainage pattern. However, Radial pattern has also been noticed around high aititudes.

SCOPE AND PURPOSE OF INVESTIGATION

The area of study lies in the north-western portion of the Kohistan island arc and is located immediately north of the Main Mantle Thrust (MMT) (Fig. 2). It could be the north-western extension of the southern Kamila amphibolite belt of Jan (1979; 1988). The arc type set up and the associated calc alkaline magmatism in Dir and Swat Kohistan (Majid and Paracha 1980, Majid et al. 1981; Hamidullah et al. 1990; Shah 1991, Shah et al. 1994) by itself forecast the existence of various types of mineral deposits, especially epithermal gold and volcanogenic massive sulfide deposits. The calc-alkaline magmatism is indicative of producing geochemical anomalies for the base metals, especially copper (Cu), Lead (Pb) and zinc (Zn) associated with basic and acidic igneous rocks. It is now determined by the modern research that various metallogenic provinces throughout the world are originated in specific tectonic setting. The massive sulfide deposits, the porphyry type deposits and epithermal precious metal deposits are mostly associated with magmatism in island arc type of setting. The significant enrichment of sulfur in acid to intermediate volcanic rocks can give rise to various sulfide deposits. These sulfide deposits in turn can develop strong indications of the existence of various other precious metal deposits, especially gold (Au) and silver (Ag) in the adjacent areas.

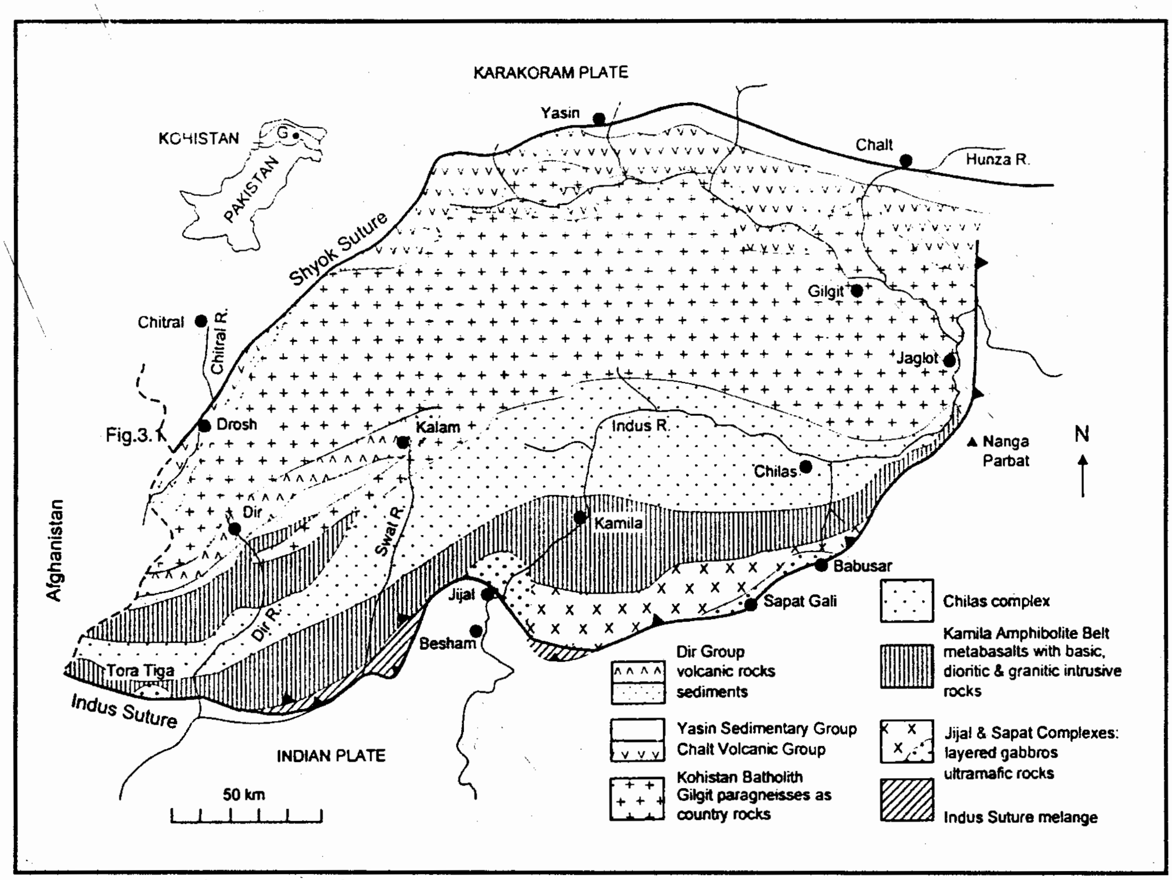

Figure 2. Regional geological map of northern Pakistan showing the location of study area, (after Khan et al. 1993).

The occurrence of hydrothermal copper mineralization in Dir area (Shah 1991; Shah et al. 1994) indicates that the area has potential for base and precious metals, as already known elsewhere in the world. Keeping in view the above mentioned facts, the regional scale preliminary geochemical investigation in Dir and Swat Kohistan area is very necessary. This study is the part of this scenario.

Many of the previous studies carried out in the region (e.g., Hyden 1915; Ahmad 1962; Jan et al. 1969; Khan,1969; Arbab and Khan 1973; Chaudhry et al. 1974; Kakar et al. 1971; Jan et al. 1983; Jan and Howie 1981; Jan and Tahirkheli 1990; Butt et al. 1980; Tahirkheli 1979; 1982; Hamidullah et al. 1990; Shah 1991; Shah and Hamidullah 1994; Shah et al.,1994; Sullivan et al. 1993) are based mainly on the geology and geochemistry of the rocks. No published stream sediment geochemical data on the area is available. However, Sarhad Development Authority (SDA) has recently started stream sediment geochemical investigations of Dir and Swat region.

The material of different media such as heavy mineral concentrates and fine fraction of <177mm (-80 mesh) show important chemical differences as these media are subjected to different influences, and underlies different geological textures (Davenport 1990; Bellehumeur et al. 1994). Based on these criteria, the present study is also based mainly on the geochemical investigations of heavy mineral concentrates and fine fractions of the stream sediments. In order to compare the stream sediment anomalies with the rocks of the area, the geochemical investigation of various rocks exposed in the catchment area were also carried out. The main objective of this reconnaissance geochemcial survey in the area is to find areas likely to contain mineralization and be worthy of follow-up work.

GEOLOGY OF THE AREA

The geology of the area has been described by Kakar et al. (1971) Chaudhry, et al. (1974), Butt, et al. (1980), Jan, et al. (1983) Sarwar (1996) and Shah et al. (in press). The geology of the area has been divided into three main complexes (i.e., Timargara, Sumergagh, and Tora Tiga). Breif geology of these complexes is given below.

TIMARGARA COMPLEX

The rocks of the complex are exposed in central and north-eastern portion of the study area (Fig. 1). This complex is mainly composed of amphibolites, metadiorite and metagabbronorites with lesser amount of metagabbro, metagrano-diorites, quartz diorites, tonalites and volcanics.

The amphibolites are mainly exposed in the southern and northern part of the study area. However, minor sheets and lenses are also exposed in the central part of the area (Fig. 1). These types of amphibolites in other parts of the Dir district are termed as Northern Dir amphibolits (para-amphibolites) by Chaudhry et al. (1974). These rocks are distinctly banded and schistose. The foliation is parallel to the layering, generally trending NE-SW. There are alternate dark and light colored bands. The dark colored bands have amphibole in higher concentration while the felsic phases (plagioclase and quartz) along with pink coloured garnet are concentrated in the light color bands. At places the bands of cherty material up to 3 cm thick are also noticed. These rocks are intruded by dioritic, aplitic and mafic dikes. The diorite intrusion in the from of small plugs are also present, which contain xenoliths of banded amphobolites.

There are isolated outcrops of banded amphibolites in the north-east of Samarbagh (Fig. 1). These out crops are in contact with porphyritic augen gneisses. The amphibolites in this zone are intensely deformed and stretched. In the central part of the study area (e.g., near Charmang and Jabagai area), these amphibolites are intruded by granititic rock which result in the formation of hornblende in the form of veins.

Metadiorites are massive in hand specimen and have medium-to coarse grained texture. These are dark gray to greenish gray on fresh surface and dirty dark brown on weathered surface. Metagabbro-norites and the metagabbros are medium to course grained, having well developed foliation. In handspecimen these are massive dark gray colored rocks on fresh surface while light brown to yellowish brown on weathered surface. Both the metadiorite and metagabbro-norites are having many similar features. The general trend of foliations of these units is NE-SW which, in turn, is in general conformity with the regional trend of the southern (Kamela) amphibolite belt. These rocks are intruded by hornblendite, aplite and micro-dioritic dikes and quartz veins. Wherever the rock has these intrusions, it has attained maximum weathering and alteration on both sides of the intrusion. Shearing along local faults is very common where quartz and epidote veining is prominent. Occasionally dark patches (about less than 30 cm thick) containing >90% amphibole, are also present within the metagabbro-norite.

Patches of volcanic rocks and volcanic porphyry dikes are exposed in the study area. These volcanics are foliated and have attained greenschist facies metamorphism. These are intruded by dioritic dikes, having chilling and alteration effects on both sides within these volcanics. The rock is generally altered to epidote and chlorite. Occasionally, the epidotization is so intense that the rock attained patchy appearance. The micro veins containing limonite, chalcopyrite and pyrite are also noticed.

SAMARBAGH COMPLEX

This complex is widely exposed in the Jandul valley, covering most of the western and north-western part of the study area (Fig. 1). The rocks of this complex extend to Afghanistan in the north-western part and to Bajaur agency in the south-western part of the study area. This complex is mainly composed of metadiorites and metagabbro-norites with subordinate amount of norite, gabbro, granodiorites, metagranites, metavolcanics and porphyry dikes.

Metadiorite can be both leuco and mela diorites. The leuco diorites are light colored and are exposed mainly on the eastern side of the Miskini Khawar while mela diorites (containing pyroxenes) are dark colored and widely exposed in the western part of the Miskini Khawar. Both the varieties are medium- to course-grained having well developed foliation. These rocks near Sarlara Qala are highly deformed and sheared. The occurrence of quartz veins is the common feature of these deformed metadiorites. The metadiorite exposures southeast of Samarbagh and northeast of Satbar (Fig. 1) are fine- to medium-grained, having unique banded structures of alternate mafic and felsic phases. These bands are deformed and exhibit micro folding. These could be primary igneous features or may be formed due to metamorphic segregation. These rocks are also intruded by pegmatitic veins, containing hornblende crystals of <cm long.

Metagabbro-norites have well developed fabric and are exposed north of Maiar (Fig. 1). These have upper gradational contact with metadiorites and are intruded by the swarm of porphyry dikes extending in the east and west directions. These rocks are medium- to coarse-grained and are topographically distinct due to their rusty dark brown weathered surfaces.

Metagranites are exposed within banded amphibolites near Derai in the centeral part of the study area (Fig. 1). These are light colored, coarse-grained granites with well developed fabrics. At places, it is intensively faulted, folded and cut by quartz and pegmatitic veins. There are other small intrusions of granite within this complex and are not shown in the map (Fig. 1).

TORA TIGA COMPLEX

The rocks of the Tora Tiga complex are exposed in the southern and central part of the study area and are well described both petrographicaly and geochemically by Banaras and Ghani (1982), Jan et al., (1983) and Jan and Tahirkheli (1990). This complex is mainly composed of amphibolites, metagabbros, ultramafics, hornblendites and other minor dikes and veins. The metagabbros occur in the southern part of the complex. These are the medium-to coarse-grained, homogeneous, gneissosed rocks. They carry dikelets and veins, as well as patches of hornblendite. The contacts of the metagabbros with the lower lying ultramafics are sharp and locally sheared. The banded amphibolites form linear belts between the metagabbros and the garnet-amphibolites. The banded amphibolites are characterized by alternate light and dark colored bands with fine to medium grained texture. The garnet-amphibolites are similar to the metagabbros with the exception of garnet porphyroblasts of varying dimension. Two main hornblendite exposures are present at Tora Tiga and Hashim village while numerous patches of variable size are present in other parts of the complex. Among ultramafic rocks the olivine ultramafites and pyroxene ultramafites can easily be distinguished. The olivine ultramafites include various types of peridotites, dunites and serpentinites. These rocks occur as elongated to subcircular bodies, or small irregular patches. These are generally medium-grained, dark green, hard compact and vitreous when fresh; light green or gray and greasy when surpentinized. The pyroxene-ultramafites are the second most abundant ultramafites and occur as east-west trending bodies. These are hard and massive rocks, generally medium-grained, though coarse- and fine-grained varieties are also found locally.

METHODOLOGY

SAMPLE COLLECTION AND ANALYSES

Representative grab samples (>5 kg) were hammered through the rock exposures in the field. Both fresh and weathered rock samples were collected in different sample bags. The crushed material along various sheared zones were also collected for analyses of base and precious metals.

Stream sediments were collected from fifty six sites arround Timargara and Samarbagh, southern Dir. The surface areas of the catchment basins (cells) vary considerably, but most of the samples were collected at the outflow sites of catchment basins ranging from 2 to 50 km^2. The average sample density was about one site per 15 km^2. Two samples were collected at each site: (a) pan-concentrate stream sediments and (b) fine fraction (-80 mesh) of stream sediments. The pan-concentrate samples were obtained by sieving to <850mm (-20 mesh) and the heavy minerals concentrates were prepared by panning. The fine fractions were obtained by sieving the clay size material to <177mm (-80 mesh) size from the same site.

Both pan-concentrates and fine fractions of stream sediments and the rock samples were digested in weak (HNO_3) and strong (aqua regia) acids in the laboratory. The digested solutions were then used for the determination of Au, Ag, Pb, Zn, Cu, Ni, Cr and Co by using Perkin Elmer Atomic Absorption spectrometer 3300. Gold, after extraction with MIBK, was determined by graphite furnace. All of these analyses were performed at the Geochemistry laboratory of the National Centre of Excellence in Geology University of Peshawar. Duplicate analyses of several samples were also carried out at the Mineral Testing Laboratory, Sarhad Development Authority, Peshawar. The results of both the laboratories match very well.

In order to have comparative interpretation, the normalization of pan-concentrate data is very necessary, especially in the case of those elements which have nugget effects (e.g., gold). The normalization is also very necessary because the concentration factor, reflected in the weight of the final concentrates, varies with the amount of heavy minerals present at the same site. However, for fine fraction the normalization is not important. The pan-concentrate data (i.e. Au, Ag, Pb, Zn, Cu, Ni, Cr and Co) of the studied samples have, therefore, been normalized to 100 g. These normalized data are then used during interpretation. Normalized geochemical data along with summary statistics of the pan-concentrates and fine fraction are given in Table 1 to 4. The geochemical data of the rocks are presented in Table 5.

Float and pan-concentrate study

Float study Float study is very useful in the areas where there is a thick vegetation cover and the rock exposures are hardly exposed. The study area is not of this type. The rocks are well exposed and the geology is very well studied by collecting rock samples from the exposures. However, during the present study the float at each srteam sediment sample site was studied. These floats are mainly of metadiorite, metagranodiorite, granite gneisses, metagabbro-norite and amphibolite. However, in some streams, floats of quartz pegmatites, hornblendite, applite dike rocks, quartz vein material, pyroxenite and volcanics etc. are also found.

Pan-concentrate Mineralogy of the pan-concentrate samples was carried out under the binocular microscope. More emphasis was given to the identification of gold in the form of pieces (>0.5 mm), specks (0.5-0.3 mm) and colors (<3 mm) in each pan-concentrate sample. The pan-concentrates are dominantly (>60%) composed of magnetite. Zircon, quartz, pyroxene, garnet, hornblende, feldspar, tourmaline, chromite, pyrite and rock fregments occur as minor constituents.

Gold in the form of pieces, specks and colors is identified in certain streams mainly in the north eastern and northwestern portion of the studied area as shown in figure 3. Gold in the form of pieces (>0.5mm) has been observed in few pan concentrates of the study area. However, no nugget of gold has been noticed in the pan-concentrates. The specks and colors are generally angular to sub angular, some time subrounded in roundness, irregular to rectangular in shape and bright yellow in color.

INTERPRETATION OF GEOCHEMICAL DATA

In geochemical mapping and exploration studies, very heterogeneous geological environments are often sampled. Changing geological units, weathering and climatological conditions are continuously refining and modifying the geochemcial background values. In soil and stream sediment surveys, the informations concerning rock materials and their transportation effects are of greater concern. Consequently, the basic problems of data processing in geochemical exploration and mapping concern the determination of different geochemical backgrounds, thresholds, and discrimination between background and anomalies. In most cases it is not possible to extract the relevant information related to surrounding rocks and mineralization from the analytical data of single element. For this purpose multielement analyses are required for routine determination. Besides the need for a well established geochemical background, sophisticated statistical methods are helpful in reducing and interpreting the resulting data sets. Reviews of useful statistical methods are given in Howarth (1983) and in Rock (1988).

Table 1. Geochemical data of the stream sediments pan concentrate from Timargara and Samar Bagh areas, southern Dir (All values are in ppm)

S.No.	Au	Ag	Pb	Cu	Zn	Co	Ni	Cr
PC1	0.05	0.50	8	65	73	47	25	103
PC2	0.05	0.50	5	31	32	22	19	128
PC3	2.48	0.50	8	72	82	60	50	239
PC4	0.05	0.50	9	78	80	61	57	244
PC6	0.10	0.50	6	55	34	40	24	180
PC7	0.05	0.50	8	86	63	45	76	570
PC8	0.59	0.50	12	90	100	68	104	602
PC9	0.99	0.50	9	95	98	58	86	398
PC11	0.07	0.71	7	38	42	24	14	47
PC12	0.98	0.50	13	99	72	57	53	242
PC13	0.85	29.00	8	98	65	97	63	301
PC14	0.56	0.50	8	110	68	78	61	279
PC15	0.06	2.31	6	83	33	15	13	129
PC16	0.04	0.50	72	18	24	16	13	88
PC17	0.07	0.50	7	32	42	27	24	270
PC18	0.05	0.50	5	48	34	40	23	79
PC19	0.03	0.50	5	16	16	10	22	118
PC20	0.06	0.50	5	19	25	13	13	152
PC21	0.76	0.50	9	120	76	82	58	230
PC22	0.06	0.50	6	28	38	19	15	136
PC23	0.07	0.50	7	30	31	13	30	137
PC24	0.58	0.50	6	19	26	17	17	83
PC25	0.05	0.50	5	41	31	25	25	113
PC26	2.54	0.50	5	51	43	16	17	105
PC27	0.05	0.50	5	16	31	15	24	186
PC28	0.27	0.50	8	43	50	68	52	142
PC29	0.59	1.29	102	429	32	41	36	139
PC31	0.04	0.50	145	40	27	20	26	126
PC32	1.56	1.07	11	105	85	43	51	320
PC33	0.04	0.50	5	8	27	16	22	139
PC35	0.06	0.50	88	33	37	21	61	201
PC36	0.04	0.50	5	32	25	19	21	108
PC37	0.10	1.02	10	65	55	35	29	117
PC38	0.63	1.31	13	39	66	39	100	603
PC39	0.05	0.50	5	15	29	15	41	465
PC40	0.47	0.50	17	173	72	48	50	89
PC41	0.05	0.50	12	90	80	85	43	241
PC42	0.94	0.50	15	93	79	53	50	147
PC43	0.05	0.50	18	94	81	51	41	152
PC44	3.47	1.04	10	36	59	40	71	585
PC45	0.21	2.09	21	63	80	59	21	105
PC46	0.49	1.29	13	36	52	28	77	851
PC47	0.09	0.85	9	19	51	26	70	530
PC48	0.04	0.50	11	10	14	10	49	620
PC49	0.09	0.89	9	37	36	28	75	1068
PC50	2.94	0.50	8	96	76	56	43	155
PC51	0.83	0.50	12	101	92	61	50	172
PC52	0.84	0.50	9	98	83	43	59	296
PC53	0.51	1.60	16	48	73	48	16	96
PC54	6.15	0.79	8	32	38	27	97	809
PC55	1.87	0.76	8	35	33	26	56	668
PC56	5.40	0.50	48	43	25	32	40	417
PC57	4.32	0.95	10	89	40	25	53	504
PC58	0.21	0.50	5	16	28	13	24	265
PC59	0.06	0.50	6	25	38	16	29	208
PC60	0.05	0.50	5	17	32	15	37	422

Table 2. Summary statistics for the stream sediment pan concentrates from Timargara and Samarbagh area, southern Dir. N; number of samples, $\bar{x}$; average (mean), Var.; variance, SD; standard deviation, C.Var.; coefficient of variance, Max.; maximim value, Min.; minimum value.

	Au	Ag	Pb	Cu	Zn	Co	Ni	Cr
N	56	56	56	56	56	56	56	56
$\bar{x}$	0.11	0.74	6.88	33.68	57.09	16.74	26.61	81.41
Var.	0.03	2.46	24.51	118.48	609.61	72.71	121.5	1492.6
SD	0.18	1.57	4.95	10.88	24.69	8.53	11.02	38.63
C.Var	1.65	2.12	0.72	0.32	0.43	0.51	0.41	0.47
Max.	0.76	12.00	21.00	74.00	127.00	43.20	81.00	298.00
Min.	0.05	0.00	0.00	18.00	25.00	7.00	12.00	30.00

A variety of methods have been devised for extracting an anomalous population out of composite population during the interpretation of data in geochemical exploration (Lepeltier 1969; Sinclair 1974, 1976; Otsu et al. 1948; Tennant and White 1959). The methods of Tennant and White (1959) and Sinclair (1974, 1976) have been used during this study. These methods seem to be most excellent in theoretical consideration, for the data processing during this study. The procedure of the data processing is as follows:

The data was ranked (arranged) in order of increasing magnitude and was divided into specific intervals of uniform width by a common formula: [K]=10.log10N; where [K] is the largest integer (number of intervals) contained in the right hand expression, and N is the number of observations. The class frequency, relative frequency, cumulative frequency and cumulative relative frequency (%) were calculated. The cumulative frequency distribution curve was then constructed for each element. This curve was further subdivided into several parts (i.e., background and low order and high order anomalous) at break points. Besides the cumulative frequency curves, the histograms of each element for both pan-concentrates and fine fractions were also constructed. Considering both these frequency distribution diagrams and other factors, a nominal threshold value for each indicator element has been selected. The data above threshold for each element was divided into low order and high order anomalous values. Both background along with low order and high order anomalous values for each element are plotted on each stream site, for both pan-concentrates and -80 mesh stream sediment samples, on a topographic map.

Table 3. Geochemical data of stream sediment fine fraction from Timargara and Samar Bagh areas, southern Dir. (All values are in ppm)

S.No.	Au	Ag	Pb	Cu	Zn	Co	Ni	Cr
SS1	0.05	0.5	5	32	38	17	15	60
SS2	0.05	0.5	5	22	38	10	17	30
SS3	0.05	0.5	8	41	95	20	30	89
SS4	0.05	0.5	7	45	71	14	18	65
SS6	0.05	0.5	5	30	40	12	15	35
SS7	0.76	0.5	8	38	80	20	81	83
SS8	0.05	0.5	5	34	80	30	32	108
SS9	0.05	0.5	7	46	95	26	28	112
SS11	0.05	0.5	5	24	37	14	13	38
SS12	0.72	0.5	7	51	96	35	30	78
SS13	0.05	0.5	7	47	78	27	32	76
SS14	0.05	0.5	6	52	76	23	26	68
SS15	0.05	0.5	5	22	39	10	18	60
SS16	0.05	0.5	5	23	45	11	13	34
SS17	0.05	0.5	11	27	35	12	12	40
SS18	0.05	0.5	5	28	42	16	17	87
SS19	0.05	0.5	7	40	51	17	37	94
SS20	0.05	3.0	16	28	49	14	18	60
SS21	0.48	0.5	13	31	103	34	32	298
SS22	0.05	0.5	6	25	48	16	27	60
SS23	0.05	0.5	5	35	43	15	32	70
SS24	0.05	0.5	6	28	44	13	17	48
SS25	0.05	0.5	5	26	58	16	27	92
SS26	0.05	0.5	6	46	53	15	29	70
SS27	0.05	0.5	5	23	39	9	25	48
SS28	0.05	0.5	5	28	45	12	37	70
SS29	0.05	0.5	5	18	42	11	30	68
SS31	0.05	0.5	5	45	49	15	33	54
SS32	0.05	0.5	5	22	39	9	25	70
SS33	0.05	0.5	5	28	41	10	23	54
SS35	0.05	0.5	5	39	42	16	58	150
SS36	0.05	0.5	5	27	48	13	25	56
SS37	0.05	0.5	5	19	37	10	21	50
SS38	0.05	0.5	5	22	34	7	23	70
SS39	0.05	12.0	20	35	32	10	30	120
SS40	0.05	0.5	15	38	80	30	32	113
SS41	0.05	0.5	17	39	94	43	40	112
SS42	0.5	0.5	13	31	117	36	32	84
SS43	0.56	0.5	16	33	127	32	31	78
SS44	0.05	0.5	5	20	42	10	20	65
SS45	0.05	3.6	6	40	52	12	27	105
SS46	0.05	0.5	5	22	38	9	17	90
SS47	0.05	0.5	5	22	35	7	23	70
SS48	0.05	0.5	5	26	32	11	25	120
SS49	0.05	0.5	5	32	25	10	16	98
SS50	0.05	0.5	14	42	108	26	34	89
SS51	0.05	0.5	16	38	84	24	34	73
SS52	0.74	0.5	18	40	93	28	32	80
SS53	0.05	0.5	5	24	50	11	22	80
SS54	0.05	0.5	5	43	53	13	30	108
SS55	0.05	0.5	5	58	40	14	24	106
SS56	0.05	0.5	5	74	43	14	24	80
SS57	0.05	0.5	7	39	46	12	18	93
SS58	0.05	0.5	21	36	53	11	18	74
SS59	0.05	0.5	8	25	58	10	21	62
SS60	0.05	0.5	5	37	45	12	24	114

Table 4. Summery statistics for the stream sediment fine-friction concentrates from Timargara and Samarbagh area, southern Dir. N; number of samples, $\bar{x}$; average (mean), Var.; variance, SD; standard deviation, C.Var.; coefficient of variance, Max.; maximim value, Min.; minimum value, D.L.; detection limit, C.A.; crustal abundance

	Au	Ag	Pb	Cu	Zn	Co	Ni	Cr
N	56	56	56	56	56	56	56	56
$\bar{x}$	0.8	1.2	16.0	62.5	51.0	37.0	43.0	11284
Var	1.8	14.5	668.3	3733	557.4	467.3	567.3	51076
SD	1.3	3.8	25.9	61.1	23.6	21.6	23.8	226.0
C.Var	1.7	3.2	1.6	1.0	0.5	0.6	0.6	0.8
Max	6.2	29.0	144.7	428.6	100	97.2	103.6	1067.5
Min	0.0	0.5	5.0	7.8	14.3	10.0	12.5	46.7
D.L.	0.1	0.5	5.0	5.0	5.0	5.0	5.0	5.0
C.A.	0.0	0.1	13.0	55.0	70.0	25.0	75.0	100

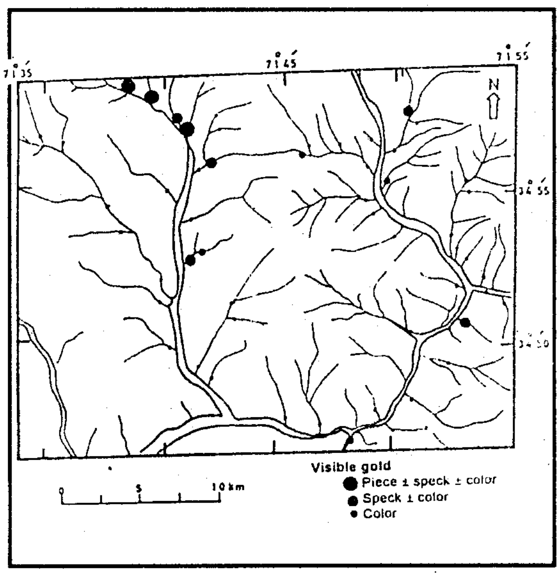

Figure 3. Distribution map of visible gold in the stream sediments of study area.

DISPLAYING AND EVALUATION OF DATA

The chemical data, obtained by analyzing the samples of pan-concentrates and fine fractions of stream sediments and rocks, have been displayed and evaluated by using single element and multi-element diagrams in order to pin point areas of most interest.

SINGLE ELEMENT PRESENTATION

Considering the statistical parameters, the distribution maps of each element on the basis of its concentration in pan-concentrate and fine fraction (-80 mesh) are prepared and are shown in figures 4 and 5 respectively. The results are discussed below.

Gold (Au) By considering the frequency distribution curves and histograms (not shown), the background, low order and high order anomalous intervals of <0.8ppm, 0.8-4ppm and >4ppm respectively are selected for the pan-concentrates while <0.4ppm, 0.4-0.6ppm and >0.6ppm respectively are selected for the fine fraction of the stream sediments. The distribution maps for gold in both pan-concentrate and fine fraction are prepared and are shown in figures 4a and 5a respectively. The distribution map of pan-concentrates (Fig. 4a) shows a wide geographical distribution of enhanced Au values (up to 7ppm) as compare to that of fine fraction (Fig. 5a). The highest, localized, Au values are found in the north and north-east of Kambat village near Sumerbagh, where metadiorite, metagranodiorite and metagabbronorite of the Samerbagh complex are exposed. The gold concentration in these rocks ranges from 0.000ppm to 0.009ppm in metadiorite, from 0.000ppm to 0.004ppm in granodiorite and from 0.000ppm to 0.007ppm in gabbronorite (Table 5). Minor gold enhancement is also observed in certain streams in north-eastern portion of the study area in the vicinity of Lal Qala where mainly the metadiorite and amphibolites of the Timargara complex are exposed.

Considering the low order and high order anomalous values of gold, the area north of Samarbagh can be pinpointed as a source of gold anomaly in the stream sediments pan-concentrates. It seems that the rocks of the area are not contributing to the high anomaly of gold in pan-concentrates. But this anomaly could be related to a specific type of mineralization, most probably in the form of quartz veins.

Silver (Ag) About 72% of pan-concentrate and 95% of the fine fractions of steam sediments in the area are below detection limit (<0.5ppm). By considering the frequency distribution curves and histogram (not shown), the background, low order and high order anomalous values of <2ppm, 2-20ppm and >20ppm respectively in pan-concentrate and <2ppm, 2-7ppm and >7ppm respectively in fine fraction are selected. Figures 4b and 5b are the distribution maps of silver in the area. The distribution pattern of silver in both pan-concentrates and fine fraction is very different. However, one sample near Maiar show low order anomaly in both the fractions (Fig. 4b and 5b). Silver concentrations in all the rock samples (Table 5) of the study area are below detection limit (<0.5) and, therefore, indicate no contribution with regard to silver.

Copper (Cu) By considering the frequency distribution curves and histograms of copper (not shown), the values of 50ppm and 24ppm are treated as the nominal threshold value for pan-concentrate and fine fraction respectively. The values of 50-130ppm and >130ppm are considered as low and high order anomaly respectively in pan-concentrates and 24-50ppm and >50ppm as low and high order respectively in the fine fraction. The distribution maps of copper for both pan-concentrates and fine fractions are shown in figures 4c and 5c respectively. The low order anomaly of copper in the fine fraction is widely distributed through out the study area as compared to the pan-concentrates. Three streams, two in the northern part of Kambat and one south of Lal Qala, have high order anomalous copper concentration in the fine fraction (Fig. 5c). Two streams have high order anomalous concentration in pan-concentrates as shown in figure 4c. Both pan-concentrate and fine fractions have, to some extent, similar distribution pattern of copper.

Low to high order anomalous values of copper, though not really high, could be attributed to the rocks of basic to intermediate composition (diorite, gabbronorite, amphibolite etc.) in the area where the Cu is ranging from about 30-140ppm (Table 5). This suggest that the Cu anomaly in stream sediments is not related to a specific type of mineralization.

Zinc (Zn) Threshold values of 40ppm for pan-concentrate and 60ppm for fine fraction have been determined by considering the frequency distribution diagrams and histograms (not shown). The low and high order anomalous values are 40-60ppm and >60ppm respectively in the pan-concentrates and 60-80ppm and >80ppm respectively in the fine fraction. The distribution pattern of Zn in figure 4d and5d indicates that it has generally high order anomalous values in both pan-concentrate and fine fraction of many streams of the studied area. Both pan concentrates and fine fractions have more or less similar distribution patterns for Zn. The concentration of zinc in various rocks of the studied area are ranging from 15 to 90ppm (Table 5). This suggests that the anomalous values, though not really high, in stream sediments could be contributed by the rocks rather than by the specific type of mineralization.

Lead (Pb) The frequency distribution of Pb in the form of frequency curves and histograms (not shown) suggest nominal threshold value of 25ppm in the pan-concentrate and 8ppm in fine fraction.

Table 5. Trace elements of various rocks from Timaragara and Samarbagh area, southern Dir. (Au is in ppb, rest are in ppm)

S.No.	Zn	Pb	Cu	Ni	Cr	Co	Ag	Au
Metdiorite and metaquartz-diorite								
TMG1	68	47	44	68	56	63	<0.5	4
TMG3	78	44	44	54	55	63	<0.5	7
TMG4	63	46	104	52	61	59	<0.5	7
TMG5	67	35	59	32	45	65	<0.5	9
TMG6	51	32	86	30	32	63	<0.5	3
TMG114	60	32	70	24	34	63	<0.5	5
TMG115	61	30	48	38	43	58	<0.5	8
TMG117	95	39	56	35	52	61	<0.5	6
TMG118	88	34	90	25	36	64	<0.5	6
TMG119	78	42	70	31	33	52	<0.5	7
SMR45	97	40	88	56	48	67	<0.5	2
SMR47	64	51	51	52	50	66	<0.5	2
SMR48	64	46	45	52	48	59	<0.5	5
SMR49	68	37	62	59	48	60	<0.5	0
SMR50	62	37	36	57	51	67	<0.5	0
Metagabbro-norites and metagabbro								
TMG28	67	31	46	52	69	58	<0.5	0
TMG29	69	32	73	49	79	62	<0.5	0
TMG30	62	41	54	77	114	61	<0.5	0
TMG31	71	52	64	51	84	65	<0.5	4
TMG33	78	53	42	41	62	64	<0.5	6
TMG35	68	43	45	59	56	47	<0.5	3
SMR37	75	40	77	92	105	68	<0.5	6
SMR38	65	36	75	86	102	67	<0.5	7
SMR39	84	55	59	-	96	70	<0.5	2
SMR40	81	44	59	59	98	67	<0.5	0
SMR41	88	47	60	66	100	51	<0.5	0
SMR42	77	48	74	67	100	58	<0.5	4
SMR51	53	52	48	86	160	71	<0.5	5
SMR53	59	43	49	-	105	68	<0.5	0
SMR54	70	47	43	76	142	66	<0.5	4
SMR55	61	29	28	66	127	58	<0.5	4
SMR56	71	50	57	49	64	54	<0.5	7
SMR57	67	38	-	48	73	64	<0.5	8
SMR58	53	34	62	74	97	52	<0.5	0
SMR59	63	44	59	52	69	71	<0.5	4
Metagranodiorites								
SMR24	43	41	52	16	24	71	<0.5	3
SMR25	30	40	56	15	13	93	<0.5	4
SMR26	15	35	44	12	8	56	<0.5	0
Metagranites								
SMR99	29	22	38	12	14	57	<0.5	2
SMR103	22	31	39	17	12	73	<0.5	4
SMR104	26	42	43	15	12	62	<0.5	5
SMR108	15	33	50	14	13	62	<0.5	2
SMR109	16	29	41	13	15	66	<0.5	0

The distribution pattern of Pb in figures 4e and 5e show that certain streams in the Jandul valley (western half) of study area have high order anomalous values of Pb in fine fraction while few streams in eastern half are also having high and low order anomalous values in the pan-concentrates. Both the pan- concentrates and fine fractions have different distribution pattern for Pb.

Various rocks of the study area have lead in the range of 20 to 55ppm (Table 5). This suggest that the anomalous values of lead in the stream sediments, though not high, can be related to the various rock types and not to the specific type of mineralization in the area.

Nickel (Ni) The frequency distribution curves and the histograms of Ni (not shown) suggest that the nominal threshold value in pan-concentrate is 30ppm while in fine fraction, it is 40ppm. Low and high order anomalous values are 30-80ppm and >80ppm respectively in pan-concentrates and 40-60ppm, and >60ppm respectively in the fine fraction of stream sediments. The concentration of nickel for each sample site in both pan-concentrates and fine fractions are plotted on the distribution diagrams (Figs. 4f and 5f). The distribution pattern of Ni in pan concentrates (Fig. 4f) shows a wide distribution of low order anomaly of Ni in the streams of the study area while the distribution pattern of fine fractions shows no anomaly in these streams. The high order anomaly in both pan-concentrates and fine fraction is restricted to three streams west of Lal Qala and a stream near Kambat in the study area (Figs. 4f and 5f).

Chromium (Cr) Threshold values of 200ppm of Cr in pan-concentrate and 130ppm in fine fractions have been selected after consulting the frequency distribution curves and histograms (not shown). The low order and high order anomaly of Cr is distinguished as 200-600ppm and >600ppm respectively in pan concentrates and 130-250ppm and >250ppm respectively in fine fraction. The data has been presented on the distribution diagrams (Figs. 4g and 5g). The distribution pattern of pan concentrates (Fig. 4g) is different from that of the fine fractions (Fig. 5g). Many streams in the western half of the area are anomalous while few streams in the north-eastern portion of the study area show low to high order anomaly in the pan-concentrates. However, only two streams have high order anomaly in the fine fraction while rest of the streams have the background values.

Cr and Ni distribution maps are analogous. Their high order anomaly in the area west of Lal

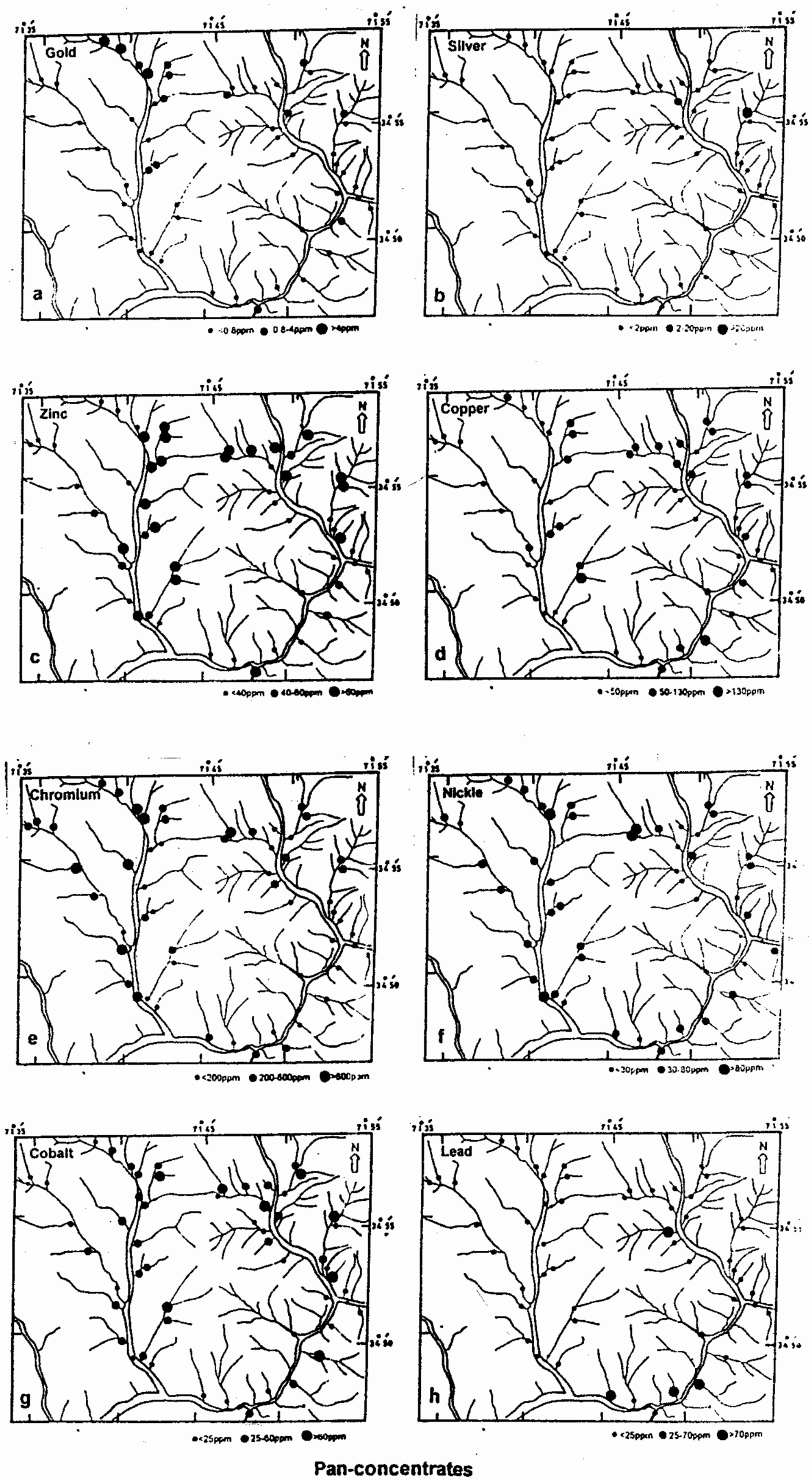

Figure 4. Distribution map of Au, Ag, Zn, Cu, Cr, Ni, Co and Pb for the pan concentrates of the stream sediments of the study area.

Table 6. The individual anomaly score for each element along with the SCORESUM of both pan concentrates and fine fraction (-80 mesh)for the drainage cells of the study area.

Sample No.	Au	Ag	Cu	Pb	Zn	Ni	Cr	Co
PC1	0	0	1	0	1	1	0	1
SS1	0	0	1	0	0	0	0	0
PC2	0	0	0	0	0	0	0	0
SS2	0	0	0	0	0	0	0	0
PC3	1	0	1	0	2	1	1	1
SS3	0	0	1	0	2	0	0	0
PC4	0	0	1	0	2	1	1	2
SS4	0	0	1	0	1	0	0	0
PC6	1	0	1	0	0	0	0	2
SS6	0	0	1	0	0	0	0	0
PC7	0	0	1	0	2	1	1	1
SS7	2	0	1	0	1	2	0	0
PC8	0	0	1	0	2	2	2	2
SS8	0	0	1	0	1	0	0	1
PC9	1	0	1	0	2	2	1	1
SS9	0	0	1	0	2	0	0	1
PC10	0	0	0	0	1	0	0	0
SS10	0	0	0	0	0	0	0	0
PC12	1	0	1	0	2	1	1	1
SS12	2	0	2	0	2	0	0	2
PC13	1	2	1	0	2	1	1	2
SS13	0	0	1	0	1	0	0	1
PC14	0	0	1	0	2	1	1	2
SS14	0	0	2	0	1	0	0	1
PC15	0	1	1	0	0	0	0	0
SS15	0	0	0	0	0	0	0	0
PC16	0	0	0	2	0	0	0	0
SS16		0	0	0	0	0	0	0
PC17	0	0	0	0	0	0	1	1
SS17	0	0	1	1	0	0	0	0
PC18	0	0	0	0	0	0	0	1
SS18	0	0	1	0	0	0	0	0
PC19	0	0	0	0	0	0	0	0
SS19	0	0	1	0	0	0	0	0
PC20	0	0	0	0	0	0	0	0
SS20	0	0	1	0	1	0	0	0
PC21	0	0	1	0	2	1	1	2
SS21	1	0	1	1	1	0	2	2
PC22	0	0	0	0	0	0	0	0
SS22	0	0	1	0	0	0	0	0
PC23	0	0	0	0	0	0	0	0
SS23	0	0	1	0	0	0	0	0
PC24	0	0	0	0	0	0	0	0
SS24	0	0	1	0	0	0	0	0
PC25	0	0	0	0	0	0	0	0
SS25	0	0	1	0	0	0	0	0
PC26	1	0	1	0	1	0	0	0
SS26	0	0	1	0	0	0	0	0
PC27	0	0	0	0	0	0	1	0
SS27	0	0	0	0	0	0	0	0
PC28	0	0	0	0	0	1	0	2
SS28	0	0	1	0	0	0	0	0
PC29	0	0	2	2	0	1	0	1
SS29	0	0	0	0	0	0	0	0
PC31	0	0	0	2	0	0	0	0
SS31	0	0	1	0	0	0	0	0

Sample No.	Au	Ag	Cu	Pb	Zn	Ni	Cr	Co
PC32	1	0	1	0	0	1	1	1
SS32	0	0	0	0	0	0	0	0
PC33	0	0	0	0	0	0	0	0
SS33	0	0	1	0	0	0	0	0
PC35	0	0	0	2	0	1	0	0
SS35	0	0	1	0	0	1	0	0
PC36	0	0	0	0	0	0	0	0
SS36	0	0	1	0	0	0	0	0
PC37	0	0	0	0	1	1	0	1
SS37	0	0	0	0	0	0	0	0
PC38	0	0	0	0	2	2	2	1
SS38	0	0	0	0	0	0	0	0
PC39	0	0	0	0	0	1	1	0
SS39	0	0	1	2	0	0	0	0
PC40	0	0	1	0	2	1	0	1
SS40	0	0	1	2	1	0	0	1
PC41	0	0	1	0	2	1	1	2
SS41	0	0	1	2	2	0	0	2
PC42	1	0	1	0	2	1	0	1
SS42	0	0	1	1	2	0	0	2
PC43	0	0	1	0	2	1	0	1
SS43	0	0	1	2	2	0	0	2
PC44	1	0	0	0	1	1	1	1
SS41	0	0	0	0	0	0	0	0
SS45	0	1	1	0	0	0	0	0
PC46	0	0	0	0	1	1	2	1
SS46	0	0	0	0	0	0	0	0
PC47	0	0	0	0	1	1	1	1
SS47	0	0	0	0	0	0	0	0
PC48	0	0	0	0	0	1	2	0
SS48	0	0	1	0	0	0	0	0
PC49	0	0	0	0	0	1	2	1
SS49	0	0	1	0	0	0	0	0
PC50	1	0	1	0	2	1	0	1
SS50	0	0	1	2	1	0	0	1
PC51	1	0	1	0	2	1	0	2
SS51	0	0	1	2	2	0	0	1
PC52	1	0	1	0	2	1	1	1
SS52	2	0	1	2	2	0	0	1
PC53	0	0	0	0	1	0	0	1
SS53	0	0	0	0	0	0	0	0
PC54	2	0	0	0	0	2	2	1
SS54	0	0	1	0	0	0	0	1
PC55	1	0	0	0	0	1	2	1
SS55	0	0	2	0	0	0	0	0
PC56	2	0	0	1	0	1	1	1
SS56	0	0	2	0	0	0	0	0
PC57	2	0	1	0	0	1	1	0
SS57	0	0	1	0	0	0	0	0
PC58	0	0	0	0	0	1	1	0
SS58	0	0	1	2	0	0	0	0
PC59	0	0	0	0	0		1	0
SS59	0	0	1	0	0	0	0	0
PC60	0	0	0	0	0	0	0	1
SS60	0	0	1	0	0	0	0	0

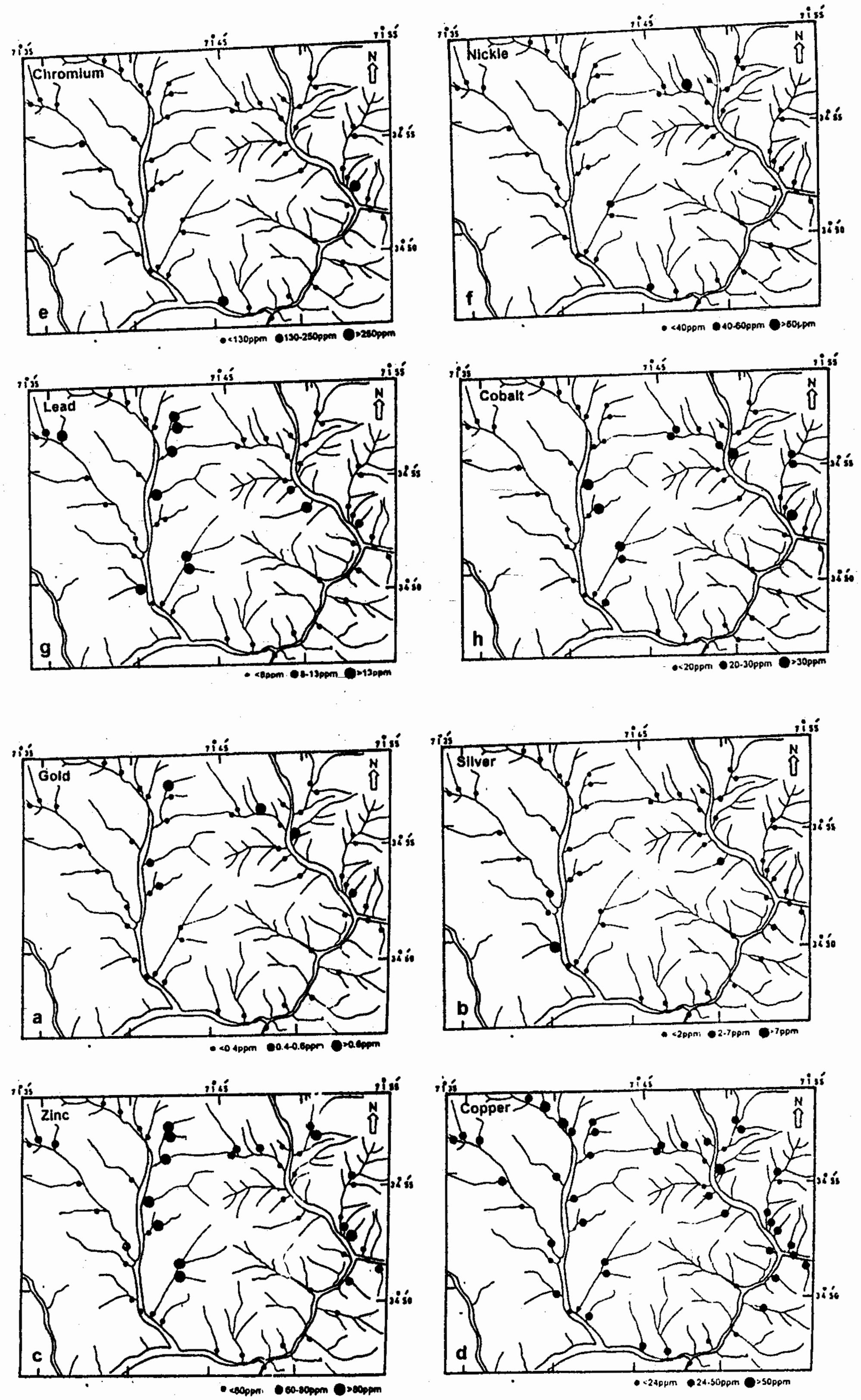

Fine fractions

Figure 5. Distribution map of Au, Ag, Zn, Cu, Cr, Ni, Co and Pb for the fine fractions (-80 mesh) of the stream sediments of the study area.

Qala, in the northeastern portion of the study area, is due to the presence of small exposure (10-15 m thick; not shown on the geological map) of ultramafic rock. The low order anomalous values of Cr and Ni in the western half of the study area can be attributed to the presence of metagabbro and metagabbro-norites of the Samarbagh and Tora Tiger complexes (Fig. 1). The high order anomalous values (maximum of 1068ppm) of Cr in this region may indicate the occurrence of ultramafic rocks. Nickel is, however, having low order anomaly in this region, except in two streams one near Kambat and another west of village Munda Qala. Basic to intermediate rocks of the study area have Ni in the range of 10 to 90ppm and Cr in the range of 10 to 160ppm (Table 5). The ultramafic rocks of the area are not analyzed during this study, however, Jan and Tahirkheli (1990) have reported Ni upto 1174ppm and Cr upto 5586ppm in the ultramafic rocks of the Tora Tiga complex of the study area. It is, therefore, suggested that the spread of enhanced Cr and Ni through out most part of the studied area could be related to the bed rocks and not to a specific mineralization.

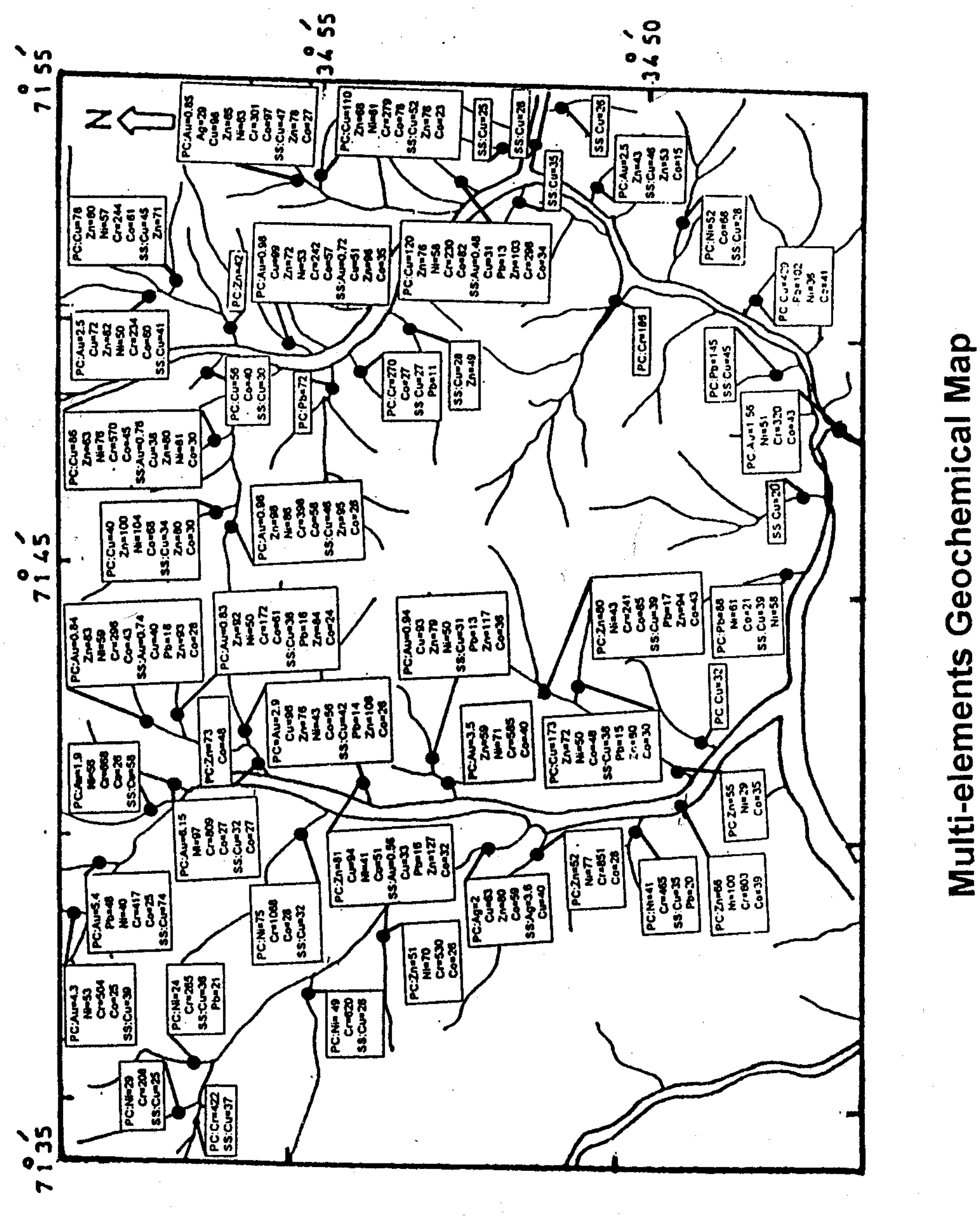

Figure 6. Map showing anomalous elements in both pan-concentrates and fine fraction (-80 mesh) of stream sediments of the study area: PC; pan-concentrate samples, SS; fine fraction samples.

Table 7. Summery of background and anomalous range for eight elements in 56 samples, each of pan-concentrates and fine fraction (-80 mesh), of the stream sediments of the study area (all values are in ppm). PC = pan-concentrates, SS = -80 mesh sample

Element	Sample type	Back-ground Value score = 0	% of sample	Anomalous samples Low order score = 1	High order score = 2
Au	PC	<0.8	74	0.8--4	>4
	SS	<0.04	91	0.4--0.6	>0.6
Ag	PC	>2	95	2--20	>2.0
	SS	>2	95	2--7	>7
Cu	PC	<160	96	160--300	>300
	SS	<24	23	24--50	>50
Pb	PC	<25	91	25--70	>70
	SS	<8	79	8--13	>13
Zn	PC	<40	48	40--60	>60
	SS	<50	59	50--80	>80
Ni	PC	<23	25	24--80	>80
	SS	<24	39	40--60	>60
Cr	PC	<170	45	170--600	>600
	SS	<150	98	150--250	>250
Co	PC	<20	29	20--60	>60
	SS	<13	50	13--30	>30

Cobalt (Co) The frequency distribution curves and histograms of Co (not shown) suggested a nominal threshold values of 25ppm in pan-concentrate and 20ppm in fine fraction of stream sediments. The low and high order anomalous values for Co in pan-concentrate are distinguished as 26-60ppm and >60ppm respectively while for fine fraction, these are considered as 20-30ppm and >30ppm respectively. The pan concentrate distribution pattern for Co (Fig. 4h) shows that most streams in the western part of the study area while some streams in the eastern part of the study area are low order anomalous. However, two streams in the western half and few streams in the eastern half of the study area are having high order anomalies in the pan-concentrates (Fig. 4h). Instead of few streams, the rest of the streams of the area have back ground values in the fine fractions of the stream sediments (Fig. 5h). The distribution pattern of Co in both the fractions (i.e., pan concentrate and fine fraction) are, therefore, not similar. Various rocks of the study area have Co in the range of 50 to 95ppm (Table 5). The spread of Co anomalies in the area, therefore, suggests that these anomalies are generated by the existing rocks and may not be attributed to the specific mineralization.

By considering the single element distribution pattern of both pan-concentrates and fine fractions, it is concluded that Cu, Pb, Zn, Ni, Cr, and Co are expected to reflect the bed rock geology of the area.

MULTI-ELEMENTS PRESENTATION

For the multi-elements presentation of the stream sediment data, a SCORSUM technique of Chaffee (1983) has been used. According to this technique the full range of chemical data for each element of interest in both pan-concentrations and fine fractions have been divided into three categories of background, low and high anomalous values as in the case of single element presentation. For simplicity the same background, low and high order anomalous values are taken as those obtained through the cumulate frequency curves and histograms plotted during the displaying of single element data in the previous section. The data is summarized in Table 6 . The background, low and high order anomalous values are scored here as 0, 1 and 2 respectively. The original chemical data set for each element, in both pan-concentrates and fine fractions, is transferred to a matrix of anomaly scores as shown in Table 7. All of the anomalous elements and their concentrations for both pan-concentrates (denoted as PC) and fine fractions (denoted as SS) for the study area are displayed on drainage map (Fig. 6). This map serves as a compilation sheet to be used for manually calculating the SCORESUM for each site. The scores obtained for each element are then summed (SCORESUM) for each site and are given in Table 7. These SCORESUMS (shown in circle) along with the scores of individual medium are then plotted on a summery drainage map (Fig. 7).

Various cells (catchment areas) in the studied area have been identified / marked as anomalous on the basis of SCORSUM technique as shown in figures 6 and 7. These anomalous areas mainly lie on the eastern side of the Samarbagh Khawar (stream) and also in the north-eastern portion of the study area. These anomalous areas have anomalies for Zn, Ni, Cr, Co and sometime for Cu (Fig. 6). However, in certain cells, especially in the north and north-eastern parts of Samarbagh, Au is anomalous from low order to high order. These areas, therefore, are interpreted to have potential for the gold mineralization. Thus this map is very useful in delineating the anomalous areas which could further be evaluated for any kind of mineralization.

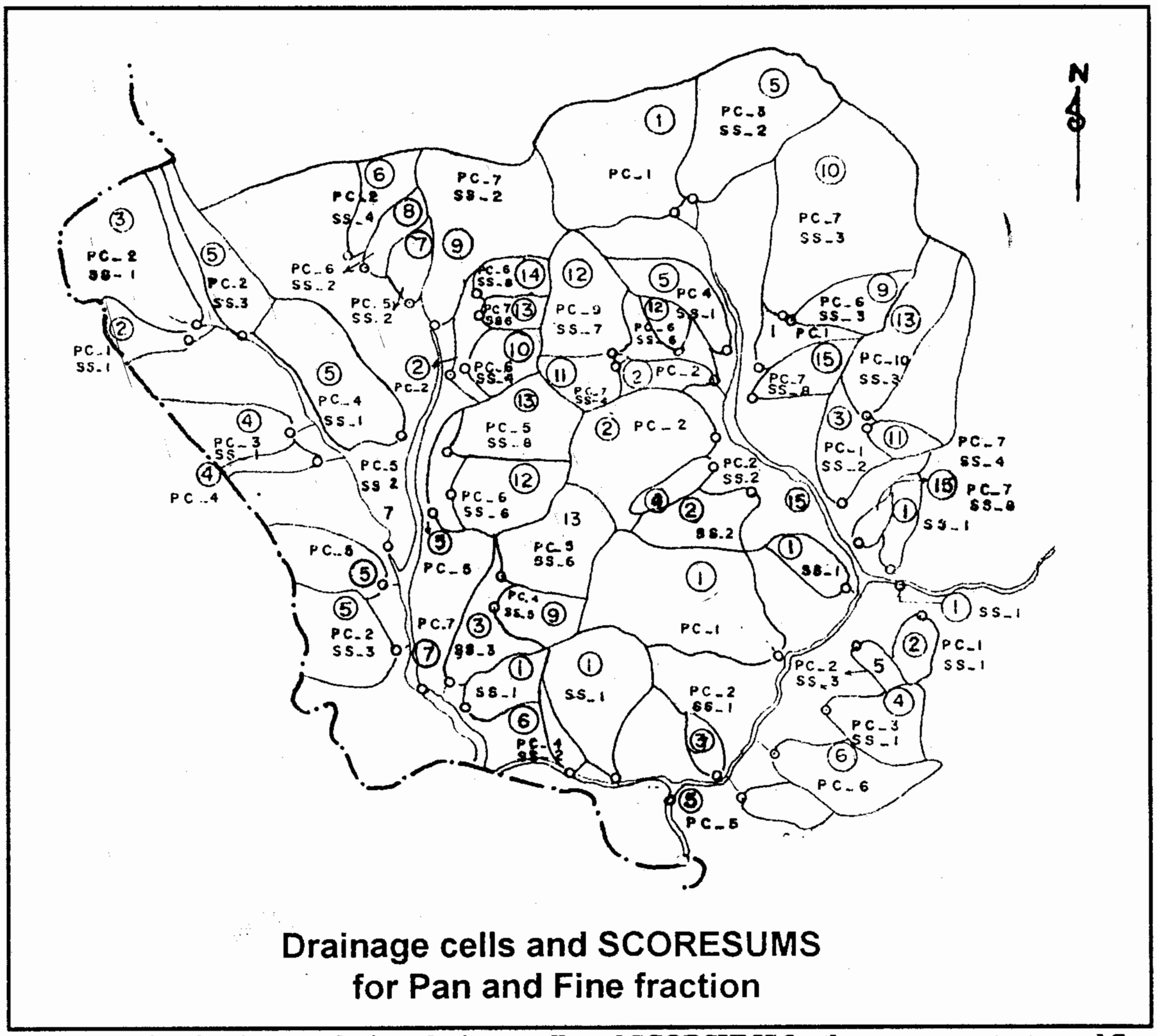

Figure 7. Map showing sample sites, drainage cells and SCORSUMS for the pan-concentrates and fine fractions (-80 mesh) of the study area. PC; pan-concentrate samples SCORSUMS, SS; fine fraction samples SCORSUMS. Number in circle is the sum of SCORSUMS for the two media. Small open circles indicate sample sites.

The concentration of various elements and summary statistics for both fine and heavy fractions of the stream sediments in tables 1, 2, 3 and 4 show that about 93% of Au and 95% of Ag in the fine fractions and 32% of Au and 82% of Ag in the pan-concentrates are equal or below the detection limit.The rest of the elements (i.e. Cu, Pb, Zn, Ni, Cr and Co) are above the detection limit. The statistical parameters further exhibit that the fine and heavy fractions have very different background levels. Most of the analyzed elements including base metals have enrichment in the heavy fractions, especially Au and Cr are highly enhanced in the pan-concentrates relative to fine fraction of stream sediments in the study area. Generally, base metals occur in silicate and sulfide phases of bed rocks of which silicates are more stable than sulfides in the stream environment. Therefore, mostly the surficial processes cause concentration of these metals in the fine fractions which are derived from the less resistant minerals such as sulfides. The less concentration of even Cu, Pb and Zn in the fine fractions of the studied samples is, therefore, unlikely as these metals are usually concentrated in the fine fractions of the stream sediments. The abundance of Au, Cr, and Ni in the pan-concentrates is obvious because of the presence of gold in the form of pieces, specks and colors and Ni and Cr-bearing minerals such as pyroxene, olivine and chromite etc. and also the rock fragments.

There could be many causes for such type of unlikely behaviour of these metals. These could be: 1) due to extreme relief of the area, the surficial weathering and erosional processes are less effective in the area. This might not have given a chance to these metals to concentrate as fine fraction of

<177mm (-80 mesh) and may have remained in the coarser fraction of the stream sediments; 2) these metals could be silicate bound (i.e., found in the resistant minerals) rather than sulfide bound in the stream sediments; 3) dissolved and particulate trace elements may fluctuate widely depending on seasonal flow rate. It is most probable that due to the individual effect or combined effect of the above mentioned factors, the fine fraction of stream sediments in the area do not provide adequate anomaly/background contrast to satisfy the requirement imposed by the sample density. However, pan-concentrates could be the right medium to pinpoint areas of interest (especially for gold) in the area of study.

CONCLUSIONS

The area of study is mainly composed of metadiorites, metagabbro-norites and amphibolites with lesser amount of metagranites, meta volcanics, aplite dikes, tonalites, hornblendites and ultramafites. The geochemical studies of these rocks do not show any kind of anomaly in regard to base and precious metals. The stream sediments studies suggest that the pan-concentrates have high concentration of all the elements (i.e. Au, Ag, Cu, Pb, Zn, Ni, Cr and Co) as compare to that of fine fraction (-80 mesh). Though Cu, Pb, Zn, Ni, Cr and Co are anomalous in the pan-concentrates of the stream sediments, they could be related to the bed rocks rather than to specific type of mineralization in the area. The anomalous gold, however, could not be directly related to the bed rocks. Its high order anomaly (both as visibly and geochemically) suggest that the area north and northeast of Samarbagh has the potential for gold mineralization.

REFERENCES

Ahmad, W., 1962. Copper showings in the Usheri region, Dir, Pakistan. Geol. Surv. Pak. Min. Inf. Circ. No,.8, p. 14.

Arbab, M.S.H. and Khan, R.N., 1973. Geology of Dir and Northern part of Timargara Quodranle, N.W.F.P. Pakistan. Geol. Surv. Pak. Inf. Rel. No.49.

Banaras, M. and Ghani, A., 1982. Petrography of the Tora Tiga complex. Munda area, Dir district, unpublished M.Sc. Thesis, Univ. Peshawar.

Bellehumeur, C., Marcotte, D. and Jebrak, M., 1994. Multi-element relationship and spatial structures of regional geochemical data from stream sediments, south-western Quebec, Canada. J. Geochem. Explor. 51, p. 11-35.

Butt, K.A., Chaudhry, M.N.and Ashraf, M., 1980. An Interpretation of petrotectonic Assemblage west of western Himalayan syntaxis in Dir District and adjoining Areas in Northern Pakistan. Geol. Bull. Univ. Peshawar. 13, p. 79-86.

Chaffee, M.A., 1983. Scoresum- Atechnique for displaying and evaluating multi-element- geochemical information, with examples of its use in regional mineral assessment programs. J. Geochem. xplor. 19, p. 361-381.

Chaudhry, M.N. and Chaudhry, A.G. 1974. Geology of Khagram area, Dir district. Geol. Bull. Punjab Univ. 11, p. 21-44.

Davenport, P.H; 1990. A comparison of regional geochemical data from lakes and streams in northern abrador: implications for mixed-media geochemical mapping. J. Geochem. Explor. 39, p. 117-151.

Hamidullah, S. and Islam, F. and Farooq, M., 1990. Petrology and goechemistry of the western part of the Dir Ignious complex, Kohsitan island arc. Northern Pakistan. In: Geology and Geodynamic evolulion of the Himalayan collision zone (Sharama, K.K. ed.). Phys. Chem. Earth, 17, p. 31-46.

Howarth, R.J., 1983. Statistics and data analysis in geochemical prespecting. In: Handbook of Exploration Geochemistry (G.J.S. Govett, ed.). Elsevier, Amsterdam, 2, 437p.

Hyden, H.H., 1915. Notes on the geology of Chitral Gilgit and Pamirs. Geol. Surv. India, 45, p. 271-335.

Jan, M.Q., Kempe, D.R.C. and Tahirkheli, R.A.K., 1969. The Geology of corundum bearing and related rock around Timargara. Geol. Bull. Univ. Peshawar, 4, p. 82-89.

Jan, M.Q., 1979. Petrology of the obducted mafic and ultramafic metamorphites from the southern part of Kohistan island arc sequence. Geol. Bull. Univ. Peshawar. 13, p. 95-107.

Jan, M.Q., and Howie, R.A., 1981. The mineralogy and geochemistry of the metamorphosed basic and ultrabasic rocks of the Jijal Complex, Kohistan, NW Pakistan. J. Petrolgoy 22, p. 85-126.

Jan, M.Q., Banaras, M., Ghani, A. andKhan, M.A., 1983. The Tora Tiga ultramafic comlex, southern Dir District. Geol. Bull. Univ. Peshawar, 16, p. 11-29.

Jan, M.Q., 1988. Geochemistry of amphibolites from the southern part of the Kohistan arc, N Pakistan. Mineral. Mag. 52, p. 147-159.

Jan, M.Q. and Tahirkheli, A.Z., 1990. The Tora Tiga complex, southern Dir, NW Pakistan; an example of mafic-ultramafic rocks in the bottom of an island arc. Geol. Bull. Univ. Peshawar,23, p. 231-251.

Kakar, S.K., Badshah, M.S., and Khan, J. 1971. The geology of the Jandul valley, western Dir. Geol. Bull. Univ. Peshawar, 6, p. 54-73.

Khan, R.N., 1969. Geology of Timargara Quadrangle, Dir. NW Pakistan. Geol. Surv. Pak. unpublished.

Lepeltier, C; 1969. A simplified statistica treatment of geochemical data by graphical representation. Econ. Geol. 64, p. 538-550.

Majid, M. and Paracha, F.a., 1980. Calc-alkaline magmatism at destructive plate margin in N.Pakistan. Geol. Bull. Univ.

Peshawar, 13, p. 109-120.

Majid, M., Shah, M.T., Latif, A; Aurangzeb; Kamal, M., 1981. Major element abundances in the Kalam Lauas . Geol. Bull. Univ. Peshawar, 14, p. 45-62.

Otsu, H., Kubotta, R. and Matsuda, Y., 1984. Partition of statistical frequency distribution of geochemical data. Min. Geol. 34, p. 51-56 (Japanese with English abstract).

Rock, N.M.S; 1988. Numerical Geology, Lecture notes in earth sciences, Springer, Berlin, 427p.

Sarwar, A., 1996. Litho and stream sediments geochemical investigation for base and precious metal in Timargara, Maidan and Jandul area, District Dir, northern Pakistan. unpublished M.Phil. Thesis, Univ. of Peshawar.

Shah, M.T., 1991.Geochemistry, mineralogy and petrology of the sulfide mineralization and associated rocks in the area around Besham and Dir, Northern Pakistan unpublished. Ph.D. Thesis Univ. South Carolina, Columbia USA.

Shah, M.T., Shervais, J.W. and Ikramuddin, M., 1994. The Dir meta-volcanic sequence: Calcalkaline magmatism in the Kohstan arc terrance, northern Pakistan. Geol. Bull. Univ. Peshawar, 27, p. 9-27.

Shah, M.T. and Hamidullah, S., 1994. Field and mineralogical constraints of the Dir metavolcanic sequence, Kohistan arc terrane, northern Pakistan. Geol. Bull. Univ. Peshawar, v. 27. P. 43-55.

Shah, M.T., Sarwar, A., Khattak, M.U.K. and Siddiqui, S.A., (in press). Petrochemical account of various types of rocks of Timargara and Samerbagh areas of southern Dir, Kohistan arc terrane, northern Pakistan.

Sinclair, A.J., 1974. Selection of threshold in geochemical data using probability graphs. J. Geochem. Explor. 3, p. 129-149.

Sinclair, A.J., 1976. "Probability graphs" Assoc. Exploration Geochemists, Spec. 4, 95p.

Sullivan, M.A., Windley, B.F., Saumders, A.D., Haynes, J.r. and Rex. D.C., 1993. A palaeogeographic reconstruction of the Dir group: evidence for magmatic arc migration within Kohistan, N. Pákistan. In: Himalayan tectonics. CP. J. Treloar and M.P. Searl, eds). Spec. Publ. No.74 Geol. Soc. London, p. 139-160.

Tahirkheli, R.A., 1979. Geology of Kohistan and adjoining eurasian and Indo-Pakistan continents, Pakistan. Geol. Bull. Univ. Peshawar. 11, p. 1-30.

Tahirkheli, R.A.K., 1982. Geology of Himalaya, Karakoram and Hindukush in Pakistan. Geol. Bull. Univ. Peshawar, 15, 54 p.

Tennant, C.B. and White, M.L., 1959. Study of the distribution of some geochemical data. Econ. Geol. 54, p. 1281-1290.

Manuscript Received 23rd July 1999
Revised Manuscript Received 29th August 1999
Accepted 1st September 1999

ACTA
MINERALOGICA
PAKISTANICA
Volume 9 (1998)

Article Reference
AMP9.1998/055-061/ISSN.0257-3660

COMPARATIVE STUDY OF MAJOR NATURAL CONTAMINANTS IN AQUIFERS OF PIEDMONT PLAIN AND VALLEY FLOOR, KUCHLAGH-BELELI AREA NEAR QUETTA, PAKISTAN

MUHAMMAD UMAR[1], ZAHOOR AHMAD[2], MUHAMMAD IQBAL KASSI[2], KHALID REHMAN[3], ABDULLAH BARYALAI[4] And ABDUL TAWAB KHAN[1]
[1] Department of Geology, University of Balochistan Quetta.
[2] Department of Statistics, University of Balochistan Quetta.
[3] Bureau of Water Resources, Government of Balochistan Quetta.
[4] Public Health Engineering Department, Government of Balochistan Quetta.

ABSTRACT

The piedmont plain along Takatu highland and downward valley floor around Beleli and Kuchlagh, was selected for study of natural contaminants in groundwater. Analyses of groundwater samples collected during field work indicate that in the piedmont plain calcium and magnesium, calcium and sulphate, magnesium and sulphate, sodium and sulphate have good positive correlation where as in valley floor sodium and chloride, sodium and sulphate, chloride and sulphate have good positive correlation. The t-test of all variables except depth of tube wells and magnesium that are salinity, alkalinity, calcium, sodium, bicarbonate, sulphate and chloride indicates a significance difference of two areas i.e; piedmont plain and valley floor. On the basis of salinity hazard and alkalinity hazard piedmont plain, transitional zone and lower valley floor aquifers fall into C2-S1,C3-S1 and C3-S2,C4-S3,C4-S4 categories respectively. The groundwater is rich in alkaline earths at piedmont plain while at valley floor it is rich in alkalies. The sodium and chloride are quite abundant in groundwater in valley floor as compared to the piedmont plain.

The soil and soluble lacustrine deposits of Bostan Formation (which is exposed in valley floor) are mainly responsible for the abundance of salt concentration and variation in salt types in two areas i.e. valley floor and piedmont plain. The consequences show that the groundwater in valley floor is not satisfactory for irrigation and it may need addition of gypsum, calcium salts, and some leaching. The sodium and salt tolerant crops may be recommended for cultivation in valley floor.

INTRODUCTION

The development of an area is commonly based on suitable and safe supply of water for different purposes like drinking, agriculture and industry. The suitability of water for different uses depends upon number of factors like concentrations of individual major and minor contaminants, salinity, alkalinity, nature of soil, extent of drainage, climate conditions, types of vegetation or industry and purpose of use i.e drinking, irrigation and industry. Among above mentioned factors two variables i.e. salinity and alkalinity hazards play most important role for irrigation use. Salinity and alkalinity may be defined in terms of electrical conductivity in microSiemens per centimeters at 25°C and sodium adsorption ratio respectively. Different organizations and research groups have studied the different aspects of groundwater including water quality, they are Khan et al. (1993), Umar et al. (1989), Kaleemullah (1990), WAPDA (1988), Kazmi and Reza (1970) and Khan et al. (1986a, b).

The purpose of this study is to describe the

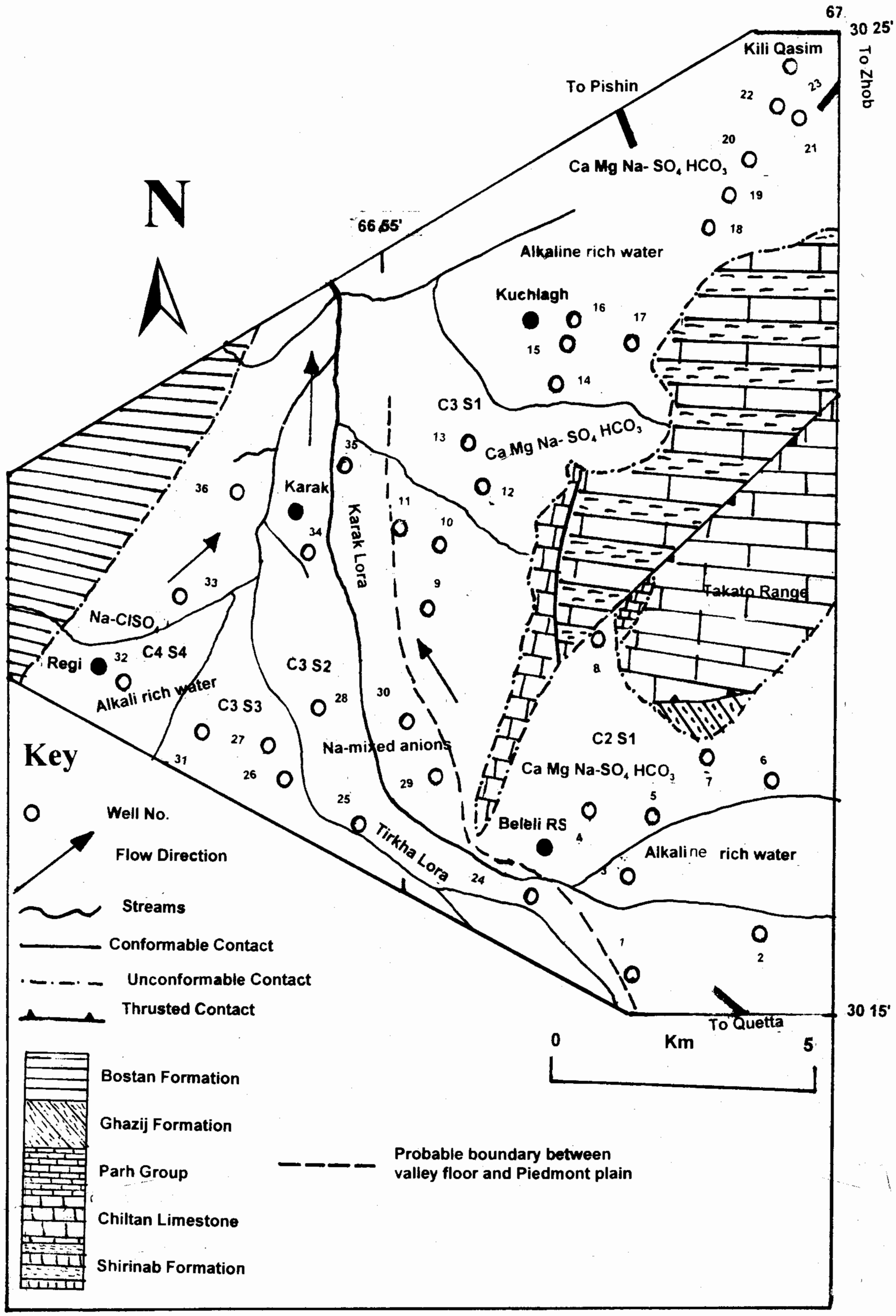

Figure 1. Map showing geology, location of tubewells, hydrochemical facies and water classes of the studied area.

comparative variations in natural contaminants and their causes both in valley floor and piedmont plain. For this purpose sampling of water has been carried out from scattered tube wells and tested in the laboratory, then statistical parameters are applied to check the variations and similarities in the groundwater of studied area. The relationship of different chemical constituents in same area (piedmont plain or valley floor), and significant results of same properties of two different areas (piedmont plain and valley floor) have been carried out by means of correlation and t-test respectively. The suitability of groundwater for irrigation in the study area is also evaluated.

The Beleli-Kuchlagh area is a part of Pishin Lora Basin and is situated around Takatu Range (~15 km north of Quetta city). Climatically the area is dry and falls into semi-arid region. Annual precipitation in the area is less then 10 inches and winters are cold. In winters commonly temperature drops down below freezing point. Along the piedmont plain mining of surface limestone of Takatu Range is in progress. Chiltan Limestone and Shirinab Formations are being mined for road and building construction material, whereas land in the valley floor is mainly used for urbanization and agriculture.

WATER ANALYSES

The specific conductivity of groundwater and intensity measurements (sodium & potassium) were obtained using BECKMAN SOLU BRIDGE model RD-26 and FLAMEPHOTOMETER PERKIN ELMER model 52 respectively. Other analyses were carried out by titration. Distilled deionized water and analytical grade reagents were used in all wet chemical analyses.

DESCRIPTION OF ANALYSES

According to World Health Organization (WHO) an average of 50,000 people die each day from diseases associated with bad water in the World (Price 1985). This alarming sentence is suffice to conclude the importance of water contamination. This study of groundwater describes and evaluates the natural contaminants by comparing different characteristics in piedmont plain and valley floor areas of Kuchlagh and Beleli. Twenty three samples from piedmont plain and thirteen samples from valley floor have been collected, from scattered tube wells and tested in the laboratory (Fig. 1). The statistical parameters such as mean, standard deviation, range, correlation and t-test were applied to make sure the consequences. The electrical conductivity of water in microSiemens per centimeters at 25°C at piedmont and valley floor are 737.9 and 2028 whereas the dispersion are 400.3 and 1060 respectively. This shows that the total dissolved solids or salinity hazards are higher in valley floor than that in the piedmont plain. Deviation from the mean (dispersion) also shows great variation of specific conductance values in valley floor. The mean and standard deviation of parameters like sodium adsorption ratio, calcium, magnesium, sodium, bicarbonate, chloride, and sulphate concentrations

Table1. Comparison of statistical parameter results of groundwater collected from piedmont plain and valley floor.

Test variables	Unit	N	$\bar{x}$	Min.	Max.	SD
PIEDMONT PLAIN						
Specific conductance	mS/cm	23	737.9	313	1816	400.3
Sodium Adsorption Ratio	-	23	1.55	0.22	5.89	1.48
Tube well depth	Feet	23	351.55	200	625	91.7
Calcium	me/litre	23	2.28	1.2	5	0.87
Magnesium	me/litre	23	3.52	2.02	10.2	1.66
Sodium	me/litre	23	2.51	0.33	6.78	1.83
Bicarbonate	me/litre	23	2.23	0.45	4.6	0.77
Chloride	me/litre	23	1.69	0.50	6.15	1.13
Sulphate	me/litre	23	4.53	0.23	14.96	3.33
VALLEY FLOOR						
Specific Conductance	mS/cm	13	2028	960	4500	1060
Sodium Adsorption Ratio	-	13	5.66	0.67	19.28	4.97
Tube well depth	Feet	13	320.8	250	360	36.5
Calcium	me/litre	13	4.5	2.2	8.4	1.75
Magnesium	me/litre	13	4.44	0.6	13.8	3.71
Sodium	me/litre	13	11.22	1.3	38.95	9.41
Bicarbonate	me/litre	13	3.65	2.3	5.7	1.35
Chloride	me/litre	13	6.67	1.75	18.5	9.1
Sulphate	me/litre	13	9.5	1.94	25.97	6.92

which appear to be greater in valley floor than that in the piedmont plain. The sodium adsorption ratio and sodium and chloride concentrations are particularly higher in valley floor (Table 1).

The t-test was made with a two tailed significance level of 95%. A null hypothesis (H_O) is defined as no significant difference exists between distribution of natural contaminants in groundwater samples collected from piedmont plain and valley floor areas and an alternate hypothesis (H_1) is defined as a significant difference exists. These results show that the depth of tube wells and concentration of magnesium are same in both piedmont plain and valley floor. But all other properties which are specific conductance, sodium adsorption, calcium, sodium, bicarbonate and sulphate concentrations have significance difference in both areas (Table 2).

Table 2. t-test with a two tailed significance level of 95% of groundwater collected from Beleli- Kuchlagh area.

Test variable	t-test value	Result
Specific conductance	5.25	Significant difference
Sodium adsorption ratio (SAR)	3.71	Significant difference
Tube well depth	-1.15	No Significant difference
Calcium	-5.09	Significant difference
Magnesium	-1.03	No significant difference
Sodium	-4.34	Significant difference
Bicarbonate	-4.03	Significant difference
Chloride	-5.51	Significant difference
Sulphate	-2.92	Significant difference

The interrelationship of different variables with correlation in the same physiographic area also have been made. The study shows that calcium-magnesium, magnesium-sulphate, sodium-sulphate, have strong positive correlation at piedmont plain while in valley floor sodium-chloride have approximately perfect correlation, sodium-sulphate and chloride-sulphate have good positive correlation. Calcium-sodium, calcium-chloride magnesium-bicarbonate, have good positive correlation at piedmont plain as shown in Table 3.

Table 3. Correlation chart of individual constituents of groundwater in same area i.e; piedmont plain or valley floor.

Correlation of variables	Piedmont plain	Result	Valley floor	Result
Ca and Mg	0.77	strong	0.15	low
Ca and Na	0.5	good	-0.004	no
Ca and HCO_3	0.44	good	0.02	no
Ca and Cl	0.55	good	0.02	no
Ca and SO_4	0.66	good	0.08	no
Mg and Na	0.37	low	0.22	low
Mg and HCO_3	0.51	good	-0.27	no
Mg and Cl	0.20	low	-0.38	no
Mg and SO_4	0.72	strong	0.23	low
Na and HCO_3	0.21	low	0.38	low
Na and Cl	0.38	low	0.92	perfect
Na and SO_4	0.78	strong	0.66	strong
HCO_3 and Cl	0.19	low	0.07	no
HCO_3 and SO_4	0.21	low	-0.55	no
Cl and SO_4	0.06	low	0.55	good

Based on sodium adsorption ratio and specific conductance (Richard et al. 1954), the groundwater of piedmont plain and valley floor in the studied area has been classified. The southern and northern part of piedmont plain is characterized by medium salinity, low sodium hazards i.e; C2-S1 (Beleli and Killi Qasim) while middle part of piedmont falls in high salinity and low sodium hazards i.e; C3-S1 (area between Beleli and Kuchlagh). On the other hand in the valley floor both salinity and sodium hazards are quite higher than in the piedmont plain. Eastern and western parts of the valley floor are characterized by high salinity, medium sodium hazards (C3-S2), and very high salinity, high to very high sodium hazards (C4-S3, C4-S4) (Fig.1). The part of valley floor adjacent to piedmont plain is characterized by high salinity and low sodium hazards (C3-S1). At piedmont plain the groundwater is of calcium magnesium sodium-bicarbonate sulphate type while in valley floor it is sodium-chloride sulphate, sodium mixed cations and calcium sodium magnesium-bicarbonate sulphate types based on trilinear diagram proposed by Hem (1970). The hydrochemical facies, deduced from chemical analyses of of groundwater are given in Table 4.

Table 4. Hydrochemical facies of the study area.

	Piedmont Plain
Southern and Middle part (Beleli & Kuchlagh)	Alkaline earths exceeds alkalies. Strong acids exceeds weak acids. No anion-cation pair exceeds 50%.
Middle part (between Beleli & Kuchlagh)	Alkaline earth exceeds alkalies. Strong acids exceeds weak acids. Non carbonate hardness (secondary salinity) exceeds 50%.
	Valley Floor
Lower part	Alkalies exceed alkaline earths. Strong acids exceeds weak acids. Non carbonate alkali (primary salinity) exceeds 50%.
Upper part	Alkaline earths exceeds alkali. Strong acids exceeds weak acids. Non carbonate hardness (secondary salinity) exceeds 50%

The above consequences clearly indicate that valley floor has quite rich concentrations of alkalies, sodium and chloride.

GEOLOGY, SOIL AND SOURCES OF CHEMICAL CONTAMINANTS IN GROUNDWATER

Physiographically the studied area may be grouped into mountain highlands (Takatu Range), piedmont plain (alluvial fans) and valley floor. The piedmont plain is consists of gravel, silt, sand, clay and their admixtures. The material is poorly sorted but due to loose arrangement of rock particles it is porous and permeable and it is the main recharge area of groundwater. The valley floor is mostly composed of finer, porous, semi permeable materials like clay and silt with minor sand. The consolidated rocks are sedimentary in origin ranging in age from Jurassic to Pleistocene. The rock units exposed at the surface are Shirinab Formation (Early Jurassic), Chiltan Limestone (Middle Jurassic), Parh Group (Cretaceous), Ghazij Formation (Eocene), and Boston Formation (Pleistocene). There are three unconformaties in the area (Fig.1);

a) between all older rock units and Recent deposits.
b) between Parh Group and Chiltan Limestone.
c) between Parh Group, Shirinab Formation and Ghazij Formation.

Chiltan Limestone is thrusted over Ghazij Formation whereas Shirinab Formation is thrusted over Chiltan Limestone (Fig.1). Shirinab Formation is composed of interbedded shale and limestone. Chiltan Limestone consists of thick bedded, massive, dark grey limestone. Parh Group has creamy white, maroon coloured, thin bedded limestone withe greenish & purple coloured shale. The Ghazij Formation contains olive grey, greenish grey shale with subordinate sandstone while Bostan Formation consists of soft, poorly consolidated assemblage of clay and silt with subordinate thin bedded salt pepper textured sandstone and conglomerate. Sand and gravel in Bostan Formation may form good recharge zones and in some localities may prove to be useful sub surface reservoirs and yield water. Ghazij Formation mainly composed of claystone, siltstone and shale which are almost impervious and are not likely to yield water. Parh Group constitute impervious limestone and shale and generally yield no significant amount of water. Jurassic rocks (Shirinab formation & Chiltan Limestone) are also impervious but in some areas they may be aquifers due to secondary porosity (Khan et al. 1993).

The soil, surface and subsurface rocks in the valley floor and piedmont plain influenced the variations in types and amount of contaminants in aquifers of the studied area. At piedmont plain the consolidated rocks are mostly carbonates with some argillaceous deposits and unconsolidated rocks are of alluvial fans. These rocks are the sources of calcium, magnesium, bicarbonate, sodium and sulphate. The valley floor is rich in clayey and silty soil and Bostan Formation which has been deposited in saline lake (Khan et al. 1993). The soil and subsurface lithology, rich in clay with silt also bears low infiltration rate (about 0.62-0.70 inches per hour) in valley floor; and the infiltration rate is higher at piedmont plain i.e. 0.74-1.0 inches per hour, (Khan et al. 1986). This means that the porosity and permeability is lower in valley floor so the time of contact of precipitated water and saline soil, clayey rich buried rocks of Bostan Formation is greater in valley floor and hence the groundwater is more saline and alkaline than at piedmont plain. Moreover, the soil of the valley floor is rich in sodium chloride, so the sodium hazard is very serious problem of lower part of valley floor especially at Karak & Regi (Fig. 1). An other cause of higher concentrations of salt in valley floor is increase in hydraulic gradient. Generally the groundwater flows from south-southeast to north-northwest, while some streams run in western part of valley floor towards east and then towards north-northwest (Khan el al. 1986a). The precipitation water which infilters and percolates down gradient from mountain highlands towards valley floor takes more time than makes a zone of saturation at piedmont plain. The precipitation water also flows through saline streams such as Karak Lora, Tirkha Lora which passes through saline Bostan Formation

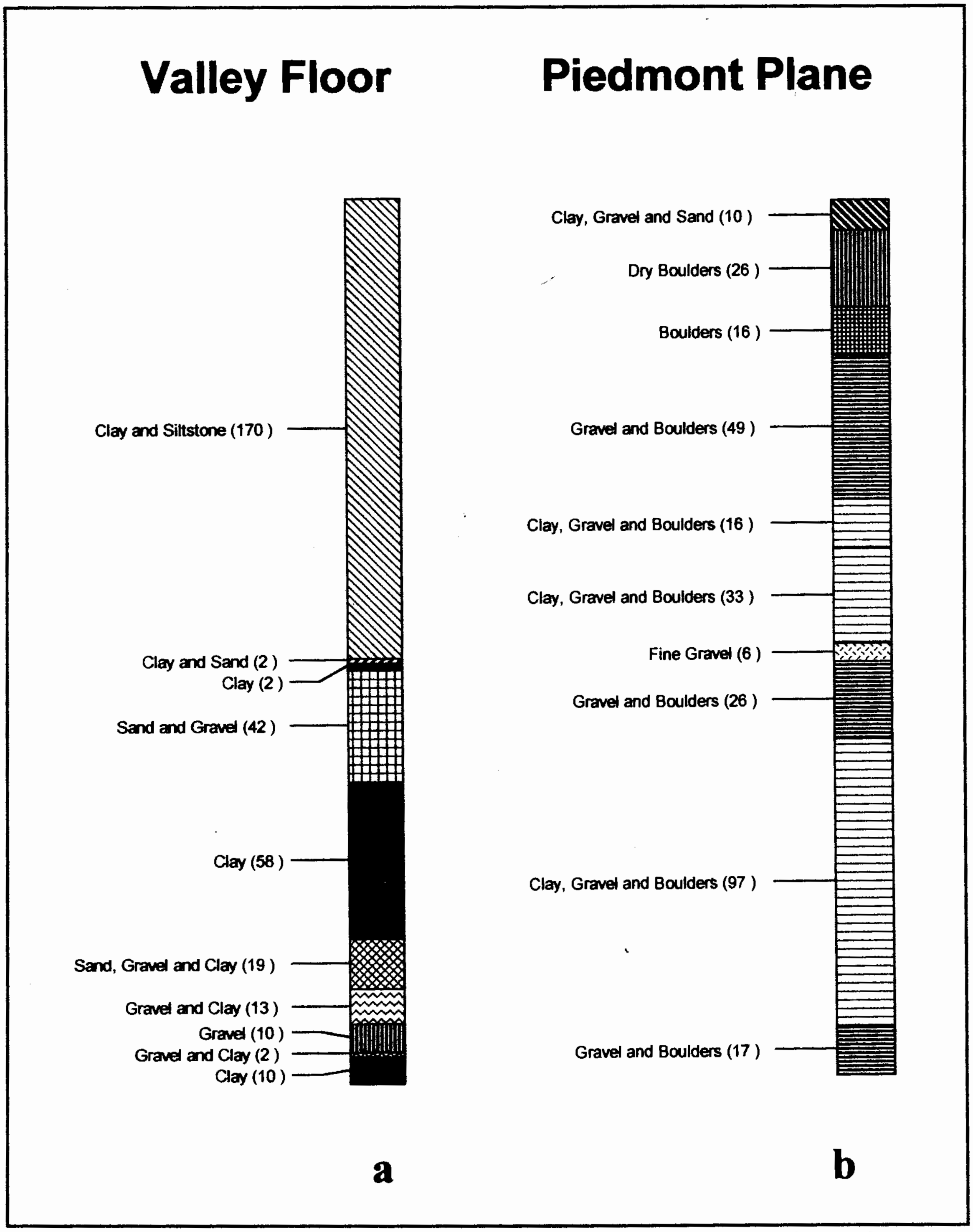

Figure 2. **Bore hole data of tubewells located (a) in valley floor (b) at piedmont plain.**

(Fig. 1). The bore hole record shows that the valley floor is rich in clay (approximately 225ft below the land surface) which is the main source of hazardous sodium, chloride and total dissolved solids concentration (Fig. 2a). On the other hand gravel, sand are the main subsurface lithology at piedmont plain (Fig. 2b) such rocks are porous, permeable and low in concentration of sodium, chloride and hence bears no sodium hazard problem.

IRRIGATION USE AND PROPOSED REMEDIES FOR IMPROVEMENT OF CONTAMINATED WATERS

For irrigation use the groundwater in aquifers of piedmont plain can be used successfully, whereas in the transitional zone (adjacent area of valley floor & piedmont plain) the groundwater can be used for only good salt tolerant crops such as onion, turnip, palm etc., providing special treatment to control salinity hazard. The groundwater in the valley floor is very harmful for drinking purpose and unsatisfactory for irrigation because it contains very high salinity and alkalinity (i.e. C3-S2, C4-S3, C4-S4 categories). The poor irrigation has also been observed during field work in the area.

In water with high amount of sodium, the addition of calcium salts such as $CaCO_3$ (lime) may greatly improve the quality of irrigation water. The addition of gypsum may greatly improve the infiltration rate and quality of water for irrigation (Richard et al 1954). In order to maintain the salt balance in the soil, it is essential to leach the salt from the soil with drainage water. It is recommended that the quality of leached salts must be at least of equal amount which is being added to the soil by the irrigation water. In case of low precipitation areas of soluble salts of the native soil will leach down and will cause an excessive accumulation of salts thus deteriorating the quality of groundwater. The artificial recharge becomes essential in these circumstances to improve the quality of groundwater (Nawaz 1980). It is suggested that high sodium and salinity in the groundwater in the valley floor may be reduced by adding gypsum, Ca-salts, with suitable leaching and artificial recharge or by reduced discharge and by maintaining the depth of water table.

REFERENCES

Hem, J.D., 1970, Study and interpretation of chemical characterstics of natural water, 2ed., U.S.G.S. water supply paper 1473, 363pp.

Kaleemullah, 1990, Groundwater quality of Quetta-Pishin districts and surrounding area, M.Sc. Thesis (unpublished) Department of Geology University of Balochistan Quetta, 180pp.

Kazmi, A.H. and Reza, S.Q., 1970, Water supply of Quetta Basin, Quetta Balochistan(pakistan), Rec. of Geol. Survey of Pakistan, Vol. 20, part 2, p. 104-113

Khan, L.A., Bhatti, M.S., Khan, A.Q., 1993, Groundwater resources of Balochistan Province Pakistan, P&D Department Government of Balochistan Quetta, Directorate of Hydrogeology WAPDA Lahore, 64, p. 114-124

Khan, S.A., Ghory, M.S., Shiekh, M.T. and Hameedullah, M., 1986a, Monitoring studies on groundwater levels in Quetta valley (Northern part) Pishin Lora Basin Balochistan, 5, p. 8-23

Khan, S.N., Younis, M.., Kazmi, S.A.H., 1986b, Environmental geology, Balochistan, Pakistan, GSP., Rec. Vol. LXXVI Environmental geology, p. 9-10

Nawaz, M.., 1980, A Text book of general Botany, Talimi Markaz Ltd. 3, Kabeer street Urdu Bazar Lahore, p. 80-82

Price M., 1985, Introducing groundwater, Gorge and Unwin Boston, Sydney.

Richard, L.A.., Allison, L.E., Bernstien, L., Bower, C.A., Brown, W.E., Fireman, M.., Hatcher, L.T., Hayword, H.E., Pearson, G.E., Reeve, S.E., and Wilcox, L.V., 1954, Daignosis and improvement of saline and alkaline soils, Agriculture handbook 60, US. Department of agriculture Oxford & IBH Pub. Co., p. 69-82

Umar, M.., Mehmood, A.., and Achakzai, A.., 1989, Study of groundwater quality of part of Quetta-Pishin districts, Balochistan, M.Sc. Thesis (unpublished) Department of Geology University of Balochistan Quetta, 50pp.

WAPDA, 1988, Groundwater levels during 1967-88, in Quetta valley, Hydrogeology project WAPDA Quetta, p. 4-17

Manuscript Received 10th October 1998
Revised Manuscript Received 7th June 1999
Accepted 1st September 1999

ACTA MINERALOGICA PAKISTANICA
Volume 9 (1998)

Article Reference
AMP9.1998/063-072/ISSN.0257-3660

GEOPHYSICAL ANALYSIS OF SUTURE ZONE AT THE COAST OF ARABIAN SEA IN PAKISTAN

NAYYER ALAM ZAIGHAM[1] AND MUJEEB AHMAD[2]
[1] Geological Survey of Pakistan, Karachi
[2] Department of Geology, University of Karachi

ABSTRACT

The north-south trending Fold-Thrust belt of Pakistan is characterized by the occurrences of ophiolites. The southernmost ophiolite zone, exposed in between Khuzdar and Uthal areas of Balochistan Province, is the largest ophiolitic occurrence in Pakistan extending over an area of 450 X 10 Km. In the south, the ophiolite zone is covered by the Quaternary sediments causing a discontinuation of relationship between the land exposures of the southern branch of the Himalayan suture zone and the submarine exotic features in the northern Arabian Sea. Modelling of gravity and aeromagnetic data pertaining to southern part of the ophiolite zone suggests that i) the ophiolite zone does not terminate in Uthal area against the Bela plain as it appears, but continues southward under the Quaternary sediments into the Arabian Sea, ii) exposed part of the ophiolite zone has been sheared off and pushed up progressively northwestward in the form of thin deformed sheet, iii) exposed part of the thrusted zone is about one kilometer thick, whereas the southern buried part is about 10 kilometers thick.

INTRODUCTION

The Bela ophiolites apparently seem to terminate in the south creating an enigmatic condition between the land and the sea geologic features (Fig.1). Is that true? To attempt this question, the gravity and magnetic data have been analyzed and interpreted in terms to geological models. Aeromagnetic data, used in this study, was collected for the geological appraisal of the southern part of the fold-thrust belt by the Geological Survey of Pakistan with the assistance of Canadian International Development Agency (CIDA) during 1975-79.

The gravity data of the Bela-Sonmiani area was interpreted at the Computer Center of the Geophysics Department, Colorado School of Mines, Golden, USA (Center for Potential Field Studies, 1984), using Upward Continuation and Spectral filtering techniques. The purpose of study was to examine the lateral and vertical trends of the ophiolite zone in the tectonic framework.

GEOLOGICAL SETTING

The fold-thrust mountainous belts of Pakistan appears to terminate against the Bela Plain before they reach the Arabian Sea. Previously, the deformed fold-thrust belt was considered as thin skinned structural manifestation thrusted southward on weak decollement above a low angled north-westward dipping basement (Sarwar & DeJong 1979), but Zaigham (1991) has described the deformed belts as a product of the convergent process within a narrow zone between Indo-Pakistan sub-continent and Makran-Bela micro-oceanic plates. Tectonically, the area is bounded by the major accretionary regime of Chagai subduction system in the west, and by the Kirthar fold-thrust mountainous belt and the Indus basin in the east. In the south, there is Arabian sea which consists of prominent submarine features such as Murray Ridge, Owen Fracture Zone, etc.

The major stratigraphic units exposed in the area range from Jurassic to Quaternary (Hunting

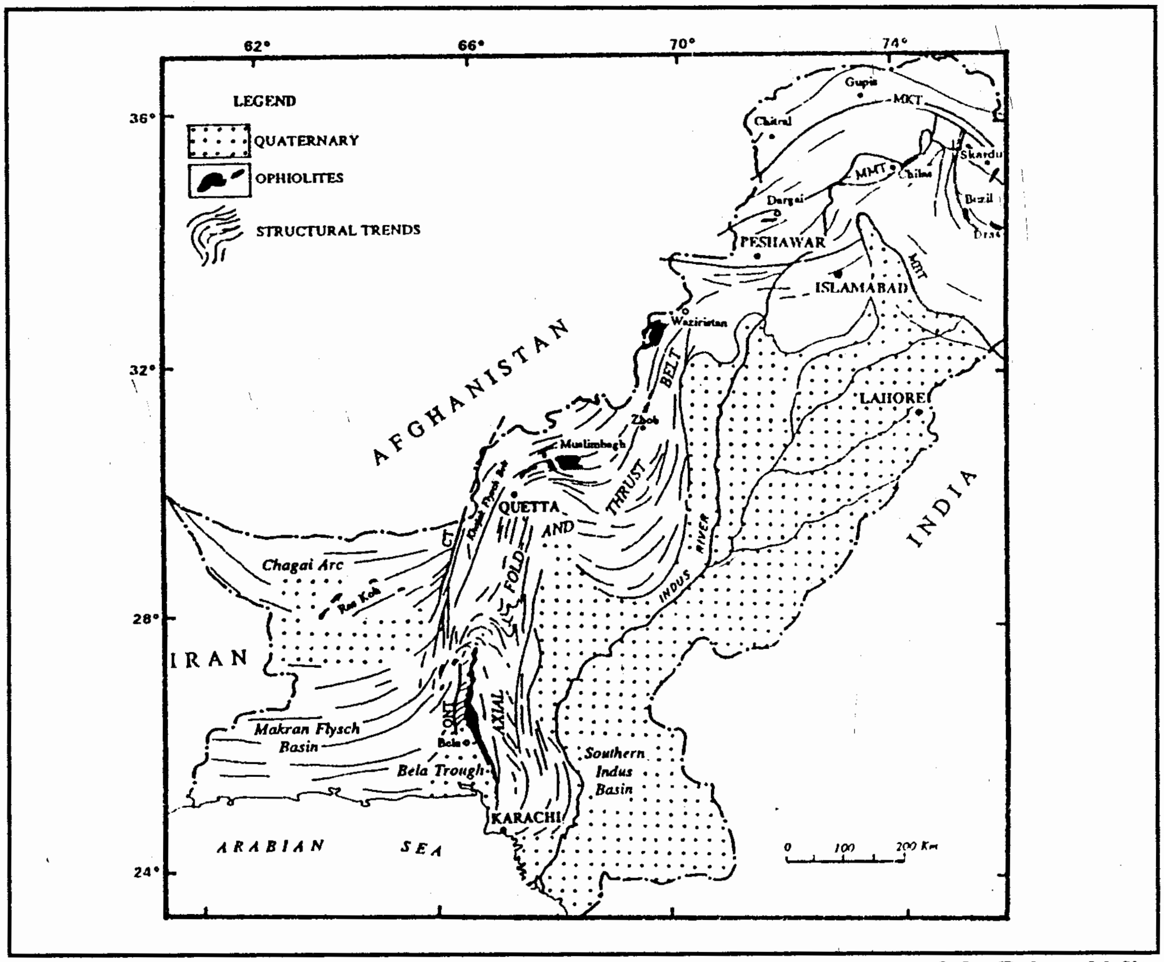

Figure 1. Map showing salient geological features in relation to occurrence of the Bela ophiolite (modified after Asrarullah, et al. 1979).

Survey Corporation 1960). The Bela ophiolite complexes are exposed only in the northeastern part of the Bela Plain. The ophiolite zone is in contact with the Neogene flysch sediments in the northwest. The remaining western side of the ophiolite zone extending towards south is buried under the Quaternary sediments. The eastern margin of the ophiolite zone has tectonic contacts with the Mesozoic rocks (Ganssar 1979). The Bela ophiolites were emplaced not before Paleocene and not after Early Eocene epoch (Allemann 1979; Sarwar & DeJong 1984).

The Bela melanges are exposed in two narrow linear belts of variable width along the western slope of Mor Range (4.5 km wide) and along the eastern slope of the Piaro Ridge (2 km wide). The eastern melange belt extends in the south discontinuously upto the Arabian Sea. In the southern most extremity, the melange is exposed in the coastal area of Gadani village and also at the mouth of Hub River in Ratti Hills. The western melange about 20 kilometers east of Bela Town, along the eastern slope of Piaro Ridge, is partly covered by alluvium, but further southward about 20 km north of Uthal Town, it is completely covered and no exposures are known. Similarly, it disappears northward under the alluvium in the vicinity of Kanar locality. The melange sequences are underlain by the Cretaceous argillites and overlain by an ophiolitic complex.

GEOPHYSICAL SIGNATURES IN RELATION TO THE OPHIOLITES AND ASSOCIATED STRUCTURES

MAGNETIC CONSIDERATIONS

Figure 2 shows an overlay of the aeromagnetic coverage of the study area over the exposed geology around Bela Plain. In the north-central part of the overlay map, a narrow zone of relatively smaller elongated magnetic anomalies, striking approximately NW-SE, appears to be associated with the exposed Bela ophiolites and the melanges sharply bounded by Mesozoic stratigraphic units

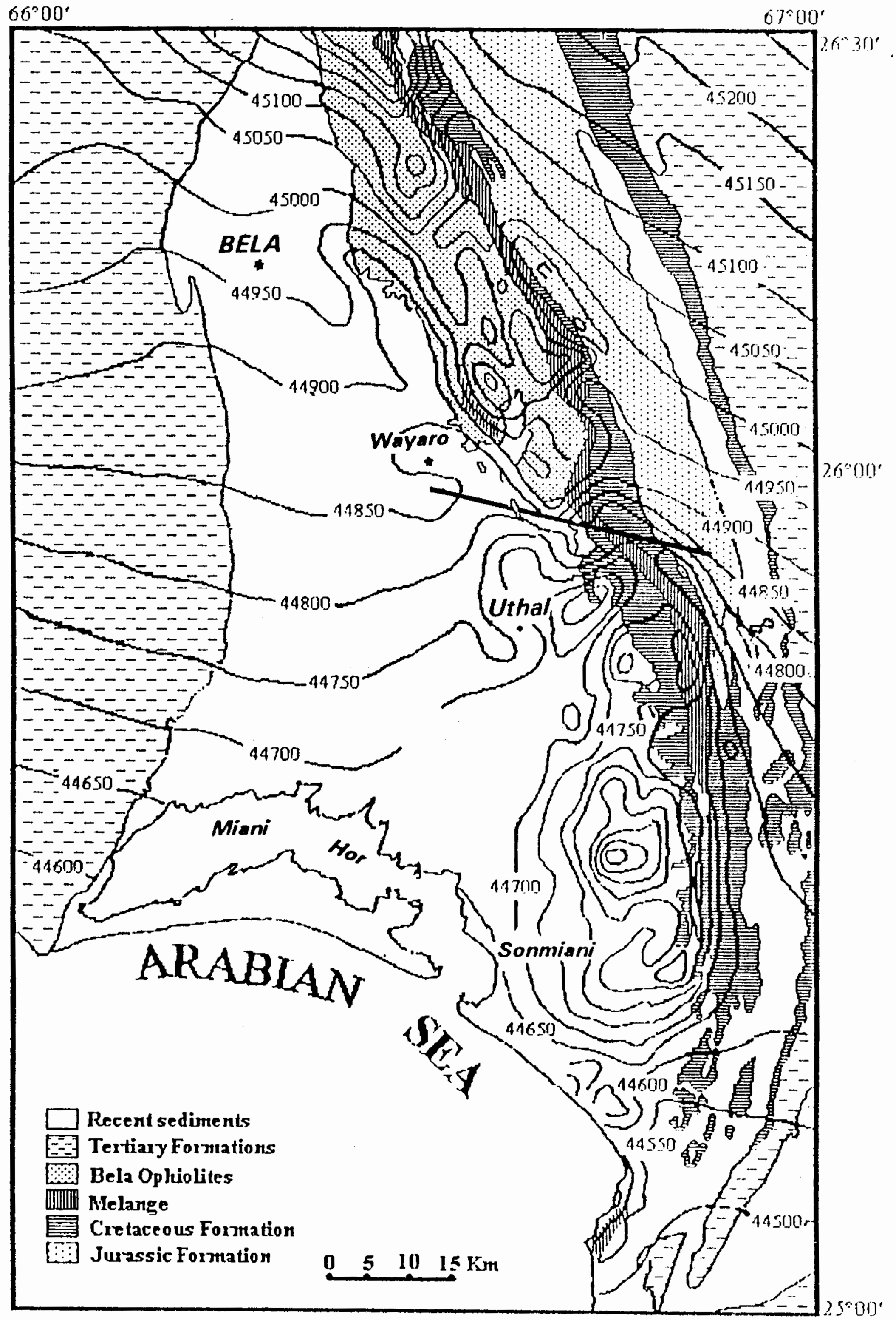

Figure 2. Aeromagnetic anomalies and the geology of the Bela region. Magnetic contour interval is 50 γ. Geology after Bakr and Jackson (1964).

exposed in Mor Range in the east and Piaro Ridge in the west.

In the south-east of Uthal a relatively broad ellipsoidal envelope, striking almost north-south and consisting of broad magnetic anomalies, appears to be associated with the buried zone of the ophiolites under the alluvial cover of Bela-Plain extending from Uthal to the coast of the Arabian Sea. The significant magnetic gradient on the eastern margin of this envelope is sharply coinciding with a very narrow N-S striking zone of irregularly exposed ophiolitic melange on the western boundary of Mesozoic sediments.

The significant change in the strike of the zones of magnetic anomalies at about 15 kilometers north-east of Uthal, is probably due to the changing trend of the narrow zones of exposed ophiolitic melange and the Mesozoic sediments. This changing trend of magnetic anomalies indicates stretch-off structure creating lateral as well as vertical oblique off-set between the two main zones of the magnetic anomalies.

The contour pattern east of Bela between Wayaro and Uthal, indicates prominently the presence of a low and narrow magnetic zone striking almost NW-SE, which is dominantly masked by the regional magnetic effects. Similarly, the contour patterns in western and north-eastern parts, are also indicating superimposed weak magnetic anomalies associated with shallow geologic features on the regional planetary effect of magnetic field. The magnetic anomalies of Bela region illustrate prominently the following geologic features:

i. Bela ophiolite and melange zone is exposed in the north and is buried in the south, but both are identifiable by high magnetization of the rocks.
ii. The ophiolite zone continues in south and extends under the Quaternary sediments into the Arabian Sea. The wavelength of the magnetic anomalies, observed over the alluvial covered area, is larger than that of anomalies observed over the exposed ophiolite zone. This indicates a thick and massive sequence of ophiolite complex buried in the Bela Plain.
iii. Magnetic flatness on western and north-eastern sides of the Bela ophiolite zone, is the indication of greater thickness of sediments.

GRAVITY CONSIDERATIONS

The predominant trend on the gravity map (Figure 3) is the elongated north-south trending high gravity anomalies bounded by steep gradients on the east and west sides plunging out north ward but extending southward into the Arabian sea. This map also shows superimposition of smaller anomalies of different origin. Similar to the magnetic results, the overlay of the gravity anomalies on the geology shows that relatively smaller anomalies in the north-west corner are associated with the exposed ophiolite units. On the other hand, most of the anomalies found in the area covered by alluvium from the coast of the Arabian sea to the north of Uthal Town are the indication of subsurface continuation of the Bela ophiolite complexes. Like in the case of magnetic gradient, the steep gravity gradients coincide with the zones of melanges. In the northeast of Uthal the trend of gravity gradient also illustrates significant change in its striking direction showing correspondence with the magnetic results.

'Upward-continuation' Filtering

In upward-continuation filtering technique, gravity data measured on one level is transformed to some higher level(s) using a particular filter operation (Dean 1958; Henderson 1970; Hildenbrand 1983; Jacobsen 1987). This technique has been applied on the gravity data of Bela area to envisage the behavior of the deep-seated regional structures for higher levels at 1, 2.5, 5, 10, 20, 25, and 35 km (Figure 4).

The comparative study of different upward-continued levels indicates that relatively short-wavelength anomalies do exist approximately upto a depth of one kilometer in the area. These short-wavelength anomalies superimpose upon an elongated north-south striking high density regional structural feature which corresponds to the buried obducted sequence of the ophiolites. The north-south striking high density regional structural feature has been filtered out on 2.5 and 5 kilometer upward-continued levels. At 10 kilometer continued-level, this gravity high plunges out just north of Uthal, but it continues from Uthal Town in the south extending into the Arabian Sea as indicated by the presence of partial gravity anomaly, which appears to continue further south of the study area. The continued-transformed levels upto 20 and 25 km indicate that the high density structural features do exist approximately upto 25 kilometers. The upward-continued levels at 35 kilometers seems to represent the possible continuation of gravity gradient due to the density contrast at that depth associated with the upper mantle.

Figure 5 shows comparative study based on the longitudinal profiles taken from different levels of Upward-Continuations. In general, it is significant that the higher density crust, which appears to be

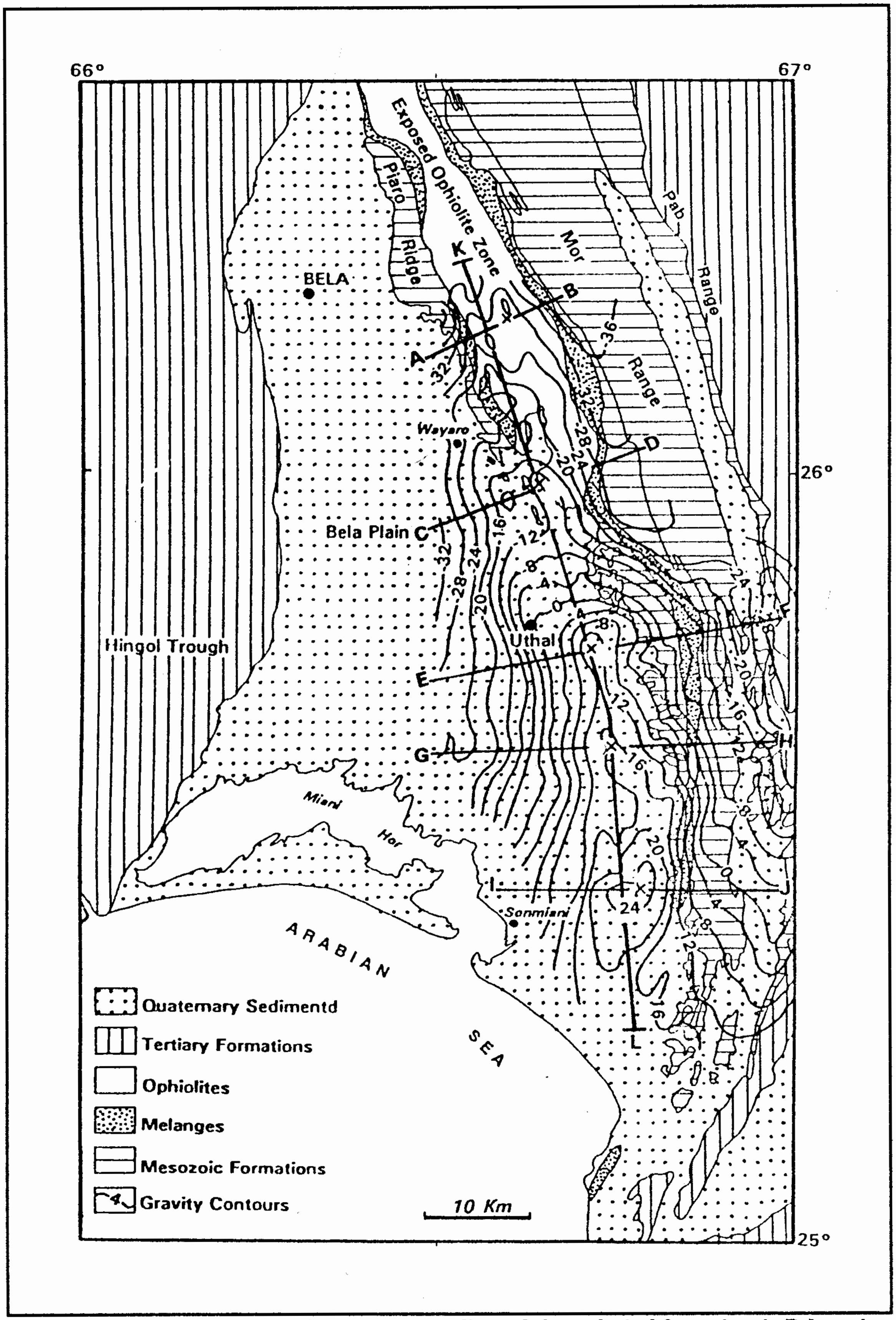

Figure 3. An overlay map of the gravity anomalies and the geological formations in Bela region. Profile lines indicate the location of power spectra profiles presented in Figure 6.

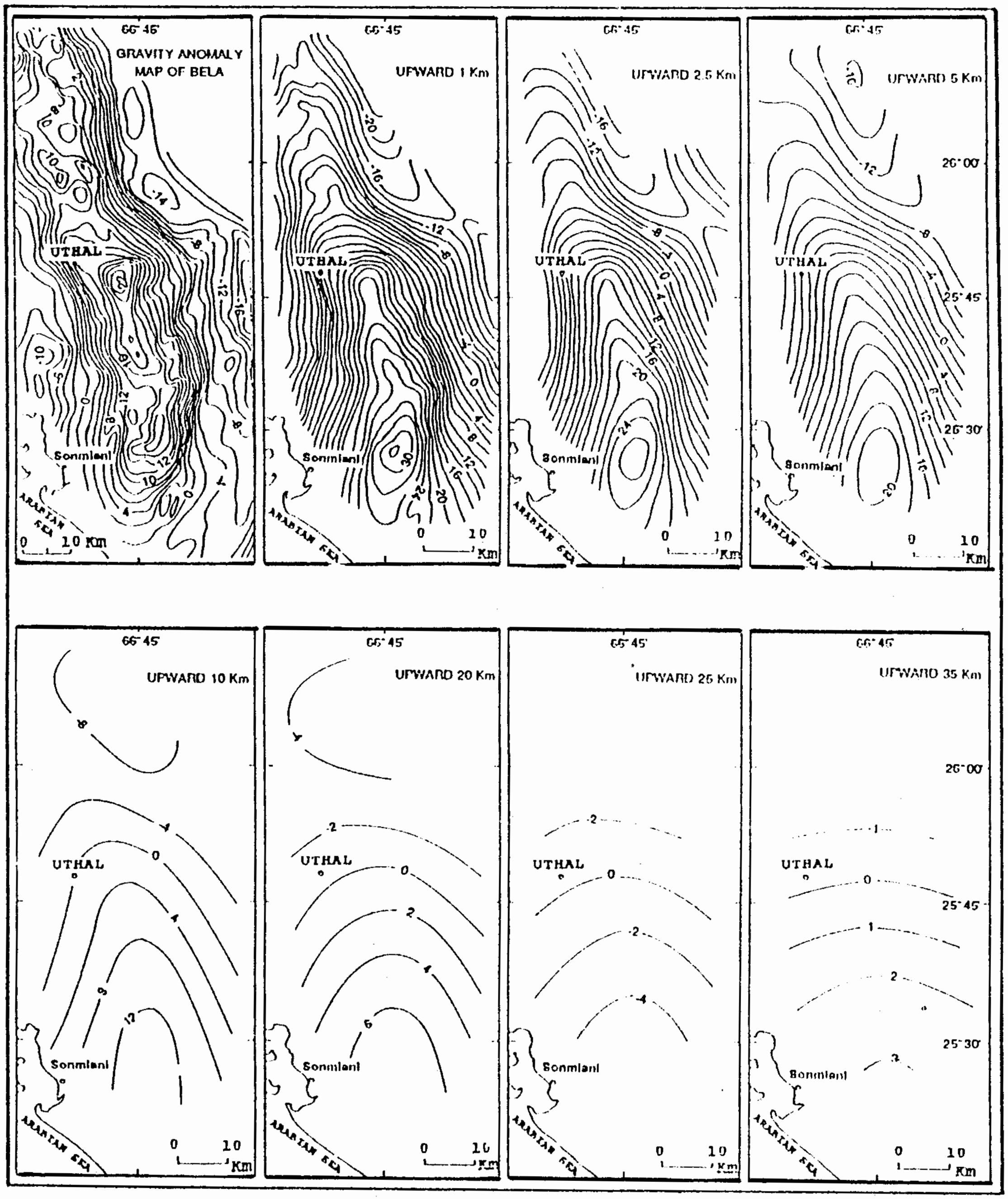

Figure 4. Maps showing results of upward-continuation filters applied to the Bela gravity data for the levels at 1, 2.5, 5, 10, 20, 25, and 35 km.

oceanic, dominates in the south but attenuates in the north with respect to the depth. A prominent zone of gravity gradient is observable on profile at 1 km and onward upto the profile at 10 km Upward Continued level. This gravity gradient appears to be associated with the zone of decollement along which the exposed part of the Bela ophiolites has been thrusted up with the older Mesozoic sediments in the north-western part of the study area (Zaigham 1991). From qualitative analysis of the Upward-continuation gravity profiles, it is inferred that the obducted Bela Ophiolites in the northern part of the study area are only restricted at shallow depth ranging from surface to a depth of one km approximately. On the other hand, relatively shorter-wavelength anomalies associated with the buried ophiolite bodies, can be seen in southern half of the profile at 2.5 km level superimposed on the deep-seated longer-wavelength anomalies.

Spectral Depth Analysis

Spectral filtering operators are designed to analyze and interpret the gravity and magnetic data for distinguishing the deep-seated crustal features from shallow origin of geological bodies. The value of the frequency domain (spectrum) of deep sources dies away more rapidly than does the spectrum of shallow sources. In this connection, Spector (1968) and Spector & Grant (1970) used a technique for spectral depth analysis of aeromagnetic maps. A similar approach has been applied to gravity data of Bela region for the spectral depth determinations.

The power spectra have been computed from gravity profiles (location of profiles is shown in Figure 3). Figure 6 displays the computed power spectra in logarithmic radial form. The parameters for definition of depth have been determined directly from a graphical analysis of the power spectrum curves. The shape of these spectra is basically bimodal and reveals (i) a very steep slope at very low frequencies and (ii) a relatively moderate decline in the remaining high frequency part of the spectrum.

In general, the bimodal trend of the power

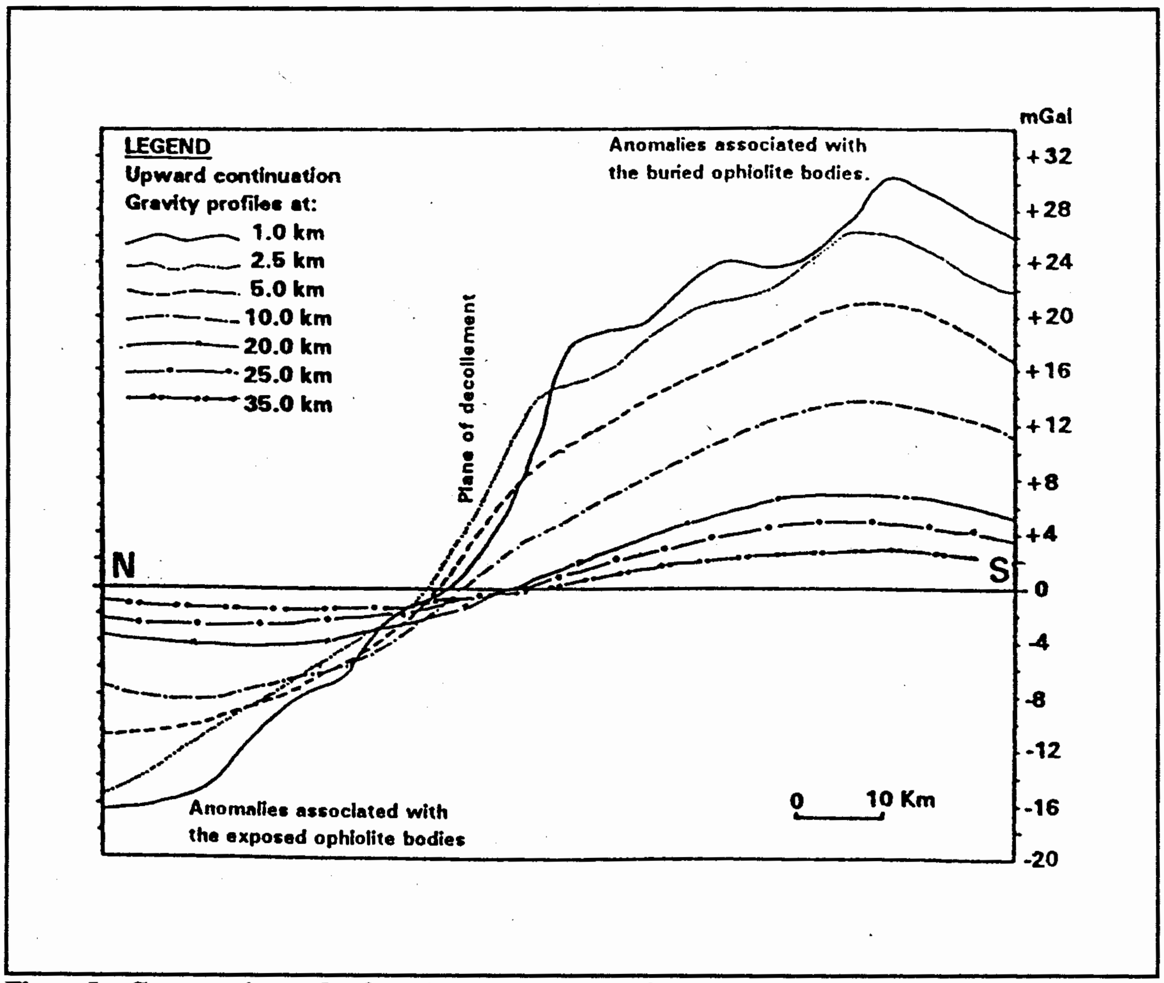

Figure 5. Comparative study of northsouth oriented profiles from the upward-continuation filter maps (Figure 4) at different levels.

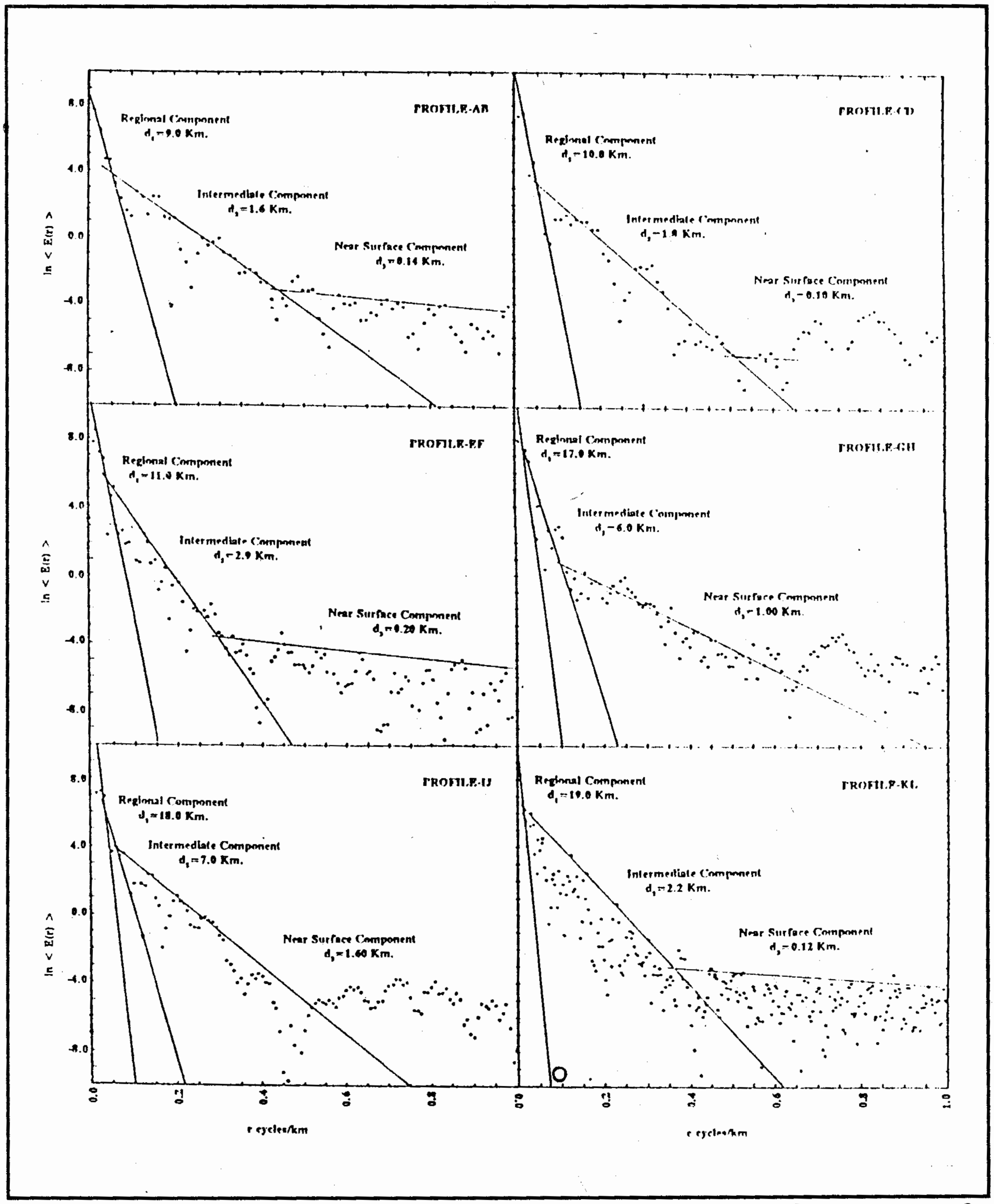

Figure 6. Graphs plotted for wave numbers versus logarithm of gravity anomaly power spectra for selected profiles in the Bela region. Location of profiles is shown in Figure3. Linear segments of the power spectra indicate the existence of discrete density boundaries, and the slopes represent their estimated mean depths (d_1, d_2, d_3).

spectrum curves indicates that the gravity data of the Bela region are due to high density rocks at greater depth ranging from 9 to 19 Km which contribute anomalies of regional gravity component. Likewise, the rocks of shallow depth ranging from 0.12 to 1.6 Km (Bela ophiolite complex) caused the anomalies of near-surface gravity component. An intermediate frequency is also evident at depth ranging from 1.6 to 7 Km which has been considered as a sheared off transition zone. In this zone the contribution from the `Regional Component' becomes progressively less significant

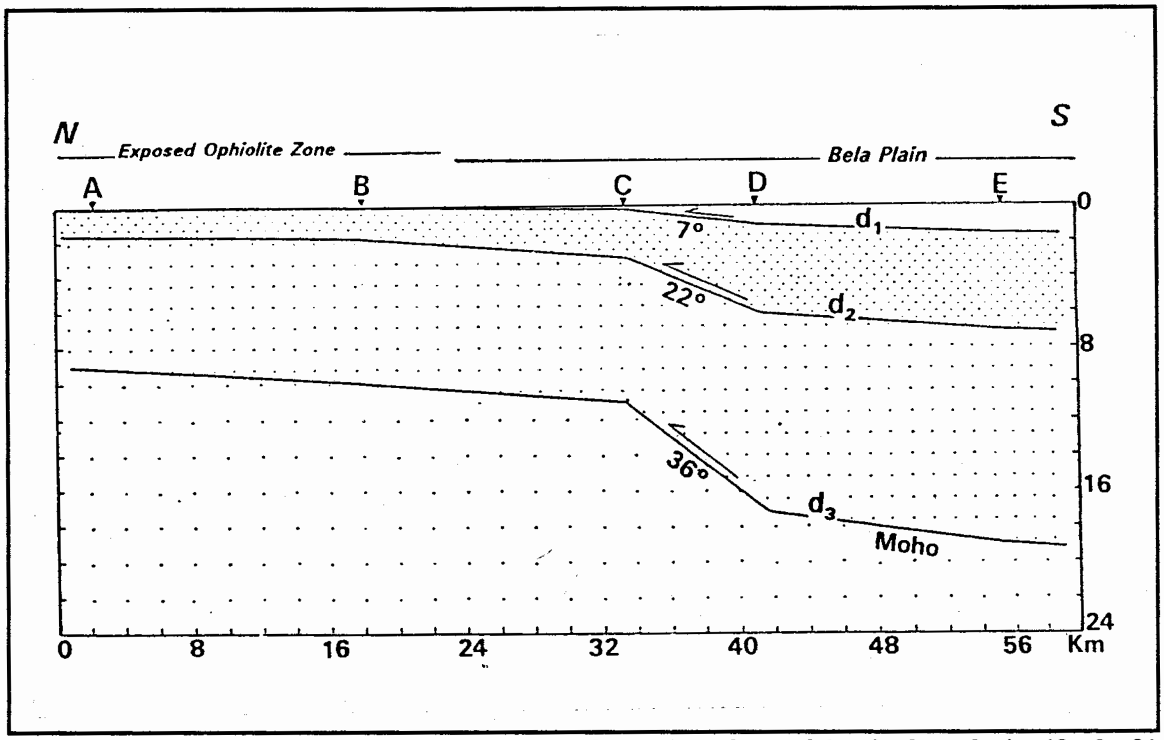

Figure 7. Proposed model to show the depths of main interfaces of density boundaries (d_1, d_2, d_3) calculated from power spectra of gravity field in the Bela region.

as compared to the Near-surface component.

A depth model (Figure 7) has been prepared in north-south direction using the depths calculated from the analyses of the energy spectra described earlier. The most significant features of this model is a zone of thrusting, which can be correlated with the deformed zone of melange at the surface in the north-east of Uthal as evident from the changing trend of the eastern Bela melange. According to this model, an increase in the angle of thrust-plane is inferred which is proportional to the increase in depth. The behavior in the change of angle of these interfaces indicates a regular increase of compressional forces in the lower crust and the upper mantle which has caused thrusting of the interfaces towards north-west along a zone of decollement (Zaigham 1991).

CONCLUSIONS

1. Bela ophiolite zone does not terminate in Uthal area as it appears, but the zone extends southward and continues under Quaternary sediments into the Arabian Sea.
2. Exposed part of the ophiolite zone has been sheared off and pushed up progressively northwestward in the form of thin deformed sheet.
3. It is inferred that the exposed part of the thrusted zone is about one kilometer thick, whereas the southern buried part is about 10 kilometers thick.
4. Based on the conspicuous trend of the elongated gravity high anomaly upto the 'Upward- Continued-Level' at 25 km, it appears that this zone of high density materials exist vertically up to considerable depth and belongs to upper mantle features.

ACKNOWLEDGMENTS

The authors wish to thank Syed Jamiluddin of Geological Survey of Pakistan, for review of the manuscript. The help, guidance and cooperation of Richard O. Hansen, Research Professor of Geophysics Department, Colorado School of Mines, during the filtering & analysis of the gravity data at the Computer Center of the School, are acknowledged with thank. We thank the *AMP* reviewer, Mubarik Ali, for his comments. We also acknowledge the assistance of Surriya Rashid, Geology Department of Karachi University, for drafting of the figures.

REFERENCES

Allemann, F., 1979. Time of emplacement of the Zhob valley ophiolites and Bela ophiolites: **In** Geodynamics of Pakistan, (eds.) A. Farah and K.A. DeJong, Geological Survey of Pakistan, Quetta, p.213-242.

Asrarullah, Ahmad,Z.,and Abbas, S.G., 1979. Ophiolites in Pakistan; An introduction: **In** Geodynamics of Pakistan,(eds.) A. Farah and K.A. DeJong, Geol. Surv. of Pakistan, Quetta, Pakistan, p.181-192.

Bakr, A., and Jackson, R. O. 1964. Geological Map of Pakistan on 1:2,000000 scale, Geological Survey of Pakistan, Quetta.

Center For Potential Field Studies, 1984. Reduction, analysis,and interpretation of gravity and magnetic survey data; a bibliography: Colorado School of Mines, Golden, Co., USA, 71p.

Dean, W. C., 1958. Frequency analysis for gravity and magnetic interpretation: Geophysics, v.23, No.1, p.97.

DeJong, K.A., and Subhani, A.M., 1979. Note on the Bela ophiolites with special reference to the Kanar area: In Geodynamics of Pakistan, (eds) A. Farah and K.A. DeJong, Geol. Surv. of Pakistan, Quetta, p.263-269.

Gansser, A., 1979, Reconnaissance visit to the ophiolites in Balochistan and Himalaya: In Geodynamics of Pakistan, A. Farah and K.A.DeJong (eds.), Geol. Surv. Pakistan, p.193-213.

Henderson, R.G., 1970. On the validity of the Upward-continuation integral for total magnetic intensity data: Geophysics, v.35, No.5, p.916.

Hildebrand, T.G., 1983. FFT FIL, A filtering program based on two-dimensional Fourier analysis of geophysical data: U.S. Geol. Sur., open-file report 83-237, 60 p.

Hunting Survey Corporation Ltd., 1960. Reconnaissance Geology of Part of west Pakistan: (Colombo Plan Coop. Project) Canadian Govt., Toronto, 550p.

Jacobsen, B.H., 1987. A case of upward continuation as a standard separation of filter for potential-field map: Geophysics, v. 52, No. 8, p.1138-1148.

Sarwar, G.,and DeJong, K.A., 1984. Composition and origin of the Kanar melange of southern Pakistan: Geol. Soc. Amer., Special Paper 198, p.127-137.

Spector, A., 1968, Spectral analysis of aeromagnetic maps: Ph.D. thesis, Physics Department, Toronto University.

Spector, A. and Grant, 1970, Statistical models for interpreting aeromagnetic data: Geophysics, v. xxxv, p. 293-302.

Zaigham, N.A., 1991, Bela ophiolites and associated mineralizations in the southern part of Axial-belt of Pakistan: Ph.D. thesis, University of Karachi, Pakistan.

Zaigham, N.A., and Mallick, K.A., 1994. Subsurface continuation of the ophiolites in the Bela Plain of Balochistan, Pakistan: Jr. Ofioliti, Vol. 19.N 2a, Florence, Italy, p.269-278.

Manuscript Received 14th November 1998
Revised Manuscript Received 10th February 1999
Accepted 1st September 1999

ACTA
MINERALOGICA
PAKISTANICA
Volume 9 (1998)

Article Reference
AMP9.1998/073-084/ISSN.0257-3660

ANOMALOUS ORIENTATION OF THE KHUDE RANGE FOLD BELT AND ENIGMA OF KHUZDAR SYNTAXIS IN SOUTHERN KIRTHAR FOLD BELT, PAKISTAN

MOHAMMAD NIAMATULLAH
Department of Geology, University of Karachi, Karachi, Pakistan.

ABSTRACT

In the northern part of the Kirthar Fold Belt, the structural trend is compatible with the northward moving Indian plate along the sinistral Ornach-Nal Chaman Transform Zone. However, the structural trends in the Bela Block and in the Khude Range Fold Belt, parts of the southern Kirthar Fold Belt, indicate more complex tectonics with some faults parallel to the sinistral Ornach-Nal Fault having dextral displacements. A possible explanation is that the oceanic lithosphere of the Arabian plate partly underthrusts the continental lithosphere of the Indian plate and has ripped off thin slivers of the latter. These slivers coupled with the Arabian plate were carried northward faster than parent mass along the dextral NS-trending Pab and Kirthar Faults.

The Khuzdar Syntaxis is a refolded complex structure. It is a thin-skinned drag in the earlier NNW-trending structures, a consequence of blocking to the NW of moving slivers at the NE-oriented Anjira-Gizan Fault, which later led to their sinistral translation along that Fault. The Makran Orocline and probably the Porali Trough also fit in the model.

INTRODUCTION

In the main Himalaya and the northern part of Pakistani Fold Belt, structures are generally EW-oriented. This indicates compression in the NS direction resulting from head on collision of the Indian continent with Eurasia (Powell 1979; Klootwijik 1979; Jacob and Quittmeyer 1979; Seeber et al. 1981; Tapponnier et al. 1986; Sengor 1985, 1986). There are lots of syntaxial bends in the Pakistani Fold Belt formed as a result of southwestward directed decollements of the near surface sedimentary cover on the Indian plate (Auden 1974; Sarwar and DeJong 1979). Paleomagnetic studies indicate a component of rotation in the earlier formed structures in the Sulaiman Fold Belt (Klootwijik et al. 1981). Along the NW-border of the Indian plate, in the northern part of Kirthar Fold Belt (KFB) structures have a NNE-trend, sub parallel to the Chaman Transform Zone (CTZ) (Fig. 1), a component of the Ornach-Nal Chaman Transform Zone (ONCTZ). Paleomagnetic studies suggest that structures in the region have not been rotated (Klootwijik et al. 1981).

Structure and tectonics of the southern KFB and adjoining areas is the main theme of this paper. In this part of the Fold Belt, south of the Anjira-Gizan Fault (AGF), structural orientation is much more complex (Hunting Survey Corporation 1961; Bakr and Jackson 1964; Kazmi and Rana 1982). There are several structural units separated by crustal faults with diversely oriented structures within them (Fig. 2). Of special attention are the NS-trending Khude Range Fold Belt Block (KRFBB) where the structures are NNW-oriented in an en-echelon pattern and are not compatible with the sinistral displacement along the ONCTZ at the NW-border of the Indian Plate. The Khuzdar Knot

(KK) is a syntaxial bend of complex nature where the fold belt is arcuate and convex northward. The tectonics of the KK has long been enigmatic. Sarwar and DeJong (1979) believe that it has formed due to counterclockwise rotation of the Khuzdar-Karachi Block as a single unit. The Khuzdar-Karachi block is a NS-elongated block whose counterclockwise rotation on the northward moving northwestern edge of the Indian plate seems incompatible. To the west of the Ornach-Nal Fault (ONF) thick flysch sequence of the Makran Accretionary Prism (MAP) is present. In far west, the structures are east west oriented and at a high angle to the ONF but in the fault's vicinity the

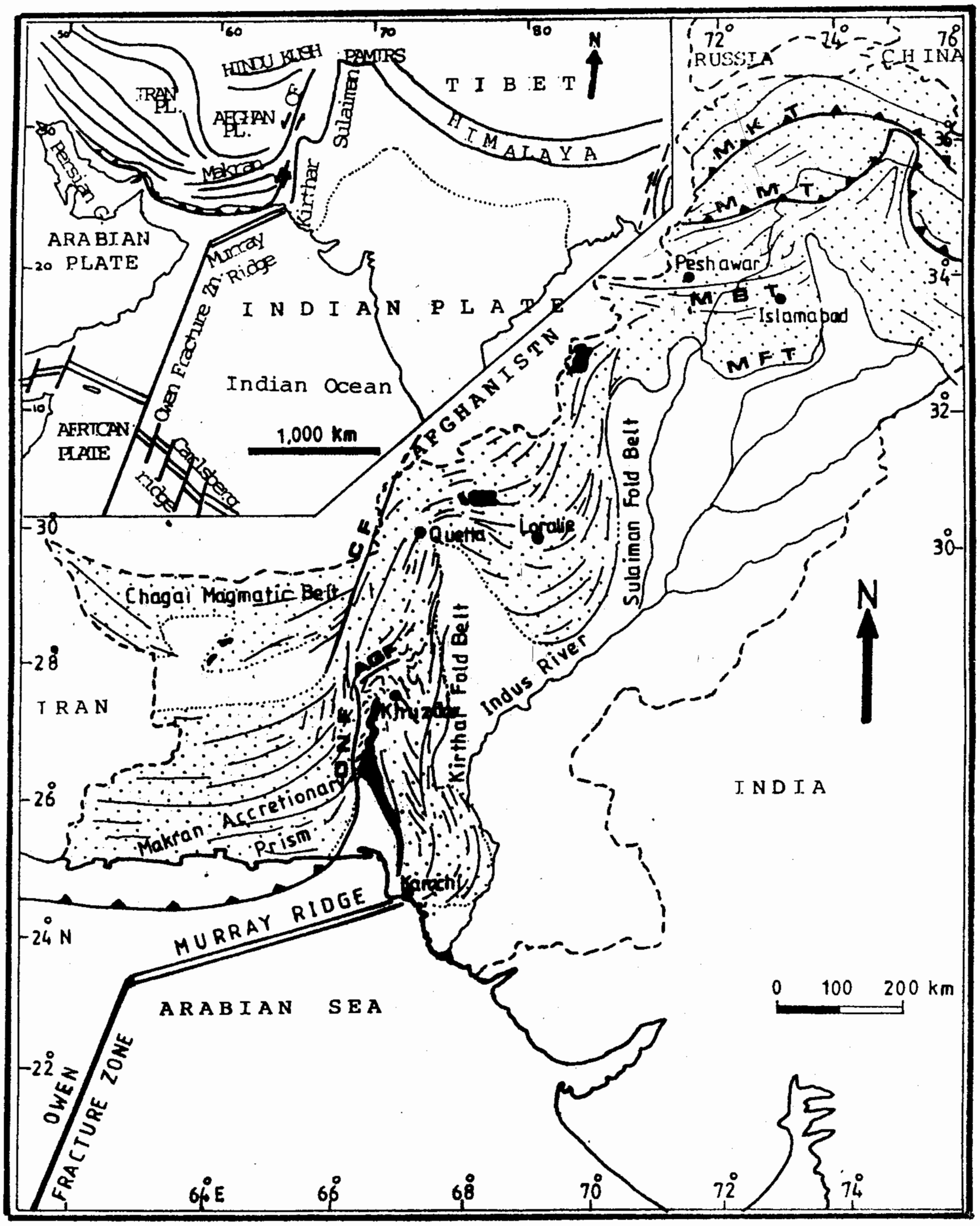

Figure 1. Structural trends in the Pakistani Fold Belt. Inset show the plate boundaries and structural trends at the Indian/Eurasian and the Arabian/Eurasian collision and subduction zones respectively.

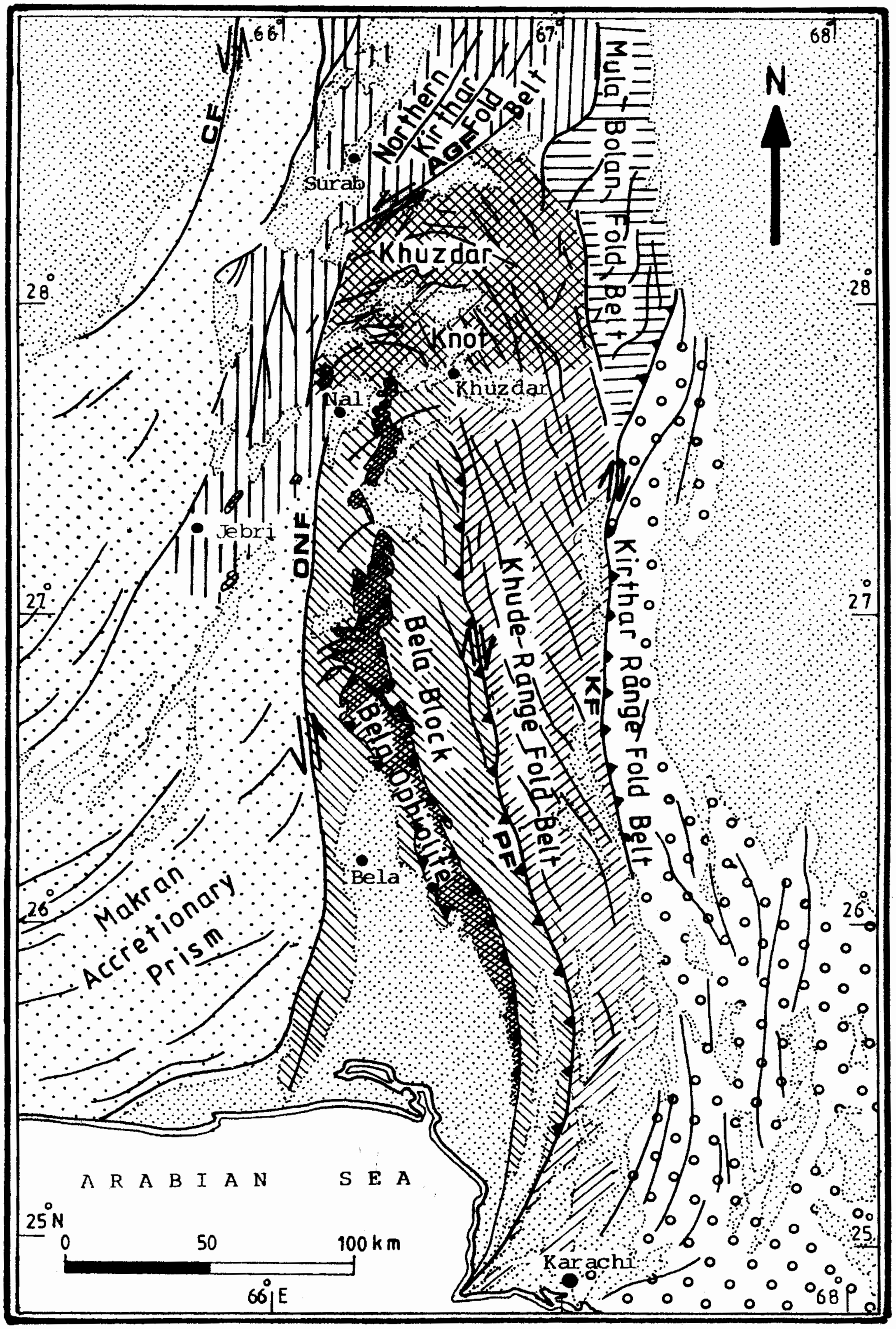

Figure 2. Various tectonic units in the southern Kirthar Fold Belt; ONF=Ornach-Nal Fault; AGF= Anjira-Gizan Fault; PF=Pab Fault, KF=Kirthar Fault & CF=Chaman Fault.

structures are arcuate and become parallel to the ONF due to a sinistral drag along it, to form the Makran Orocline (Sarwar and DeJong, op cit.). The MAP is underlain by the oceanic lithosphere of the Arabian Plate converging northward (Farhoudi and Karig 1977; Arthurton et al. 1982; DeJong 1982).

STRUCTURAL DISCONTINUITIES

The structural discontinuities which divide the southern Kirthar Fold Belt into various blocks, exhibiting diversely oriented structures are: the Kirthar Fault (KF), the Pab Fault (PF), the Ornach-Nal Fault (ONF) and the Anjira-Gizan Fault (AGF, see Fig. 2). With the exception of the NE-oriented AGF, all others are generally NS-trending faults.

The NS-trending KF separates the KRFBB to the west from the Kirthar Range Fold Belt (KRFB) to the east. Major part of it is an east dipping underthrust, while on its northern extreme it becomes vertical and then dips westward with a slight swing to the east (Hunting Survey Corporation 1961).

The PF is located to the west of the KF and is somewhat arcuate on the map convex eastward. The PF and the KF get closer to each other to the south near Karachi, and probably are connected at a high angle with the NE-end of the Murray Ridge in the Arabian sea (Kemal 1991). A right-stepping en-echelon fold pattern in the KRFBB, which is bounded by the KF and the PF indicates a dextral displacement, at least along the PF. Compressional and extensional structures may develop on restraining and releasing bends along the strike slip faults (Woodcock and Fischer 1986). Seismic activity and disrupted recent sediments indicate that the faults are still active (Kazmi 1979). P-wave first motion analysis of an earthquake in 1974 in the northern part of the PF indicates an oblique movement. On its northern segment where its geometry is close to a restraining bend a component of thrusting accompanies dominant dextral displacement (Quittmeyer et al. 1979). On the other hand normal displacement is evidenced and reported in the southern part of the Pab Fault (Nakata et al. 1989) where its orientation is close to a releasing bend.

The ONF, which is the NW-boundary of the Indian plate in the region, is the southern most fault of the ONCTZ (Lawrence et al. 1981; Farah et al. 1984) and separates the Bela Block (BB) to the east from the MAP to the west. Arcuate outcrop of the MAP in plan convex southward adjacent to the ONF, is a drag in the accretionary prism indicating a sinistral displacement along it (Sarwar and DeJong 1979).

TECTONIC BLOCKS

KHUDE RANGE FOLD BELT BLOCK (KRFBB)

This is a NS-oriented tectonic block, more than 350 km long, bounded to the east by the KF and to the west by the PF. To the north, it merges with the southern extremity of the KK, where it is more than 50 km wide while to the south it gets taper and extends up to Karachi. Folds in the block are NNW-oriented and arranged in en-echelon pattern counterclockwise to the length of the block (Figs. 3a, 3b).

Folds arranged in an en-echelon pattern are usually found along large convergent strike-slip faults (Sylvester 1988), or in a transpression zone bounded by two strike-slip faults (Aydin and Page 1984; Ramsay and Huber 1987). Folds arranged in an en-echelon patterns oblique to the shear direction are also present along the San Andreas fault (Dibblee 1977). Ideally the hinges of en-echelon folds should make an angle of 45 degree in plan view to the faults, representing the shortening component of the bulk strain, but the folds in generally rotate towards elongation of fault zone and vary from 10 to 30 degrees to the strike (Harding and Lowell 1979). A low angle between the PF, KF and the en-echelon folds of the KRFBB indicate that the folds may have been rotated.

During sinistral movement, folds form with their axes oriented clockwise to the length of the shear, while dextral shears results in fold axes oriented counterclockwise to main fault (Sylvester 1988). In the KRFBB counterclockwise orientation of the folds in the zone suggest dextral displacements in the zone bounded between the PF and the KF.

BELA BLOCK (BB)

This is also a NS-oriented elongated block, over 350 km long bounded between the PF to the east and the ONF to the west. The northern part is about 50 km wide and reaches about 100 km wide near the Arabian coast. In addition to sediments, this block is also underlain by Bela Ophiolites for more than 350 km. These ophiolites were obducted from west during Paleocene-Early Eocene time on to the Indian continental lithosphere (Allemann 1979; Ahmed and Abbas 1979; Sarwar and DeJong 1984; Sarwar 1992). To the south, except along the eastern edge, this block contains a triangular depression filled with recent sediments pointing northward, the Porali Trough (Kazmi and Rana 1982).

On the eastern border of the block structures are parallel to the PF, whereas its western side is covered over by recent sediments. In the northern part, smaller faults generally traverse to the block

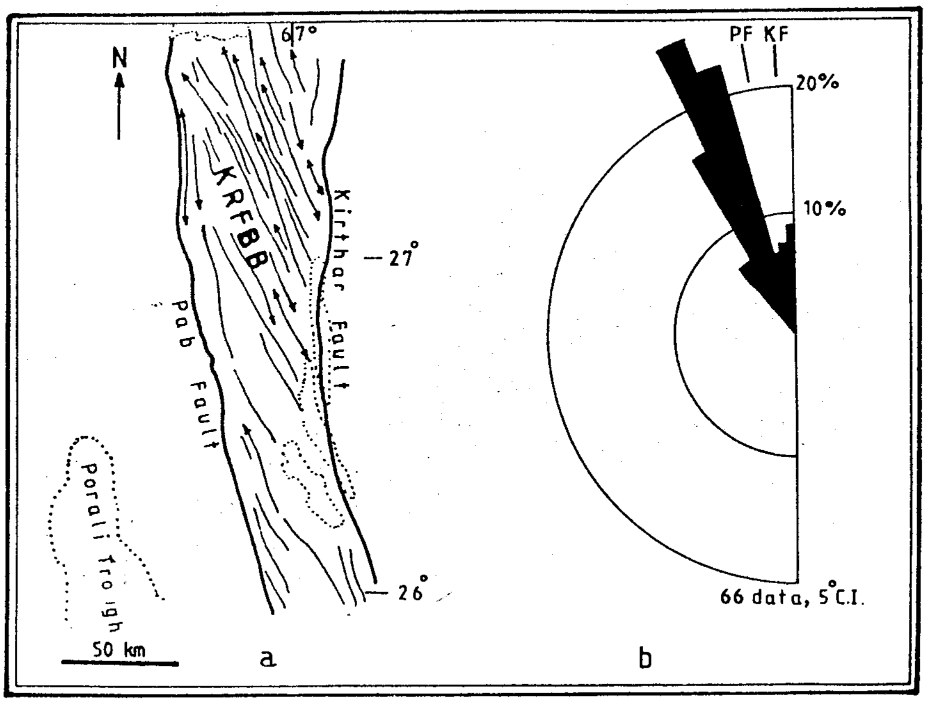

Figure 3. The en-echelon pattern of the folds, oriented clockwise to the length of the Khude Range Fold Belt Block (KRFBB). a, A sketch of the KRFBB, b, Rose diagram of the folds with 5 counting interval in the KRFBB. The PF and the KF are the average trends of the Pab Fault and the Kirthar Fault in the Block.

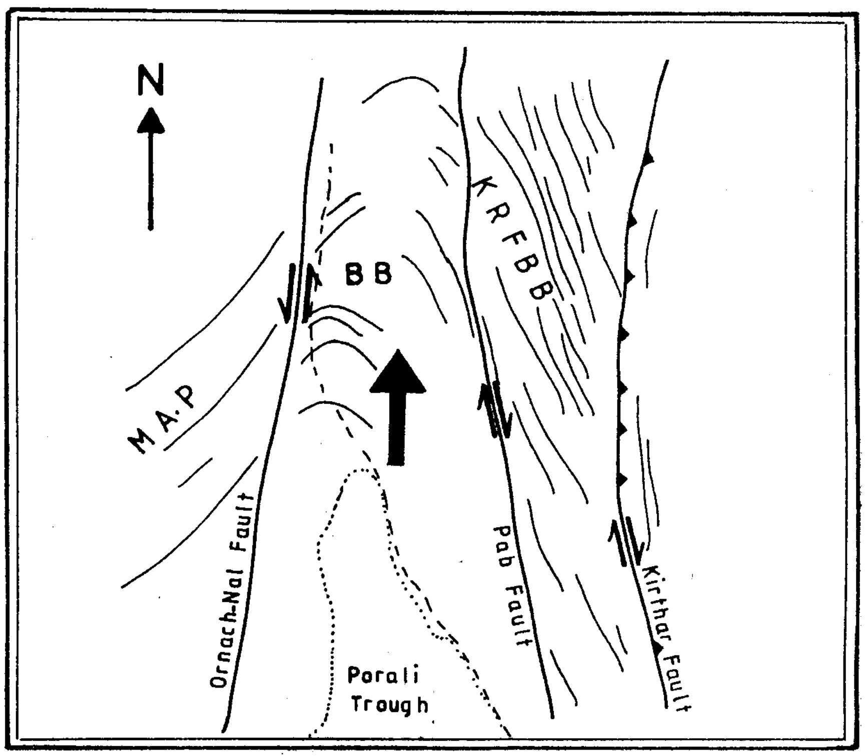

Figure 4. Sketch showing the structural trends in various tectonics blocks are due to a drag, indicating sense of displacement along the Ornach-Nal and the Pab faults, hence facilitating northward movement of the Bela Block. KRFBB; Khude Range Fold Belt Block, BB; Bela Block and MAP; Makran Accretionary Prism.

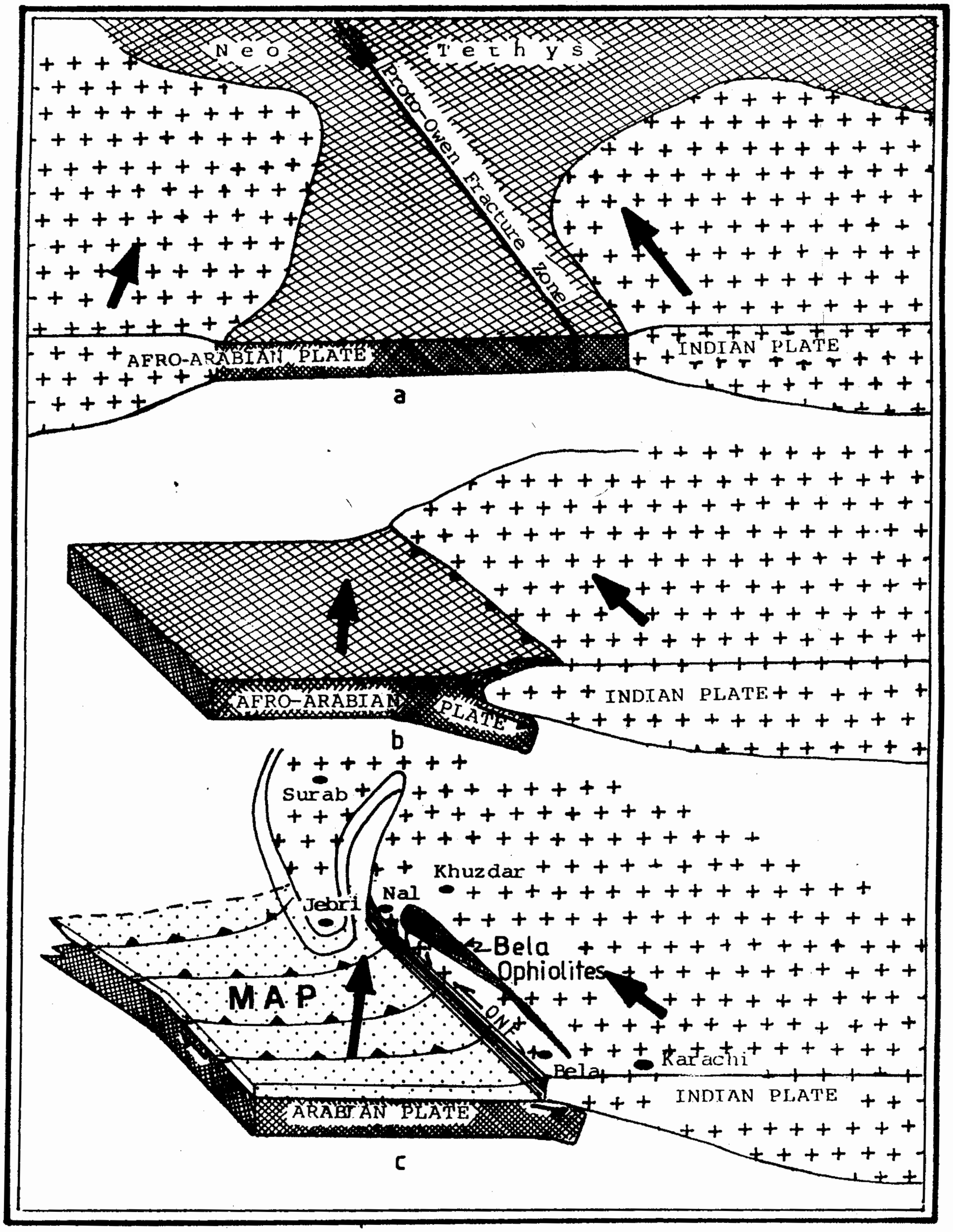

Figure 5. **Developmental stages of structures in the southern Kirthar Fold Belt as a result of interaction of continental lithosphere of the Indian plate and oceanic lithosphere of the Arabian plate. ONF = Ornach-Nal Fault, AGF = Anjira-Gizan Fault, PF = Pab Fault, KF = Kirthar Fault, MAP = Makran Accretionary Prism, BB = Bela Block, KRFBB = Khude Range Fold Belt Block, KK = Khuzdar Knot. a) Northward movement of the Indian plate along the Proto Owen Fracture Zone, b) Obduction of the Afro-Arabian plate on the continental lithosphere of the Indian plate, c) The Arabian plate although mainly subducting beneath Eurasia, also partly underthrusting the continental lithosphere of the Indian plate,** *(continued on facing page)*

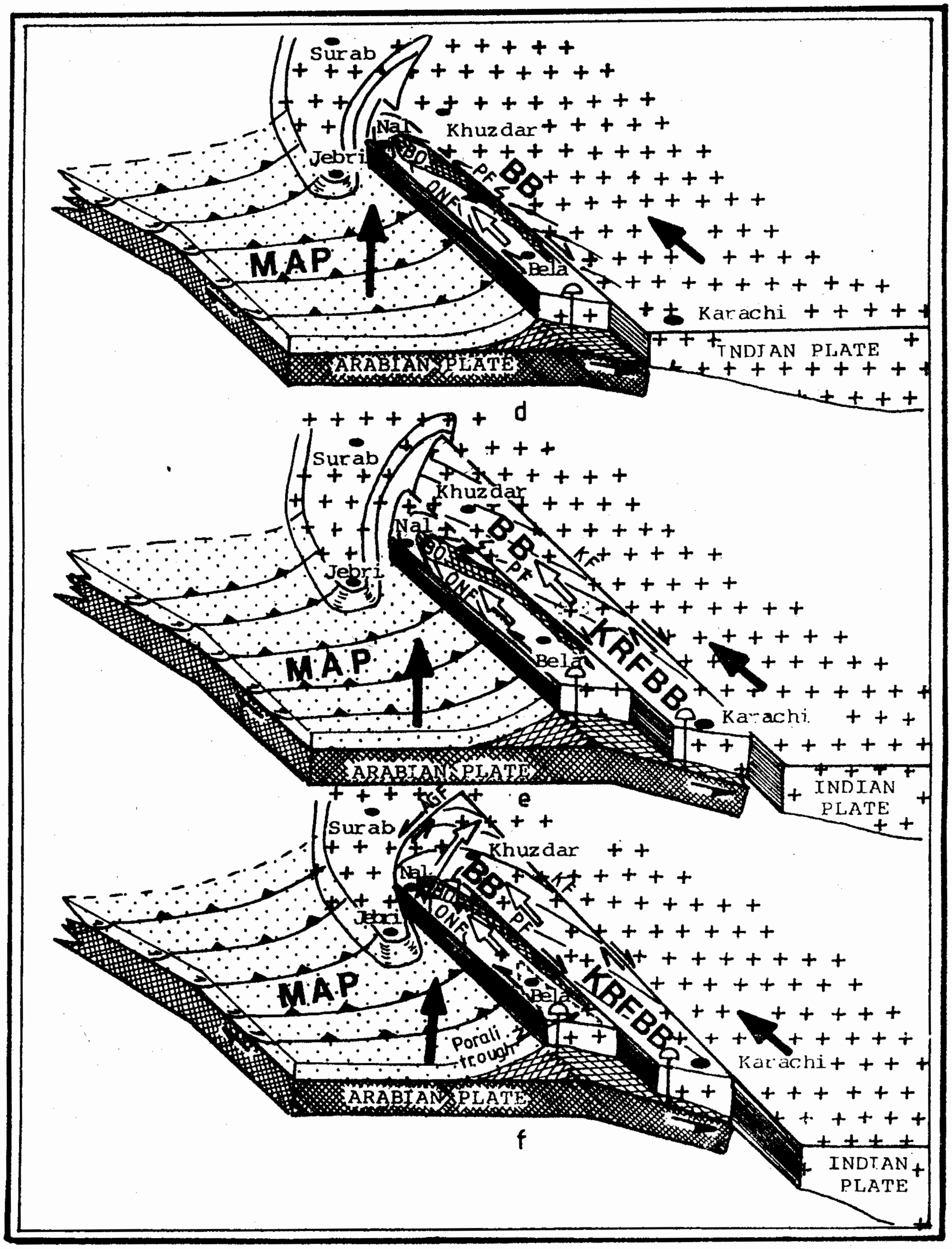

(Continued from previous page) **d) Faster movement of the Arabian plate has ripped off a sliver i.e. the Bela Block from the Indian continental lithosphere and carried it northward coupled with it, e) Further underthrusting of the Arabian plate has ripped off another sliver,the Khude Range Fold Belt Block from the continental lithosphere of the Indian plate and carried both slivers northward, f) Northward movement of the Bela Block and the Khude Range Fold Belt Block chocked the gap between the slivers and the southern extension of the northern Kirthar Fold Belt i.e. Surab-Jebri zone along the Anjira-Gizan Fault. Later translation of the slivers along the Anjira-Gizan Fault has refolded the earlier structures in Khuzdar Knot.**

are arcuate in plan view and convex northward. Close to the ONF, to the north of the Bela town, these smaller arcuate faults have disrupted the ophiolitic slices as well as sediments of Pliocene age (Hunting Survey Corporation 1961, map No. 11).

KHUZDAR KNOT (KK)

It is a complex swirling structure right in the middle of the KFB (Sarwar and DeJong 1979). It is a block bounded to the east, north and west by the KF, the AGF and the ONF respectively. The fold axes, although zigzag in plan, are arcuate on the map, convex northward. In the eastern part of the knot the folds are oriented parallel to the en-echelon folds of the KRFBB and merge with them. The folds are EW-oriented in the central part of the knot, but swing towards SW in its western part where they are terminated against a fault parallel to the ONF.

To the west of the KK and across the ONF, structures are a continuation of the northern part of the KFB and continue further southwest as far as Jebri (Bakr and Jackson 1964), the western most part of the Indian continental lithosphere. On its south side, the KRFBB and the BB grades into it, while the PF terminates against it, at least surface manifestations of PF.

KINEMATICS AND DISCUSSION

The complexity of structures in the southern Kirthar Fold Belt include the NNW-trending en-echelon folds of the KRFBB; different types of displacements along PF at bends along it; northward convex arcuate structures in the BB and swing in these on the map. All these structures were developed in a thin-skinned fashion and indicate sinistral displacement along the ONF but dextral along the PF. This leads to a conclusion that the BB has moved at a faster rate, than adjacent KRFBB to the east and the MAP to the west (Fig. 4).

It is now widely accepted that India has moved northward from southern latitudes from Cretaceous onward (Powell 1979, Klootwijik 1979). It has drifted northward along a NS-oriented huge transform fault on its western border, the Proto-Owen Fracture Zone (Fig. 5a; McKenzie and Sclater 1971 & 1973; Nortan and Sclater 1979; McCormic 1989). In Cretaceous times, India was moving at a faster rate, which drastically reduced when it collided with Eurasia in Paleocene-Early Eocene (Powell 1979; Klootwijik 1979; Schwan 1985; Patriat and Segoufin 1988). As a consequence of collision with Eurasia, the convergence direction of India also changed and it rotated counterclockwise (Powell 1979; Klootwijik 1979) with a close pole to the west. Rotation of the Indian plate caused obduction of the Kanar Melange (Sarwar and DeJong 1984) and the later Bela Ophiolites on the western edge of the Indian plate (Fig. 5b, DeJong and Subhani 1979; Sarwar 1992). According to Brookfield (1977) many ophiolites were emplaced along transform zones bordering the continental margins during change in the direction of plate motion. Later the Arabian plate rifted from Africa along the Red Sea in Late Eocene and moved northward (Colmen 1974; Kazmin 1991). The Indian and Arabian plates both are converging northward toward Eurasia, the latter at a faster rate (McKenzi and Sclater 1971; Jacob and Quittmeyer 1979). To the east of the Oman line oceanic lithosphere of the Arabian Plate, which is covered by a thick pile of sediments forming an accretionary prism, is subducting under Eurasia (Arthurton et al. 1982; DeJong 1982; Jacob and Quittmeyer 1979; Sengör 1985 & 1986). The accretionary prism is so thick that it is elevated up to about 2 km above sea level. Mismatch between seismic activity in the region and Arabian/Eurasian convergence suggest aseismic slip in the subsurface (Quittmeyer et al. 1979). This indicates that the Arabian plate is moving at a faster rate than the overlying accretionary prism where thrust slices are stacked up in an EW-direction.

In post Oligocene/Miocene times, the oceanic lithosphere of the Arabian Plate underthrust the continental lithosphere of the Indian Plate and ripped off a sliver, coupled with it carried along the PF at a faster rate than the parent mass (Figs. 5c & 5d). This was analogous to the northward movement of the coastal California, coupled with the Pacific Plate moving along the San Andreas Fault (Anderson 1971). The PF is analogous to a trench-linked strike slip-fault formed at an oblique subduction margin (Woodcock 1986). The absence of a well developed trench and a magmatic arc in the region is because of the low angle between the plate boundary along the ONF and the movement vector of the Arabian Plate with respect to India (Jacob and Quittmeyer 1979). However, the subduction was probably enough to produce a fore arc depression in the form of Porali Trough, filled with recent sediments (Hunting Survey Corporation 1961; Bakr and Jackson 1964). Later when the Arabian Plate further plunged beneath the continental lithosphere of the Indian Plate, the KF formed with a probable dextral component (Fig. 5e). The northward movement of the BB and the KRFBB were probably facilitated either by the presence of a thin continental lithosphere or due to a gap in continental lithosphere and presence of ocanic lithosphere along AGF. Geophysical studies

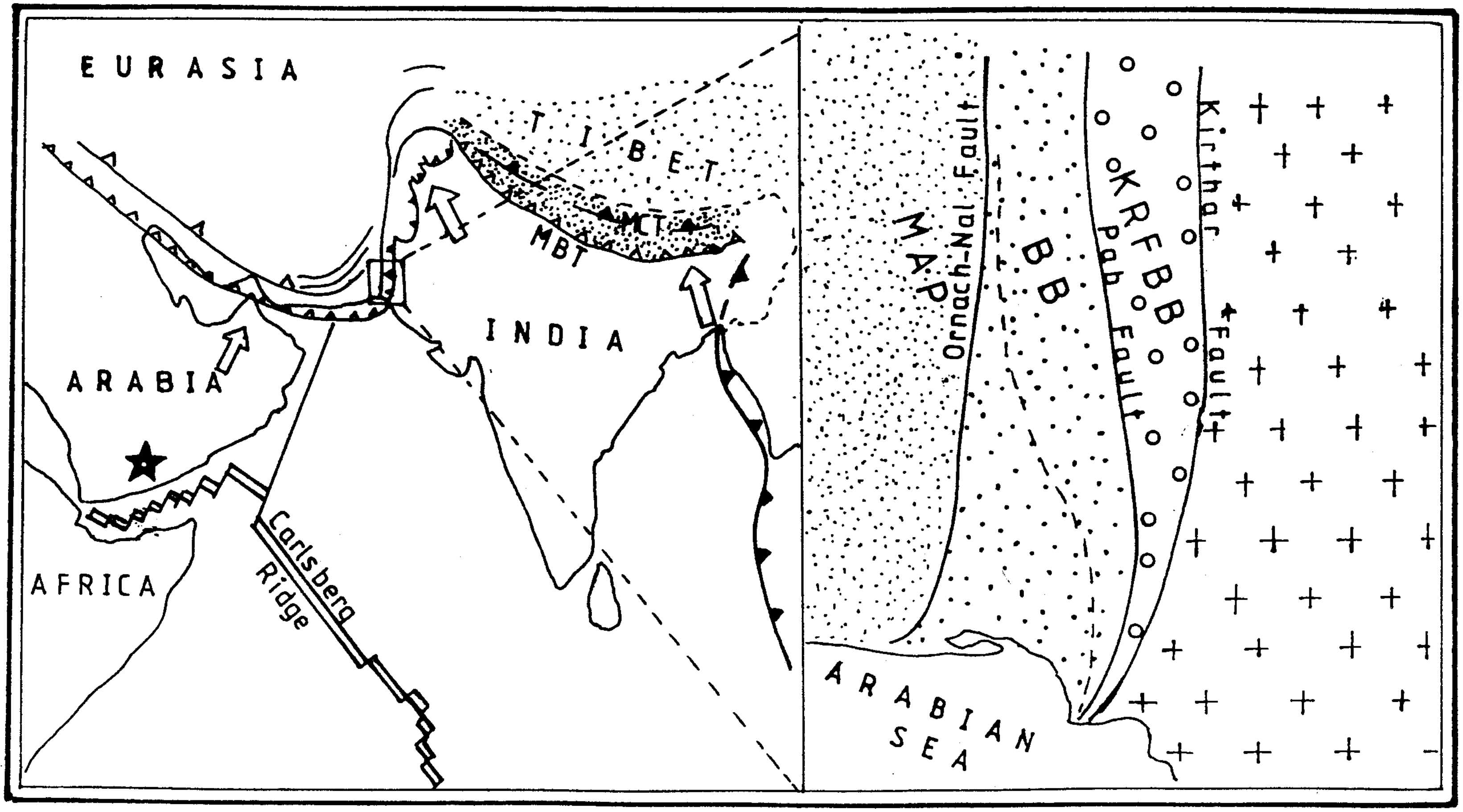

Figure 6. Counterclockwise rotation of the Indian plate resulting in asymmetry in the Himalaya (thick stipples) and Tibet (thin stipples). Reflection of this is asymmetry is also present in the southern Kirthar Fold Belt where slivers of the Indian plate : the Bela Block and the Khude Range Fold Belt Block became wider towards north. a, Map of the region with the pole of rotation of India/Eurasia convergence is located in Arabia (modified after Powell 1979), b, A sketch of the southern Kirthar Fold Belt. Discontinuous line in the Bela Block is the boundary of rock exposures limited to the east of it. MCT = Main Central Thrust & MBT = Main Boundary Thrust, rest of the abbreviations are same as in Figure 4.

indicate a deeper Moho about 20 km in the coastal region which gets shallower northward and it is only 10 km deep in the Bela region (Zaigham 1991). These two slivers i.e. the BB and the KRFBB after their detetchment from the Indian continental lithosphere have moved northward in conjunction with the oceanic Arabian lithosphere collided with the northern Kirthar Fold Belt along the AGF (Fig. 5f). The evidence for this is the presence of small ophiolitic fragments along the AGF on the Quetta-Karachi highway. Aeromagnetic data also indicate that the northern part of the Bela Ophiolites was also effected by north-south oriented compressive forces (Allan Spector and Associates 1981).

The BB and the KRFBB have translated along the sinistral AGF and produced a drag in the north northwesterly oriented fold belt of the Khude Range. Consequently, the folded sedimentary cover in the northern part of the KRFBB and folded sediments of the BB along with some ophiolitic fragments have rotated counterclockwise in a thin-skinned fashion up to about 90 degree to produce the KK. Aeromagnetic studies also indicate a counterclockwise rotation of the ophiolitic slices present in the northern portion of the Bela Ophiolites (Zaigham 1991). It is interpreted that the displacement of the BB and the KRFBB along the AGF produces an eastward deflection in the KRFB and probably are also causative for a change in the dip direction of the KF. Geophysical studies support the model which is based on detailed analysis of gravity, aeromagnetic and seismicity indicate that the Arabian Plate dips at about 20 degree eastward below the Indian continental lithosphere (Zaigham, op cit.).

In Miocene and onward the Indian plate further rotated counterclockwise on a close pole (at about 16 N, 48.3 E) in the southern Arabia (Powell 1979). The effect of this rotation was the variation in the width of the Himalayan orogen and the distance between the Main Central Thrust and the Main Boundary Thrust in the main Himalaya which decreases from east to west. Moreover, the width of the Tibetan Plateau where crustal thickness is double the normal 35 km (Gupta and Narain 1967; Kano 1974; Choudhry 1975) also decreases from east to west. The rate of convergence between the Indian Plate and the Tibet Plateau decreases from 5.4 cm/yr in the eastern Himalaya to 3.7 cm/yr in the Punjab Himalaya (Minster et al. 1974). The southward tapering of the KRFBB and the BB, excluding the Porali trough, at the northwestern edge of the Indian Plate is also attributed to this counterclockwise rotation of India on this close pole of rotation (Fig. 6). This rotation leads to a greater convergence and hence underthrusting of the Arabian plate in the northern part of the ONF as compared to the southern part of the ONF and an ultimate southward tapering slivers of the KRFBB and the BB excluding of course, the Porali Trough.

CONCLUSION

In the southern Kirthar Fold Belt, there are NS-trending tectonic units separated from each other by faults of crustal depth. In the Khude Range Fold Belt Block bounded between NS-trending the Pab and the Kirthar faults, folds are NNW-oriented, arranged in an en-echelon pattern counterclockwise to the fault's trend. This indicate a dextral displacement along the Pab Fault and probably also along the Kirthar Fault. The Bela Block which is bounded between the Ornach-Nal Fault and the Pab Fault is also NS-oriented. The drag of the Makran Orocline and the presence of smaller faults, arcuate in plan convex northward in the Bela Block indicate a sinistral displacement along the Ornach-Nal Fault. All of this indicates a northward movement of the Bela Block with respect to it's surroundings.

The northward translation of the Bela Block is attributed to the northward converging Arabian plate. The oceanic lithosphere of the Arabian plate although underthrusting the Eurasia, partly underthrusts the Indian plate, ripped off sliver of continental lithosphere of the latter, coupled with it carried northward at a faster rate than the parent Indian mass. Further plunge of the Arabian lithosphere ripped off another sliver, the Khude Range Fold Belt Block, coupled with it carried northward. This northward displacement of the slivers was facilitated by a gap in the Indian continental crust at the site of the Anjira-Gizan Fault, evident by the presence of ophiolitic fragments along it. By northward drift of the Bela Block and the Khude Range Fold Belt Block and their collision with the northern Kirthar Fold Belt along the Anjira-Gizan Fault, the NNW-oriented folds of the Khude Range Fold Belt refolded into a zigzag pattern. This was accompanied or followed by a sinistral movement along the Anjira-Gizan Fault, ultimately resulted in a drag in the NNW-trending folds of the Khude Range Fold Belt causative for the formation of the Khuzdar Knot.

REFERENCES

Ahmed, Z., and Abbas, S.G., 1979. The Muslim Bagh Ophiolites. **In:** Farah, A., and DeJong, K.A. (eds), Geodynamics of Pakistan. Geological Survey Pakistan, Quetta. p. 243-249.

Allan Spector and Associates, 1981. Report on Interpretation of Aeromagnetic Survey Data, Baluchistan Province, Pakistan. Toronto, Canada project J223.

Alleman, F., 1979. Time of Emplacement of the Zhob Valley Ophiolites, Balochistan (Preliminary Report). **In**: Farah, A., and DeJong, K.A. (eds), Geodynamics of Pakistan. Geological Survey Pakistan, Quetta. p. 215-242.

Anderson, D.L., 1971. The San Andreas Fault. **In**: Tuzo Wilson's Continents Adrift and Continents Aground (1976). W.H. Freeman and Co., San Francisco. p. 87-102.

Arthurton. R.S., Farah, A. and Ahmed, W., 1982. The Late Cretaceous-Cenozoic history of Western Baluchistan, Pakistan the northern margin of the Makran subduction complex. **In**: Leggett, J.K. (ed), Trench-Forearc Geology. Geological Society Special Publication 10: p. 373-385.

Auden, J.B., 1974. Afghanistan-West Pakistan, **In**. Spencer, A.M. (ed), Mesozoic-Cenozoic belts, data for orogenic studies. Geolical Society Special Publication 4, p. 235-253.

Aydin, A., and Page, B.M., 1984. Diverse Pliocene-Quaternary tectonics in a transform environment, San Francisco Bay Region, California: Geological Society America Bulletin v. 95, p. 1303-1317.

Bakr, M.A., and Jackson, R.O., 1964. Geological Map of Pakistan (1: 2,000,000) Geological Survey Pakistan, Quetta, Pakistan, 1964.

Brookfield, M.E., 1977. The emplacement of giant ophiolite nappes. Mesozoic-Cainozoic complexes. Tectonophysics, v. 37, p. 247-303.

Choudhury, S.K., 1975. Gravity and crustal thickness in the Indus-Gangetic Plains and Himalayan region, India:Royal Astronomical Society Geophysics Journal, v. 40, p. 441-452.

Colmen, R.G., 1977. Ophiolites. Springer-Verlag, Berlin.

DeJong, K.A., 1982. Tectonics of the Persian Gulf, Gulf of Oman, and Southern Pakistan Region. **In**: Nairn, A.E.M., and Stehli, F.G. (eds), The Ocean Basins and Margins. 6, The Indian Ocean. Plenum Press, New York. p. 315-351.

DeJong, K.A., and Subhani, A.M., 1979. A note on the Bela Ophiolites, with Special Reference to the Kanar Area. **In**: Farah, A., and DeJong, K.A. (eds), Geodynamics of Pakistan. Geological Survey Pakistan, Quetta. p. 263-269.

Dibblee, T.W.Jr., 1977. Relations of hydrocarbon accumulations to strike slip tectonics of the San Andreas fault system, **In**: Nilsen, T.H.(ed), Late Mesozoic and Cenozoic sedimentation in California. Bakersfield, California, San Joaquin Geophysical Society p.135-143.

Farah, A., Abbas, S.G., DeJong, K. A. and Lawrence, R. D., 1984. Evolution of the Lithosphere in Pakistan. Tectonophysics, v. 105, p. 207-227.

Farhoudi, G., and Karig, D.E., 1977. Makran of Iran and Pakistan as an active arc system. Geology, v. 5, p. 664-668.

Gupta, H.K., and Narain, H., 1967. Crustal structures in the Himalayan and Tibet plateau region from surface waves dispersion. Seismological Society America Bulliten, v. 57, p. 235-248.

Harding, T.P., and Lowell, J.D., 1979. Structural style, their plate tectonic habitats, and hydrocarbon traps in petroleum provinces. American Association Petroleum Geologists Bulletin, v. 63, p. 1016-1058.

Hunting Survey Corporation, 1961. Reconnaissance Geology of part of West Pakistan. Colombo Plan Coop(rative Project, Toranto, Government of Canada.

Jacob, K.H., and Quittmeyer, R.L., 1979. The Makran Region of Pakistan and Iran: Trench Arc System with Active Plate Subduction. **In**: Farah, A., and DeJong, K.A., (eds), Geodynamics of Pakistan. Geological Survey Pakistan, Quetta. p. 303-317.

Kano, M., 1974. Gravity anomalies in east Nepal and their implications to the crustal structures of the Himalayan: Royal Astronomical Society Geophysical Journal, v. 39, p. 283-300.

Kazmi, A.H., 1979. Active Fault Systems in Pakistan. **In**: Farah, A., and DeJong, K.E. (eds), Geodynamics of Pakistan. Geological Survey Pakistan, Quetta. p. 285-294.

Kazmi, A.H., and Rana, R.A., 1982. Tectonic Map of Pakistan (1:2,000,000). Geol. Surv. Pakistan, Quetta, Pakistan.

Kazmin, V. G., 1991. Collision and rifting in the Tethys Ocean: geodynamic implications. Tectonophysics, v.196, p. 371-384.

Kemal, A., 1991. Geology and New Trends for Petroleum explorationon in Pakistan. **In**: Ahmed, G., Kemal, A., Zaman, A.S.H., and Humayon, M. (eds), Proceedings in New directions and strategies for accelerating petroleum exploration and production in Pakistan. Ministry of Petroleum and Natural Resources, Govt. of Pakistan. p. 16-57.

Klootwijk, C.T., 1979. A Review of Paleomagnetic Data from the Indo-Pakistani Fragment of Gondwanaland. **In**: Farah, A., and DeJong, K.A. (eds), Geodynamics of Pakistan. Geological Survey Pakistan, Quetta. p. 41-80.

Klootwijik, C.T., Nazirullah, R., DeJong, K.A., and Ahmed, H.A., 1981. Paleomagnetic reconnaissance of northeastern Baluchistan, Pakistan. Journal Geophysical Research, v. 86, p. 289-306.

Lawrence, R.D., Khan, S.H., DeJong, K.A., Farah, A. and Yeats, R.S., 1981. Thrust and strike slip fault interaction along Chaman transform zone, Pakistan. **In**: McClay, K.R. and Price, N.J., (eds), Thrust and Nappe Tectonics. Geological Society Special Publication 9, p. 363-370.

McCormic, G.R., 1989. Geology of Baluchistan (Pakistan) portion of the southern margin of the Tethys Sea. **In**: Sengor, A.M.C. (ed), Tectonic evolution of the Tethyean Region. Kluwer Academic Publishers. p. 277-288.

McKenzie, D.P., and Sclater, J.G., 1971. The evolution of the Indian ocean since the Late Cretaceous: Royal Astronomical Society Geophysics Journal, v. 24: p. 437-528.

McKenzie, D.P., and Sclater, J.G., 1973. The evolution of the Indian Ocean. **In**: Tuzo Wilson's Continents Adrift and Continents Aground (1976). W.H. Freeman and Co. p. 138-148.

Minster, J.B., Jordan, T.H., Molnar, P. and Haines, E., 1974. Numerical modelling of instantaneous plate tectonics: Royal Astronomical Society Geophysics Journal, v. 36, p. 541-576.

Nakata, T., Khan, S.H. and Tsutsumi, H., 1989. Photogrametric study on active faults of Pakistan. **In**: Okimura, Y., and Fatmi, A.N.,(eds), Tectonics and Sedimentation of the Indo-Eurasian Colliding Plate Boundary Region and it's Influence on the Mineral Development in Pakistan. Hiroshima University, Hiroshima. p. 69-82.

Norton, I.O., and Sclater, J.G., 1979. A model for the evolution of the Indian Ocean and the breakup of Gondwanaland. Journal Geophysical Ressearch, v. 84, p. 6803-6830.

Patriat, P., and Segoufin, J., 1988. Reconstruction of the Central Indian Ocean. Tectonophysics, v. 155, p. 211-234.

Powell, C.McA.A., 1979. Speculative Tectonic History of Pakistan and Surroundings: Some Constraints from the Indian Ocean. **In**: Farah,A., and DeJong, K.A., (eds), Geodynamics of Pakistan. Geolical Survey Pakistan, Quetta. p. 5-24.

Qureshi, M.J., Tariq, M.A., and Abid, Q.Z., 1993. Geological Map of Pakistan (1:1000,000). Geol. Surv. Pakistan, Quetta, Pakistan.

Quittmeyer, R.C., Farah, A., and Jacob, K.H., 1979. The seismicity of Pakistan and its Relation to Surface Faults. **In**: Farah, A., and DeJong, K.A., (eds), Geodynamics of Pakistan. Geological Survey Pakistan, Quetta. p. 271-284.

Ramsay, J.G., and Huber, M.I., 1987. The Techniques of Modern Structural Geology, V.2. Academic Press Inc., London.

Sengor, A.M.C., 1985. The story of Tethys: How many wives Did Okeanos Have ? Episodes, v. 8, p. 3-12.

Sengor, A.M.C.,1986. The dual nature of the Alpine-Himalayan system: progress, problems and prospects. Tectonophysics, v. 127, p.177-195.

Sarwar, G., 1992. Tectonic setting of the Bela Ophiolites, southern Pakistan, Tectonophysics, v. 207, p. 359-381.

Sarwar, G., and DeJong, K.A., 1979. Arcs, Oroclines, Syntaxes: the Curvatures of Mountain Belts in Pakistan, **In**: Farah, A., and DeJong, K.A., (eds), Geodynamics of Pakistan. Geolical Survey Pakistan, Quetta. p. 341-349.

Sarwar, G., and DeJong, K.A.,1984. Composition and origin of the Kanar Melange, southern Pakistan. Geological Society America Special Paper, 198, p. 127-137.

Schwan, W., 1985. The worldwide active Middle/Late Eocene geodynamics episode with a peak at + 45 and + 37 m.y. B.P. and implications and problems of orogeny and sea floor spreading : Tectonophysics, v.115, p. 197-234.

Seeber, L., Armbruster, J.G., and Quittmeyer, R.C., 1981. Seismicity and continental subduction in the Himalayan Arc. **In**: Gupta,H.K., and Delnay, F.M., (eds), Zagros, Hindu Kush, Himalaya: Geodynamic Evolution. Geodynamic Series V. 3. American Geophysical Union, p. 215-242.

Sylvester, A. G., 1988. Strike-slip faults. Geological Society America Bulletin, v. 100, p. 1666-1703.

Tapponier, P., Peltzer, G., and Armijo, R., 1986, On the Mechanism of collision between India and Asia. **In**: Coward, M.P., and Ries, A.C., (eds) Collision Tectonics. Geological Society Special Publication, 19, p. 115-158.

Woodcock, N.H., 1986. The role of strike-slip fault system at plate boundaries, Philosophical Transcripts Royal Society London, A 317, p. 13-29.

Woodcock, N.H., and Fischer, M., 1986. Strike-slip duplexes, Journal Structural Geology, v. 8, p. 725-735.

Zaigham, N. A., 1991. Bela Ophiolites and Associated Mineralization in southern part of Axial Belt of Pakistan. Ph.D. thesis (unpublished). University of Karachi.

Manuscript Received 25th October 1999
Revised Manuscript Received 10th November 1999
Accepted 10th November 1999

The paper was presented by the author in the Second South Asia Geological Congress (GEOSAS-II) held at Colombo, Sri Lanka, January 19-24, 1995.

ACTA
MINERALOGICA
PAKISTANICA
Volume 9 (1998)

Article Reference
AMP9.1998/085-102/ISSN.0257-3660

ORE MINERALOGY AND MINERAL PARAGENESIS OF THE BASE METAL DEPOSITS NEAR KHUZDAR, BALOCHISTAN, PAKISTAN.

SHAMIM AHMED SIDDIQUI
Centre of Excellence in Mineralogy, University of Balochistan, Quetta Pakistan

ABSTRACT

Field study of the sediment-hosted lead-zinc-barite mineralization in Khuzdar district reveals that barite occurs in association with base metals only at Gunga, other locations (i.e., Surmai, Malkhor, and Sekran) are devoid of any barite. The mineralization at Gunga occurs in two zones: upper and lower mineralized zones separated by a relatively thin barren zone. The upper zone is primarily a sulfate zone composed mainly of huge massive bed of barite containing also some base metal sulfide mineralization in its lower and middle parts. The lower zone is a sulfide zone cropping out as huge gossan on the surface which contains unaltered sulfide minerals at depth. Sphalerite, galena, pyrite and marcasite are the dominant while chalcopyrite and cinnabar are the minor sulfide minerals of the base metal mineralization at Gunga, Surmai, Malkhor, Sekran and elsewhere in the district. Gangue minerals include barite, quartz, chalcedony, siderite, calcite, etc. The mineralization is of both cavity-filling and replacement types. It occurs in dissemination and forms veins, streaks, patches, lenses, mineralized breccia, and replaced beds. There could be more than one generation of mineralization. The microscopic studies of polished thin sections reveal that there could be two paragenetic sequences of ore minerals in the area: 1) sphalerite-galena-Pyrite/marcasite-siderite-quartz; and 2) simultaneous crystallization of sphalerite, galena and pyrite.

INTRODUCTION

The Balochistan province of Pakistan has a variety of volcanic, plutonic and sedimentary rocks ranging in age from Triassic to Recent. These rocks not only contain large fuel deposits (natural gas and coal) but also contain a host of minerals, including chromite, fluorite, barite, magnesite, iron ore, and copper minerals such as chalcopyrite and chalcocite, which are commercially important. Minerals like sphalerite and galena, containing the base metals zinc and lead respectively, are among those whose presence in the province is proven but further exploration and development work must be done to determine if these prospects can be economic.

Base-metal mineralization is observed at several locations in a region known as the Khuzdar-Lasbela metallogenic zone, which extends for about 400 km from Khuzdar in the north to Lasbela in the south. Gossans, representing underlying unaltered Pb-Zn mineralization, are exposed sporadically in the area. Noteworthy among these locations are those of Gunga, Malkhor, Sekran and Surmai in the north, and Duddar far to the south in the Lasbela district. This northerly trending metallogenic zone occurs mainly in the Mesozoic shallow marine continental shelf deposits which are for the most part in contact with the famous Bela ophiolites. The Jurassic Zidi Formation hosting lead-zinc-barite mineralization in the area consists of a thick sequence of alternating beds of limestone and shale deposited at the edge of the Indo-Pakistan continental plate.

The project area (Fig. 1) lies almost at the centre of the Balochistan province, in the vicinity of Gunga which, in turn lies about 9 km to the west of Khuzdar. The town of Khuzdar lies midway along the RCD Highway that links Khuzdar with Quetta 304 km to the north, and with Karachi 370 km to

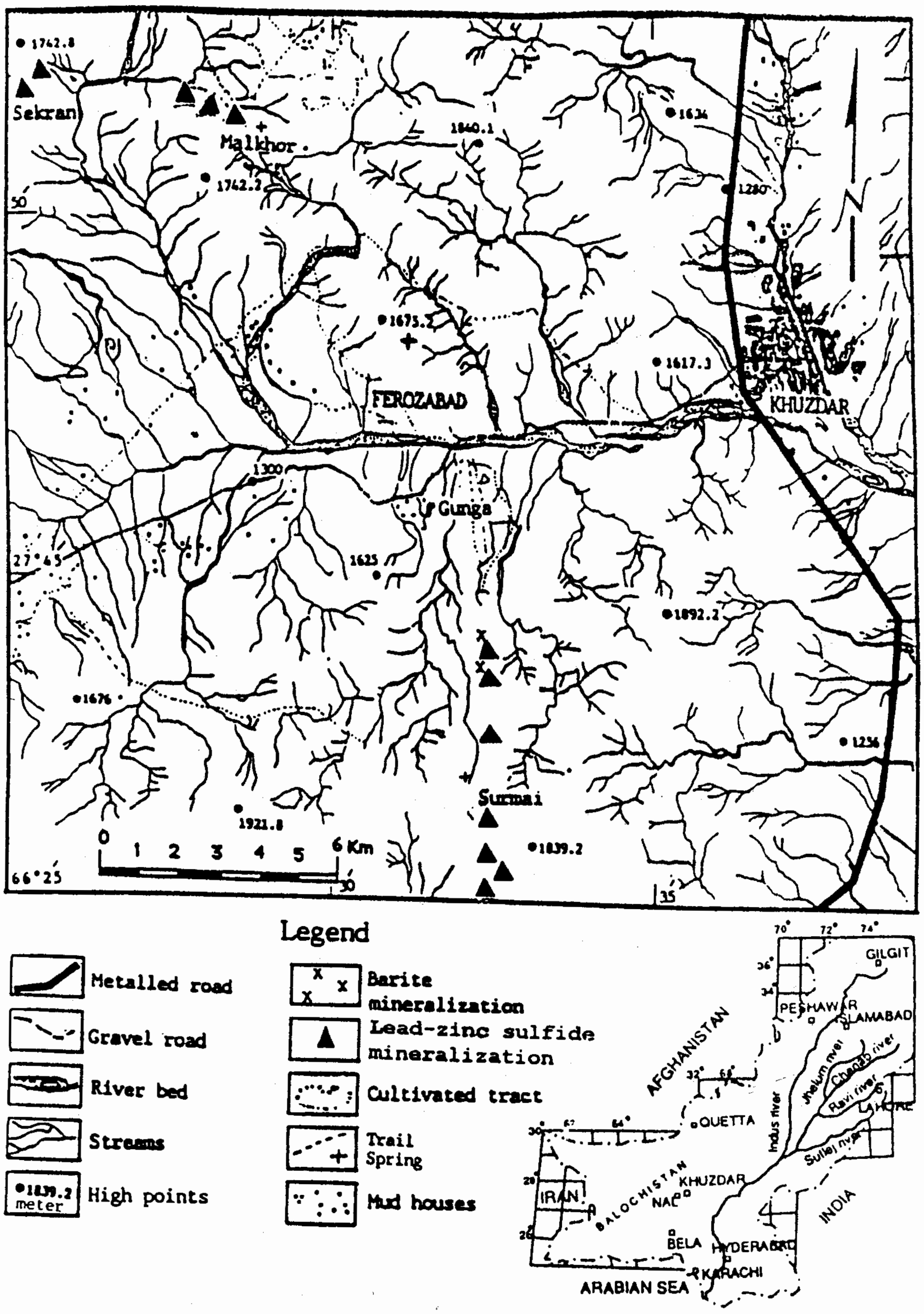

Figure 1. Map showing locations of barite and lead-zinc mineralization near Khuzdar, Pakistan.

the south. The deposits lie west of Khuzdar close to a gravel road which, passing through Nal, leads to Turbat and Makran. A large barite deposit and underlying gossan is exposed close to Gunga; hence the name Gunga lead-zinc-barite deposit. The other locations, namely, Surmai, Malkhor and Sekran lie south and NW of Gunga within a distance of not more than 18 km.

The massive barite deposits of Gunga near Khuzdar were first discovered by Waheeduddin Ahmad, a geologist of the Geological Survey of Pakistan, long ago in 1950. Then in 1960, the deposits were described and their reserves calculated by the Hunting Survey Corporation, Canada (HSC 1961), while working under a joint project with Geological Survey of Pakistan. Schmidt et al. (1961) also reported the presence of barite in the area. Klinger and Ahmed (1967) studied the barite deposit at Gunga and revised the reserves. They also noted the presence of fine grained galena as well as small specks of cinnabar within barite. Around 1979, the lead-zinc mineralization was discovered by geologists of the Geological Survey of Pakistan. Hoagland (1981) investigated Fe-Pb-Zn-Ba mineralization in the region and described its geology. The first systematic geological and scientific exploration of the lead-zinc mineralization in the area was carried out under a joint project between the Geological Survey of Pakistan and the UNDP during 1981-1983. Under this project geological and geophysical investigations were conducted and bore holes were drilled in the Gunga area. During 1986 to 1989, Japan International Cooperation Agency (JICA) undertook, as a joint project with Geological Survey of Pakistan, geological, geophysical and geochemical investigations in Surmai locality which lies a few km south of Gunga deposit. In this paper field and mineralogical aspects of lead-zinc-barite mineralization in the Khuzdar area are discussed in context with the mineral paragenesis.

GEOLOGIC SETTING

The Khuzdar Pb-Zn-Barite deposits occur in the Kirthar Range (Fig. 2) which runs north-south for about 600 km. The Kirthar Range is the southern component of the vast fault and fold zone known as the Pakistan Fold Belt resulting from collision between Indian and Eurasian plates which started 55 m.a. and continues till today. The Pakistan Fold Belt, first runs east-west in northern Pakistan giving rise to important geological features and famous mountain ranges, then, it makes sharp syntaxial bends while turning around the strike through 90 degrees so as to run north-south in the western part of the country. These north-south trending mountains comprise two major ranges: the Sulaiman Range towards north and the Kirthar Range to the south.

The strike of the ranges in the Khuzdar area changes so abruptly and so repeatedly from north-south to east-west and back again to north-south that the area was termed by Jones (1961) as "Khuzdar Knot" because of its knot-like appearance on the map. The Khuzdar-Bela metallogenic province extending southward for about 350 km to the Arabian Sea is bounded by the Kirthar fault on the east and by the Ornach-Nal fault and Gazan fault systems on the west and north respectively. It is believed that the block which is located on the margin of the Indo-Pakistan subcontinent has not only dragged along Ornach-Nal fault in a left lateral manner, but also may have rotated counterclock-wise as an independent tectonic unit (Sarwar and DeJong 1979).

The terrain is mainly comprised of Jurassic and Cretaceous sequences of marine sediments which were deposited on the shelf under fluctuating conditions (Fatmi 1986). The Pb-Zn-Barite mineralization is found associated with the interbedded limestone and shale sequences of the Upper and Middle units of the Jurassic Zidi Formation (Ferozabad Group).

MODE OF MINERALIZATION

GUNGA DEPOSIT

At Gunga the mineralized part of the Jurassic sedimentary sequence is about 100 to 200 meter thick (Plate 1 to 2) which is confined to the Upper Member (Anjira) of the Zidi Formation. This mineralized sequence could be divided into two distinct zones: the lower and upper mineralized zones separated by a predominantly barren zone of interbedded limestone and shale.

Lower Mineralized Zone

This zone consists of 30-70 meter thick highly silicified interbedded carbonaceous shale and siltstone and subordinate limestone. The surface expression of the mineralized zone is represented by a siliceous gossan which crops out in the form of a more than 1000 meter long hog-back ridge striking north-south. Siliceous gossan is composed of leached and silicified calcareous siltstone and red and yellowish brown oxides of Fe (Plate 3 and 4). This consists of alternate hard and soft beds, perhaps depending upon the amount of iron content present in each case. At places it is almost goethite. The total Zn and Pb metal contents of the siliceous

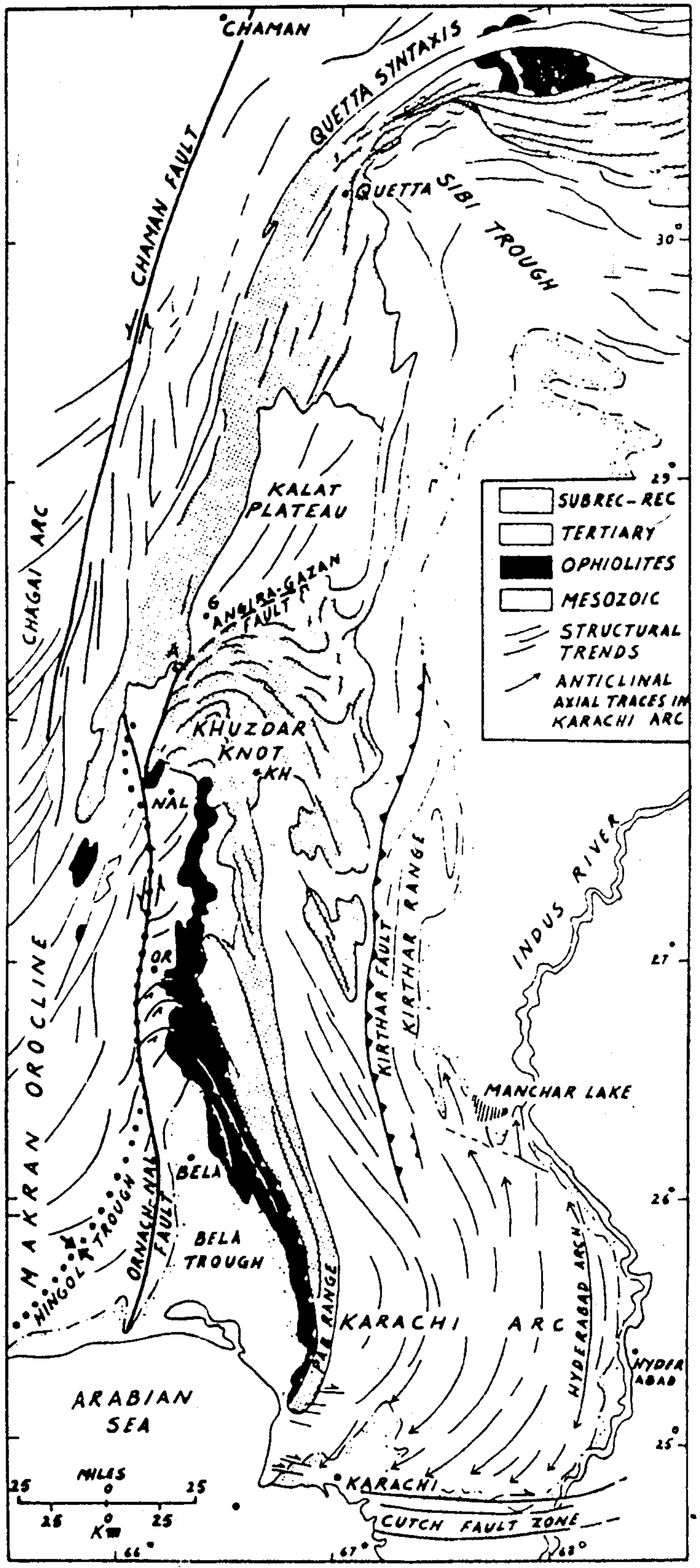

Figure 2. Map showing Kirthar Range and other important geological features in the area stretching between Quetta and Karachi (after Sarwar et al. 1979).

gossan ranges between 0-4 % (Jankovic 1986). The subsurface sulfide mineralization was found to extend for about 400 meters down the dip in the bore-holes drilled by Geological Survey of Pakistan. This lower zone of mineralization is associated with a sequence of hydrothermally altered sediments, e.g. siliceous sinter, siltstone, and siderite.

The siltstone matrix or groundmass contains variable amount of detrital grains with occasional muscovite and disseminated organic matter. The shales are rich in organic material and also contain detrital quartz and muscovite. Limestone is argillaceous and has very fine grained calcite, and the groundmass carries disseminated organic material. The argillaceous limestone frequently contains disseminated tiny grains of framboidal pyrite and marcasite. Rhombohedral grains of disseminated siderite occur locally in the limestone.

The lower mineralized zone is overlain by the relatively barren sequence of interbedded black, dark-gray, bituminous, fossiliferous and argillaceous limestone and shale with siltstone. Angular as well as rounded grains of quartz are occasionally present within this zone. This bed commonly contains disseminated tiny grains of spheroidal pyrite. Transition from the lower mineralized zone to the relatively barren zone (20-50 meter thick) is gradual.

Upper Mineralized Zone

Above this relatively barren band lies another mineralized zone whose base consists of siliceous sinter intermixed with brownish argillaceous material. Dark brown disseminated bituminous matter is frequently found in the basal part of this zone. This part of the upper mineralized zone is devoid of Pb-Zn mineralization except for some specks of barite and pyrite/marcasite.

The actual upper mineralized zone begins with a transitional zone characterized by increasing amounts of disseminated barite, iron, zinc and lead sulfides. The whole upper zone is virtually comprised of a lenticular barite bed (Plate 5 and 6) which varies in thickness from a few meters to about 80 meters. A relatively thin band (a few meters thick) of barite runs parallel to the gossan ridge for about 200 meters and ultimately pinches out in the southward direction.

The barite body is composed mainly of massive barite and the barite intermixed with carbonates and siliceous material. In the lower part ore minerals occur as streaks, patches, and lenses. These tabular and lenticular bodies of zinc, lead, and iron sulfides are 10-40 meter thick (Jankovic 1986). The concentration of sphalerite, galena and pyrite/marcasite generally occurs in the central part of the barite bed. The upper part of this body consists of barite with traces of galena and marcasite and rare sphalerite. A few meters thick bed of siliceous sinter containing limestone, some barite grains and argillite as impurities caps the topmost part of the upper mineralized zone. Interbedded limestone and shale containing traces of zinc near its contact with siliceous sinter lies on top of the upper mineralized zone.

Various types and shapes of mineralization in Gunga deposit include dissemination and thin layers, lenses and patches, mineralized breccia, open space fillings, and massive marcasite/pyrite beds at depth formed by the process of replacement. Ore minerals such as sphalerite, galena, and pyrite/marcasite are found in dissemination as well as forming thin layers within the host siltstone and dark shale. Massive Pb-Zn and Fe sulfides form lenses and patches within siltstone.

SURMAI DEPOSIT

As in Gunga, mineralization in Surmai area is also indicated by gossan, which represents the oxidized zone outcropping at several places in this area. There are at least three main discontinuous north-south trending bodies of gossan known as Surmai-1, Surmai-2, Surmai-3. All of the three mineralized bodies at Surmai are contained within the Middle Member (Loralai Limestone) of Zidi Formation.

The mineralization occurs along bedding planes, fissures, joints, and other cracks and fractures in the form of crosscutting veins and veinlets. It is also seen as extending outward from the fractures and bedding planes into the limestone beds, partly replacing it. Islands of unmineralized limestone are present within the strata replaced by mineralization (Fig. 3). Unlike Gunga deposit, no barite mineralization was observed in the Surmai area.

Gossan

It is mainly composed of yellowish brown, reddish brown and at some places almost black color limonite, dark gray siderite, silicified and dolomitized limestone with dark brown limonitic veins. Light yellow spots commonly found in the oxidized zone probably are formed of lead ochers. Yellowish and greenish crustification is most probably smithsonite (see also Jankovic 1986). Many veins contain massive galena which is associated with limonitic boxwork and has a colloform texture. At places, euhedral to subhedral disseminated grains of galena are also frequently noticed in the gossan. Euhedral quartz crystals commonly fill the cavities and vugs. Apart from galena and quartz, radiating aggregates of marcasite, partially or completely altered to limonite, are also observed. Silicification and sideritization of gossan occur due to metasomatic replacement of limestone caused by the ore-bearing solutions (Jica 1988).

MALKHOR-SEKRAN DEPOSIT

Malkhor-Sekran is another site of Pb-Zn mineralization which is represented by several discontinuous gossan outcrops roughly aligned along a line trending almost east-west. These gossans are individually named as Malkhor, Ranjlaki, and east and west Sekran deposits. They are located about 20 km west of Khuzdar and 16 km northwest of Gunga. The mineralization is hosted, as in Surmai area, by the Loralai Limestone Member of Zidi Formation. The mineralization at Malkhor occurs on the southern limb of a syncline which trends ENE and the mineralized beds are either vertical or dip very steeply. It consists of both replacement and cavity filling types of mineralization. The Ranjlaki mineral deposit is the largest in the area and consists of 7-8 sheets of bedded ore bodies accompanied by crosscutting veinlets. The West Sekran itself seems to be divided into east and west deposits by the intervening fluvial bed. This mineralization consists of several bedded ore bodies accompanied by crosscutting veinsand are in contact with the sandstone of the Spingwar Member.

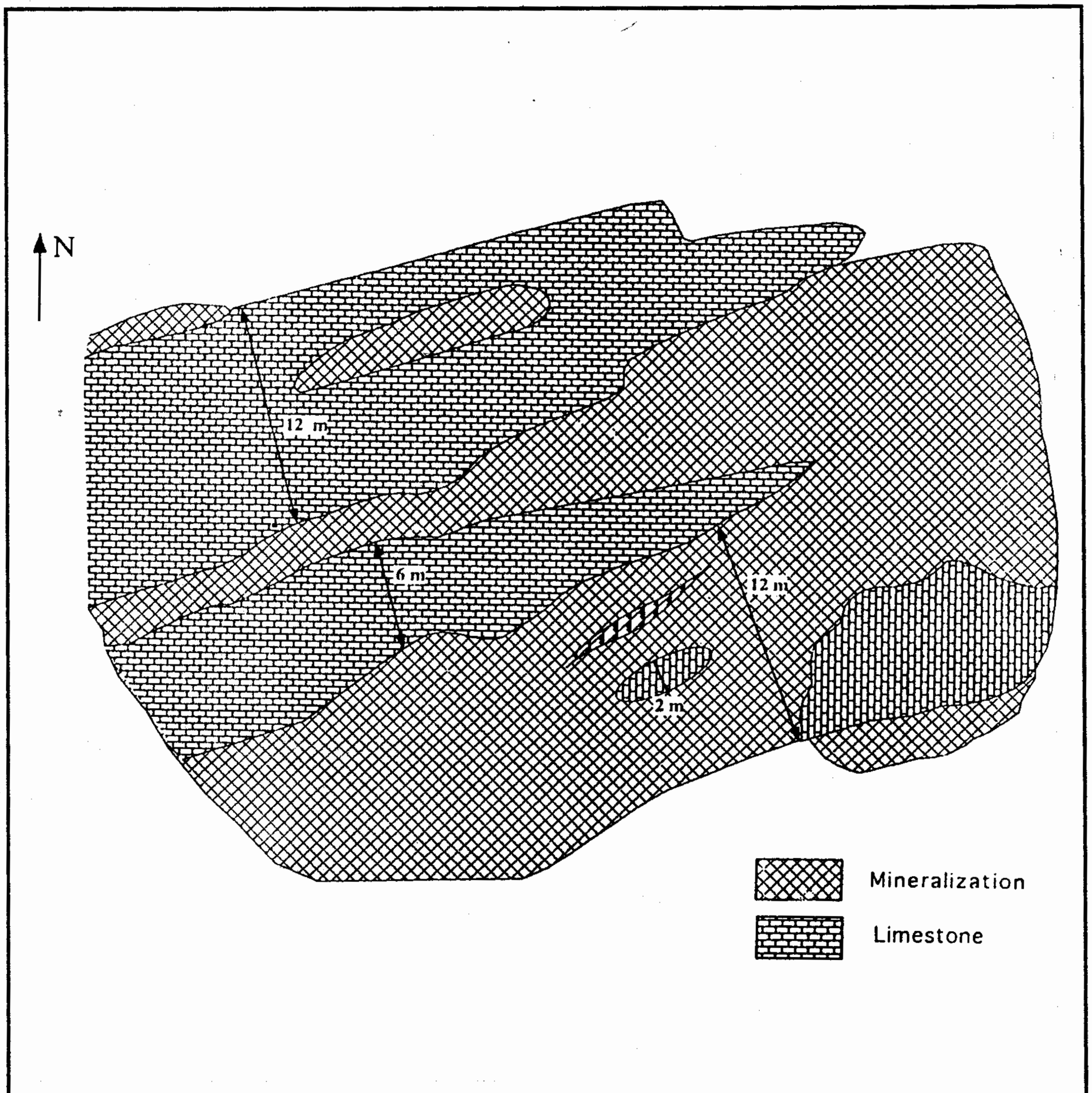

Figure 3. Field sketch showing replacement of limestone by pervasive Pb-Zn mineralization.

ORE MINERALOGY

All the studied deposits consist primarily of pyrite/marcasite, sphalerite, and galena. Minor occurrences of chalcopyrite, cinnabar, and exceptionally pyrrhotite, along with sulphosalts of Pb and Sb have also been reported (see also Jankovic 1986). Gangue minerals include barite, quartz, chalcedony, and carbonates. Traces of native sulfur can be observed with barite and in the oxidation zone. Gypsum and anhydrite are rarely present within barite. Carbonates include siderite, calcite and minor dolomite. Quartz and chalcedony are also observed. The important feature of the Gunga deposit is the colloform texture of almost all of its minerals.

MINERALOGY OF BARITE ZONE

Barite varies in color from almost colorless through white to gray . It is stained with limonite and hematite giving it a rusty brown or reddish brown color. Limonitic veins often cross cut barite adjacent to the oxidized zone. At places reddish brown patches of cinnabar can be recognized (see also Jankovic 1986). Barite occurs as coarse crystalline grains to very fine grained amorphous material forming the groundmass. The coarser-grained barite which generally has prismatic or radiating crystals often occurs as veins or vug fillings. Sometimes calcite is also found in association. This type of barite belongs to second generation which deposited as vein and cavity fillings at a later stage within the fine grained barite. Fine grained barite is the most abundant and forms groundmass. It is usually hydrothermally altered at the contact with coarse grained barite veins to give rise to leached and porous structures partly filled in by silica and pyrite. Quartz, calcite and certain clays are present as impurities. Sometimes native sulfur forms cavity lining. Limonite frequently covers the cleavage surfaces in barite. Galena occurs generally as small euhedral disseminated crystals. However, at places large grains of individual galena crystals are also noticed. Pyrite with golden metallic luster occurs as fine grained disseminated phase.

MINERALOGY OF OXIDIZED ZONE (GOSSAN)

The rocks in the oxidized zone are of yellowish brown and reddish brown color due to the presence of limonite, haematite, and goethite in them. Smithsonite, jarosite, cerrusite, and iron oxides are also present. The rocks are silicified and contain veinlets of darker brown limonite. Small euhedral quartz crystals make lining in the cavities. Smithsonite occurs as yellowish and greenish crustification. Yellow spots on the surfaces are perhaps zinc ochers. Lead ochers have also been reported. Massive galena veins occur in brown limonite boxwork showing colloform texture which are pseudomorphs after marcasite. Unoxidized lenses contain disseminated brownish sphalerite, galena and siderite.

MINERALOGY OF SULFIDE ZONE

Sphalerite

Sphalerite occurs as small grains, collomorphic concentrations, large grains (Plates 7 and 8), small inclusions in other minerals, and as elongated nodular lenses and bands. Small grains are mostly euhedral or subhedral which are disseminated preferably through the siltstone matrix. Collomorphic aggregates occur in close association with marcasite and pyrite or as individual globules (Plates 9 and 10). Some sphalerite globules form coarser grained aggregates, but they show original concentric layers. Large grains of sphalerite are intergrown with galena, pyrite, marcasite (Plates 11 and 12) and gangue minerals. Sphalerite also occurs as small inclusions in certain minerals such as pyrite, marcasite and also in gangue minerals such as barite. Occasionally, the irregular large grains of sphalerite occur as interstitial phase to gangue minerals especially carbonates. At places sphalerite forms banded structures resulting from open space filling. It also is locally concentrated as massive lenticular bodies.

Sphalerite is generally brown or reddish brown in color. However, light brown to yellowish brown grains are also noticed. Color zoning (Plate 8) having dark brown core surrounded by rims of lighter colors is the common feature of the studied sphalerite. The intensity of color depends upon the increase in the amount of iron content of these sphalerite which varies from 1.2 to 5.7 % (Jankovic 1986). It is noticed that the dark brown to reddish brown sphalerites having higher contents of iron are usually found in close association with marcasite and pyrite. Sphalerite which deposited with gangue minerals showed low content of iron.

Colloform sphalerite occurs in the form of tiny globules characterized by spherical growth and /or rhythmic alteration with marcasite and pyrite or even with barite. Some colloform sphalerite may have reniform textures and some concentrically developed sphalerite have framboids of pyrite at the core. Many sphalerite grains have relics of colloform textures in their cores which are surrounded by recrystallized homogeneous sphalerite. Banded structures are often found in which the regularly spaced alternating bands might have been formed by the intermittent precipitation of ore-forming fluids (also see Jankovic 1986).

Sphalerite is not only present as inclusions in the other minerals but it also contains inclusions of other minerals in it such as marcasite, galena, pyrite, carbonates and occasionally chalcopyrite. Inclusions of pyrrhotite were also found in one sample (Jankovic 1986). This association for the low temperature Gunga deposit is rather anomalous. Sphalerite also contains fluid inclusions; a few samples were analyzed by the author to find out homogenization temperature and the nature of ore-forming fluids. The results indicate rather low trapping temperatures: 100-110°C and around 150°C; and somewhat high (16-17 eq. wt. % NaCl) salinities (Siddiqui 1994). The mineralogy and texture suggest that there could be three generations of sphalerite formation: first, primary precipitation, second, diagenetic transformation, and third, late-stage recrystallization (also see Jankovic 1986). Sphalerite is often replaced by marcasite, pyrite, and galena along margins.

Galena

Galena occurs in aggregates of euhedral to subhedral cubic crystals (Plate 13 and 14). It may be massive but also occurs in disseminations. It is rarely found making veins in the host rocks. The size of the individual crystals ranges from 0.1 mm to >1 mm. Some crystals are as large as 5 mm or even more. Occasionally it is also found as small globules composed of fine grains which are often surrounded by sphalerite. Galena may have been precipitated as colloidal material but owing to its strong tendency to crystallization, all the galena became crystallized from the mixed gel. Thus the original gel and colloidal textures are better developed in sphalerite, marcasite and pyrite than in galena (also see Jankovic 1986). Galena is sometimes found to enclose blebs of chalcopyrite. According to Jankovic (1986) the studied galena carries rather high silver content (1200-3000 ppm). It is also noticed that galena with high silver, possesses high Sb (upto 3000ppm) content as well.

Marcasite

Marcasite is an ubiquitous mineral in these deposits. There are two modes of occurrence of marcasite: 1) Marcasite associated with sediments containing large amount of organic compounds; and 2) Marcasite associated with ore minerals. The first type of marcasite occurs in dark argillic limestone, siltstone, dark shale, etc. This type of marcasite occurs as framboids that might result from bacterial activity in an anaerobic environment. The second type of marcasite occurs as colloform and as euhedral coarse grained aggregates of crystals formed in open space fillings and replacement of carbonate minerals (Plate 15). Colloform textures are quite common at Gunga and probably represents deposition from colloidal material that took place in close association with carbonaceous material (Bateman 1967).

Transformation of marcasite to stable pyrite and simultaneous precipitation of both minerals can also be seen. In the Gunga deposit occasional occurrence of rhythmic alteration of extremely thin layers of pyrite and marcasite is also observed. Marcasite precipitated in several generations and it contains inclusions of other minerals; but it is also found as inclusions in other minerals of the deposit (see also Jankovic 1986).

Pyrite

Pyrite is quite commonly found in these deposits at all the locations of the district; though, it is less abundant than marcasite (Plate 16). It occurs as rounded grains and disseminated cubic crystals. It also forms veins in the host rock. Tiny pyrite framboids, being resistant to recrystallization are widely distributed in these deposits. Mineralization of pyrite essentially occurs in rhythmic sequence of argillaceous, silicified, and pyrite rich layers.

In the brecciated portions of the deposit cataclastic cracks might have probably provided conduits to the incoming solutions which brought about replacement of already existing materials.. Mineralization of pyrite by the process of replacement is quite commonly observed in these deposits. Several minerals including sphalerite, galena and carbonates replace pyrite (Plates 17 and 18) and are themselves replaced by the latter (Jankovic 1986).

Siderite

Siderite is one of the common minerals of the mineral assemblage present in these deposits. It occurs as vein filling in association with sphalerite, galena and marcasite, and also as euhedral grains within the calcite. Its rhombohedral grains and small rounded bodies are also found disseminated in pelitic groundmass Sometimes there is a rhythmic alternation of siderite and chemically precipitated silica (chalcedony) in thin layers which points to a colloidal origin for both of these minerals (see also Jankovic 1986). It is also found replacing the oolites and small fossil-shell fragments in calcareous siltstone and limestone.

Quartz

Quartz and chalcedony occur in several forms Quartz is found as beautiful euhedral, at places doubly terminating, crystals filling vugs in the host rock, particularly limestone. It is also present as detrital angular grains in the siltstone. Quartz is also seen forming veins and veinlets along with other minerals within pyrite (Plate 18). At places large quartz grains are found replacing sphalerite, galena and pyrite. Fine grains of quartz/chalcedony are dispersed along with grains of marcasite and pyrite. Chalcedony is found replacing oolites and shell fragments. They form rhythmic alternations with carbonates (Jankovic 1986).

MINERAL PARAGENESIS

Ore microscopic study as well as visual examination of samples suggest the following paragenetic sequence of minerals in these deposits: 1) Sphalerite--galena--marcasite/pyrite--siderite--quartz / chalcedony, and 2) the simultaneous crystallization of sphalerite, galena, and pyrite. The first paragenetic sequence is established after considering the textural and boundary relationships between various coexisting mineral phases. For example, sphalerite appears to be replaced by almost all the sulfides. It is most frequently replaced by marcasite / pyrite and quite often by galena and is, therefore, considered to be the first sulfide mineral formed. The replacement of galena and sphalerite along margins by marcasite / pyrite suggests that the latter has formed after the formation of galena. The occurrence of quartz and chalcedony in the form of veins within the microfractures of pyrite suggests that veining was the last event and, therefore, quartz and chalcedony were formed at the later stage after the precipitation of sulfides.

The coexistence of sphalerite, galena, and pyrite, on the other hand, without replacing one another in certain samples also suggests that these phases were crystallized simultaneously from sulfide rich ore-forming fluids.

ACKNOWLEDGMENTS

This research was carried out by the author as part of the Ph.D. dissertation project, which was sponsored and funded by the United States Agency for International Development (USAID) through Ministry of Education, Government of Pakistan. The author is particularly grateful to Prof. W.E. Sharp who provided valuable guidance and support as Research Supervisor at the University of South Carolina, Columbia. The help and cooperation extended to the author by the friends and officials at the Geological Survey of Pakistan is also thankfully acknowledged.

REFERENCES

Ahmad, W., 1950, Summary of field notes on the areas between Khuzdar and Nal, Kalat Division: Geol. Surv. Pakistan, File No. 173.

Bateman, A.M., 1967 , Economic Mineral Deposits, 2nd ed., John Wiley and Sons (publ), p. 33.

Fatmi, A.N., 1986, Zidi Formation (Ferozabad Group) and Parh Group (Monajhal Group), Khuzdar district, Balochistan, Pakistan: Rec. Geol. Surv. Pakistan, 75, 32 p.

Hoagland, A.D., 1981, Programme, recommendations and comments on zinc-lead-barite-fluorite project, Baluchistan, Pakistan: Mission report, Pak/79/016 (unpublished), UNDP, Islamabad.

Hunting Survey Corporation (HSC), 1961, Reconnaissance geology of part of West Pakistan: report published for Government of Pakistan by the Government of Canada, Toronto, 550 p.

Jankovic, S., 1986, The mineral association and genesis of the lead-zinc-barite deposits of Gunga, Khuzdar district, Baluchistan, Pakistan. Rec. Geol. Surv. Pakistan, 71, 22 p.

JICA, 1987, 1988, 1989, Reports on the Cooperative Mineral Exploration in the Khuzdar area of Balochistan, Phase 1, 2 and 3: published by Japan International Cooperation Agency and Metal Mining Agency of Pakistan.

Jones, A.G., 1960, Reconnaissance geology of part of West Pakistan: A Colombo Plan Cooperative Project: Govt. of Canada, Toronto, 550 p.

Klinger, F., and Ahmad, M.I., 1967, Barite deposits near Khuzdar, Kalat Division, West Pakistan: Geol.Surv. Pakistan.

Sarwar, G., and DeJong, K.A., 1979, Arcs, oroclines, Syntaxes: The curvature of mountain belts in Pakistan: **In** Farah and DeJong (eds) Geodynamics of Pakistan, p. 341-349.

Schmidt, R.G., Ahmad, M.I., and Asad, S.A., 1961, Mineral commodity reference file: Geol. Surv. Pakistan.

Siddiqui, S.A., 1994, Genesis of sediment-hosted Pb-Zn-Barite mineralization near Gunga, Khuzdar district, Balochistan, Pakistan: Ph.D. dissertation (unpublished), University of South Carolina, Columbia, U.S.A., 227 p.

Manuscript Received 3rd March 1998
Revised Manuscript Received 28th August 1999
Accepted 1st September 1999

Plate 1. Gossan outcrop at Gunga, as viewed from the west in the dip-slope direction.

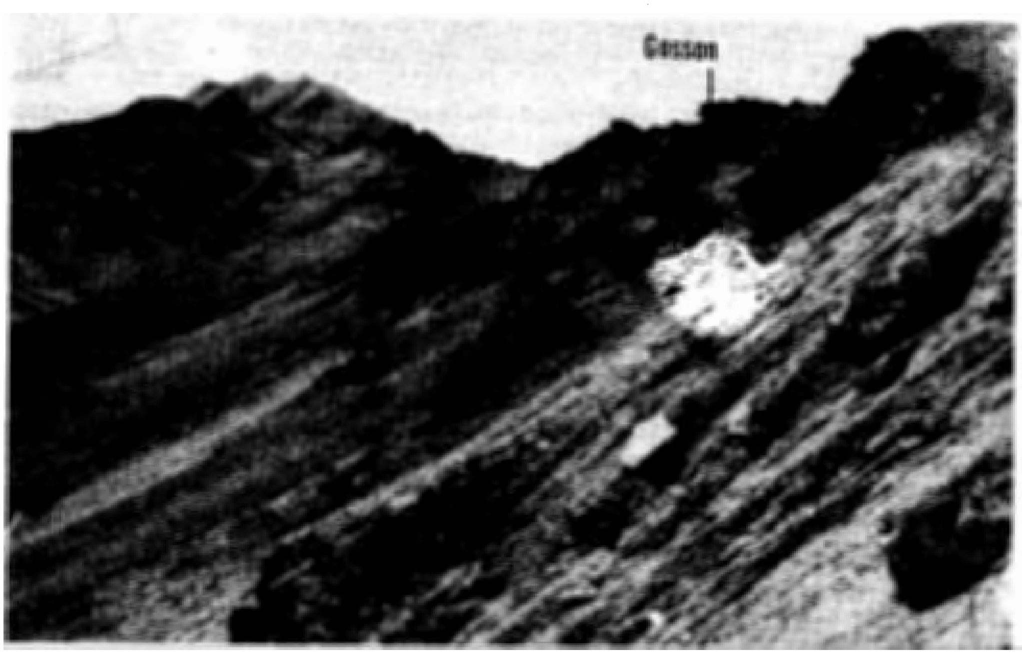

Plate 2. Gossan outcrop and scree from barite mine at Gunga, as viewed from the east towards escarpment slope.

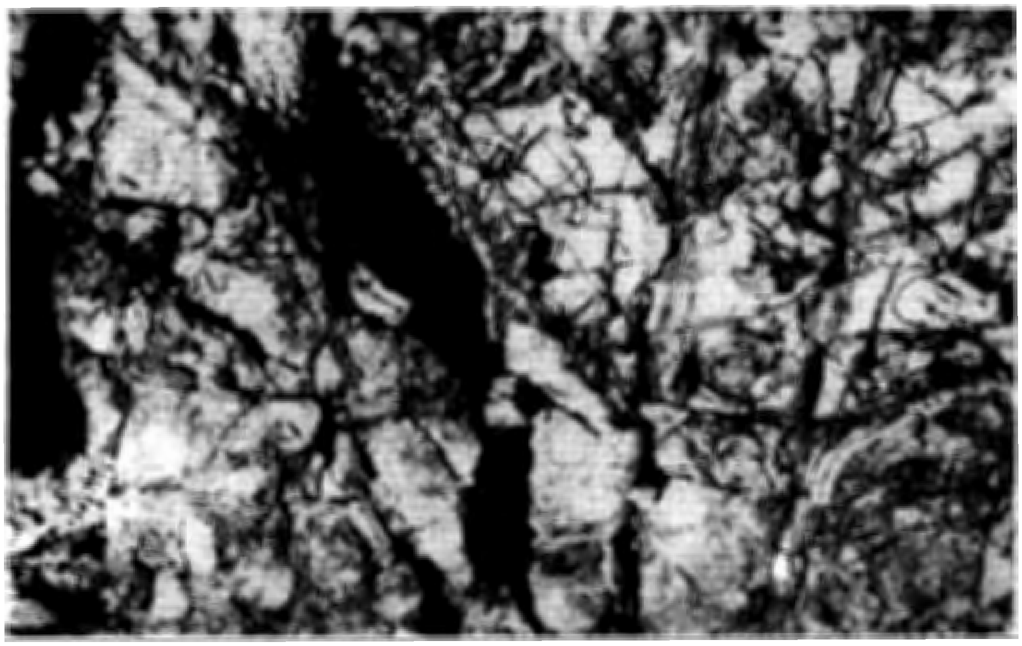

Plate 3. Weathered and leached surface of siliceous gossan developed in silt and mudstone.

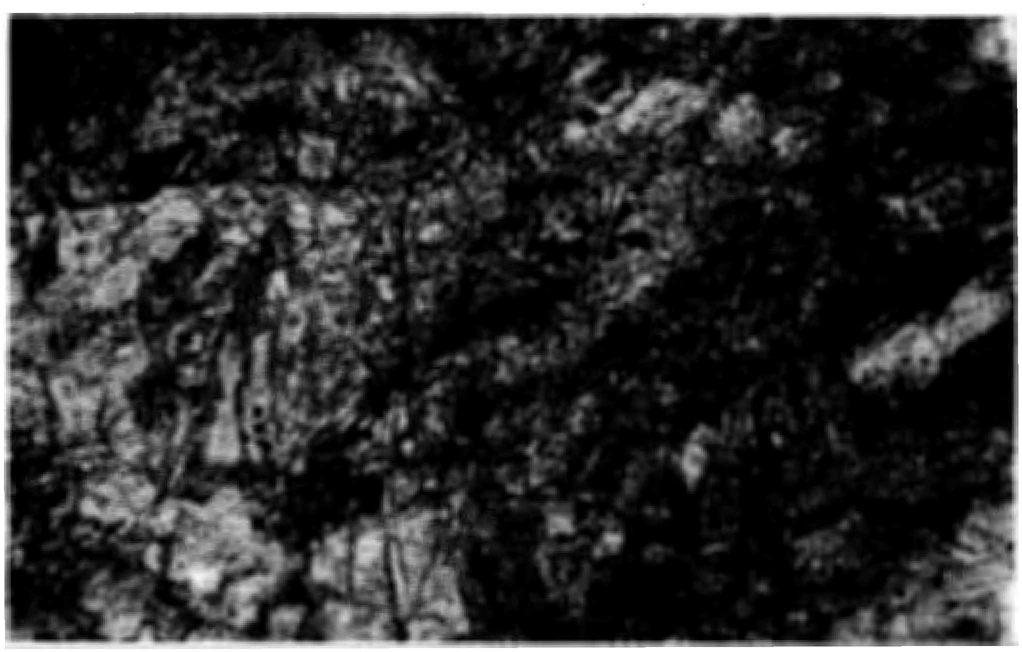

Plate 4. Weathered and leached surface of siliceous gossan developed in silt and mudstone.

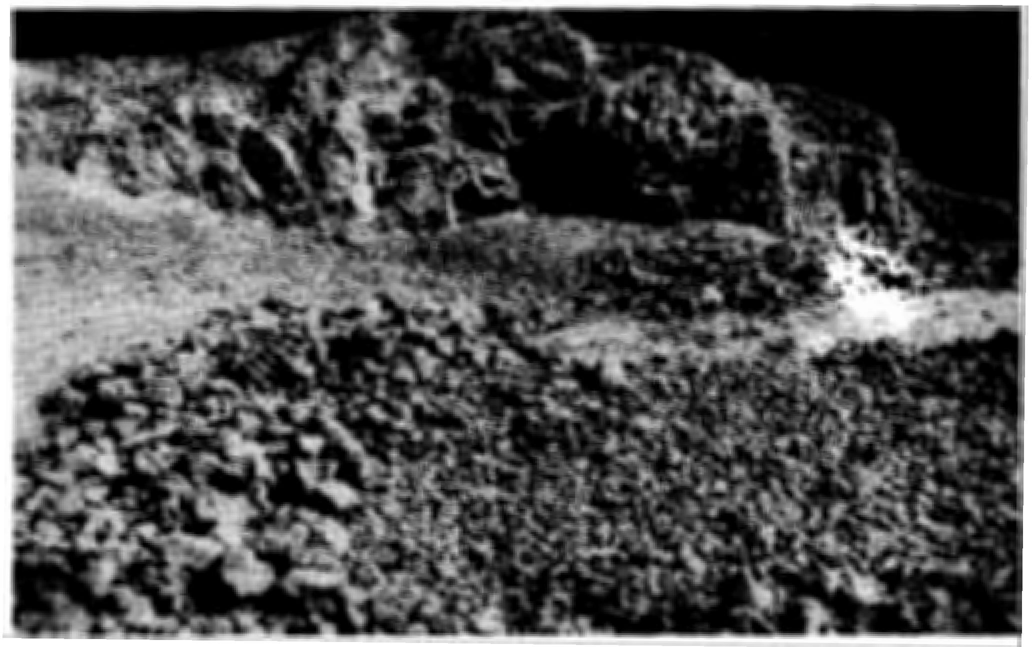

Plate 5. A view of the barite open-pit mine at Gunga showing limonitic surfaces.

Plate 6. Barite mine at Gunga overlooking plunging anticline to the NNW.

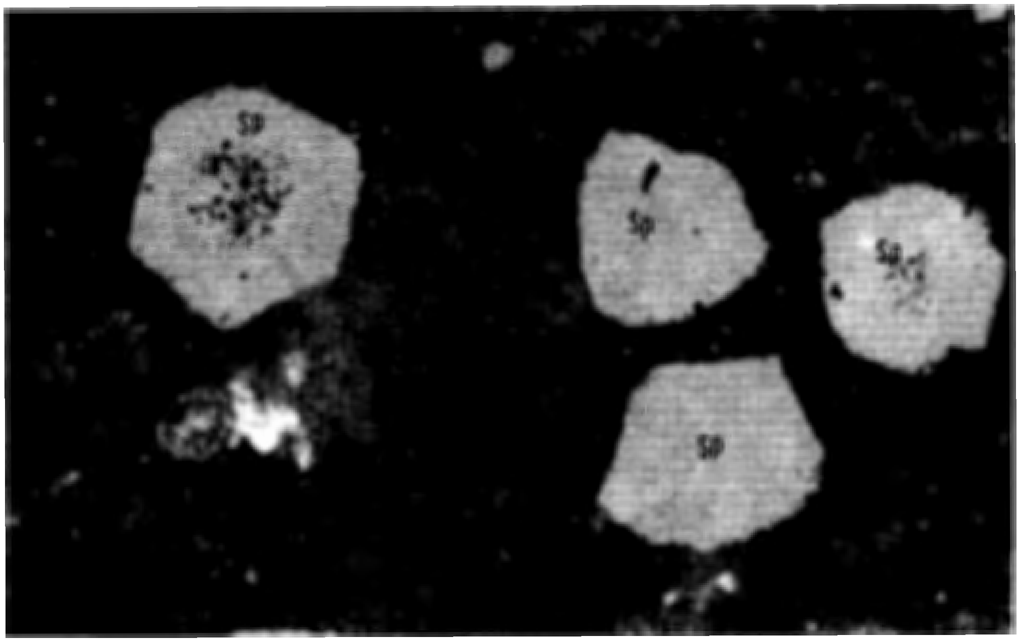

Plate 7. Photomicrograph in the reflected light showing large euhedral to subhedral sphalerite (Sp) grains along with other minerals, such as pyrite (Py), marcasite, (X5).

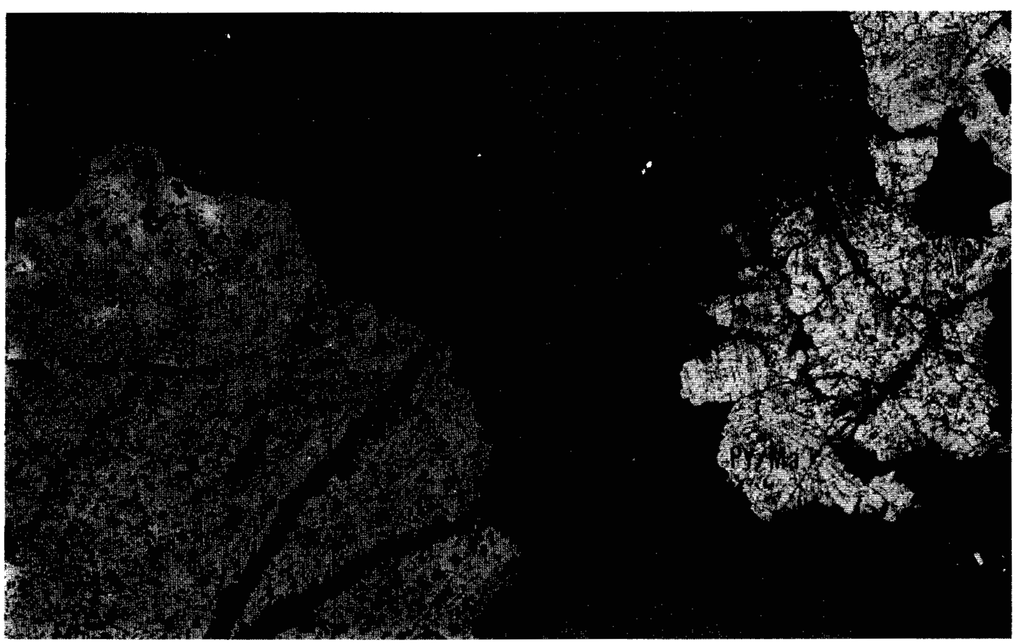

Plate 8. Photomicrograph showing color zoning in transmitted light within the large and medium grained sphalerite (Sp), (X5). (Ca = carbonates)

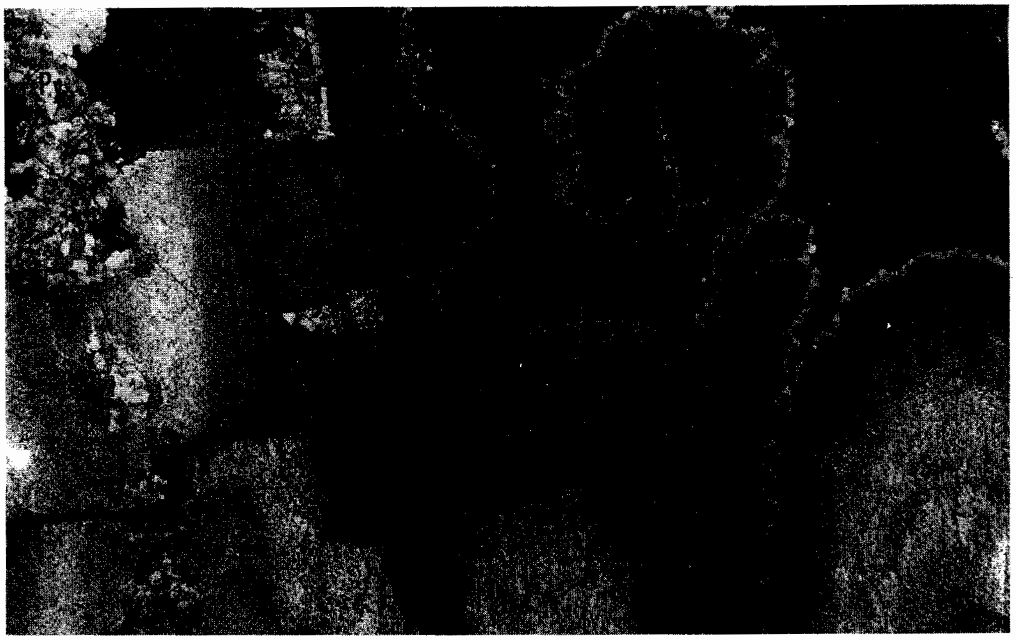

Plate 9. Photomicrograph in reflected light showing concentric banding in sphalerite (Sp) which is being replaced by the pyrite (Py) along rims, (X5). (Ca = carbonates)

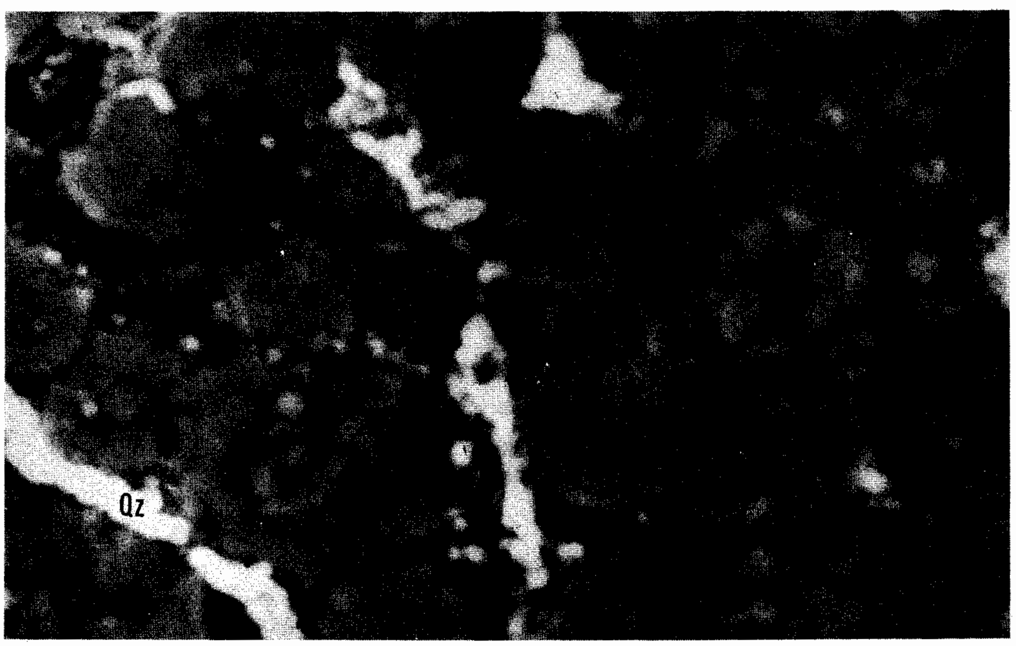

Plate 10. Photomicrograph (transmitted light) showing globular aggregate of sphalerite (Sp), still maintaining internal zoning, (X5). (Qz= quartz).

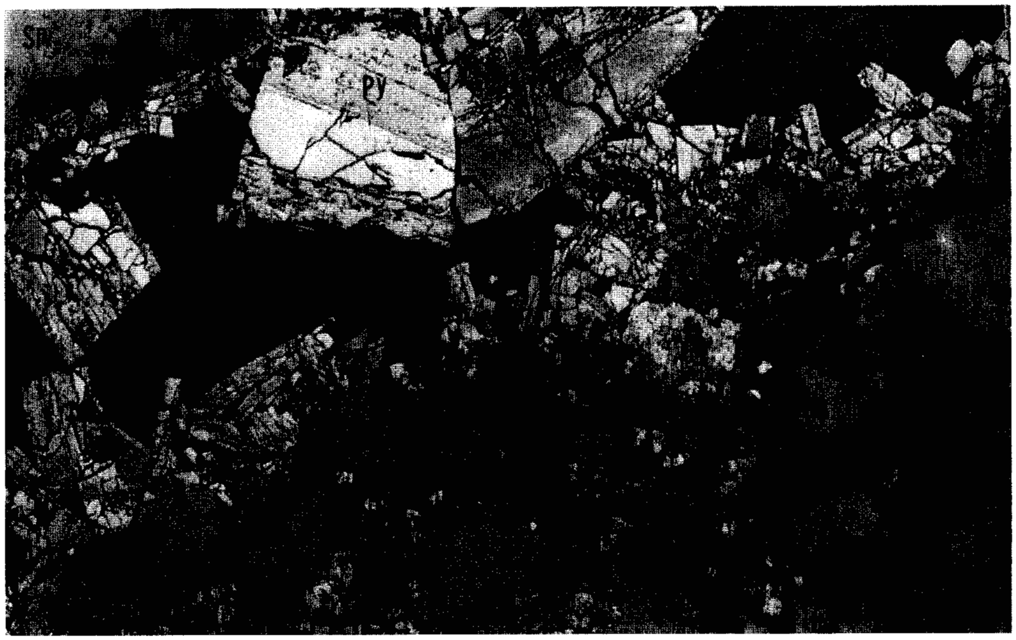

Plate 11. Photomicrograph in reflected light showing intergrowths of sphalerite (Sp), pyrite Py), marcasite, and other minerals, (X5). (Ca = carbonates)

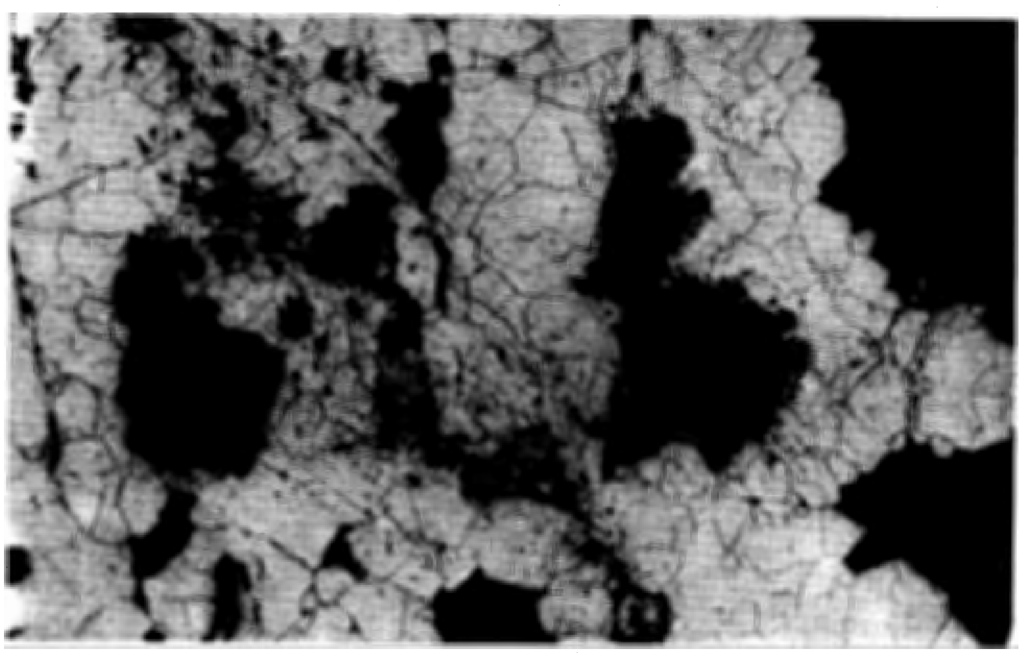

Plate 12. Photomicrograph in reflected light showing large fractured grain of sphalerite (Sp) alongwith other minerals, e.g. pyrite (Py) marcasite, (X5).

Plate 13. Photomicrograph in reflected light showing the formation of cubic galena (Ga) crystals by replacement of the host rock, (X5).

Plate 14. Photomicrograph in reflected light showing a large grain of galena (Ga) having sharp contact with calcite (Ca), (X10).

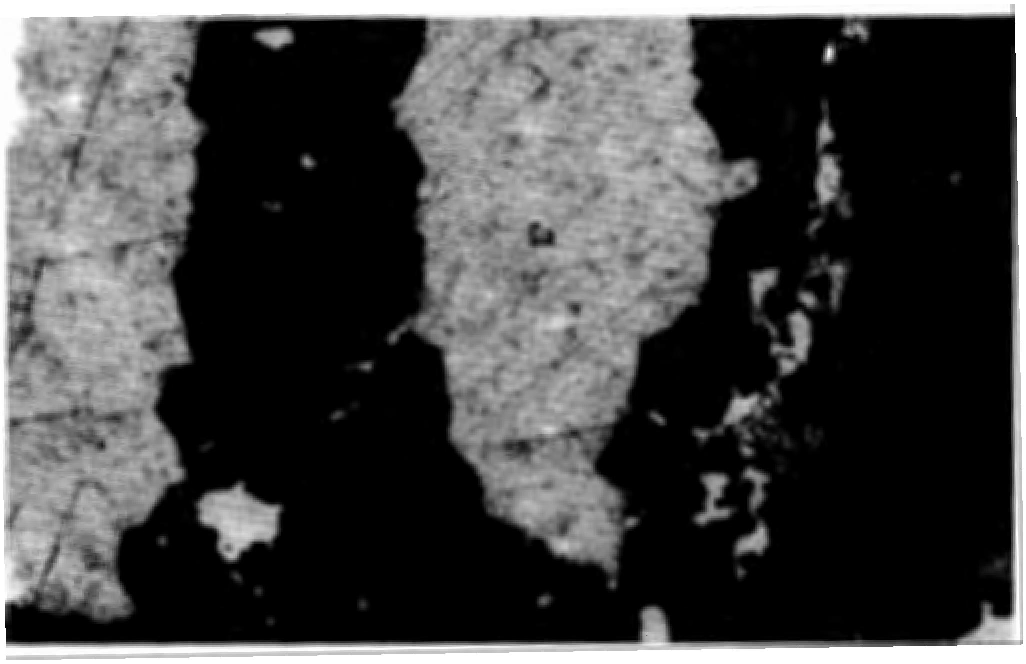

Plate 15. Photomicrograph in reflected light showing development of euhedral marcasite/pyrite (Py) by the replacement of carbonates (Ca), (X5).

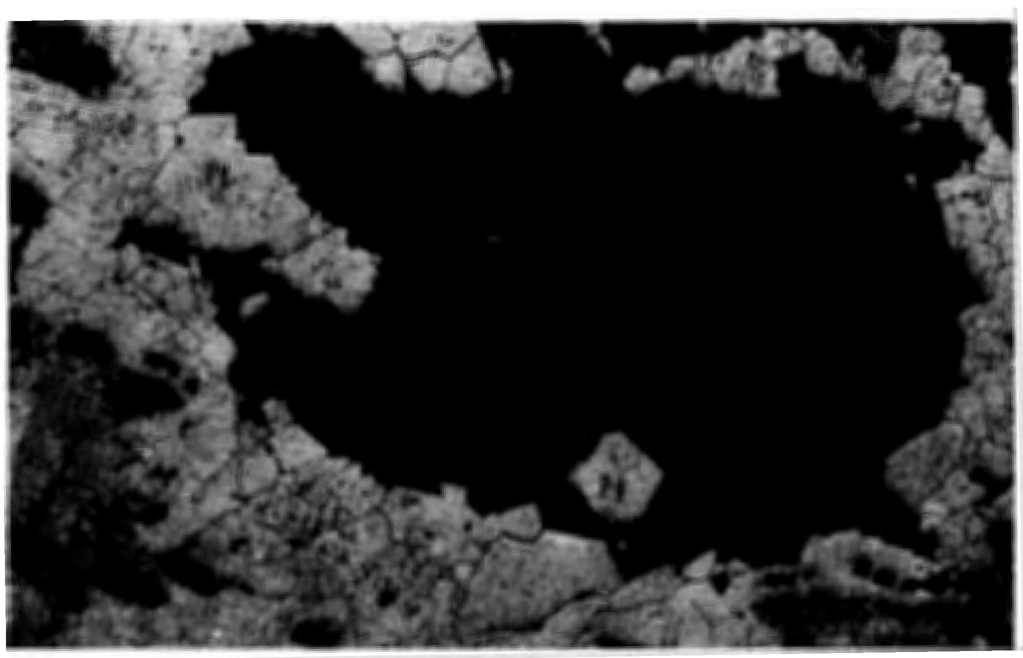

Plate 16. Photomicrograph in reflected light showing pyrite (Py) surrounding and perhaps replacing limestone rock, (X5).

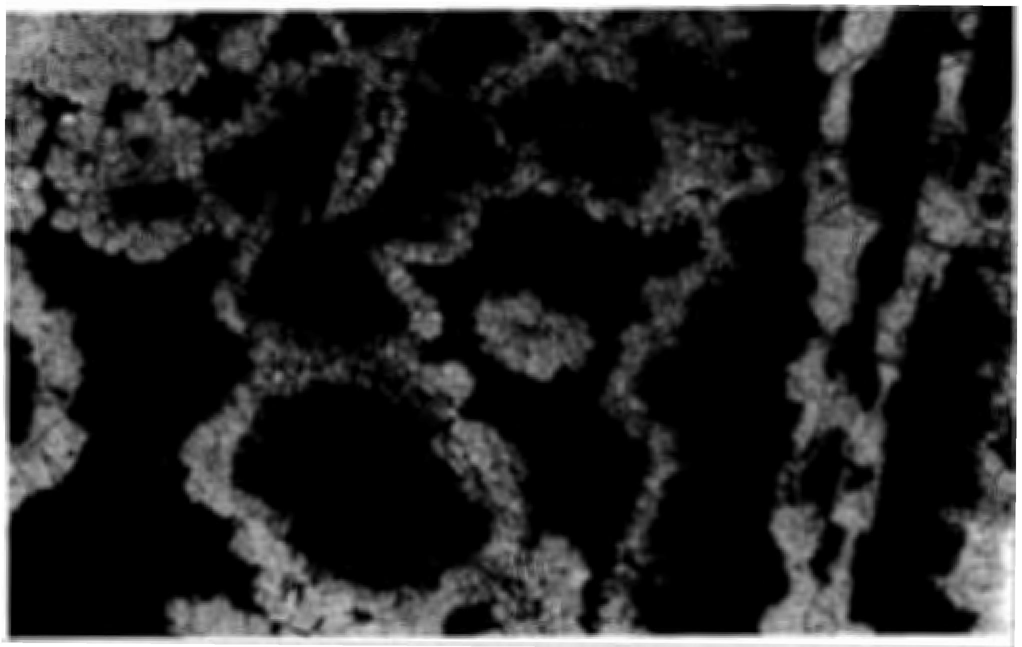

Plate 17. Photomicrograph in reflected light showing replacement of sphalerite (Sp) by pyrite (Py), (X5).

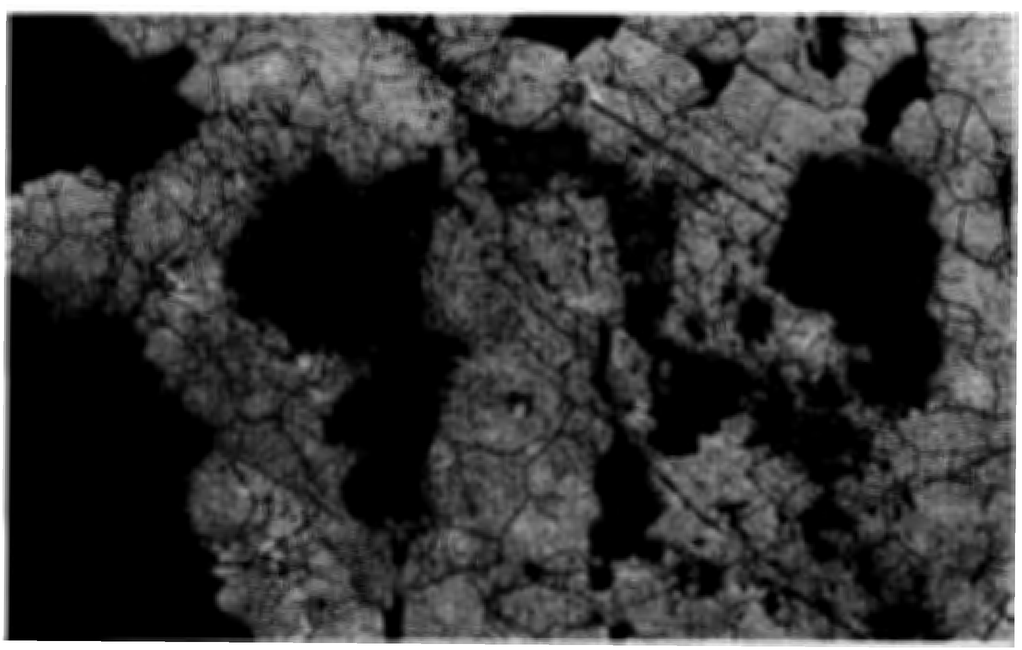

Plate 18. Photomicrograph in reflected light showing the same as in Plate 17; it also shows a fracture filled vein of quartz (Qz) within pyrite (Py), (X5).

ACTA
MINERALOGICA
PAKISTANICA
Volume 9 (1998)

Article Reference
AMP9.1998/103-109/ISSN.0257-3660

EXPLORATION PROSPECTS OF GEOTHERMAL ENERGY IN BALOCHISTAN

SYED MOBASHER AFTAB[1] AND MOHAMMAD AHMAD FAROOQUI[2]
[1] Public Health Engineering Department, Government of Balochistan, Quetta Pakistan
[2] Centre of Excellence in Mineralogy, University of Balochistan, Quetta Pakistan

ABSTRACT

The geodynamic setup of Balochistan signifies that the existing geothermal springs are fraternized as geopressurised systems, seismotectonic and Neogene-Quaternary volcanism. A geothermal resource map of Balochistan is presented here with extricate data collected for disparate geologic, geothermic, geodynamic, structural, tectonic and seismic investigations. To exploit the geothermal reservoirs for development of remote and undeveloped areas of Balochistan, a preliminary but detailed plan is proposed here that is needed for electricity generation.

INTRODUCTION

Geothermal resources are found all over the Earth. High-temperature geothermal resources are concentrated along Earth's crustal plates. In such regions volcanic activities, geysers, fumaroles, thermal springs, fossil seeps, mud volcanoes and thermal, mineral and gaseous springs originate. The Circum-Pacific Belt is one of the most tectonically active region which retains world's largest and hottest geothermal resources. Oceanic spreading centers also give rise to hot crustal material. Continental spreading produces "rifts" that are the pathways for molten rock and geothermal heat release. Geothermal resources also occur in regions, i) where hot spots occurred due to local magmatic disruption, ii) where the earth's crust is thin and heated the groundwater, iii) where radioactive rocks found in significant proportions, and iv) where heat is trapped by a thick sedimentary sequence of deep basins. Hydrothermal systems or geothermal resources consist of hot water or steam trapped in fractured or porous rocks. Fluid temperature from these systems vary considerably but can be as high as 350°C, and are used for the generation of electricity.

GEOTECTONICS OF BALOCHISTAN

Balochistan is dominated by three geologic segments namely i) Chaghi-Raskoh Volcanic Arc ii) Makran-Khojak-Pishin Flysch Zone and iii) West Pakistan Fold Belt. The sedimentary rocks are widely exposed in most of the segments that are mainly calcareous and arenaceous. Limestone, shale, marl and clay are dominant in the oldest rocks of Permian age. The Mesozoic and Cenozoic rocks are mainly composed of limestone, shale and sandstone. Rocks of igneous origin range from Cretaceous to Oligocene and are mostly exposed in the Chaghi-Raskoh Arcs. Bela and Muslimbagh Ophiolites of Cretaceous age are predominantly composed of ultramafic rocks and doleritic dykes. In order to evaluate the geothermal resources the geotectonic history of all these areas are reviewed and contemplated.

CHAGHI AND RASKOH ARCS

The Chaghi and Raskoh Arcs are further divided into five segments namely Chaghi Hills Geanticline, Dalbandin Trough, Raskoh Geanticline, Raskoh-Mirjawa Flysch Belt, and Mashkhel Depression (Bender 1995).

The Chaghi Hills Geanticline is a complex of granite-andesitic rocks (Pre-Maestritchtian) that are consists of tuffs, andesitic lavas and volcanic agglomerates, with boulders of hippuritic limestone, granodiorite, diorite and granitic intrusions.

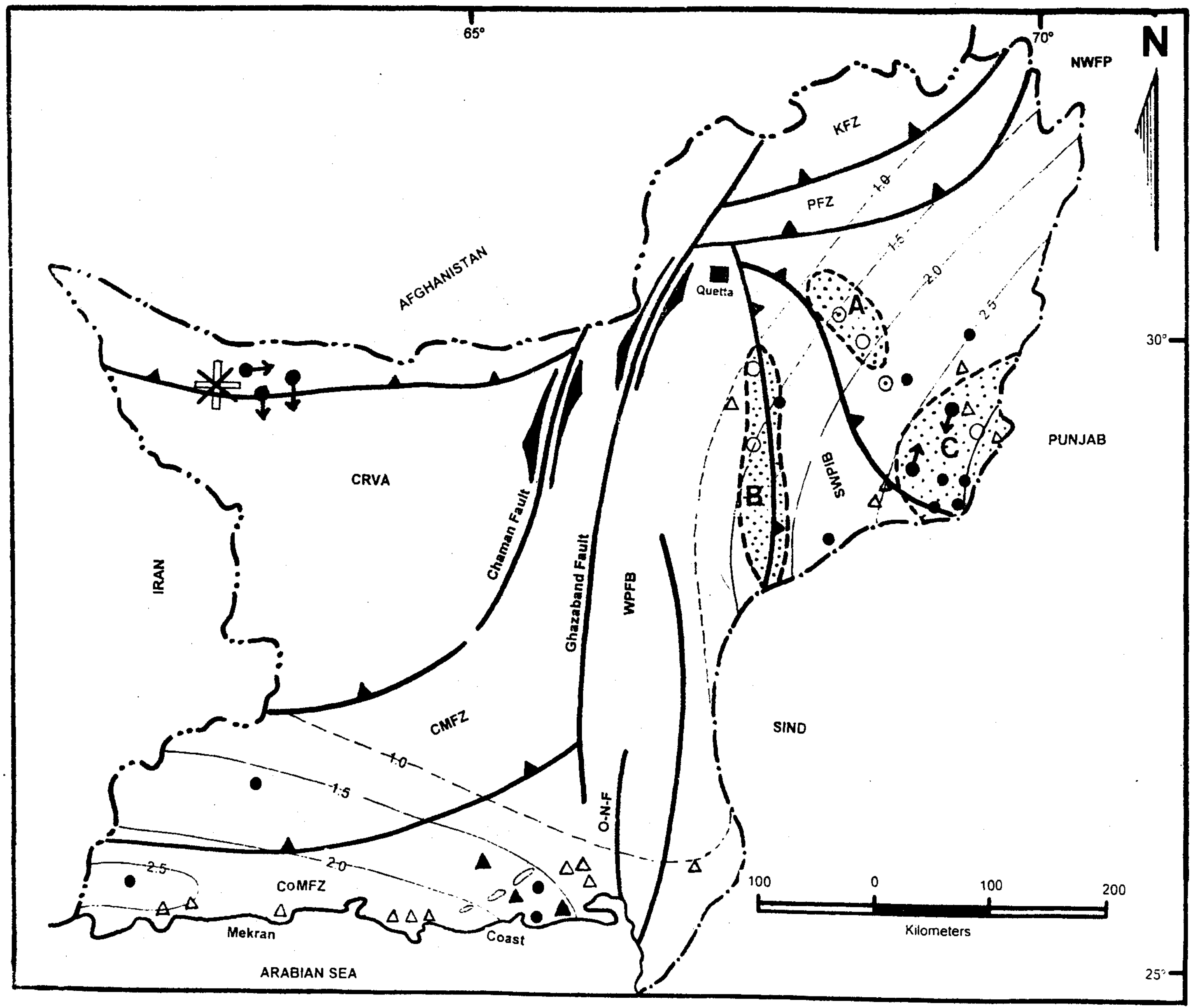

Figure 1. Geothermal Resource Map of Balochistan. Modified after Schoepple (1977), Raza (1989a and 1989b) and Khan et al. (1986). *(for explanation see facing page).*

EXPLANATIONS (Figure 1)

Major sedimentary basins of Balochistan with approximate maximum thickness (in kilometers) of sediments given in parenthesis.

CRVA	Chaghi-Raskoh Volcanic Arc (4)	**CMFZ**	Central Makran Flysch Zone (15)
CoMFZ	Coastal Makran Flysch Zone (14)	**WPFB**	West Pakistan Fold Belt (6 km)
SWPIB	S-western Part of Indus Basin (10)	**KFZ**	Khojak Flysch Zone (8)
PFZ	Pishin Flysch Zone (6)	**A**	Harnai Geopressurised System
O-N-F	Ornach-Nal Fault	**B**	Sanni Geopressurised System
		C	Sui Geopressurised System
	Dominant Thrusts		Gas seepage at surface
			Zone of gas seepage at surface
	Active Fault Zones		Oil seepage at surface
			Zone of oil seepage at surface
	Zone of Mud Volcanoes		
	Thermal springs with surface temperature <50°C		
	Oil or gas well/test hole with average geothermal gradient between 1.5-3.5°C/100m		
	Neogene-Quarternary volcanic system with thermal springs of anomalous silica concentration.		
2.5	Generalized isothermal contours: dashed lines indicate area of less certain control.		
	Area favourable for the development of low temperature Geothermal resources.		

It is tectonically active area where Paleocene and Miocene magmatism produced Shor Koh Intrusions of doleritic (diabase) sills and dykes in the western part of the Geanticline and eruptions of Koh-e-Sultan Volcano (Chaghi), Koh-i-Taftan (Iran) and Bazman Volcano (Iran) simultaneously during Pliestocene produced volcanic rocks. These recent volcanic activities have generated a number of hot water springs in the area.

The Dalbandin Trough is almost straight northeast-striking valley south of the Chaghi Hills Geanticline that ends in the Hamun-e-Mashkhel. The trough is composed of volcanics, fluvial and lacustrine deposits ranging from Masestritchtian to Pliestocene. During Pliocene two tectonic phases influenced the Dalbandin Trough; one produced folds with axis that change from northeast near Yak Mach to east near Dalbandin, whereas, the second phase produced major reverse faulting and folding along arcuate thrusts convex to the south.

The Raskoh Geanticline has more or less similar lithostratigraphic units as those in Chaghi Geanticline. During Late Cretaceous about 6000m of volcaniclastics accumulated in this area. Andesitic lava flows are less widespread in Raskoh than those in Chaghi Hills.

The Raskoh-Mirjawa Flysch Belt is composed of mudstone, shale, and turbiditic, volcanoclastic sandstone ranging in age from Maestritchian to Eocene. Earliest folding occurred during Early Paleocene which coincided with the obduction of ophiolites in the Bela-Waziristan Ophiolite Zone indicating the collision of the Indo-Pakistan Plate with Arabian Plate and simultaneously with the southern margin of Eurasian Plate. Up to the end of Middle Eocene the Raskoh Flysch Belt moved northward against the Chaghi Geanticline and both structures formed a single landmass. During Late Eocene the marine sedimentation stopped and the entire Chaghi, Mirjawa, and Raskoh area finally emerged.

The Mashkhel Depression is a flat area that includes Hamun-e-Mashkhel Playa lake and the Kharan Desert covered by Quaternary sand. The depression is about 100Km wide starting from Mirjawa-Raskoh Ranges in the north to North Makran Flysch Ranges in the south. Mashkhel depression is thought to be the forearc basin of the ancient subduction zone below the Makran Flysch.

MAKRAN-KHOJAK-PISHIN FLYSCH ZONE

The Makran-Khojak-Pishin Flysch Zone is a part of the continental margin of the Afghan Block in the southern part of the Eurasian Plate. It is a continuous zone of sediments, mostly of flysch nature locally grading into orogenic mollasse sediments. Based on tectonic style the zone is divided into three segments.

The Makran Flysch Segment is the best exposed arc-trench gap in the world. The accretionary wedge is exceptionally broad, extending more than 300km northward from the wedge front which lies 100 km south of the present coast line in the Gulf of Oman. Boundaries of the segment are 1) Oman Line (Iran) in the west, 2) north trending Chaman, Ghazaband, and Ornach Nal Faults in the east, 3) Active subduction trench of the Gulf of Oman in the south and 4) Chaghi-Raskoh Arcs in the north.The age of the segment ranges from Cretaceous in the north to Recent in the south along the subduction zone. Most of the sediments in this segment are turbiditic sandstone, siltstone, and shale with some isolated exposures of reefoid limestone.

The Khojak Flysch Segment lies east of 65°E and north of 28°N. The structures of the Makran Flysch Segment gradually change from east-trending to the north-trending of the Khojak Flysch segment which extends from Chaman Fault in the west and the Ghazaband Fault in the east. The sediments in the segment are of Oligocene to Miocene and are cut parallel to bedding planes by numerous strike slip faults.

The Pishin Flysch Segment lies approximately 30 km north of Quetta and bends to the northeast while changing its internal structure progressively from tight and imbricate sediment wedges into undeformed strata. It is wedged between Kabul Block of the Eurasian Plate in the north and the Bela-Waziristan Ophiolite zone in the south. The sediments in the segment are of Paleocene through Pliocene and are 7000 to 8000 meters thick. It contains a large number of nappes in which broad synclines occur with their axis commonly plunging at both ends. Anticlines are much smaller in size, or absent and replaced by faults.

WEST PAKISTAN FOLDBELT

This fold belt marks a general western boundary of Indo-Pak Plate and occupies the area east of Makran-Khojak-Pishin Flysch Zone and west of Indus Plain. It was folded during the collision process when the Indo-Pakistan Plate underwent basement segmentation. The rocks overlying the basement of the Indo-Pakistan Plate in the Foldbelt range from Triassic to Pleistocene and Recent. The Foldbelt includes a zone of oceanic seafloor rocks known as "Bela-Waziristan Ophiolite Zone" which contains the Ophiolite complexes of Bela, Muslimbagh, and Zhob. It has experienced multiple phases of mountain building which developed a very complex configuration of the structural features. Nappes and thrusts, synclines and anticlines are common structural features of the Foldbelt which are assumed to abruptly terminate along the eastern boundary of the Foldbelt under the unfolded sediments of the Indus Plain.

GEOTHERMAL SYSTEMS OF BALOCHISTAN

The geology and tectonics of Balochistan impersonate a consequential role in the occurrence and association of geothermal reservoirs. On the basis of geotectonics a Geothermal Resource Map of Balochistan has been prepared (Fig. 1). The map incorporates dominant thrusts, active faults, sedimentary zones, thickness of sedimentary deposits, geopreassurised zones, geothermal gradients and other relevant features. The thickness of sediments in different sedimentary zones varies from region to region. The maximum sedimentary thickness is in Central Makran Flusch Zone (CMFZ) whereas over all thickness in all the zones ranges from 4 to 15 kilometers. The exploratory wells drilled for oil and gas show that the average geothermal gradient increases from 1.5-3.5°C per 100 meter. The geothermal gradient increases towards eastern and costal regions of the province. Due to active tectonism and geopreassurised systems, gas seepage has been observed at land surface in costal regions and oil seepage in eastern Balochistan. The geotectonic setup signifies that the existing geothermal springs are fraternized as geopreassurised systems related to basin subsidence, seismotectonic or suture-related systems and Neogene-Quaternary volcanism (Kazmi 1995). Chaman Fault, Ghazaband Fault and Ornach-Nal Fault are the major active fault zones of the province. The neotectonics reflects that numerous other seismic zones and seismotectonic features are associated with the active faults. The northern Kirther Seismic Zone lies between Quetta and Kalat and bounded to the east by Kachhi Plain and to the west by the Ghazaband Fault. The latter separates it from the Chaman Fault Seismic Zone. The high seismicity of this region is indicated by several teleseismic events. Numerous springs are associated along these fault zones but geothermal springs of considerable surface temperature has not been reported. In Sulaiman Seismic Zone, the Harnai-Kohlu high-seismicity belt lies which is arcuate and 25-50 Km long. In Harnai area thermal springs are present north-northeast of Spintangi Railway Station (Bakr 1965), associated with Harnai and Tatra faults (Kazmi 1979). Seismically it is an active region and earthquakes of magnitudes 6-7 on Richter scale have been recorded and higher geothermal gradient is expected. In the Kirther Foldbelt, geothermal springs are fraternized in the foothill region of Kirther Range west of Dhadar, near Sanni. They appear along Mach and Kirther faults (Kazmi 1979) at the western edge of Kirther

Foredeep which has 10 km thick sediments with high seismicity (Kazmi 1979, Quittmeyer 1979). In Zhob Valley two thermal springs (Abid 1975) are associated with a series of imbricate faults (Bakr 1965) in a region of high seismicity.

The geopressurised system exists in Mari-Bughti fold belt (Kazmi and Rana 1982) and in nearby Sui gas field area, where the geothermal gradient is about 3.0-3.49°C/100m. In this region, the thermal springs have been recorded (Bakr 1965) at Uch (28° 45'N; 68° 40'E) and Gram Aab at Mari Hills (29° 33'N; 69° 40'E). In the costal and central zones of Makran evidence of geothermal activity and occurrence of mud volcanoes are known since late 1950s (H.S.C., 1960). A concentric zone of active mud volcanoes lies between 25° 30'-26° 30'N; 65° 00'-66°30'E and a wide area containing extinct mud volcanoes is situated about 30km north of Gawadar. The main tectonic control in this region is the active subduction of the Arabian Plate beneath the Eurasian Plate and is characterized by shallow seismicity. Several high level coastal terraces and platforms provide geomorphological evidence of vertical uplift and high seismotectonic activity in this zone. In Santsar area near Diz and southeast of Garruk, thermal springs are situated along major faults and in the regions of high seismicity. The geophysical evidences represent the existence of a geothermal system in Hamun-e-Mashkhel region (Spector 1981), which lies in between the Chaghi Arc in the north and Makran Convergence Zone in the south. In Chagai District at Miri Crater of Koh-i-Sultan the thermal springs are associated with the Neogene-Quaternary volcanism of the Chagai Arc. Surface investigations indicate that very high geothermic gradient is expected in this region, no considerable subsurface studies and exploratory drilling have been carried out to substantiate this hypothesis. The preliminary investigations of Koh-i-Sultan volcanogenic geothermal zone were carried out by the Geological Survey of Pakistan; the relevant information of spring analysis are given in Table 1.

In the Koh-i-Sultan geothermal system an acidic alteration zone has been developed with silicified segmentation. Hydrogen sulphide and sulphur deposits were also reported from the area (Zaki 1975; Zaki and Siddiqui 1993). The temperature of spring waters ranges from 25.6-36°C. The estimated reservoir temperature on the basis of the silica geothermometer ranges from 150-175°C (Shuja 1984; 1988). It is anticipated that this region has the highest geothermal potential in the country and economically exploitable geothermal reservoir is expected which may be utilized for electricity generation.

Table 1. Important properties of Koh-i-Sultan thermal springs.

Springs	Schoeppel,	Todaka,
Sampling points	10	04
Sources of water	Springs	Springs
Discharges	-	< 1 litre/min.
Water temperature	26.0-36.0°C.	25.6-30.2°C.
pH	-	2.0-7.4
EC	-	> 10,000 mohs
Silica content	33-183 ppm	27-188 ppm

DEVELOPMENT OF GEOTHERMAL RESOURCES

In practice the geothermal resource assessment involves determination of the location, size and geologic characteristics of each resource area to calculate the thermal energy stored in the reservoir and the thermal energy recoverable at the wellhead (Edwards 1982). Identified geothermal resource areas must meet the criteria that a reservoir with sufficient permeability to supply long-term production exists and that reservoir temperature exceeds a defined temperature-depth relation. The summary of the applied concepts (Aamodt and Riecker 1980) required for the basic research to discriminate the geothermal systems are summarized in Box 1.

Box 1. Basic research required for the development of Geothermal energy systems (Aamodt and Riecker 1980).

1. Origin of geothermal flux
   - Oceanic crust
   - Subduction zones
   - Continental heat flow
2. Transport of geothermal energy
   - Conductive transport
   - Convective transport
3. Geothermal reservoirs
   - Hydrothermal systems
   - Geopressured systems
   - Conductive systems
4. Rock-water interactions
5. Geophysical and geochemical exploration
6. And above all specific studies and research required for the contemplated assessment, exploitation and development of geothermal reservoirs.

The drilling deep wells and their heat flow testing provides conclusive evidence for the presence of a geothermal resource. After making a discovery, step-out wells are drilled in order to determine the extent, life and physical structure of the reservoir system. Flow testing, core analysis and formation evaluation techniques are used to determine production capacity. Finally, the results of these investigation shall help prepare the appropriate design of the power plant, machinery installation and electricity generation. The economics and commercial feasibility issues are the reservoir temperature, engineering and technology related to production capacity, life of the reservoir and performance of the power plant. The financial and management issues include exploration and plant costs, selling price of the produced energy, anticipated rate of return, operating and maintenance costs, ownership and regularity matters. The exploration of geothermal energy entails considerable risks, there probable assessment and reformatory appraises a vital role in the economics. The success rate of wildcat wells is 10% or less, and the exploration well costs more than $1 million (Edwards, 1982).

CONCLUSIONS AND RECOMMENDATIONS

Geothermal energy has been produced commercially for nearly a century, and on the scale of hundreds of megawatts (MW) for over four decades for electricity generation and direct use in 46 countries in the world (Fridleifsson, 1998). Electricity generation in these countries is about 44 terrawatt hours annually (TWh/a), and direct use amounts to about 37 TWh/a. While on the other hand, Pakistan faces an energy crises and in Balochistan electricity is supplied from other provinces by stretching hundreds ofkilometer power lines through national grid system. This system antecedented frequent breakdowns, low voltage and continuous fluctuations in the regular supply of power. In Balochistan no river has enough potential to generate considerable quantity of hydropower. Establishment of thermal and nuclear power plants are calamitous and in prevailing circumstances their prospects are negligible. To surmount the problem a detailed investigation plan is recommended for systematic exploration and development of the geothermal energy resources for electricity generation:

a) Fundamental geological studies and detailed geo-logical mapping.
b) Study of tectonic mechanism, geodynamic setup, variation in altitude and horizontal position of potential sites with the assistance of remote sensing and satellite imageries.
c) Volcanic activities, radioactivity and emplacement mechanism of igneous intrusions.
d) Hydrogeological studies including groundwater circulation, effects of tectonic stress on permeability, convection and recharge srtudies are imperative for hydrothermal evolution of geothermal systems.
e) Gravity survey for the evaluation and recording of anomalous heat flow.
f) Seismic, electric, magnetic, aeromagnetic, magnetotelluric, and electromagnetic sounding surveys to establish a sub-surface three dimensional model.
g) Reservoir temperature estimation with geochemi-cal thermometric data.
h) Geothermal gradient estimation and drilling of deep exploration and production wells.
i) Physical properties and behavior of rock-fluid samples at elevated temperatures and pressures.
j) Electricity generation and economic issues for geothermal energy exploration.

REFERENCES

Aamodt, R.L., and Riecker, R.E., 1980, Basic Research Needed for the Geothermal Energy. United States Department of Energy. LA-8562-MS, UC-66a.

Abid, M.S., 1975, Evaluation of geothermal resources in Pakistan. Proceedings of the symposium on World Energy Crises and its Implications with Particular Reference to the Developing Countries, held at Karachi November 1-7.

Bakr, M.A., and Jackson. R.O., 1964, Geological Map of Pakistan 1:2,000,000. Geological Survey of Pakistan.

Bakr, M.A., 1965, Thermal springs of Pakistan. Geological Survey of Pakistan. Rec. 16, p 3-4.

Bender, F.K., and Raza, H.A., (ed.), 1995, Geology of Pakistan. GB Berlin-Stuttgart, Germany. 414 p.

Bannert, D., Raza, H.A., Iqbal, M., Cheema, A., and Achmed, A., 1993, LANDSAT-MSS Annalysis of the West Pakistan Foldbelt. Proceedings of the Ninth Thematic conference on Geologic Remote Sensing Pasadena, Cal. p. 751-52, Ann Arbor, Michigan.

Edwards, Chilingar, Rieke III, Fertl, 1982, Handbook of Geothermal Energy. Gulf Publishing Company, Houston, USA.

Fridleifsson, Ingvar., 1998, Geothermal Direct Use Around the World. Geothermal Bulletin, Vol. 27, No. 8, p. 235-239.

H.S.C., 1960, (Hunting Survey Corporation), Reconnaissance geology of part of West Pakistan: Report published for Government of Pakistan by the Government of Canada, Toronto, 550 p.

Kazmi, A.H., 1979, Active fault system in Pakistan. In Farah and DeJong, (ed) Geodynamics of Pakistan. p. 286-294,

Geological Survey of Pakistan.
Kazmi, A.H., 1979, Seismotectonic Map of Pakistan, Scale 1:2,000,000. Geological Survey of Pakistan Map Series.
Kazmi, A.H. and Rana, R.A. 1982, Tectonic Map of Pakistan. Scale 1:2,000,000. Geological Survey of Pakistan Map Series.
Khan, M.A., Ahmed, R., Raza, H.A., and Kemal, A., 1986, Geology of Petroleum in Kohat Potwar depression Pakistan; Bull. Amer. Asso. Petrol. Geol. 70(4), p. 369-414.
Quittmeyer, R.C., Farah, A., and Jacob, K.H., 1979, The seismicity of Pakistan and its relation to surface faults. **In** Farah and DeJong (eds.) Geodynamics of Pakistan, Geol. Surv. Pak., p. 271-284.
Raza, H.A., Ahmed, R., Alam , S., and Ali, S.M. 1989(a), Petroleum Prospects: Sulaiman Sub-Basin, Pakistan; Pak. J. of Hydrocarbon Res., 1(2), p. 1-19
Raza, H.A., Ahmed, R., Ali, S.M., Ahmed, J., 1989(b), Petroleum Prospects: Sulaiman Sub-Basin, Pakistan; Pak. J. of Hydrocarbon Res., 1(2), p. 21-56
Schoeppel, R.J. 1977, Prospects for geothermal power in Saindak area, Balochistan Province, Pakistan. Final report for Oil and Gas Development Corporation, Pakistan.
Shuja, T.A. and Khan, A.L. 1984, Prospects of geothermal energy in Pakistan. Geological Survey of Pakistan I.R. No. 242.
Shuja, T.A., 1986, Goethermal areas in Pakistan. Geothermics, Vol. 15, No. 5/6, p. 719-723.
Shuja, T.A., 1988, Small Geothermal Resources in Pakistan. Geothermics, Vol. 17, No. 2/3, p. 461-464.
Spector, A. and Associates Ltd., 1981, Report on interpretation of aeromagnetic survey data, Balochistan Province, Pakistan. Canada-Geological Survey Pakistan, Quetta, 107 p.
Zaki, A., 1975, Geology of Mineral Deposits of Baluchistan, Geological Survey of Pakistan. Rec. 36, 178 p.
Zaki, A., and Siddiqui, R.A., 1993, Minerals and Rocks for Industry; Vol. II, Geological Survey of Pakistan p. 601-618

Manuscript Received 10th October 1998
Revised Manuscript Received 14th May 1999
Accepted 1st September, 1999

ACTA
MINERALOGICA
PAKISTANICA
Volume 9 (1998)

Article Reference
AMP9.1998/111-116/ISSN.0257-3660

OXYGEN ISOTOPIC SIGNATURE OF THE HYDROTHERMAL COPPER MINERALIZATION IN DROSH-SHISHI AREA, CHITRAL, PAKISTAN

TAZEEM TAHIRKHELI, MOHAMMAD TAHIR SHAH AND MOHAMMAD ASIF KHAN
National Centre of Excellence in Geology, University of Peshawar, Peshawar Pakistan

ABSTRACT

Copper mineralization in Drosh-Shishi area is a part of the upper crust of Kohistan arc terrane in Chitral, northern Pakistan. It is generally confined to the Gawuch Formation in the area. This formation comprises of variably metamorphosed volcanics and sediments intruded by plutons of diorite and granodiorite. Copper mineralization is related to the hydrothermal activity and is mainly associated with altered diorites and quartz veins.

Nine samples of mineralized quartz veins in Drosh Shishi area were analyzed for oxygen isotopic ratios. The $\delta^{18}O$ values of quartz veins range from 14.49 to 18.32 ‰ with a mean value of 16.63‰. The $\delta^{18}O$ value of the mineralizing fluid of the area has been calculated at the mean temperature (255°C) as determined by fluid inclusion studies. The estimated $\delta^{18}O$ value of the mineralizing fluid ranges from 5.79 to 9.62 ‰ with a mean value of 7.98‰. This indicates the involvement of magmatic fluids in the formation of quartz veins and associated copper mineralization in the investigated area.

INTRODUCTION

Copper mineralization in the Drosh Shishi area, Chitral occurs in a narrow belt of 100m wide and 15Km long in the vicinity of Shyok suture zone, at the north-western margin of the Kohistan Island-arc terran (Fig 1). Metabasalts/meta-andesites with common intercalation of carbonate lithologies (limestone and marble) form the cover sequence in this part of the Kohistan terran. These lithologies, included in the Gawuch Formation (Pudsey et al. 1985) are western equivalents of the better known Chalt-Yasin Group of Yasin and Hunza valleys (Tahirkheli and Jan 1979; Petterson and Windley 1991). The Gawuch Formation is abundantly intruded by sills of diorites and granodiorites composition belonging to the Early Eocene Lowari pluton of the Kohistan batholith. Minor intrusions of diorites and granodiorite in the Gawuch Formation, together with intimately associate quartz veins, host the copper mineralization in the Drosh-Shishi area.

This paper is based on a detailed oxygen isotopic study of quartz veins containing sulfide mineralization. The isotope composition of the quartz from the studied quartz veins suggests that the copper mineralization is related with hydrothermal activity, some of heavy fluids involved in the formation of sulfide mineralization.

GEOLOGICAL SETTING

The Shyok suture separates the Eurasian plate to the north from the Kohistan terrene to the south (Tahirkheli and Jan 1979; Bard et al. 1980). The northern part of the Kohistan terrene comprises three principal tectonic units, that from north to south include: 1) Shyok suture melange, 2) sedimentary-volcano cover sequence and 3) Kohistan batholith. The Shyok suture melange, as the name signifies, defines the collision zone between Kohistan and Eurasian plates and marks the closure of the northern branch of the Neotethys, termed the Shyok ocean (Khan et al. 1997). It ranges from a razor-sharp fault to a 4 km wide zone and consists of lenticular blocks of highly variable

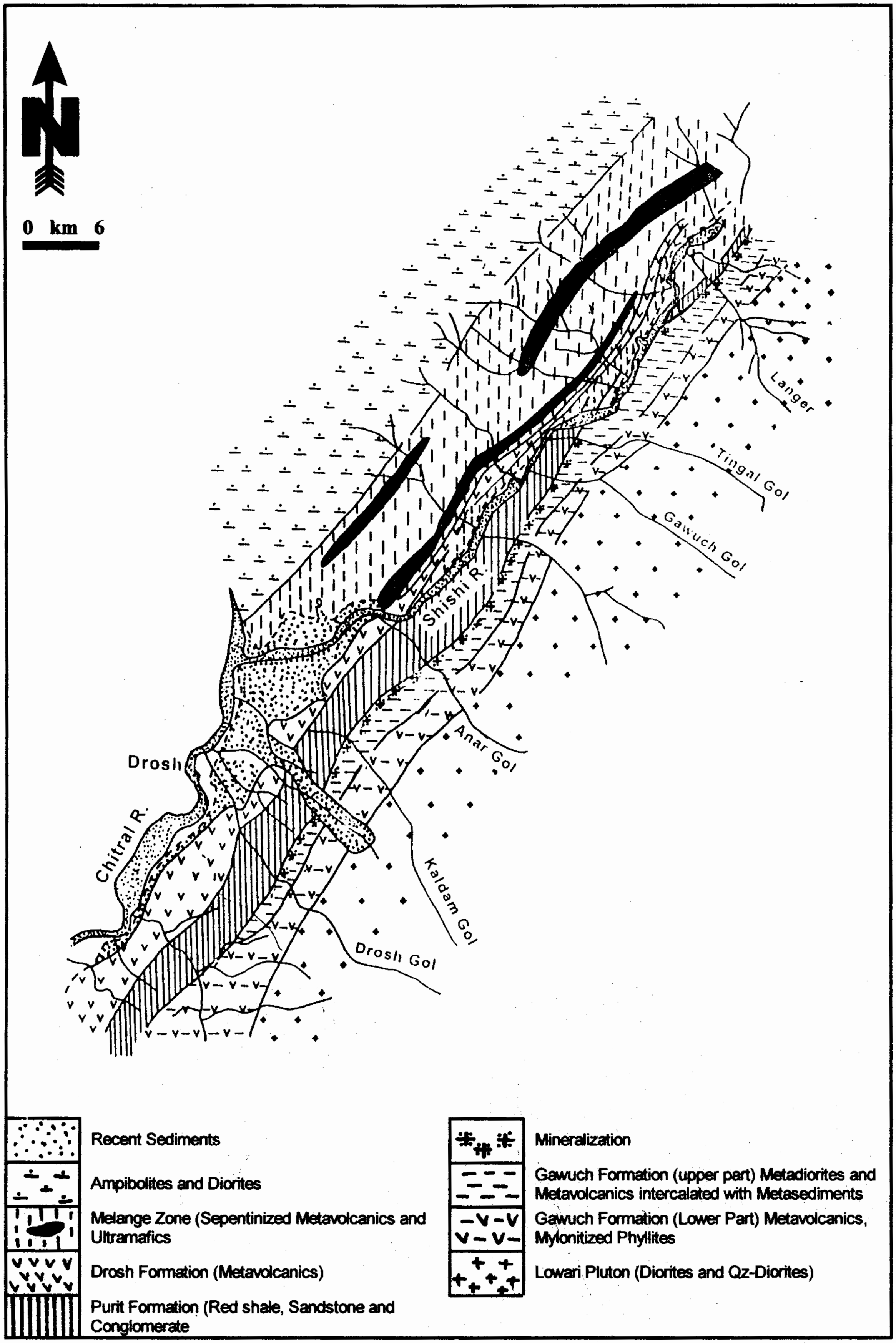

Figure 1. Geological map of Drosh-Shishi area, Chitral, Northern Pakistan.

lithology including serpentinites, marbles, conglomerates, sandstones and basalts, mostly set in a pellitic matrix comprising slates of turbidite origin (Pudsey 1986). In the Yasin area, limestone blocks are reported to contain Albian-Aptian fauna. The volcano-sedimentary cover sequence in the Kohistan terrene occurs as a lenticular belt of variable width squeezed between the Shyok suture in the north and the Kohistan batholith in the south. The sequence comprises a thick succession of metabasalts at the base (the Chalt volcanics; Petterson and windley 1991) overlain by a succession of quartzites, limestones and turbidites (Pudsey et al. 1985; Pudsey 1986), termed the Yasin Group. The Yasin Group contains Early Cretaceous fauna and is marine in origin (Pudsey 1986). Khan et al. (1994) have named the succession of paragneisses, schists and amphibolites, some containing pillow structures as the Gilgit Formation that occupies the base of the Chalt Volcanics. The Kohistan batholith occupies the central spine of the Kohistan terrene and is intrusive into the first two tectonic elements mentioned above. The batholith is composite and consists of plutons of a wide range of compositions from gabbros, through diorites, tonalites and granodiorites to granites. The igneous activity related to the Kohistan batholith is 102 to 29 Ma old (Patterson and Windley 1985).

The geology of the NW margin of the Kohistan terrane in Chitral including the Drosh-Shishi area, contains all the three tectonic elements outlined above. The Shyok suture melange in this area comprises lenticular blocks of ultramafics, limestones etc. The volcano-sedimentary succession in this area, is however, much more complex than that of the Yasin-Hunza segment. Pudsey et al. (1985) recognized three formations, which from south to north include 1) Gawuch Formation, 2) Purit Formation and 3) Drosh Formation. The Gawuch Formation comprises metabasalts and limestones and is probably marine in origin, whereas the Purit Formation comprises red, fluvial conglomerates, sandstones and shale (Pudsey et al. 1985). Occurrence of a succession of andesite/dacite volcanics of the Drosh Formation to the north and probably over the Purit Formation points to the possibility of a phase of Eocene volcanic event similar to that of Dir-Utror (Shah and Jan 1993). Towards the south the Gawuch Formation, the host of the copper mineralization, is in contact with the Lowari pluton belonging to the Kohistan batholith. The contact, probably intrusive in origin, is now strongly sheared and is occupied by phyllites derived from metavolcanics of the Gawuch Formation through mylonitization. Much of the lower half of the Gawuch Formation is occupied by metabasalts, which are locally strongly sheared and transformed into phyllites. The upper half of the succession making the Gawuch Formation comprises commonly intercalated metabasalts and limestone/marble. This part of the Gawuch Formation is additionally commonly intruded by sills of diorite and granodiorite composition, which are themselves pervasively intruded by quartz veins. The contact between the Gawuch Formation and the overlying Purit Formation is occupied by a 10-m thick band of marble. Copper mineralization in this formation is related to hydrothermal activity and is mainly associated with altered diorites and quartz veins.

The mineralized rocks of the study area are divided in to three units on the basis of both field and petrographic studies such as 1) sulfide-bearing quartz veins, 2) sulfide-bearing altered diorites and 3) sulfide-bearing shear zone. Based on field observations, four types of copper mineralization are recognized in the area; 1) copper mineralization along quartz veins, 2) copper mineralization along foliation planes, 3) disseminated copper mineralization and 4) supergene copper enrichment.

METHODOLOGY

Out of many samples collected during the field work, 13 sample of mineralized quartz veins were selected and analyzed for oxygen isotopic studies. Quartz separates were made by standard techniques of heavy liquids, hand picking, and short cold HF bath. Quartz was 100% pure. Oxygen was extracted by a new technique, in which 1 mg of silicate was heated by laser and reacted with BrF_5 (Sharp 1990) and then converted CO_2 on a hot carbon rod (Taylor and Epstein 1962). Isotopic composition of the prepared gas was measured on gas ratio (Nier type) mass spectrometers. All analytical work related to the isotopic studies was carried at the Oregon State University, Corvallis, USA.

RESULS AND DISCUSSION

$\delta^{18}O$ IN MINERALIZED QUARTZ VEINS

Quartz in 9 samples of mineralized quartz veins, having mainly tetrahedrite with subordinate galena chalcopyrite, bornite, pyrite and magnetite, were analyzed for oxygen isotope composition. The $\delta^{18}O$ values of quartz veins range from 14.49 to 18.32 with a mean of 16.63 (table 1). The oxygen isotope composition of the quartz from the studied quartz veins suggests that the mineralization in the area is related to a hydrothermal event which has

Table 1. Oxygen isotope composition of quartz from the mineralized quartz veins of the Drosh area, Chitral, and $\delta^{18}O$ values of the mineralizing fluids.

Sample No.	^{18}O quartz	$\delta^{18}O$ fluid %
GR73	16.84	8.74
KG168	17.17	8.47
KG203	16.83	8.13
KG12	14.49	5.79
KG17b	16.72	8.02
GR74	17.78	9.08
GR75	18.32	9.62
GR76	14.61	5.91
GR81b	17.36	8.66
Average*	**16.68**	**7.98**

**Average $\delta^{18}O$ (fluid)=7.98 % at 255°C*

produced a high $\delta^{18}O$ signature in the mineralized quartz veins and most probably also in the associated altered host rocks.

$\delta^{18}O$ VALUES OF HYDROTHERMAL FLUID

The $\delta^{18}O$ value of mineralizing fluid of the Gawuch Formation were calculated from the fluid inclusion data for the quartz veins which is indicates a range of temperature form 160-350°C with a mean value of 255°C. The isotopic composition of water in equilibrium with the quartz veins was calculated at the mean temperature (255°C) using the empirically determined quartz-water fractionation equation 1000In∂=3.34 (106 T-2) –3.31 or the curve of Matsuhisa et al. (1979). This temperature yields the average $\Delta^{18}O$ (quartz-water) value of 8.70 for mineralized quartz veins. These values fall within the range of values accepted for waters of metamorphic (4-25 ‰) and magmatic (5-9‰) origin (Taylor 1974) (Figure 2).

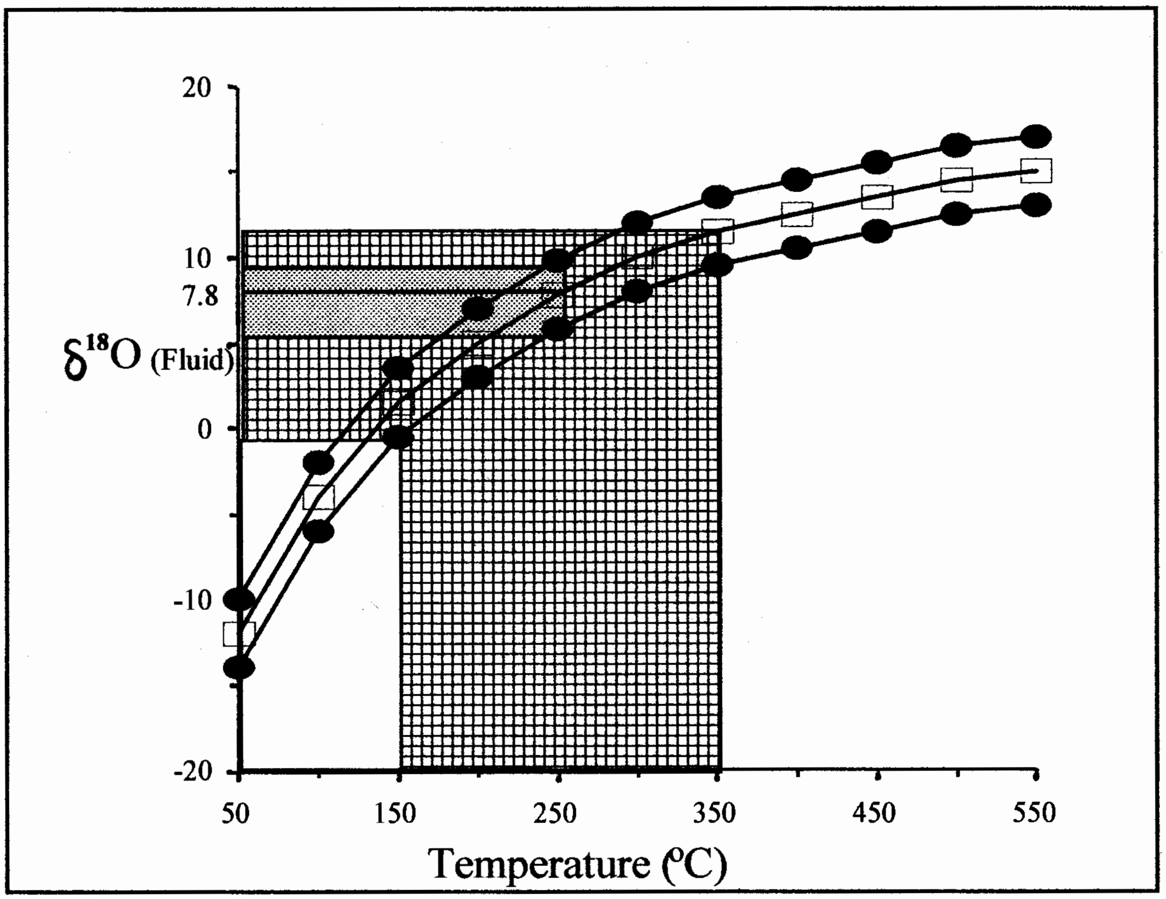

Figure 2. Oxygen isotope composition of parental water calculated at a series of temperatures from the measured oxygen isotope composition of quartz from the Gwauch Formation. The lightly shaded area represents the range of the fluid inclusion homogenization temperature (150-350°C) and the range of corresponding oxygen isotope composition (calculated) of parental waters. The inset with lighter shade represents the range of oxygen isotope-composition of the magmatic water.

The high oxygen isotopic signature of the studied quartz veins, however, rules out the possibility of involvement of meteoric water and shows that heavy fluids played an important role in the formation of quartz veins and associated Cu-mineralization and alteration.

The rocks of the area are metamorphosed to greenschist- and at places, to epidote-amphibole facies metamorphism. These rocks have well-developed fabric, faulting and shearing. The Cu mineralization occurs within the granodiorite sills, dikes and plugs, suggesting the involvement of either magmatic or metamorphic water for Cu mineralization in Gawuch Formation.

The development of high $\delta^{18}O$ values, in the region affected by low-grade regional metamorphism can be attributed to the metamorphic dehydration (Spooner et al. 1974; Paterson 1982). During this process the metals leach out of the host rocks and concentrate in the metamorphic dehydration fluids (Paterson 1982). The higher $\delta^{18}O$ signature of the mineralizing fluids in Gawuch Formation may be related to this type of dehydration. However, the development of hydrous mineral phases and the higher amount of water in the mineralized rocks of the Gawuch Formation do not favor the possibility that the metamorphic dehydration or dewatering is the cause of ore-forming fluid in the area.

The presence of igneous activity in the form of diorite-granodioritic plugs, sills, and dykes, hosting the mineralization, suggest a role of magma in the generation of hydrothermal system rather than metamorphism. It is, therefore, hypothesized that the diorite-granodiorite plutons existing at depth beneath the mineralized zone could have been sources of brine metalliferous fluids. These fluids have precipitated the Cu-sulfide phases along silica, mainly in the form of quartz vein at shallow level.

CONCLUSION

Hydrothermal copper mineralization in Drosh-Shishi area is present in the upper parts of Gawuch Formation and is generally confined to the diorite/granodiorite intrusions and associated quartz veins. The oxygen isotope composition of quartz veins shows $\delta^{18}O$ values ranging from 14.49 to 18.32‰ with a mean value of 16.63‰. The estimated $\delta^{18}O$ value of the mineralizing fluid ranges from 5.79‰ to 9.62‰ with a mean value of 7.98‰. This indicates the involvement of magmatic fluids in the formation of quartz veins and associated Cu-minerals in the investigated area.

REFERENCES

Bard, J. P., Maluski, H., Matt. P. H. and Proust, F., 1980. The Koshistan squence; Crust and Mantle of an obducted island arc. Geological Bulletin University of Peshawar; v.13, p.87-93.

Khan, M. A., Stern, R. J., Gribble, R. F and Windley, B. F., 1997. Geochemical and isotope constraints on subduction polarity magma source and paleogeography of Kohistan intra-oceanic arc, northern Pakistan Himalaya. Geol. Society of London, (in press).

Khan, M. Nawaz, 1986, Geological Map of Drosh Area Chitral, Northern Pakistan, (unpublished Report) Sarhad Development Authority, NWFP, Peshawar.

Khan, T., Khan, M. A. and Jan, M. Q., 1994. Geology of a part of the Kohistan terrane between Gilgit and Chilas, northern areas, Pakistan. Geological Bulletin University of Peshawar; v.27, p.99-112.

Matsuhisa, Y., Goldsmith, J. R. and Clayton, R. N., 1979. Oxygen isotopic fractionation in system quartz- albite-anorthite-water: Geochim Cosmochim Acta; v. 43, p. 1131-1140.

Paterson, C. J., 1982. Oxygen isotopic evidence for the origin and evolution of a scheelite ore forming fluid, Glenorchy, New Zealand Econ. Geol.; v. 77, p. 1672-1687.

Petterson, M. G. and Windley, B. F., 1985. Changing source regions of magmas and crustal growth in the Trans-Himalayas: Evidence from the Chalt volcanics and Kohistan batholith, Kohistan, N. Pakistan. Earth and Planetary Sciences Letters; v. 102, p. 326-346.

Pudsey, C. J., 1986. The northern suture, Pakistan : Margin of a Cretaceous island arc. Geological Magazine; v.13, p.405-423.

Pudsey, C., Coward, M. P., Luff, I. W., Shackleton, R. M., Windley, B. F. and Jan, M. Q., 1985. Collision zone between the Kohistan arc and the Asian plate in NW Pakistan. Trasactions of Royal Society, Edinburgh (Earth Sciences); v. 76, p. 463-479.

Shah, M. T. and Jan. M. Q., 1993. Mineralogical constraints of Shergarh Sar amphibolites of Allai Kohistan, Northern Pakistan. Geological Bulletin University of Peshawar; v.26, p.59-73.

Sharp, Z. D., 1990. A laser-based microanalytical method for insitu determination of oxygen isotope ratios of silicates and oxides; v. 54, p. 1354-1357.

Spooner E. T. C., Beckinsale R. D.,Fyfe, W. S. and Snewing, J. D. 1974. 18O enriched ophiolitic metabasic rocks from E. Liquria (Italy), Pindos (Greece), and Troodos (Cyprus). Contrib. Mineral. Petrol.; v. 47, p. 41- 62.

Tahirkheli, R. A. K. and Jan. M. Q. 1979. A preliminary geological map of Kohistan and the adjoining areas, N. Pakistan.

Geological Bulletin University Peshawar, v. 11.
Taylor, H. P., Jr., and Epstein, S., 1962. Relationship between $^{18}O/^{16}O$ ratios in coexisting minerals of igneous and metamorphic rocks. Part 1: Geologcial Society of America; v. 73, p. 461-480.
Taylor,H. P., Jr., 1974. The application of Oxygen and hydrogen isotope studies to problems of hydrothermal alteration and ore deposition : Economic Geology; v. 69, p. 843-883.

Manuscript Received 20th October 1999
Revised Manuscript Received 15th December, 1999
Accepted 16th December, 1999

ACTA MINERALOGICA PAKISTANICA
Volume 9 (1998)

Article Reference
AMP9.1998/117-122/ISSN.0257-3660

Short Communication

VOLCANICLASTIC SEDIMENTS OF THE UPPER CRETACEOUS BIBAI FORMATION, KACH-ZIARAT VALLEY, BALOCHISTAN

ABDUL TAWAB KHAN[1], AKHTAR MOHAMMAD KASSI[1] AND ABDUL SALAM KHAN[2]
[1] Department of Geology, University of Balochistan, Quetta Pakistan
[2] Centre of Excellence in Mineralogy, University of Balochistan, Quetta Pakistan

The Upper Cretaceous Bibai Formation of Kazmi (1955), exposed in the western part of the Sulaiman Thrust-Fold Belt, is mainly composed of volcaniclastic sediments including volcanic conglomerate, volcanic breccia, sandstone, mudstone and minor proportion of volcanic rocks in Kach-Ziarat valley and Muslimbagh area, whereas, in Chinjun Spera Ragha valley mainly the *in-situ* volcanic rocks with minor proportion of volcaniclastic succession (Fig. 1). The formation is overlain conformably and transitionally by the Albian-Cenomanian Parh Limestone and underlain conformably by the Upper Cretaceous rocks of Pab Sandstone, Mughal Kot Formation and Palaeocene Dungan Limestone. In the Spera Ragha-Chinjun valley the *in-situ* volcanics are overlain disconformably by the Maestrichtian Fort Munro Formation.

The Bibai Formation is the lateral equivalent of the Mughal Kot Formation and Porali Agglomerate, which was previously designated as part of the Bela Volcanic Group (Hunting Survey Corporation 1960), and Duccan Trap Volcanics (Vredenburg 1901, Williams 1959, Yoshida et al. 1995). Kazmi (1955, 1995) has assigned it Campanion to Middle Maestrichtian, whereas, Sawada et al. (1995) have proposed 71.4 $\pm$ 3.4 Ma (K-Ar) to the *in-situ* Bibai Volcanics of the Spera Ragha-Chinjun valley.

Study of the sedimentary facies and facies associations of the volcaniclastic succession of Kach-Ziarat valley (Fig. 2) show that volcaniclastic succession comprises volcanic conglomerate (VC), sandstone (SS), sandstone rhythmically interbedded with mudstone (SSMS), mudstone (MS), volcanic breccia (VB), limestone (LS) and *in situ* volcanics (VOL) facies.

The VC and SS facies resembles with the facies classes and groups A and B of Pickering et al. (1986) which are the product of high concentration turbidity currents, of upper flow regime and generated at higher gradient. These facies have concave-up erosive bases, lenticular morphology and general fining-upward trends which are characteristic of channels. The SSMS facies of rhythmically interbedded sandstone and mudstone, possessing sedimentary structures like grading, sole marks and Bouma T_{abcde}, T_{bcde}, T_{cde}, T_{de} sequences (Bouma 1962), resemble with the facies C2 of organised sand-mud couplets (Pickering et al. 1986). They indicate deposition by moderate to high concentrated turbidity currents and grain-by-grain deposition from suspension and traction transport. Muddy upper divisions are the product of low concentration turbidity currents and/or hemi-pelagic/pelagic sedimentation or deposition by mud-rich turbidity currents. Close association the SSMS facies, and their frequent truncation by the VC-SS facies, indicate that they are deposits of the overbank (-levee) complex in which thicker beds with concave-up erosive bases and lenticular morphology show crevasse channels.

Association of coherent folded and contorted strata (facies class F of Pickering et al. [1986]) indicates slides, slumps and high gradient soft

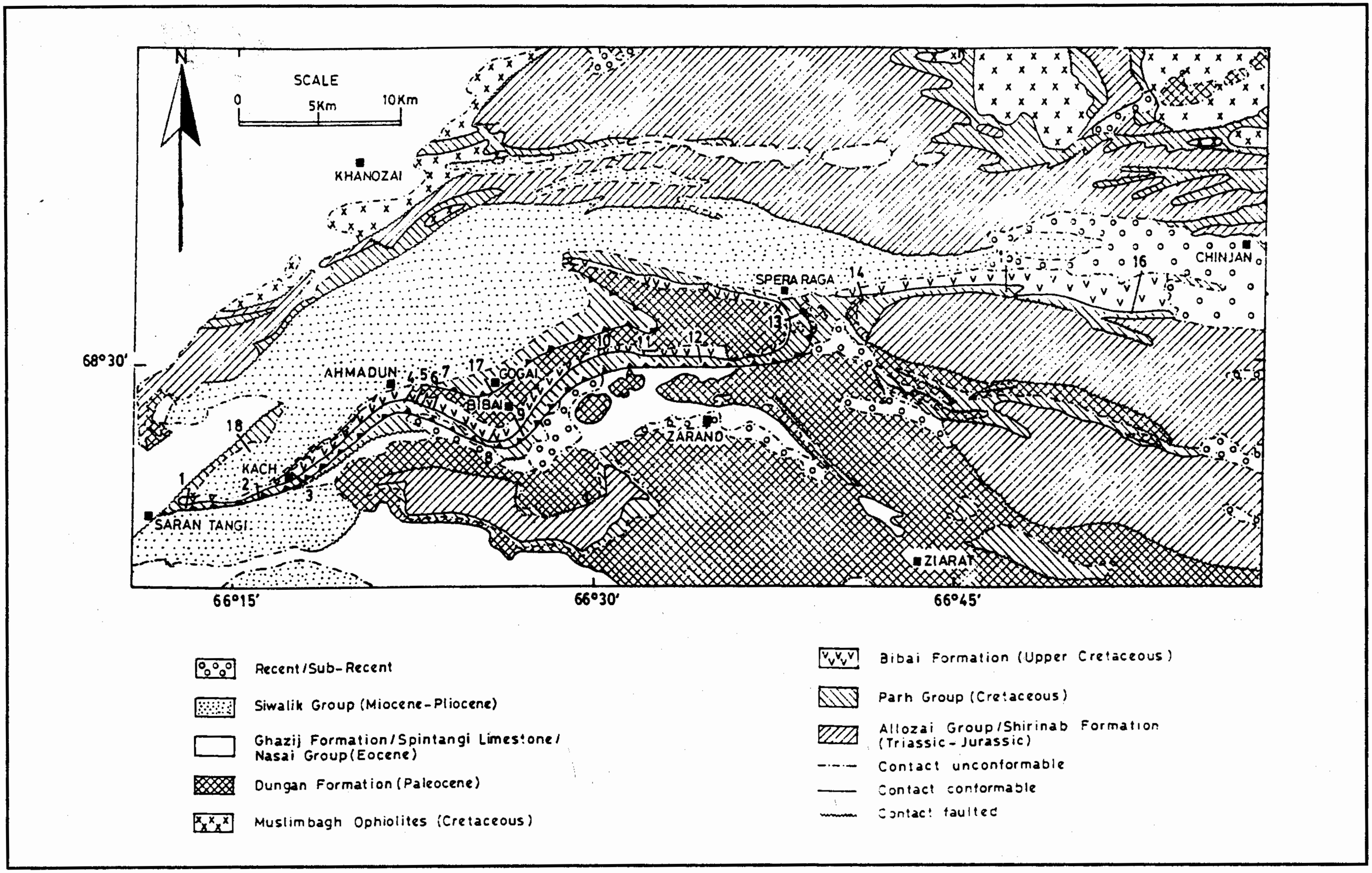

Figure 1. **Geological Map of the study area (modified after HSC 1960) showing positions of various studied sections and localities mentioned in text.**

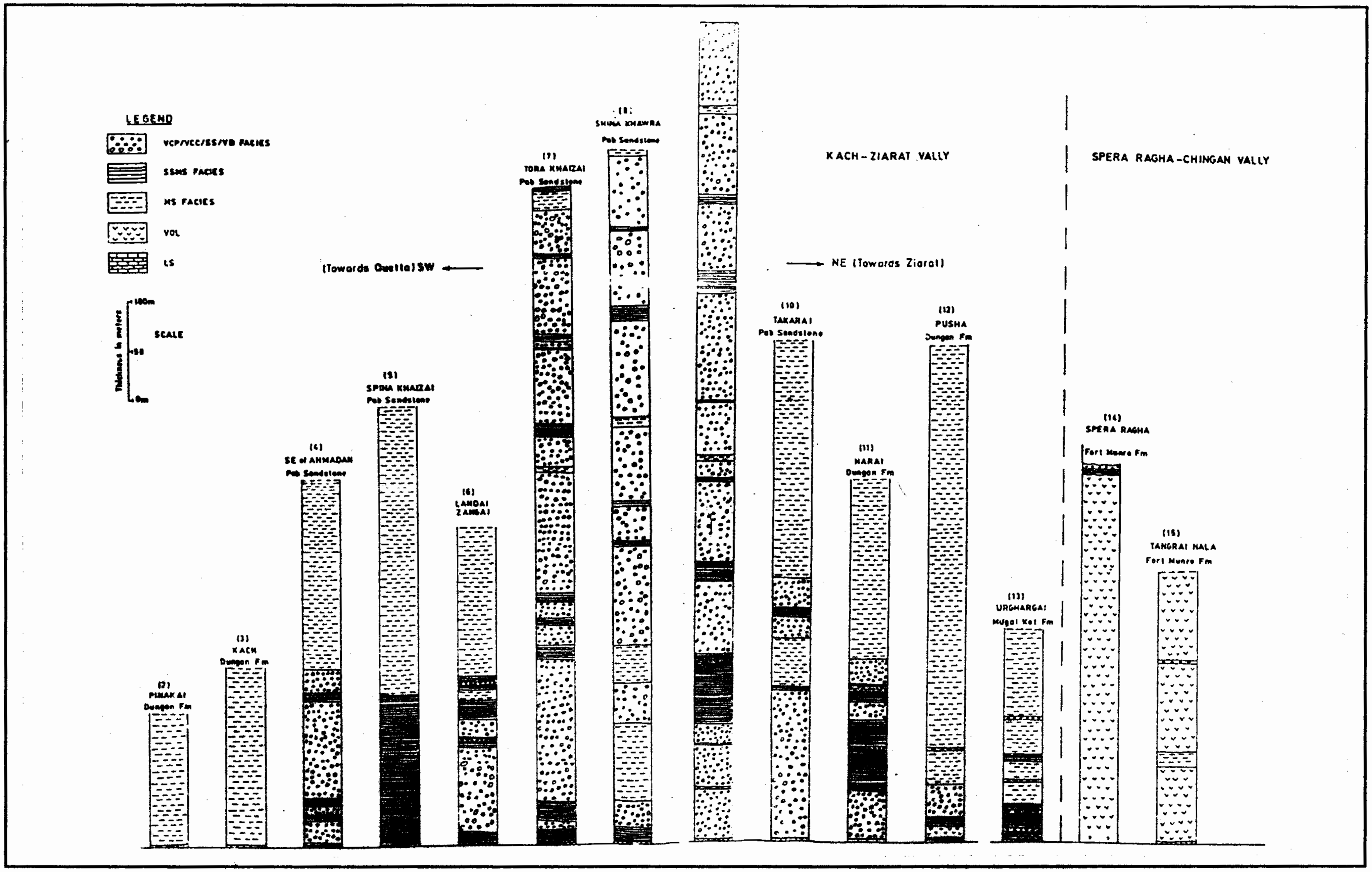

Figure 2. **Figure showing comparison of columnar profiles of the studied sections and vertical and lateral variations within the studied area.**

sediment deformation, overloading of weekly lithified sediments and/or influence of eruptive/ seismic activity. The MS facies of claystone, siltstone with occasional thin sandstone beds dominate in various sections of the distal areas northeast and southwest of the Bibai Peak. Their upper parts contain shallow marine fossils. The MS facies resemble with the facies classes D and E of Mutti and Ricci Lucchi (1975) and Pickering et al. (1986) and are deposited by mud-rich, very low-concentration turbidity currents and lateral transfer of hemipelagic / pelagic material by ocean currents. Within the proximal area near Bibai Peak facies MS occurs at certain levels in cyclic manner with those of the VC-SS and SSMS facies associations which may be manifestation of global sea-level fluctuations (Vail et al. 1977, Shanmugam et al. 1985). In such successions sea-level rise (highstand) is represented by development of fine grained clastic facies (basin plane) and sea-level fall (lowstand) by coarse clastic facies (submarine fans).

Volcanic breccia (VB) is present mostly in lower part of the succession, in proximal part of the area, and associated with highly distorted and slumped facies. Characters of the VB facies resemble with the debrite facies model of Stow (1985) or F1 (exotic clasts) of the chaotic deposits of Pickering et al. 1986). The Limestone (LS) facies, interbedded with the volcaniclastic facies in lower part of the Formation, is very finely crystalline (biomicritic) and possesses microforaminifera of the *Globotruncana* family (Kazmi 1995). Its characters resemble with the underlying Parh Limestone (Allemann 1979) which are interpreted to have been deposited by pelagic sedimentation in lower shelf - upper slope conditions during calm periods between the volcaniclastic sedimentation. The *in-situ* volcanic rocks (VOL), in some cases intercalated with the volcaniclastic facies, has been interpreted as those of the hotspot origin (McCormick 1985, 1989, Siddiqui et al. 1996).

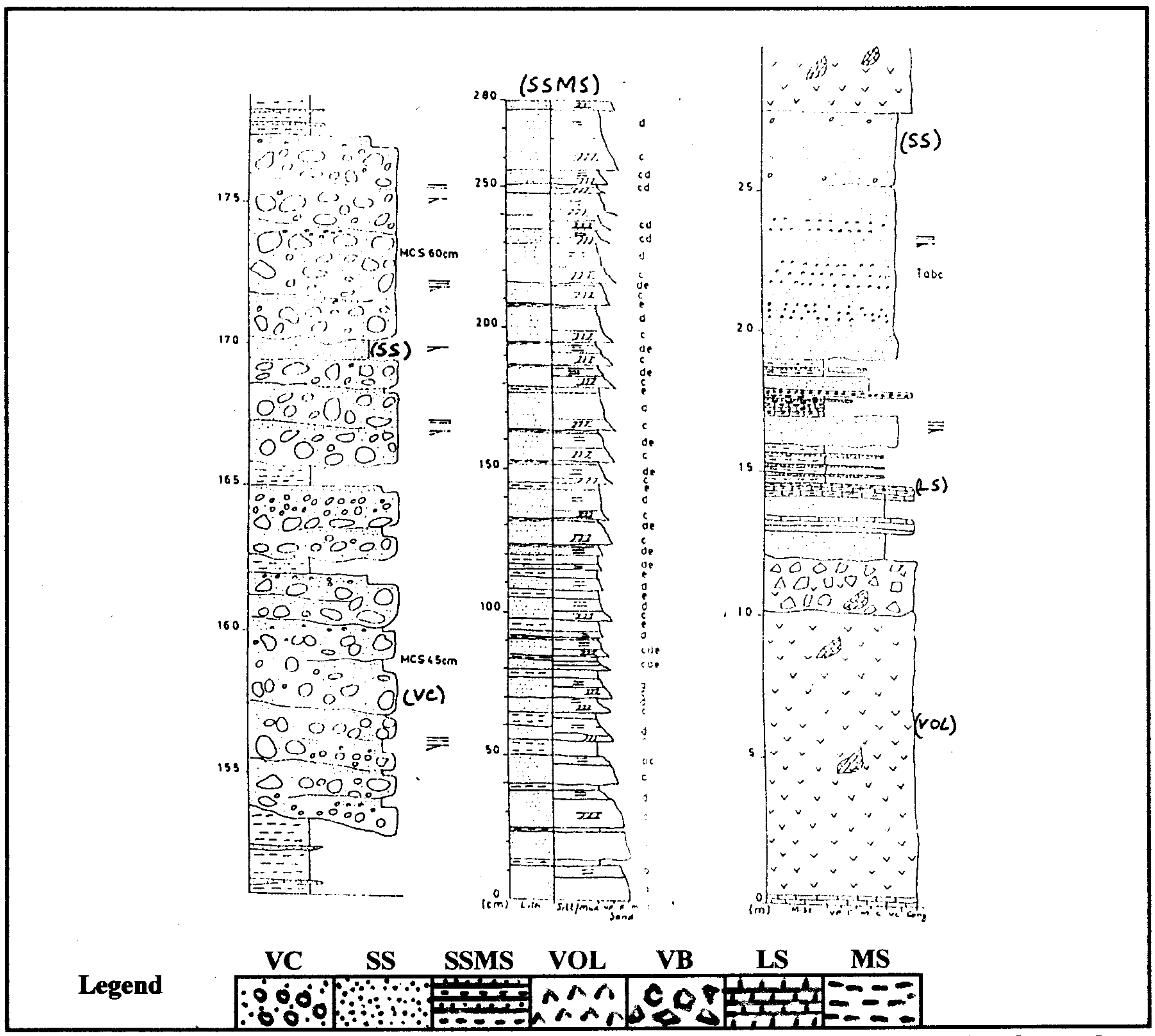

Figure 3. Parts of the columnar profiles of the Bibai Formation showing varios facies observed.

Various associations of facies, comparison of various sections, paleocurrent pattern, the concept of the submarine fan models proposed by early workers and presence of the facies deposited by sediment gravity flows (Middleton and Hampton 1973) suggest that the Bibai Formation in Kach-Ziarat valley comprises special category of a "channel (-levee) -overbank complex". This complex developed on slope of a series of seamounts (hotspot volcanos) whereby its material was derived from a volcanic terrain. Lithofacies and their associations clearly define the distributary channels (mid-fan), inter-channel (overbank-levee) and lower fan / basin plane components of the submarine fan. Absence of the thickening-upward cycles suggest that the Bibai Submarine Fan is Type-III system of the three types of models of Mutti (1985), which comprises the channel-levee complex. Among the four types of submarine fans of Shanmugam and Moiola (1988), the Bibai Submarine Fan resembles with those of "mixed setting" as it has particularly developed on the basin-ward slope of the seamounts (hotspot volcanics) on northwestern (and northward drifting) margin of the Indo-Pakistan Plate. The very coarse grained (conglomeratic) nature of the Bibai Submarine Fan is comparable presumably with the steep, short and radial character of the active margin fans.

Paleocurrent pattern (Fig. 4) indicate a south-southwest paleo-flow direction and a source area to the north-northeast of Bibai Peak. Rock fragments of the volcanic conglomerate and sandstone of the Bibai Formation are alkalic in character and have been derived from hotspot-related volcanic source. We suggest that the Bibai Volcanics, exposed prior to the deposition of Siwaliks, to the north of Bibai Peak is the possible source, the lateral extention toward Spera Ragha-Chinjun has been interpreted as hotspot related volcanics (McCormick 1985, Khan 1986, 1994, Siddiqui et al. 1996).

Based on study of the lateral facies variations (Fig. 3), paleocurrent directions, composition and provenance of the volcaniclastic succession of Bibai Formation we have also proposed a paleogeographic model. According to the proposed model the Bibai Submarine Fan formed on slope of a series of sea mounts (hotspot volcanos) that grew on the northwestern margin of the Indo-Pakistan Plate over the pelagic limestone succession on the Tethyan sea-floor and which later-on emerged and provided volcaniclastic detritus to the submarine fan. We suggest that the present trend of paleocurrent directions observed within the Bibai Submarine Fan (from

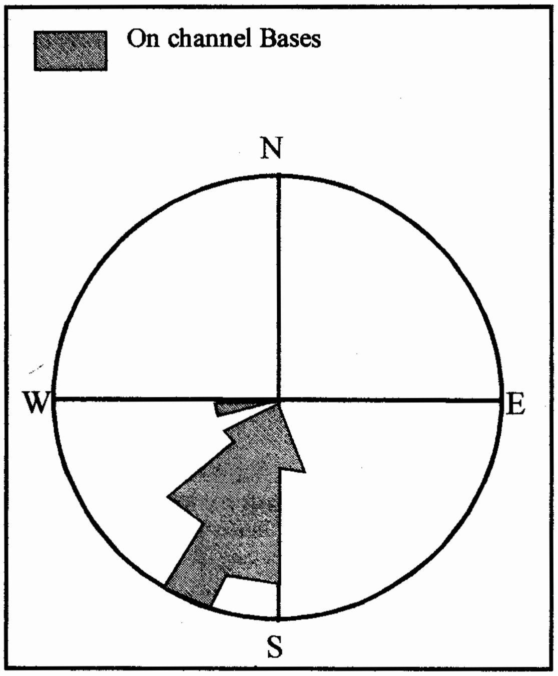

Figure 4. Comprehensive rose diagram of paleocurrent pattern based on longitudinal ridges and flute marks; Scale: 1cm = 4 readings; n = 83.

north-northeast to south-southwest) has been rotated considerably anticlockwise along with the north-northeastward drift and anticlockwise rotation of the Indo-Pakistan Plate which continued during the Upper Cretaceous and later periods till present time. This interpretation concurs with the Powel (1979). The general rotation of the Indo-Pakistan continent in a clockwise direction to its 71.4$\pm$3.4 My position would bring the present south-southwest trend of paleo-flow directions back to the original west-northwest direction, justifying the original paleo-slope of northwestern margin of the Indo-Pakistan Plate. Development of the submarine fan, associated with emergence and denudation of sea mounts was followed by submergence and deposition of shallow marine succession along with folding, thrusting and obduction of the Bela-Waziristan Ophiolites.

REFERENCES

Allemann, F., 1979. Time of emplacement of the Zhob Valley Ophiolites and Bela Ophiolites, Balochistan, In Farah, A. and DeJong, K. A., (eds.), Geodynamics of Pakistan: Geological Survey of Pakistan, Quetta, 215-242.

Bouma, A. H., 1962. Sedimentology of some flysch deposits - a graphic approach to the facies interpretation: Elservier, Amsterdam, 165p.

Hunting Survey Corporation, 1960. Reconniassance Geology of part of West Pakistan: A Colombo Plan Coorporation

Project, 550p., Toronto, Canada.

Kazmi, A. H., 1955. Geology of the Ziarat-Kach-Zardalu area of Balochistan: D.I.C. thesis, Imperial College of Science andTechnology, London (unpubl.), 157 p., London.

Kazmi, A. H., 1979. The Bibai and Gogai Nappes in the Kach-Ziarat area of northeastern Balochistan: **In** Farah, A. and DeJong, K. A., (eds.), Geodynamics of Pakistan: Geological Survey of Pakistan, Quetta.

Kazmi, A.H., 1995. Sedimentary Sequences: In F.K. Bender and H.A. Raza, (eds) Geology of Pakistan. Pub. in Berlin. p. 61-124

Khan, W., 1986. Geology and petrochemistry of part of the Parh Group Volcanics near Chingun: M. Phil. desertation, Centre of Excellence in Mineralogy, University of Balochistan, Quetta (unpubl.).

Khan, W., 1994. Geology, geochemistry and tectonic setting of the volcanic rocks of Chinjun and Ghunda Manra areas, northeastern Balochistan, Pakistan: Ph.D. dessertation (unpubl.), University of Lowa, 257p.

McCormick, G. R., 1985. Preliminary study of the volcanic rocks of the South Tethyan suture in Balochistan, Pakistan: Acta Minralogica Pakistanica, 1, p. 2-9.

McCormick, G. R., 1989. Geology of the Balochistan (Pakistan) portion of the southern margin of Tethys sea: **In** Sengor, A. M. (ed.), Tectonic evolotion of the Tethyan region. P. 277-288, Kluwer Academic Publishers.

Middleton, G. V. and Hampton, M. A., 1973: Sediment gravity flows - Mechanics of flow and deposition. **In** Middleton, G. V. and Bouma, A. H., (eds.), Turbidites and Deep-Water Sedimentation, Pacific Section: Soc. Econ. Paleontol. Mineral., Los Angeles, California, p. 1-38.

Mutti, E., 1985. Turbidite system and their relations to depositional sequences: **In** Zuffa, G. G., (ed.), Provenance of arenites: D. Reidel Publishing Company, Dordrecht, p. 65-93.

Mutti, E. and Ricci Lucchi, F., 1975. Turbidite facies and facies associations: *in* Examples of turbidite facies and facies associations from selected formations of the Northern Apennines: Field Trip Guide Book, A-11. Int. Sediment. Congr., 1X, Nice, p. 21-36.

Pickering, K. T., Stow, D. A. V., Watson, M. and Hiscott, R. N., 1986. Deep-water facies, processes and models - a review and classification scheme for modern and ancient sediments: Earth Sci. Rev., 22, p. 75-174.

Powell,C.M., 1979. A Speculative Tectonic History of Pakistan and surroundigs. Some constraints from the Indian Ocean. **In** Farah, A and Dejong, K. A., (eds.) Geodynamics of Pakistan, Geol.Surv. Pakistan, Quetta, p.325-31.

Sawada, Y., Siddiqui, R. H. and Khan, S. R., 1995. K-Ar Ages of the Mesozoic Igneous and Metamorphic Rocks from the Muslim Bagh area, Pakistan: Proc. Geosci. Colloq., 12, p.73-90.

Shanmugam, G. and Moiola, R. J., 1988. Submarine fans - Characteristics, models, classification and reservoir potential: Earth Science Reviews, 24, 383-428.

Shanmugam, G., Moiola, R. J. and Damuth, J. E., 1985. Eustatic control of submarine fan development: **In** Bouma, A. H., Normark, W. R. and Barnes, N. E., (eds.), Submarine Fans and Related Turbidite Systems: Springer-Verlag, New York, p. 23-28.

Siddiqui, R. H., Khan, I. H. and Aziz, A., 1996. Geology and Petrogenesis of Hotspot Related Magmatism on the Northwestern Margin of the Indian Continent: Proc. Geosci. Colloq. Geosci. Lab. GSP, 16, p. 115-48.

Stow, D. A. V., 1985. Deep sea clastics - Where are we and where we are going ?: *in* Brenchley, P. S. and Williams, B. P. J., (eds.), Sedimentology - recent developments and applied aspects: Geol. Soc. (London), Spec. Publn., 18, p. 67-93.

Vail, P. R., Mitchum, R. M. and Thompson, III, S., 1977. Seismic stratigraphy and global changes of sea-level, Part 4 - Global cycles of relative changes of sea-level: **In** Payton, C. E., (ed.), Seismic Stratigraphy - application to Hydrocarbon Exploration: AAPG Memoir 26, p. 83-97.

Vredenburg, E. W., 1901. A geological sketch of the Balochistan and part of eastern Persia: Geol. Surv. India Mem., 31, p. 137- 302, Calcutta.

Williams, M. D., 1959. Stratigraphy of the lower Indus basin, West Pakistan: Proc. 5th World Petroleum Congress, Sec. 1, 19, p. 337-391.

Yoshida, M., Khadim, I. M. and Zaman, H., 1995. Paleomagnetism of pillow basalts in the Muslim Bagh area, Balochistan, Pakistan - Late Cretaceous trace of Re-Union Hotspot: Geologica, Res. Bull. Geosci. Lab., GSP, 1, p. 77-90.

Manuscript Received 12th October 1998
Revised Manuscript Received 25th October 1998
Accepted 1st September 1999

ANNUAL REPORT
(1998)

NATIONAL CENTRE OF EXCELLENCE IN MINERALOGY, QUETTA

ACADEMIC STAFF

Director

Dr. Akhtar Mohammad Kassi, Professor of Geology, University of Balochistan has been given additional charge of the Director, C.E.M. The appointment of a permanent Director is still awaited. Dr. Kassi is Ph.D. from U.K. and is teaching geology at the Department of Geology for the last 22 years.

		Date of Joining C.E.M.
Associate Professors		
Shamim Ahmad Siddiqui	*Ph.D. (U.S.A.)*	01-Jan-1998
Abdul Salam Khan	*Ph.D. (U.K.)*	01-Jan-1998
Javed Ahmad	*M.Phil. (Balochistan Universty)*	01-Apr-1980
Khalid Mahmood	*Ph.D. (France.)*	05-Nov-1989
Mohammad Ahmad Farooqui	*Ph.D. (U.S.A.)*	05-Nov-1989
Assisstant Professors		
Mehrab Khan	*M.Phil. (Balochistan University)*	05-Nov-1989
Visiting Professors		
Mohammad Niamatullah	*Ph.D. (U.K.)*	
Syed Mobasher Aftab	*Ph.D. (Turkey)*	
Din Mohammad Kakar	*M.Phil. (Balochistan University)*	

ADMIN./TECHNICAL STAFF

S. Shahabuddin	Administrative Officer	28-May-1977
Mirza Manzoor Ahmad	Accounts Officer	07-May-1980
Khushnood Ahmad	Senior Technician	13-Jul-1976
Abdul Ghafoor	Assistant Librarian	02-May-1985
Lal Mohammad	Superintendent	12-May-1973
Hussainuddin	Photographer	16-Jun-1981
Ghalib Shaheen	Stenotypist	17-Jul-1985
S.R. Mahjoor	Stenographer	06-Jun-1990
Ahmad Khan Mangi	Draughtsman	01-Jul-1981
Musa Khan	Laboratory Supervisor	20-Aug-1977
Sher Hassan	Store Keeper	22-Aug-1977
Mohammad Anwar	Assistant	18-Sep-1973
Juma Khan	Assistant	12-Jun-1985
Abdul Malik	Senior Clerk	28-Apr-1987
Manzoor Ahmad	Junior Clerk	26-May-1995
Ali Mohammad	Driver	17-Jul-1984
Saleh Mohammad	Driver	18-Aug-1990
Ghulam Rasool	Junior. Mechanic	20-Aug-1977
Mohammad Rafiq	Peon *(Naib Qasid)*	12-Oct-1978
Sikandar Khan	Peon *(Naib Qasid)*	30-Apr-1976
Atta Mohammad	Peon *(Naib Qasid)*	25-Mar-1986
Abdul Wadood	Chowkidar	26-Jan-1992
Nazir Masih	Janitor	01-Apr-1977

ACADEMIC ACTIVITIES

Mohammad Ayub Baloch successfully completed his M.Phil. Project under the Supervision of Dr. Abdul Haq (late) and Dr. Abdul Salam Khan, and defended his thesis on "Petrography of the Ophiolitic rocks of Goth Shahi Mohammad, Khuzdar District Balochostan". His thesis has been approved by the University of Balochistan.

Mehrab Khan successfully completed his Ph.D. work under the supervision of Khalid Mahmood and Abdul Salam Khan, and defended his Dissertation in December 1998. The dissertation is yet to be approved by the Committee for Advanced Studies and Research and the Syndicate of the University of Balochistan.

Abdul Tawab Khan also completed his research work for Ph.D. under the supervision of Akhtar Mohammad Kassi and Abdul Salam Khan. He is expected to defend his Dissertation during the first quarter of 1999.

By the end of December 1998, the C.E.M had four Ph.D. and fourteen M.Phil. students working on the following aspects of the Geology of Balochistan:

Student	Supervisor	Co-Supervisor	Project Title
		Ph.D. PROJECTS	
Mehrab Khan Baloch	Abdul Salam Khan	Khalid Mahmood	Petrological and Structural (Kinematic) Studies of the Igneous Rocks of the Baran Lak Area Bela, Khuzdar District, Balochistan.
Abdul Tawab Khan	Akhtar Mohammad Kassi	Abdul Salam Khan	Sedimentology and Petrology of the Volcaniclastic Succession of the Bibai Formation (Cretaceous), Ziarat District, Balochistan, Pakistan.
Din Muhammad Kakar	Akhtar M. Kassi	Mohammad Ahmad Farooqui	Geology of The Tertiary Khojak Formation of Pishin, Muslimbagh And Chaghi Districts, Balochistan
Ghulam Nabi	Abdul Salam	Javed Ahmad	Petrography And Depositional Environment of Ghazij Formation (Eocene). Balochistan
		M. PHIL. PROJECTS	
Atif Saleem	Khalid Mahmood	Mehrab Khan Baloch	Nature of Mafic Intrusions in the Mantle Section of Saplai Tor Ghar Ophiolite related to Mantle Rocks, Muslim Bagh, Balochistan.
Ahmad Jan	Abdul Salam Khan	Jawed Ahmad	Sedimentological and Structural Studies of the Coal Bearing Ghazij Formation Near Khost/Shahrig, Balochistan.
Khalil-Ur-Rehman	Mohammad Ahmad Farooqui	Akhtar Mohammad Kassi	Petrology and Provenance of Paleocene (?) Ispikan Conglomerate, SW Makran and its implications on the tectonic evolution of makran Region.
Mohammad Zahir Kakar	Mohammad Ahmad Farooqui	Din Mohammad Kakar	Depositional Environment And Diagenesis of Lower Cretaceous Sembar Formation, Balochistan.
Syed Ashrafuddin	Mohammad Ahmad Farooqui	Mehrab Khan Baloch	Study of K-T Boundary in the western Sulaiman Foldbelt, Pakistan
Mohammad Rahim Jan	Mohammad Ahmad Farooqui		Geology and Mineral Resources of part of Makran Coast, Balochistan.
Azhar Hussain	Mohammad Ahmad Farooqui	Khalid Mehmood	Petrology, Stratigraphy and Lithofacies Analysis of Dungan Formation (Paleocene), Sulaiman Foldbelt, Balochistan.

Student	Supervisor	Co-Supervisor	Project Title
Abdul Rahim Kassi	Abdul Salam	Mohammad Ahmad Farooqui	Facies Distribution And Environmental Analysis of The Parh Group, Balochistan.
Shahzad Baig	Mohammad Niamatullah	Mohammad Ahmad Farooqui	Geology And Hydrocarbon Potential of Part of Makran Coast, Balochistan.
Shah Zaman Kakar	Javed Ahmad	Abdul Salam Khan	Facies Analysis And Reservoir Properties of Chiltan Formation (Jurassic) Northern Balochistan.
Khawar Sohail	Abdul Salam	Javed Ahmad	Petrology, Sedimentology And Diagenesis of (Mio-Pliesto) Hinglaj Formation, District Khuzdar and Bela Balochistan.
Hussain Buksh	Mobasher Aftab	Javed Ahmad	Hydrogeological Investigations of Kalat Sub-Basin, Balochistan.
Abdul Hadi	Mobasher Aftab	Mehrab Khan Baloch	Hydrogeological Investigation of Pishin Sub-Basin Balochistan.
Arif Ali	Mobasher Aftab	Javed Ahmad	Assessment of Groundwater Budget of Mangocher Valley, Balochistan.

Faculty members continued supervision of their research students. A number of students completed their field studies/work. Following field studies were carried out during 1998:

Research Supervisor	Student	Program of Study	Areas visited
Mohammad A. Farooqui and Abdul Salam Khan	Khalil-Ur-Rehman and Khawar Suhail	M.Phil. M.Phil.	Khuzdar, Bela districts (7 days): to study Khojak Flysch and Hinglaj Formation.
Khalid Mahmood	Atif Saleem	M.Phil.	Saplai Tor Ghar Massif, Muslim Bagh (20 days): to study the ophiolites.
Abdul Salam Khan	Khawar Suhail	M.Phil.	Khuzdar and Bela Districts (20days): to study the Hinglaj Formation in detail.
Mohammad Ahmad Farooqui	Khalil-Ur-Rehman	M.Phil.	Ispikan (Mand) and surrounding areas, Makran (15 days): to study in detail the Ispikan Conglomerate, Wakai Limestone (Nisai Formation), and Siahan Shale & Turbat Group (Khojak Flysch).
Javed Ahmad and Mobasher Aftab	Hussain Buksh	M.Phil.	Mastung, Mangocher and Kalat districts (5 days): To study the hydrogeol-ogical characters of groundwater basins.
Akhtar Mohammad Kassi	Khalil-Ur-Rehman	M.Phil.	Ispikan and Surrounding areas, Makran (5 days): To study Ispikan Conglomerate
Mohammad Ahmad Farooqui and Abdul Salam Khan	Mohammad Zahir, Azhar Hussain and Abdul Rahim	M.Phil. M.Phil. M.Phil.	Kach, Ziarat, Harnai, Loralai, and Sinmjavi, and Jindaran areas (13 days): to study Cretaceous Parh Group and Paleocene Dungan Formation.
Mohammad Ahmad Farooqui and Mohammad Niamatullah	Sghahzad Baig and M. Rahim Jan	M.Phil. M.Phil.	Panjgoor, Turbat, Ispikan, Pasni, Gawadar and Jiwani areas of Makran (12 days): to study the geology and mineral resources along the coast of Makran.
Abdul Salam Khan	Mehrab Khan	Ph.D.	Bela and Khuzdar areas (20 days): to study Bela Ophiolites.

Abdul Salam Khan attended one day seminar on "Mapping Trends in the 21st Century", held at Rawalpindi in May 1998, organized by the Survey of Pakistan, Rawalpindi.

Mohammad A. Farooqui organized a ten day workshop on *"Computer Applications in Geology"* in October, 1998. All the faculty members of the C.E.M. and the Department of Geology attended the workshop.

Abdul Salam Khan attended 13th Himalyan-Karakoram-Tibet International Workshop held in Peshawar from April 19-22, 1998 and presented a paper extracted from the research work of Ph.D. student Mehrab Khan.

Khalid Mahmood started the initial work on the structural and textural characteristics of Muslim Bagh ophiolites for which he and Mehrab Khan (co-investigator) made several visits to the Muslim Bagh ophiolites.

The Faculty members remained involved in independent research projects also. Out of four, three research projects have been approved and funded. Details of the projects are as under:

Title of the Project	Principal Investigator	Co-Investigators	Funded By
Structural & Textural studies of mantle rocks from Muslim Bagh ophiolites.	Khalid Mahmood	Mehrab Khan Baloch	University Grants Commission.
Facies distribution, depositional environments and Petroleum prospects of the Foreland Basin sediments, Kirthar fold-belt, Balochistan, Pakistan.	Abdul Salam Khan	Akhtar Mohammad Kassi	Pakistan Science Foundation
Study of Sedimentological and Structural Aspects of Selected Sites in the Makran Accretionary Belt, Pakistan.	Akhtar Mohammad Kassi	Abdul Salam Khan, Mohammad Ahmad Farooqui and Din Mohammad Kakar	University Grants Commission.
Geothermal Energy Prospects of Balochistan. *(Approval and funding awaited)*	Syed Mobasher Aftab	Mohammad Ahmad Farooqui	Submitted for funding to Federal Ministry of Science and Technology, under Grants-in-aid Contractual Research Project.

ERRATA

Plate 8 on page 97 and plate 12 on page 99 are printed incorrectly. The correct photographs with correct captions are as follows.

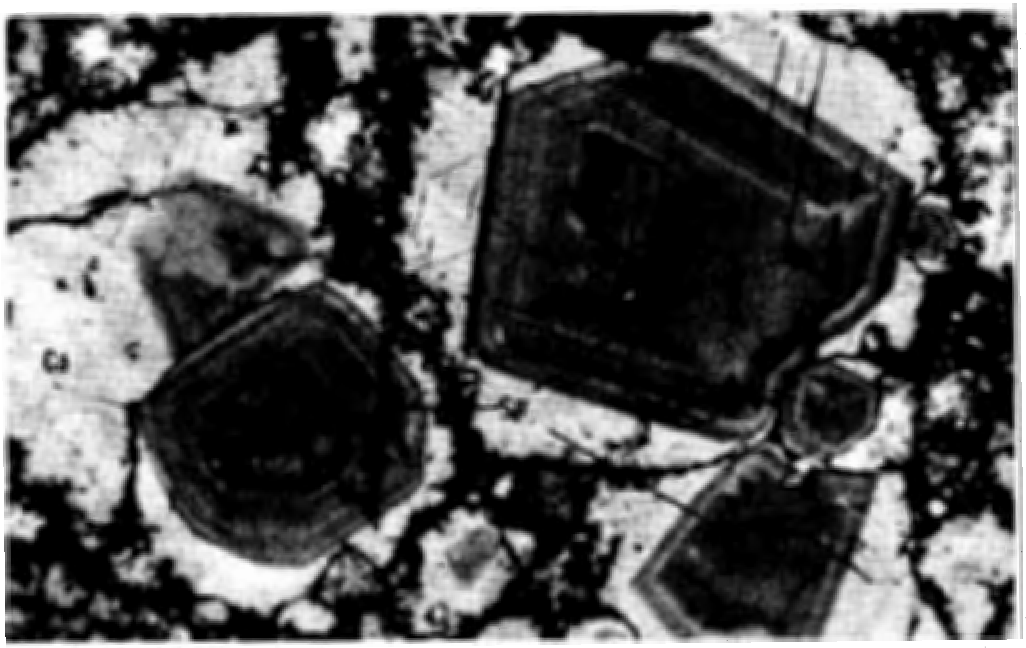

Plate 8. Photomicrograph showing color zoning in transmitted light within the large and medium grained sphalerite (Sp), (X5). (Ca = carbonates)

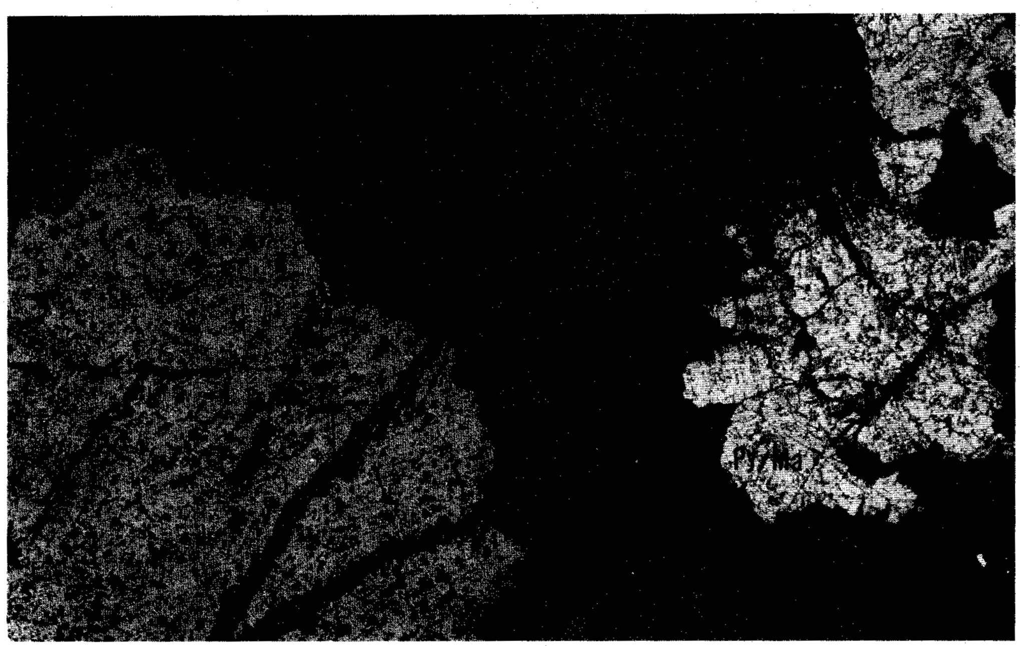

Plate 12. Photomicrograph (in reflected light) of large fractured grain of sphalerite (Sp) along with other minerals, e.g. pyrite/marcasite (Py/Ma), (X5).

INSTRUCTIONS FOR AUTHORS

Send three unbound copies, not stapled, of the complete manuscript to Editor *Acta Mineralogica Pakistanica*, Centre of Excellence in Mineralogy, University of Balochistan, Quetta Pakistan, along with a computer disk. Create and format your document in WordPerfect 5 or higher (for windows), or MS Word, however, manuscripts saved in any major wordprocessor will also be accepted. Mark the computer disk with the name of the principal author, abbreviated title of the paper, name of the file and the software in which the document was created. We will not retype manuscripts! Except for minor editing, content will be printed as it is received on computer disk or returned to be redone if required. **Please note that manuscripts received without a computer disk shall not be considered for publication.**

Type or laser print manuscripts, single sided, double spaced on A4 size paper including abstract, references, figure captions, appendices and tables. Leave one inch margin on all four sides and do not use extremely small fontsize. Number all pages begining with the abstract. Exact format of the title page is unimportant because it will be changed upon computer formatting for electronic typesetting, but supply the following items clearly differentiated in the following order

- running head: a descriptive condensation of the title, not exceeding 80 characters, in all capital letters
- title, in all capital letters
- list of authors, in all capital letters, all in single paragraph, with first names or initials first, with supercripts to indetify the addresses
- list of addresses, in capital and small letters, superscripted to correspond to the list of authors (use asterisks to indicate current address when different from original address).
- the word 'manuscript received' with a generous space for a date stamp

In the text, use the following format for heading

first order headings are **BOLD CAPITAL CENTERED;**

second order headings are ***BOLD ITALIC CAPITALS CENTERED;***

third order headings are left indented **bold Small Letter**

fourth order headings are left indented ***bold Italic Small Letter***

FIGURES: All line figures (maps, drawings etc.) and photographs should be clear, sharp, and legible originals in black and white colours only. Submit figures and photographs as large as possible but no larger than 8½" x 11". Line figures and photographs may be reduced during printing for the prupose of saving space, therefore, lettering on figures should be large enough to be $\geq$1.5mm when figure is reduced to final width. Photographs should be of superior quality, black and white only, glossy, ideally 5" x 7". If necassary authors should indicate crop lines on photos before submittal. Composite photos, line drawings and multi-part figures must have identifying Roman capital Letters applied firmly and permanently in the upper left corner. Publisher shall not be responsible for such letters falling off during review and production. Itentify all figures on the back by authors name and figure number. List figure captions on a separate page or pages at the end of the manuscript. In the text the word *figure* is capitalized and spelled out e.g. Figure 1; it is capitalized and abberviated when used parenthetically e.g. (Fig. 1). Colour plates and foldouts can only be published if the author bears the full extra cost in advance of publication; contact the Editor for details. All permissions for quotations, photographs, illustrations, etc. are the author's responsibility and should be acknowledged in the paper.

KINDS OF CONTRIBUTIONS

Research Papers Articles dealing with original unpublished research results in the multifaceted field of Earth Sciences covering Economic Geology, Petroleum Geology, Mineral Exploration, Mineralogy, Petrology, Crystallography, Tectonics, Structural Geology, Hydrogeology, Aqueous Geochemistry, Geophysics, Tectonophysics, Geochemistry, Mineral Chemistry, Geochronology, Historical Geology, Environmental Geology, Engineering Geology, Paleontology, Stratigraphy, Sedimentology, Oceanography, Coastal Geology, Marine Geology and Geology Education

Review Articles Articles reviewing the research results, theories, models, or opinions presented in the already published literature.

Book Reviews: Reviews of books useful to the readers of the Acta Mineralogica Pakistanica.

Short Communications Short articles (up to four printed pages) dealing with more personal or opion-oriented viewpoints or observation on any aspect of the Earth Sciences.

Abstracts Abstracts of original unpublished research results shall also be considered for publication. The abstracts should not be longer than one printed page, including figures if any.

Announcements Announcements of events of interest to the readers of Acta Mineralogica Pakistanica.

Please make sure that your contribution/s fulfill the following criteria of scientific publications:

Original data and information,

Clear conceptual approach of analysis,

Usefull information from academic and practical considerations, and

Simple style and straight expression

ACTA MINERALOGICA PAKISTANICA
VOLUME 9, 1998

CONTENTS

ARTICLES

SHORT COMMUNICATIONS

REPORTS